

ISTANBUL TECHNICAL UNIVERSITY ★ EURASIA INSTITUTE OF EARTH SCIENCES

**SIMULATION OF ¹³⁷CS TRANSPORT AND DEPOSITION AFTER THE
CHERNOBYL NUCLEAR POWER PLANT ACCIDENT AND
RADIOLOGICAL DOSES OVER THE ANATOLIAN PENINSULA**

Ph.D. THESIS

Volkan ŞİMŞEK

Department of Climate and Marine Sciences

Earth System Science Program

NOVEMBER 2014

**SIMULATION OF ¹³⁷Cs TRANSPORT AND DEPOSITION AFTER THE
CHERNOBYL NUCLEAR POWER PLANT ACCIDENT AND
RADIOLOGICAL DOSES OVER THE ANATOLIAN PENINSULA**

Ph.D. THESIS

**Volkan ŞİMŞEK
(601062006)**

Department of Climate and Marine Sciences

Earth System Science Program

**Thesis Advisor: Prof. Dr. Tayfun KINDAP
Co-advisor : Assist. Prof. Dr. Luca Pozzoli**

NOVEMBER 2014

İSTANBUL TEKNİK ÜNİVERSİTESİ ★ AVRASYA YER BİLİMLERİ
ENSTİTÜSÜ

**ÇERNOBİL NÜKLEER GÜÇ SANTRALİ KAZASI SONRASI ¹³⁷Cs TAŞINIMI
VE ÇÖKELİMESİNİN SİMULASYONU VE ANADOLU YARIMADASINDAKİ
RADYOLOJİK DOZLAR**

DOKTORA TEZİ

Volkan ŞİMŞEK
(601062006)

İklim ve Deniz Bilimleri Anabilim Dalı

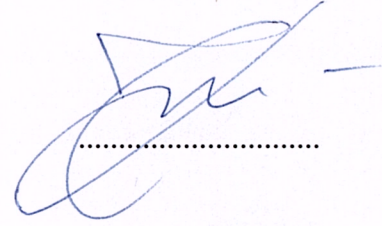
Yer Sistem Bilimi Programı

Tez Danışmanı : Prof. Dr. Tayfun KINDAP
Eşdanışman : Yard. Doç. Dr. Luca Pozzoli

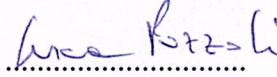
KASIM 2014

Volkan ŞİMŞEK, a Ph.D. student of ITU Eurasia Institute Of Earth Sciences student ID **601062006**, successfully defended the **dissertation** entitled “**Simulation of ¹³⁷Cs transport and deposition after the chernobyl nuclear power plant accident and radiological doses over the Anatolian Peninsula**”, which he prepared after fulfilling the requirements specified in the associated legislations, before the jury whose signatures are below.

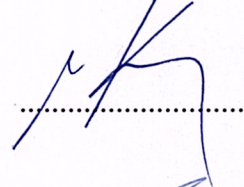
Thesis Advisor : **Prof. Dr. Tayfun KINDAP**
İstanbul Technical University



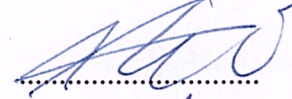
Co-advisor : **Assist. Prof. Dr. Luca POZZOLI**
İstanbul Technical University



Jury Members : **Prof. Dr. Mehmet KARACA**
İstanbul Technical University



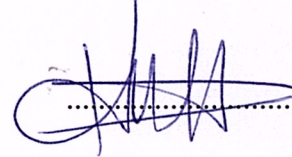
Assoc. Prof. Dr. Alper ÜNAL
İstanbul Technical University



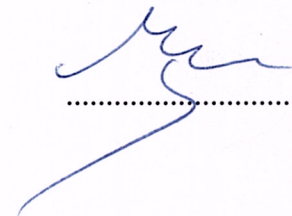
Assoc. Prof. Dr. Gürsel KARAHAAN
TAEK-ÇNAEM



Prof. Dr. Göksel DEMİR
Bahçeşehir University



Prof. Dr. Mete TAYANÇ
Marmara University



Date of Submission : 17 September 2014
Date of Defense : 25 November 2014

To my family,

FOREWORD

‘People will fight for energy and water in the near future’ said the Minister of Energy while watching news on TV with my family. As a boy fight was gripping. I found this as interesting as when Peter Parker had mutation and became the Spiderman after he was bitten by a spider.

Then I heard about Chernobyl accident on TV. I did not understand it but it was said to be something bad. On the other hand, nuts, eggs and milk were brought to us at school. People were arguing if these were the food which were radioactively contaminated because of the Chernobyl accident. Maybe Chernobyl was not something bad because of delicious nuts? Energy, mutation, nuclear, radioactive... These were interesting words for me when I first heard them. Even now, they still are. Afterwards, I had undergraduate degree diploma at Physics. I started to work at Mugla University Physics Department as a research assistant. During a technical visit, I visited Çekmece Nuclear Research and Training Center with my students. I remembered the Chernobyl accident. I really wanted to work here. In 2006, I started to work at the Health Physics Department of Çekmece Nuclear Research and Training Center.

I wanted to pursue a PhD that is closely related to what I do in ÇNAEM. Luckily, I met with my advisor Prof. Dr. Tayfun KINDAP who was also interested in Chernobyl accident. And the long way to get PhD degree started...

This study was conducted at Istanbul Technical University, Eurasia Institute of Earth Sciences.

I would like to acknowledge ITU for their support at EGU 2012 which I presented a poster about this study.

I am grateful to meet Prof. Dr. Tayfun KINDAP. I owe great thanks to him for believing that we can do this study and never gave up on me.

It was a big chance to meet my co-Advisor Dr. Luca Pozzoli. Many thanks to him for being patient to me and sharing his experience, time and knowledge.

I sincerely express my thanks to Assoc. Prof. Alper Ünal and Prof. Mehmet KARACA for their academic support and constant encouragement in this work.

I would like to thank Deniz Vural for his help about WRF, my friend Res. Assistant Dr. Tuğba AĞAÇAYAK for her help about almost everything and her friendship , and many thanks to Seden BALTACIBAŞI for her help about R.

I also want to thank my friends at Çekmece Nuclear Research and Training Center mostly Levent ÖZDEMİR, for sharing their time and experience at this study.

And my family. I'm happy to have such great family and to have their love all the time. As I promised to my father İrfan ŞİMŞEK and my mother Saniye ŞİMŞEK, I continued my education to the last. And I am happy to have such a good sister Çiğdem ŞİMŞEK.

I want to thank my wife, friend, Funda, who can turn a gray sky to blue with her smile, who is always beside me.

I hope my daughter Asya will do better than her parents in life and I wish her a good, successful life.

September 2014

Volkan ŞİMŞEK

TABLE OF CONTENTS

	<u>Page</u>
FOREWORD	ix
TABLE OF CONTENTS	xi
ABBREVIATIONS	xiii
LIST OF TABLES	xxv
LIST OF FIGURES	xvii
SUMMARY	xix
ÖZET	xxi
1. INTRODUCTION	1
1.1 Motivation.....	2
1.2 Purpose.....	3
2. LITERATURE REVIEW	5
2.1 Overview of the Chernobyl NuclearPower Plant Accident	5
2.1.1 Chernobyl Nuclear Power Plant	5
2.1.2 RBMK-1000 design nuclear reactors	6
2.1.3 Chernobyl Nuclear Power Plant accident	6
2.1.4 Source term and releases from the reactor.....	7
2.1.5 The Atlas Project: Caesium-137 Contamination of Europe after the Chernobyl Accident	10
2.1.6 CNPP Accident and Modelling studies	14
2.2 Biological Effects of Ionizing Radiation	16
2.3 Pathways of Released Radioactive Material to The Environment and to the Human Body	19
2.3.1 ¹³⁷ Cs and it's effects on the body.....	20
2.3.2 Radiation doses and health effects after CNPP accident	21
3. METHODOLOGY	27
3.1 WRF (Weather Research Forecast model)	28
3.2 HYSPLIT	30
3.3 HYSPLIT Simulations setup.....	31
3.4 Radiaiton Dose Calculations.....	34
3.4.1 Effective dose calculation from UNSCEAR and Radiological Toolbox ..	35
3.4.1.1 Radiological Tool Box	35
3.4.1.2 Dose from ground deposition.....	35
3.4.1.3 Cloud gamma doses	36
3.4.1.4 Inhalation doses.....	36
3.4.2 Effective dose calculation from WHO.....	36
3.4.2.1 Dose from Ground Deposition	36
3.4.2.2 Cloud Gamma Doses.....	37
3.4.2.3 Inhalation Doses.....	37
3.5 REM Database	38
4. RESULTS AND DISCUSSION	39
4.1 Meteorology.....	39

4.2 Air Concentrations and Deposition of ¹³⁷ Cs over Europe.....	41
4.2.1 Air concentrations of ¹³⁷ Cs over Europe.....	41
4.2.2 Deposition of ¹³⁷ Cs over Europe.....	46
4.2.3 Radiological doses over Europe.....	52
4.3 Air Concentrations and Deposition of ¹³⁷ Cs over Turkey and Radiological Doses.....	54
4.3.1 Air concentrations and deposition of ¹³⁷ Cs over Turkey.....	54
4.3.2 Radiological doses over Turkey.....	58
5. CONCLUSIONS.....	65
REFERENCES.....	69
APPENDICES.....	77
Appendix A.1: Maps.....	78
Appendix A.2: Tables.....	95
CURRICULUM VITAE.....	135

ABBREVIATIONS

CNPP	: Chernobyl Nuclear Power Plant
¹³⁷Cs	: Caesium-137
DNA	: Deoxyribonucleic acid
DREAM	: Danish Rimpuff and Eulerian Accidental release Model
FNPP	: Fukushima Dai-ichi Nuclear Power Plant
GHG	: Greenhouse Gas
HYSPLIT	: Hybrid Single Particle Lagrangian Integrated Trajectory Model
¹³¹I	: Iodine-131
IAEA	: International Atomic Energy Agency
INES	: International Nuclear Event Scale
JRC	: Joint Research Centre
LADAS	: Long-range Accident Dose Assessment System
MNPP	: Metsamor Nuclear Power Plant
NCRP	: National Council on Radiation Protection and Measurements
NEA	: Nuclear Energy Agency
OECD	: The Organisation for Economic Co-operation and Development
RBMK	: (Reaktor Bolshoy Moshchnosty Kanalny, High-Power Channel Reactor)
REM	: The Radioactivity Environmental Monitoring
UNSCEAR	: United Nations Scientific Committee on the Effects of Atomic Radiation
WRF	: Weather Research and Forecasting Model
WHO	: World Health Organisation

LIST OF TABLES

	<u>Page</u>
Table 2.1 : Current estimate of radionuclide releases during the CNPP accident	9
Table 2.2 : Summary of deposition measuring techniques and data.....	12
Table 2.3 : Dose results after CNPP accident, natural background and medical applications.....	25
Table 3.1 : Summary of the simulations performed with HYSPLIT..	32
Table 3.2 : Source term after CNPP accident according to Brand et al., 2002..	33
Table 3.3 : Source term after CNPP accident according to Suh et al.,2009.....	33
Table 3.4 : Source term after CNPP accident according to Evangeliou et al.,2013..	34
Table 4.1 : Cumulative ¹³⁷ Cs deposition results for Europe after CNPP accident....	51
Table 4.2 : Calculated maximum adult doses.	53
Table 4.3 : BR1 Simulation results for Turkish Provinces.	57
Table 4.4 : Mean, minimum, maximum, and standard deviation (6 simulations) of ¹³⁷ Cs adult dose values (mSv/year) for each province in Turkey (UNSCEAR approach).....	61
Table 4.5 : Mean, minimum, maximum, and standard deviation (6 simulations) of ¹³⁷ Cs adult dose values (mSv/year) for each province in Turkey (WHO approach).....	63
Table B.1 : List of REM database stations used for comparisons with simulated ¹³⁷ Cs air concentrations..	94
Table B.2 : BR2 Simulation results for Turkish Provinces.....	95
Table B.3 : CONT Simulation results for Turkish Provinces.	97
Table B.4 : EV1 Simulation results for Turkish Provinces.....	99
Table B.5 : EV2 Simulation results for Turkish Provinces.....	101
Table B.6 : SU1 Simulation results for Turkish Provinces.	103
Table B.7 : SU2 Simulation results for Turkish Provinces.	105
Table B.8 : Calculated doses for Turkish Provinces by using BR1 simulation results (UNSCEAR Approach).....	107
Table B.9 : Calculated doses for Turkish Provinces by using BR1 simulation results (WHO Approach)	109
Table B.10 : Calculated doses for Turkish Provinces by using BR2 simulation results (UNSCEAR Approach).....	111
Table B.11 : Calculated doses for Turkish Provinces by using BR2 simulation results (WHO Approach)	113
Table B.12 : Calculated doses for Turkish Provinces by using EV1 simulation results (UNSCEAR Approach).....	115
Table B.13 : Calculated doses for Turkish Provinces by using EV1 simulation results (WHO Approach)	117
Table B.14 : Calculated doses for Turkish Provinces by using EV2 simulation results (UNSCEAR Approach).....	119
Table B.15 : Calculated doses for Turkish Provinces by using EV2 simulation results (WHO Approach)	121

Table B.16 : Calculated doses for Turkish Provinces by using SU1 simulation results (UNSCEAR Approach).....	123
Table B.17 : Calculated doses for Turkish Provinces by using SU1 simulation results (WHO Approach).....	125
Table B.18 : Calculated doses for Turkish Provinces by using SU2 simulation results (UNSCEAR Approach).....	127
Table B.19 : Calculated doses for Turkish Provinces by using SU2 simulation results (WHO Approach).....	129
Table B.20 : Calculated doses for Turkish Provinces by using CONT simulation results (UNSCEAR Approach)..	131
Table B.21 : Calculated doses for Turkish Provinces by using CONT simulation results (WHO Approach).....	133

LIST OF FIGURES

	<u>Page</u>
Figure 1.1 : Purpose diagram of the thesis.....	4
Figure 2.1 : Chernobyl Nuclear Power Plant before the accident.....	5
Figure 2.2 : RBMK-1000 nuclear reactor design.....	6
Figure 2.3 : Chernobyl Nuclear Power Plant after accident..	7
Figure 2.4 : Daily release rate of radioactive substances into the atmosphere.	8
Figure 2.5 : Daily releases of iodine-131, iodine-133, tellurium-132 and caesium-137 from the CNPP.....	10
Figure 2.6 : Ground deposition of ¹³⁷ Cs in Europe after the CNPP accident	14
Figure 2.7 : Direct versus indirect action of ionizing radiation	17
Figure 2.8 : The pathways of radionuclides to the body.....	20
Figure 2.9 : ¹³⁷ Cs decay scheme.....	21
Figure 2.10 : Spatial distribution of the effective doses to European populations for the 1986–05 time period	24
Figure 3.1 : Diagram of methodology.....	27
Figure 3.2 : WRF system components.....	29
Figure 3.3 : Model domain and land/sea mask used of the WRF simulation..	30
Figure 3.4 : Measured (REM) total deposition of ¹³⁷ Cs over Europe... ..	38
Figure 4.1 : Daily mean wind speed, sea level pressure and precipitations for the days: a)26/04/1986. b)29/04/1986. c)02/05/1986. d)04/05/1986.	39
Figure 4.2 : Daily 850 hPa level pressure for the days: a) 26/04/1986. b) 29/04/1986. c) 02/05/1986. d) 04/05/1986.....	40
Figure 4.3 : BR1 simulation results (Bq/m ³) showing transport of radioactive clouds between 27/04/1986 and 08/05/1986.....	42
Figure 4.4 : Observed and simulated Caesium-137 maximum air concentrations at REM database measuring stations.	45
Figure 4.5 : Box and Whisker plots of the surface activity concentrations (Bq/m ³) of ¹³⁷ Cs.	46
Figure 4.6 : Total depositions of ¹³⁷ Cs over Europe after Chernobyl accident for six simulations.	47
Figure 4.7 : Box and Whisker plots of the cumulative deposition (kBq/m ²) of ¹³⁷ Cs	49
Figure 4.8 : Effective dose values for Europe for two approaches. a) UNSCEAR Approach, b) WHO Approach	53
Figure 4.9 : Mean ¹³⁷ Cs concentration values for Turkey.....	55
Figure 4.10 : Total ¹³⁷ Cs deposition amounts of Turkey with 6 different simulations	56
Figure 4.11 : Mean ¹³⁷ Cs effective dose values for 6 simulations (CONT300 excluded) for adults (left), child (<10 years age, center), and infants (<1 year age, right), and with UNSCEAR (top) and WHO (bottom) methodologies	60

Figure A.1 : Daily mean wind speed, sea level pressure and precipitation amounts for a) 27 April 1986. b) 28 April 1986. c) 30 April 1986. d) 01 May 1986. e) 03 May 1986. f) 05 May 1986	78
Figure A.2 : Daily mean wind speed, Sea level pressure and precipitation amounts for a) 06/05/1986. b) 07/05/1986. c) 08/05/1986. d) 09/05/1986. e) 10/05/1986..	79
Figure A.3 : Caesium-137 air concentrations [Bq m^{-3}] simulated by HYSPLIT at surface for the BR2 simulation, 27/04/1986–08/05/1986.....	80
Figure A.4 : Caesium-137 air concentrations [Bq m^{-3}] simulated by HYSPLIT at surface for the CONT simulation, 27/04/1986–08/05/1986..	82
Figure A.5 : Caesium-137 air concentrations [Bq m^{-3}] simulated by HYSPLIT at surface for the EV1 simulation, 27/04/1986–08/05/1986.....	84
Figure A.6 : Caesium-137 air concentrations [Bq m^{-3}] simulated by HYSPLIT at surface for the EV2 simulation, 27/04/1986–08/05/1986.....	86
Figure A.7 : Caesium-137 air concentrations [Bq m^{-3}] simulated by HYSPLIT at surface for the SU1 simulation, 27/04/1986–08/05/1986.	88
Figure A.8 : Caesium-137 air concentrations [Bq m^{-3}] simulated by HYSPLIT at surface for the SU2 simulation, 27/04/1986–08/05/1986.	90
Figure A.9 : Adult dose results (mSv) of the simulations for Europe calculated by UNSCEAR Approach : a)BR2 b) CONT c)EV1 d) EV2. e) SU1. f) SU2.	92
Figure A.10 : Adult dose results (mSv) of the simulations for Europe calculated by WHO Approach : a)BR2 b) CONT c)EV1 d) EV2. e) SU1. f) SU2.. ..	93

SIMULATION OF ¹³⁷CS TRANSPORT AND DEPOSITION AFTER THE CHERNOBYL NUCLEAR POWER PLANT ACCIDENT AND RADIOLOGICAL DOSES OVER THE ANATOLIAN PENINSULA

SUMMARY

The Chernobyl Nuclear Power Plant (CNPP) accident occurred on April 26 of 1986, was the most serious accident ever to occur in the nuclear power industry. It is still an episode of interest, due to the large amount of radionuclides dispersed in the atmosphere. After CNPP accident main releases occurred during first 10 days of the accident. First estimation about releases was that 100% of the core inventory of the noble gases (xenon and krypton) was released, and between 10% and 20% of the more volatile elements of iodine, tellurium and caesium. From the radiological point of view, the releases of ¹³¹I and ¹³⁷Cs, estimated to have been 1,760 and 85 PBq, respectively, are the most important to consider.

Caesium-137 (¹³⁷Cs) is one of the main radionuclides emitted during the Chernobyl accident, can travel long distances in the air before being brought back to the earth by rainfall and gravitational settling. It has a half-life of 30 years, which can be accumulated in humans and animals, and for this reason the impacts on population are still monitored today. One of the main parameters in order to estimate the exposure of population to ¹³⁷Cs is the concentration in the air, during the days after the accident, and the deposition at surface.

The transport and deposition of ¹³⁷Cs over Europe occurred after the CNPP accident has been simulated using the WRF-HYSPLIT modelling system. Meteorological conditions and dispersion of radionuclides were simulated by using the WRF meteorological model and the HYSPLIT dispersion model. Four different vertical and temporal emission rate profiles have been simulated, as well as two different dry deposition velocities.

The model simulations could reproduce fairly well the observations of ¹³⁷Cs concentrations and deposition, which were used to generate the 'Atlas of caesium deposition on Europe after the Chernobyl accident' and published in 1998. An additional focus was given on ¹³⁷Cs deposition and air concentrations over Turkey, which was one of the main affected countries, but not included in the results of the Atlas.

We estimated a total deposition of 2-3.5 PBq over Turkey, which would rank Turkey at the 5th place if compared to the country totals in the Atlas. The radioactive cloud interested Turkey from the 2nd of May until the 8th of May. Air concentrations values reached 25 Bq/m³ in the province of Edirne, and larger than 10 Bq/m³ in many provinces of Black Sea and Marmara regions. Deposition results shows that 2 main regions affected, East Turkey and Central Black Sea coast until Central Anatolia, with values between 10 kBq m⁻² and 100 kBq m⁻².

Mean radiological effective doses from simulated air concentrations and deposition has been estimated for Turkey reaching with two different approaches. First approach includes some coefficients from United Nations Scientific Committee on

the Effects of Atomic Radiation (UNSCEAR) report after CNPP and dose coefficients from Radiological Toolbox, developed for the U.S. Nuclear Regulatory Commission (NRC). The second approach was done according to World Health Organization report (WHO) which includes effects of Fukushima Nuclear Power Plant accident. Estimated doses reached up to 0.15 mSv/year in the North Eastern part of Turkey even if the contribution from ingestion of contaminated food and water is not considered, the estimated levels are largely below the 1 mSv limit indicated by the International Commission on Radiological Protection.

ÇERNOBİL NÜKLEER GÜÇ SANTRALİ KAZASINDAN SONRA ¹³⁷Cs TAŞINIMI VE ÇÖKELMESİNİN SİMULASYONU VE ANADOLU YARIMADASINDAKİ RADYOLOJİK DOZLAR

ÖZET

26 Nisan 1986 tarihinde Ukrayna'nın Kiev iline bağlı Çernobil kentinde bulunan Çernobil Nükleer Güç Santralinde meydana gelen kaza nükleer endüstride günümüze kadar meydana gelen en büyük kazadır.

Rus dizaynı RBMK tipi olan reaktörün 4. ünitesinde meydana gelen kaza, elektrik kesintisi durumunda kalp soğutmasının sürdürülebilirliği ile ilgili yapılan deney sırasında meydana gelmiştir. Ancak personel arası iletişim ve bilgi eksikliği, yeterli güvenlik önlemlerinin alınmaması gibi birçok neden kazanın oluşmasına neden olmuştur. Bir diğer önemli husus da kazanın oluşumunun dünya kamuoyuna duyurulmasının şeklidir. Kaza ilk kez İsveç'te bilimadamları tarafından yapılan ölçümlerde farkedilmiştir. Yapılan modelleme çalışmaları ile de kazanın yeri belirlenmiş ve dünya kamuoyuna açıklanmıştır.

Yüksek miktarlardaki radyonüklid salınımı sonrasında kazanın etkileri sadece kendi civarında değil bütün Kuzey yarımkürede hissedilmiştir. Reaktörde oluşan patlamalar ve çıkan yangın atmosferin üst kısımlarına radyonüklidlerin ulaşmasına neden olmuş ve bu da atmosferik hareketlerle radyonüklidleri uzak mesafelere taşımıştır. Radyonüklidlerin tamamına yakını kazayı takip eden 10 gün içinde atmosfere salınmıştır. Daha sonraki günlerde salınımlar meydana gelse de miktarı düşük kalmıştır. Kaza sonrası yapılan hesaplamalar reaktör kor envanterindeki asal gazların (xenon ve krypton) %100'ünün, İyot, tellür ve sezyum elementlerinin %10 ila %20'sinin salındığını göstermektedir. Öte yandan yapılan hesaplamalarda hala %50' ye yakın belirsizlikler olması salınan radyonüklid miktarlarının daha fazla olabileceğini düşündürmektedir. Çernobil nükleer santral kazasının gerek çok geniş bir alanda etkilerinin gözlemlenmesi gerekse de salınan radyonüklid miktarlarındaki belirsizlikler kazaya olan bilimsel ilgiyi canlı tutmaktadır.

Bir nükleer güç santrali kazası sonrasında atmosfere salınan radyonüklidler incelendiğinde özellikle uzun mesafelere taşınabilmeleri sebebiyle iyot ve sezyum izotopları radyolojik açıdan en önemli olanlardır. İyot-131 radyoizotopu 8 günlük yarıömre sahiptir. Özellikle kaza sonrasındaki ilk dönemlerde radyolojik açıdan I-131 radyoizotopu önem taşımaktadır. Öte yandan 30 yıl yarı ömrü olan Sezyum-137 radyoizotopu özellikle çökme yaptığı bölgelerde, Çernobil nükleer santral kazası sonrasında insanların maruz kaldığı radyasyon dozunda uzun vadeli olan etkisi ile ön plana çıkmaktadır. Bunun iki nedeni vardır. İlki toprak yüzeyindeki ¹³⁷Cs miktarına bağlı olarak dış ışınlanmadır. İkincisi ise toprak yüzeyinden zamanla yer altı sularına ve bitkisel ürünlere geçiş yapması ve uzun yarıömürü sayesinde beslenme yoluyla insan vücuduna girebilmesidir. Özellikle insan vücudunda kaslarda biriken ¹³⁷Cs , 15 ila 150 günlük biyolojik yarıömre sahiptir. Ayrıca kazayı takip eden günlerde meteorolojik olaylara da bağlı olarak solunum yoluyla ve havadan ışınlanma ile insan sağlığına etki etmiştir.

Çernobil nükleer santral kazasından sonra gerek ülkemizde gerekse dünyada kazanın etkileri ile ilgili birçok bilimsel çalışma yapılmıştır. Çalışmaların içeriği temelde reaktörden salınan radyonüklid miktarları üzerine hesaplama ve modellemeleri, salınan radyonüklidlerin taşınımı ve üzerine olan etkileri, bitkisel ve hayvansal numunelerde, tüketici ürünlerinde radyoaktivite miktarları ve son olarak bunların insan sağlığına etkiler üzerinedir. Ülkemizdeki çalışmalara bakılacak olursa, özellikle ölçüm anlamında Türkiye Atom Enerjisi Kurumu tarafından ölçümler yapılmıştır. Öte yandan bugüne kadar özellikle meteorolojik olarak Çernobil Nükleer santral kazasının modellemesi ve parçacık dağılımının simülasyonu ilk olarak Dr. Tayfun KINDAP ve arkadaşları tarafından yapılan çalışmadır. Ayrıca Avrupa Birliğinin desteği ile yapılan bir projede, Avrupadaki her ülkenin kendi ölçüm sonuçlarını derleyerek, ¹³⁷Cs çökeltme miktarlarını içeren bir atlas oluşturmuş ve 1998 yılında yayınlamıştır. Atlasta Avrupa ülkelerinin hemen hemen tamamına dair sonuçlar yer almaktadır. Her ülke için onlarca bazen binlerce olan veri, ölçüm sayısı Türkiye için bir adet ve sadece Trakya bölgesi için mevcuttur. Türkiye'nin kazanın meydana geldiği bölgeye yakınlığı ve kapladığı alan göz önüne alındığında bir noktadaki verinin yetersiz olduğu anlaşılacaktır.

Bu çalışmada Çernobil nükleer santral kazası sonrasında atmosfere salınan radyonüklidlerin meteorolojik koşullara bağlı olarak dağılımı simüle edilmiştir. Meteorolojik koşullar Weather Research and Forecasting (WRF) model kullanılarak 26 Nisan 1986 ile 8 Mayıs 1986 tarihleri arasında simüle edilmiştir. Elde edilen meteorolojik model çıktıları Hybrid Single Particle Lagrangian Integrated Trajectory (HYSPLIT) dağılım modeline girdi olarak kullanılmıştır. HYSPLIT dağılım modeli ile 7 farklı salınım koşulunda ¹³⁷Cs radyonüklidinin dağılımı Türkiye ve Avrupa kıtası için simüle edilmiştir.

HYSPLIT modeli ile elde edilen simülasyon sonuçlarında ¹³⁷Cs radyonüklidinin dağılımı literatürdeki çalışmalarla kıyaslanmıştır. Dağılım sonuçlarının literatürle uyumlu olması sonucunda bulunan hava konsantrasyonu değerleri öncelikle domainimiz içinde kalan ülkelerde kaza sonrası yapılan hava konsantrasyonu ölçümlerini içeren Avrupa Birliği veritabanı ile kıyaslandırılmıştır. Yapılan simülasyonlar sonucunda elde edilen ¹³⁷Cs çökeltme miktarları Atlas'taki değerlerle karşılaştırılmış ve istatistiksel olarak değerlendirmeler yapılmıştır. Gerek ¹³⁷Cs radyonüklidinin hava konsantrasyonu değerlerinin veritabanı ile gerekse çökeltme miktarlarının Atlas ile uyumlu olduğu gözlemlenmiştir.

Simülasyon sonuçları, radyoaktif bulutların ilk beş günlük süreçte İskandinav Yarımadası ile Orta ve Doğu Avrupa da etkili olduğunu göstermektedir. Takip eden beş günlük süreçte ise radyoaktif bulutların Balkanlar ve Türkiye üzerinde yoğunlaştığı sonucu elde edilmiştir. İlk olarak 2 Mayıs 1986 tarihinde Türkiye sınırlarına Trakyadan giren radyoaktif bulutların iki gün boyunca Türkiye sınırlarında Ege Bölgesini de etkileyecek şekilde kaldığı görülmüştür. 4 Mayıs 1986 tarihinden itibaren de radyoaktif bulutların etkisini Karadeniz Bölgesi ve buna müteakip Türkiye'nin doğusu'nda 8 Mayıs 1986 tarihine kadar gösterdiği anlaşılmaktadır. Bu süreçte hesaplanan ¹³⁷Cs hava konsantrasyonu değerleri Edirne ili için 25 Bq/m³ değerine ulaşmıştır. Karadeniz Bölgesi ve Marmara Bölgesinde ise 10 Bq/m³ üzerinde ¹³⁷Cs hava konsantrasyonu değerleri görülmüştür. Radyoaktif bulutların kaldığı süreler içinde meydana gelen yağış gibi hava olayları ¹³⁷Cs radyonüklidinin çökeltme miktarlarını belirlemiştir.

Atlas sonuçlarına göre Avrupa sınırları içinde ^{137}Cs radyonüklidinin toplam çökeltme miktarı 44,3 PBq (10^5 Bq)dir. HYSPLIT dağılım modeli ile yapılan yedi simülasyon sonuçları incelendiğinde Avrupa sınırlarında toplam çökeltme miktarı 33.8 PBq ile 44.6 PBq arasında değişmektedir. Çökeltme miktarlarının %90'ı sekiz Avrupa ülkesinde meydana gelmiştir. Bu ülkeler Belarus, Ukrayna, Finlandiya, İsveç, Norveç, Avusturya, Romanya ve Almanyadır. Avrupa geneline bakıldığında simülasyonlar arasında toplam radyoaktivite değeri arasında bütün Avrupa için %8 ile %10 fark varken, çökeltmenin fazla olduğu ülkelerde ise bu fark %20 ile %30 arasında gerçekleşmiştir. Simülasyonlardaki değişkenlerden birisi olan kuru çökeltme hızının etkisi ise bütün Avrupa'da toplamda %10 azalma yönünde olmuştur. Kuru çökeltme hızının etkisi ülkeler bazında incelenirse kaza bölgesine yakın yerlerde çökeltmenin azalmasına, uzak bölgelerde artmasına neden olmuştur. Örneğin Ukrayna da %20 ile %15 arasında, Belarus ta %6 ile %10 arasında azalma, Almanya' da ise %8 ile %25 arasında artış vardır.

Kaza sonrasında Türkiye'de meydana gelen ^{137}Cs radyonüklidinin çökeltme miktarları incelenecek olursa simülasyon sonuçlarına göre 2 PBq ile 3.5 PBq arasında olduğu görülmektedir. Bu değerler gözönüne alındığında Atlas'ta yer almayan Türkiye'nin ^{137}Cs çökeltme miktarının en yüksek beşinci değer olduğu görülecektir. Bütün simülasyon sonuçları ^{137}Cs çökeltme miktarlarının Türkiye'nin doğusu ile Karadeniz sahil şeridinin ortasından Ankara ve Konyaya kadar güney batı uzanımlı iki ana bölgede 10 kBq/m^2 ile 100 kBq/m^2 arasında olduğunu göstermektedir.

Elde edilen hava konsantrasyonu ve çökeltme değerleri kullanılarak Avrupa ve Türkiye için insanların maruz kaldığı toplam etkin doz değeri hesaplanmıştır. Toplam etkin doz hesabı ^{137}Cs aktivitesine bağlı olarak iç ve dış ışınlanma değerlerini içermektedir. Dış ışınlanma yer yüzeyindeki toplam ^{137}Cs aktivitesinden kaynaklanan radyasyon dozu ile radyoaktif bulutun bulunduğu zaman aralığından kaynaklanan radyasyon dozu değerlerini içermektedir. İç ışınlanma için ise hava konsantrasyonu dikkate alınarak solunumdan kaynaklanan doz değerleri hesaplanmıştır. Hesaplama sırasında Birleşmiş Milletler Atom Enerjisi Komisyonu'nun (UNSCEAR) Çernobil Kazası sonrası yayınladığı rapor ile Dünya Sağlık Örgütü'nün (WHO) Fukushima Nükleer Santral Kazası sonrasında yayınladığı raporda yer alan iki farklı metod ve koşullar kullanılmış ve kazadan sonraki ilk yıl için yetişkin, çocuk (10 yaşından küçük) ve bebek (1 yaşından küçük) dozları hesaplanmıştır.

Avrupa kıtasındaki radyolojik doz değerleri incelendiğinde ilk yıl için 0 ila 5 mSv üzerinde olduğu gözükmektedir. Özellikle Ukrayna'da santral etrafında yaşayan insanlar için 5 mSv üzerinde doz değerleri olduğu belirlenmiştir. Öte yandan yine Ukrayna ve Belarus için bazı bölgelerde doz değerlerinin yıllık 1 mSv ' i aştığı gözlemlenmiştir. Polonya ve Moldova için ise $0,5 \text{ mSv}$ ile 1 mSv arasında doz değerleri hesaplanmıştır.

Kaza sonrasındaki ilk yıl için Türkiye’de yaşayan yetişkin insanlar için yapılan doz hesaplarına göre; Birleşmiş Milletler Atom Enerjisi Komisyonu (UNSCEAR) yaklaşımına göre yıllık $1,40 \times 10^{-4}$ mSv ve $1,15 \times 10^{-1}$ mSv, Dünya Sağlık Örgütü (WHO) yaklaşımına göre ise yıllık $9,36 \times 10^{-5}$ mSv ile $7,56 \times 10^{-2}$ mSv arasındadır. Bu iki yaklaşım arasında %66 ile %77 arasında değişen uyumluluk mevcuttur. Sonuçlar incelendiğinde Dünya Sağlık Örgütü raporu ile de uyumlu olarak, yer yüzeyi aktivitesinden kaynaklanan doz değerlerinin diğer bileşenlere göre daha yüksek oranda olduğu görülmektedir. Yeryüzeyi aktivitesinden kaynaklanan doz değeri toplam doz değerine göre %25 ile %100 arasında bir orana sahipken solunumdan kaynaklanan doz değerleri %1 ile %74 arasında değişmektedir. Öte yandan radyoaktif bulutun geçişi sırasında maruz kalınan radyasyon dozunun toplam doza oranı oldukça küçük olup %1’ in altındadır.

Kaza sonrasındaki ilk yılı dikkate alarak Türkiye için yapılan doz hesaplarına göre radyasyon dozu değerleri yıllık yaklaşık 0,15 ile 0,01 mSv arasında değişmektedir. En yüksek radyasyon dozu değerleri Türkiye’ nin kuzey illeri (Ardahan, Bayburt, Kastamonu), ile Orta ve Doğu Anadolu illerinde (Kars, Kırıkkale, Iğdır, Erzurum) hesaplanmıştır.

Yapılan çalışma sonucunda elde edilen doz değerleri Uluslararası Radyasyondan Korunma Komitesi (ICRP) tarafından tavsiye niteliğinde belirlenen toplum üyesi kişilerin bir yılda medikal uygulamalar dışında maruz kalabileceği doz değeri 1 mSv’in ve ICRP hesaplamalarına göre bir bireyin doğal yollardan bir yılda maruz kaldığı yıllık 4,2 mSv değerinin altındadır. Ancak bu çalışma sırasında elde edilen doz değerleri kişilerin beslenme yoluyla alabilecekleri dozu kapsamamaktadır. Bu yolla alınabilecek doz değerlerinin hesaplanması bütün besin öğelerinin spektrometrik analizi ve halkın tüketim eğilimleri göz önüne alınarak yapılabileceğinden bu çalışmanı kapsamı dışında kalmaktadır.

Günümüzde operasyon halindeki nükleer santrallerin büyük çoğunluğu Türkiye’ye yakın olan Avrupa ve eski Sovyet Sosyalist Cumhuriyetler birliği toprakları içinde yer almaktadır. Özellikle sınırimıza 16 km uzaklıkta olan Metsamor Nükleer Güç Santrali eski Rus teknolojisi olmasına ve sismik açıdan riskli bir alanda olmasına rağmen işletme halindedir. Ayrıca her ne kadar yeni nesil reaktörler arttırılmış güvenlik önlemlerine sahip olsalar da Fukushima Nükleer Santral kazası gibi beklenmeyen ve sıradışı kazalar meydana gelebilmektedir. Bütün bunlar gözönüne alındığında bu çalışmada kullanılan yöntemin, herhangi bir nükleer santral kazası sonrasında acil müdahale ve önlem amaçlı kullanıma uygun olduğu görülmektedir.

1. INTRODUCTION

With the increasing need of energy, due to the decrease in amount and increase in costs of fossil fuels, alternative energy sources are needed. Nuclear energy is one of the alternatives. As of March 11, 2014 there are 435 nuclear power plant units in operation with an installed electric net capacity of about 372 GW in 31 countries and 72 plants are under construction with an installed capacity of 68 GW in 15 countries. And for the date January 2012 there is a total of 187 nuclear power plant units in Europe (five of them in the Asian part of the Russian Federation) and 18 units were under construction in six countries (Url-1). According to the 2012 projections (IAEA-RDS-1/32, 2012), the global installed nuclear power capacity expanded from 369 gigawatts electrical output (GW(e)) at the end of 2011 to 456 GW(e) in 2030, i.e. a decrease of 9% compared with previous projection. Nuclear power plants provide an alternative energy source with low level emissions of greenhouse gases (GHG), as carbon dioxide (CO₂). IAEA Report on CO₂ emissions by power source mentions that nuclear power does not generate carbon dioxide from spent fuels. Also CO₂ emissions from uranium mining and enrichment, as well as carbon emissions from the processes of plant operation and dismantling, is only 1-2% of that of other fossil fuels and it is either equal to or even lower than that of other renewables. On the other hand the level of radioactivity around research or power reactors is an important safety concern (Sadeghi and Sadrnia, 2011). Due to the inevitable presence of personnel within the site and the population outside the site, radioactivity should be monitored frequently and properly. Besides, accidents occurred at power plants had shown that results were harmful for not only the power plants environment but also for the entire world. The attention on nuclear reactor accidents increased again after the Fukushima Dai-ichi Nuclear Power Plant (FNPP) accident, happened in Japan on 11 March 2011 and caused by a tsunami following 9.0 magnitude earthquake. Radioactive materials were emitted into the atmosphere and transferred to the land and ocean through wet and dry deposition (Povinec et al., 2013). FNPP accident was not the first nuclear reactor accident ever happened. The accident at the

Chernobyl Power Plant (CNPP) that occurred on 26 April 1986 was the most severe accident ever to occur in the nuclear power industry. The reactor was destroyed in the accident and considerable amounts of radioactive material were released to the environment (Url-2). Considerations between CNPP and FNPP accidents show that the consequences of the CNPP accident clearly exceeded those of the FNPP accident. In both accidents, most of the radioactivity released was due to volatile radionuclides (noble gases, iodine, caesium, and tellurium). However, the amount of refractory elements (including actinides) emitted in the course of the CNPP accident was approximately four orders of magnitude higher than during the FNPP accident (Steinhauser et al., 2014). The definition of the magnitude of a nuclear reactor accident is done by the most severe NPP disasters, defined as International Nuclear Event Scale (INES). This scale depends on many factors such as reactor type, capacity and fuel (and burn-up of the fuel). While Three Mile Island (Pennsylvania, United States) accident in 1979 was categorized as an INES level 5 accident, FNPP and CNPP were categorized as an INES level 7 accidents (Lelieveld et al., 2012).

1.1 Motivation

People, animals and environment are exposed to ionizing radiation due to the released radioactive gases and particles. Ionizing radiation has harmful effects on health including causing cancer and mortality. Total exposure is generally separated into external and internal exposure. External exposure is determined by the radionuclides deposited on the ground and suspended in the atmosphere, the dose due to radionuclides suspended in the atmosphere is commonly called cloud gamma dose. The internal exposure is the one determined by inhalation from air and ingestion from food of radioactive material, caesium-137 (^{137}Cs) is the main source of the internal and external exposure of the population for long term after a nuclear power plant accident due to its long half life. Belarus, the Russian Federation and Ukraine were the most effected countries because of the CNPP accident. Up to the year 2005 more than 6,000 cases of thyroid cancer were reported in children and adolescents who were exposed at the time of the accident, and more cases can be expected during the next decades. Furthermore after CNPP accident the released radionuclides were measurable in all countries of the northern hemisphere (Url-3).

The CNPP accident in 1986 deposited ^{137}Cs along with other radioactive debris over large parts of Europe. The European Commission coordinated a study to create the “Atlas of ^{137}Cs deposition over Europe after the CNPP accident” (de Cort et al., 1998). The Atlas provides estimates of ^{137}Cs deposition only for the European side of Turkey, which represents only a small fraction of the entire Turkish territory, and based only on one soil sample. Previous studies showed that after CNPP accident emitted radioactive cloud caused deposition of radioactive material in Turkey, especially over Thrace and the Eastern Black Sea regions (e.g., Cetiner and Ozmen, 1995).

Beside on-site studies (in situ and laboratory measurements) also modeling studies of distribution and deposition of radionuclides after such accidents have been widely used (e.g. Schöppner et al., 2012). The first modeling study simulating the atmospheric dispersion and deposition of radionuclides over Turkey after the CNPP accident was conducted by Kindap et al. (2009). The study remarked, contrary to public opinion, that northern parts of Turkey were mostly affected by the CNPP accident; Marmara Region, the Aegean Region, and even the Central Anatolian Region were influenced as well.

1.2 Purpose

The release of radioactive material after CNPP accident affected almost all Northern Hemisphere (OECD/NEA, 2002). The main objectives of this study are:

1. to model ^{137}Cs dispersion and deposition by using available information about the accident;
2. to estimate in particular ^{137}Cs deposition and air concentrations over the Anatolian peninsula, to close a historic gap in the “Atlas of Caesium deposition over Europe after the CNPP accident”;
3. to estimate radiological doses for Europe and Turkey by using simulation results as illustrated in Figure 1.1.

Meteorological conditions and dispersion of radionuclides were simulated by using the WRF meteorological model and the HYSPLIT dispersion model. Due to the large

uncertainty related to the temporal and vertical distribution of the emitted radioactive material (Evangelidou et al., 2013), four different source distributions, average constant emissions at constant altitude and three different time and vertical profiles used in recent studies were tested. Radiological doses from simulated air concentrations and deposition has been estimated for Europe and Turkey according to two separate methodologies based on the UNSCEAR (1998) and WHO (2012) reports, respectively.

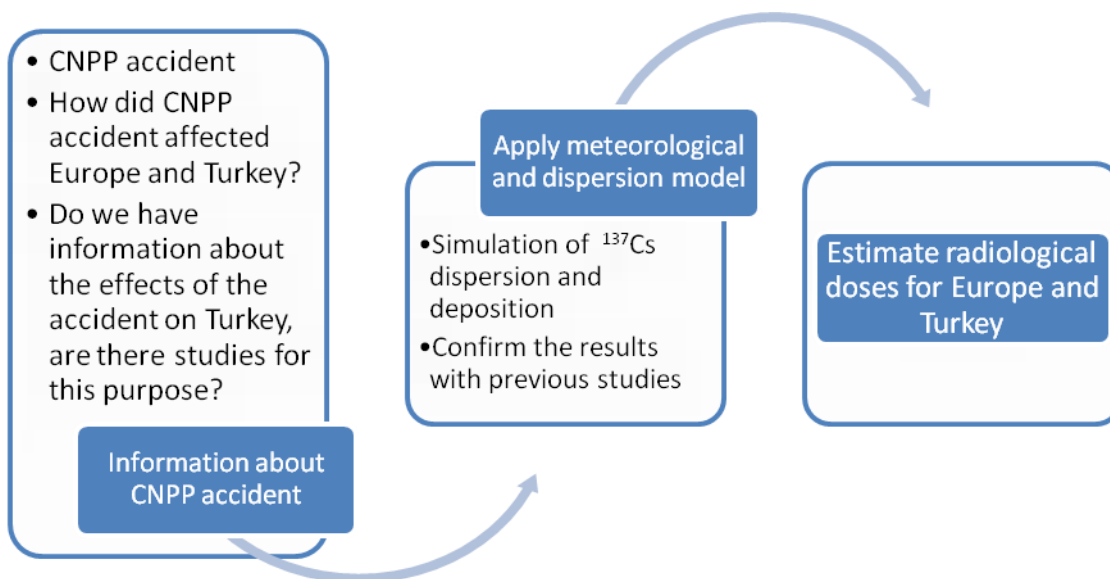


Figure 1.1: Purpose diagram of the thesis.

2. LITERATURE REVIEW

2.1 Overview of the Chernobyl Nuclear Power Plant Accident

2.1.1 Chernobyl Nuclear Power Plant

The CNPP is located at northwest of the city of Chernobyl, Ukraine and 16 km's away from the Ukraine–Belarus border. Reactor was consisted of four nuclear reactors of the RBMK-1000 design, units 1 and 2 being constructed between 1970 and 1977, while units 3 and 4 of the same design were completed in 1983 (Url-8). Figure 2.1 shows the CNPP before the accident.

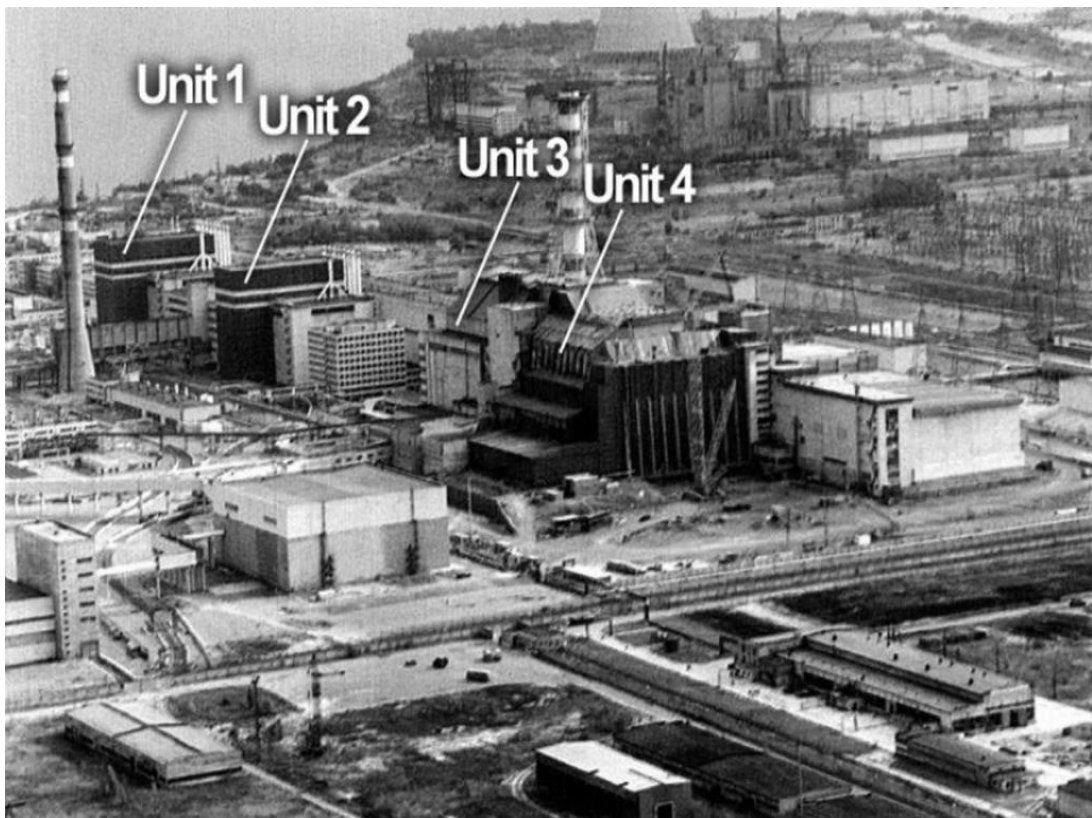


Figure 2.1: Chernobyl Nuclear Power Plant before the accident (Url-8).

2.1.2 RBMK-1000 design nuclear reactors

The RBMK-1000 (Figure 2.2) is a Soviet designed and built graphite moderated pressure tube type reactor, using slightly enriched (2% ^{235}U) uranium dioxide fuel. It is a boiling light water reactor, with direct steam feed to the turbines, without an intervening heat-exchanger. As seen in Figure 2.2 water pumped to the bottom of the fuel channels boils as it progresses up the pressure tubes, producing steam which feeds two 500 MWe [megawatt electrical] turbines (Url-9). At 31 December 2012 there were 12 RBMK-1000 type nuclear reactors (11 in operation and 1 was under construction). All these reactors belong to Russia (IAEA-RDS-2/33, 2013).

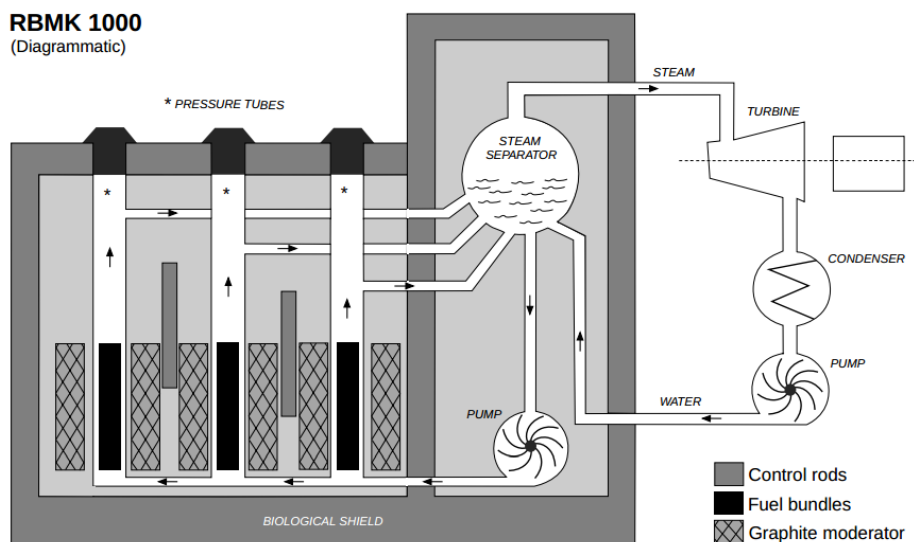


Figure 2.2: RBMK-1000 nuclear reactor design (OECD/NEA, 2002).

2.1.3 The Chernobyl Nuclear Power Plant accident

The accident happened at CNPP was at reactor unit 4. The accident occurred at 01:23 AM on Saturday, 26 April 1986. The reason of the accident was the scheduled tests of power supply mode in case of external sources loss. Despite constructional and physical characteristics of RBMK-1000 reactor did not allow the staff to effectively control its work at such low capacity, the CNPP staff lowered the reactor capacity down to inadmissible low level (20% from the nominal capacity). With sharp increase in reactivity, reactor power growth and the reactor overheated. This caused intense generation of steam and two explosions destroyed the core of Unit 4 (Figure 2.3) and the roof of the reactor building (Kortov and Ustyantsev, 2013 and Mould,

2000). The two explosions sent fuel, core components and structural items and produced a shower of hot and highly radioactive debris, including fuel, core components, structural items and graphite into the air and exposed the destroyed core to the atmosphere (OECD/NEA, 2002). For the following 10 days, the explosions and fire continued. Also the melt of reactor core resulted with the release and deposition of radioactive particles to the environment.

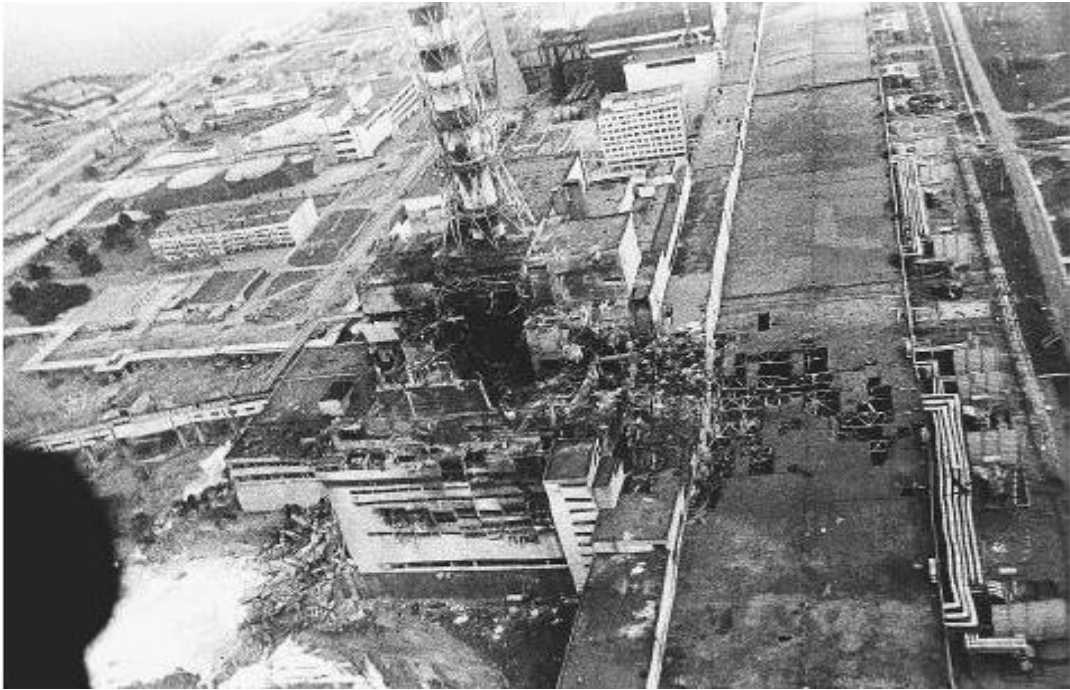


Figure 2.3: Chernobyl Nuclear Power Plant after accident (Url-8).

2.1.4 Source term and releases from the reactor

After a nuclear power plant accident to have information about releases to environment, the technical expression ‘source term’ is used. The source term is defined as the magnitude, composition, form (physical and chemical) and mode of release (puff, intermittent or continuous) of radioactive elements (fission and/or activation products) released during a reactor accident (IAEA SRS53, 2008).

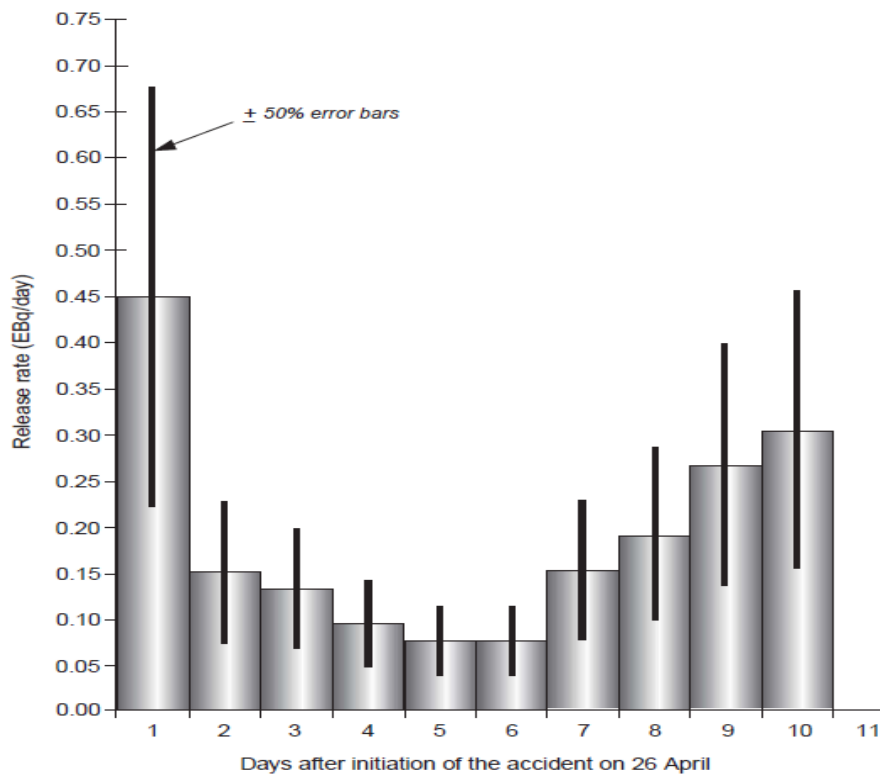


Figure 2.4: Daily release rate of radioactive substances into the atmosphere (OECD/NEA, 2002).

Source term is important to assess the magnitude of the accident and radiological doses received by the general populations (Thakur. et al., 2013). After CNPP accident main releases occurred during first 10 days of the accident. At the first days of the accident, with the affect of the explosions the emissions occurred at relatively high altitudes and were larger due to the mechanical fragmentation of the fuel. According to Waight et al. (1995) it mainly contained the more volatile radionuclides such as noble gases, iodine and some caesium. The second large release in the end of this period was caused by the high temperatures reached in the core melt (Evangelidou et al., 2013).

First estimations about radionuclide amount released to the atmosphere were done by Soviet scientists based on deposited radionuclide data only on the territory of Soviet Union since there was not any data available for Europe and elsewhere then. Soviet scientist's estimations about releases were presented at the IAEA Post-Accident Assessment Meeting in Vienna in 1986. Their estimation was that 100% of the core inventory of the noble gases (xenon and krypton) was released, and between 10% and 20% of the more volatile elements of iodine, tellurium and caesium. The early estimate for fuel material released to the environment was $3 \pm 1.5\%$ (UNSCEAR, 2000).

Table 2.1 Current estimate of radionuclide releases during the CNPP accident.

Radionuclide	Radioactive half-life	Core inventory (PBq)	Activity released (PBq)
Noble gases			
⁸⁵ Kr	10.7 a	33	33
¹³³ Xe	5.25 d	6500	6500
Volatile elements			
¹³² Te	3.26 d	4200	1040
¹³¹ I	8.04 d	3200	1760
¹³³ I	20.8 h	4800	910
¹³⁴ Cs	2.06 a	170	54
¹³⁷ Cs	30.0 a	260	85
Intermediate			
⁹⁰ Sr	29.1 a	220	10
¹⁰³ Ru	29.3 d	3800	>168
¹⁰⁶ Ru	368 d	850	>73
Refractory (including fuel particles)			
⁹⁵ Zr	64.0 d	5800	196
¹⁴⁴ Ce	39.3 d	3900	116
²⁴⁰ Pu	368 d	0.96	0.03

Table 2.1 shows the estimated inventories and releases of some of the radionuclides involved in the CNPP accident on 26 April 1986 based on Sichert et al., 1994, Belyaev et al., 1991, Begichev et al., 1990, Buzulukov et al., 1993, Devell et al., 1996, Dreicer et al., 1996, Kruger et al., 1996, OECD,1995 (Bennett et al., 2000).

On the other hand modeling studies had been done to simulate the accident scenario and to estimate the emission amounts of radionuclides. The facts that the exact emission values for CNPP are still not known (50 % uncertainty of the emissions) and there is heterogeneity of measurements (Evangelidou et al., 2013), there can be large differences between simulated and observed radionuclide activities.

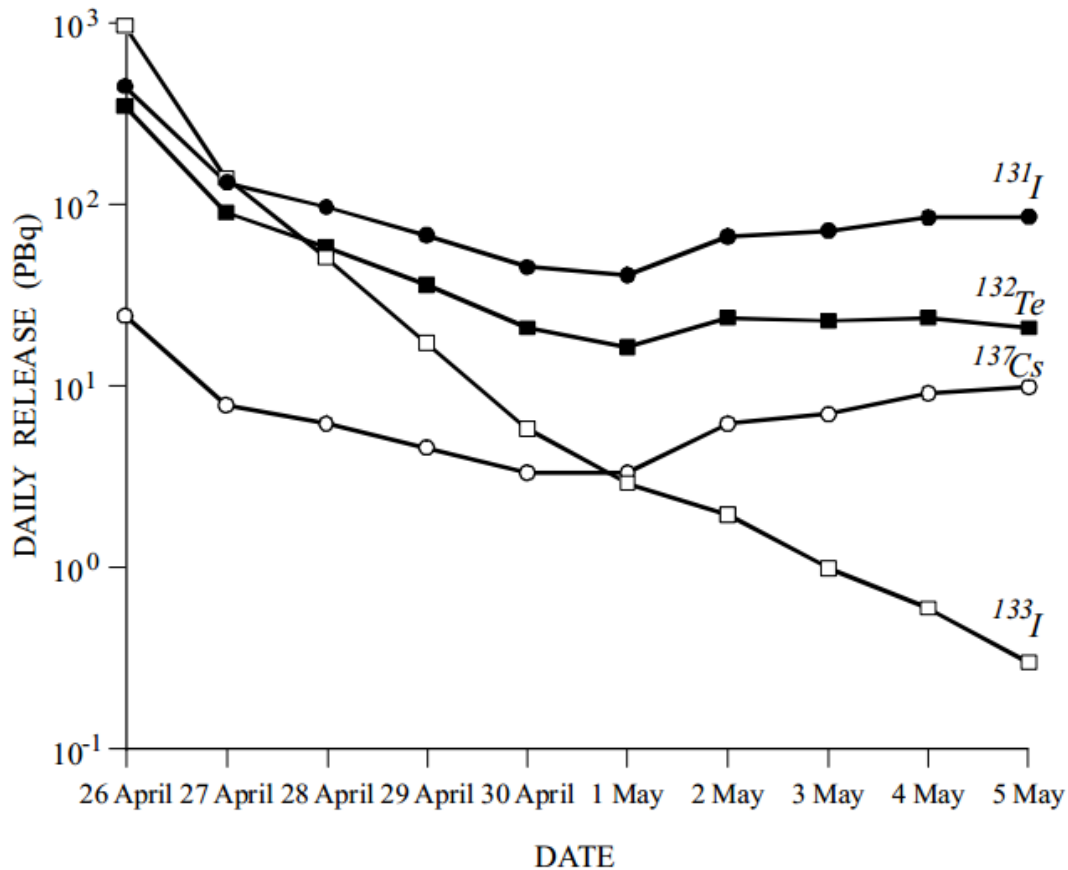


Figure 2.5: Daily releases of iodine-131, iodine-133, tellurium-132 and caesium- 137 from the CNPP (OECD/NEA, 2002).

The radionuclides which are volatile are presented in Figure 2.5. Since these radionuclides can travel long distances after a nuclear accident depending on the atmospheric conditions, their release amounts are important also for people living far from the location of the accident. From the radiological point of view, the releases of ¹³¹I and ¹³⁷Cs, estimated to have been 1,760 and 85 PBq, respectively, are the most important to consider as they can travel long distances and their impacts on human health (Burton et al., 2000). For short time after accident (days and week) iodine compounds are the main cause of the radiation doses, whereas the effects of caesium compounds can be relevant for several decades.

2.1.5 The Atlas Project: Caesium-137 Contamination of Europe after the Chernobyl Accident

After CNPP accident many of studies involving radioactivity measurements have been done and still many of studies are carried on. Above all European

Commission's 'The Atlas Project: Caesium-137 Contamination of Europe after the Chernobyl Accident' is the main reference study for Europe. Since ^{137}Cs has long life and widely dispersed across the continent, the European Commission accepted a proposal on a joint study to compile "The Atlas of caesium contamination of Europe after the Chernobyl accident". The goals of the Atlas were:

- Providing generalized and detailed information on the distribution of ^{137}Cs in soil and the total amount of ^{137}Cs deposited over the whole European territory, and separately by countries.
- Making an estimation for external gamma dose because of ^{137}Cs from the CNPP accident
- To familiarize the general public, governmental and municipal bodies with a comprehensive view of the pattern of caesium-137 across the whole of the European continent.

Atlas was compiled under the Joint Study Project (JSP6) of the CEC/CIS Collaborative Programme on the Consequences of the CNPP accident. It summarizes the results of numerous investigations undertaken throughout Europe to assess the ground contamination by caesium-137 after CNPP accident (Izrael et al., 1996). The Atlas was based on radiological data provided by participating scientific institutes and competent authorities of more than thirty European countries and have been integrated in an information platform by the CEC Joint Research Centre Ispra (JRC-Ispra, EC), Roshydromet (Moscow, Russia), the Institute of Global Climate and Ecology (Moscow, Russia), the Committee for Hydrometeorology (Minsk, Belarus) and Minchernobyl (Kiev, Ukraine) (Url-4). Atlas resulted with ^{137}Cs deposition data and deposition maps at national and international level. Figure 2.6 shows the ground deposition of ^{137}Cs in Europe after the CNPP accident (De Cort et al., 1998) which was created in this study. Atlas estimates a total 64 PBq deposited activity for Europe (land mass). And the deposition amounts were estimated between 2 kBq/m² and larger than 1480 kBq/m². The values smaller than 2 kBq/m² are thought to be because of past nuclear weapons testing. The data used in the Atlas were obtained by measurements of soil sample activity, measurement done by airborne gamma surveys, in situ measurements of gamma dose rates and spectrometry, measurements of soil profiles (often to different depths).

The number of data used in compiling the maps are indicated in Table 2.2. They do not, however, necessarily represent the actual number of measurements for some countries especially like Belarus and Ukraine as the reported data are often aggregates of many measurements (eg, to be representative of particular settlements) made in more extensive monitoring campaigns. Also the values for same location were averaged by the project staff, after orrection for radioactive decay. Airborne gamma spectrometry was used for those regions exhibiting the highest density of data (eg, Russian Federation, Sweden, limited areas in the UK) (De Cort et al., 1998).

Table 2.2: Summary of deposition measuring techniques and data (De Cort et al., 1998)

Country	Surface (1000 km ²)	Number of data used ⁽¹⁾	Type of Sampling	Soil depth (mm)	Modifications made to the reported data ⁽²⁾
Austria	83.9	1780	SAL	30-400	
Belarus	208	19058	SAL	200	
Belgium	30.05	11	SAL	20	
Croatia	56.5	4	SAL	50-100	
Czech Republic	78.9	776	SAL	30	correction to include global fallout: (Reported level -0.5) × 1.25 + 2.8 kBq/m ²)
Denmark	43.1	15	SAL	100	
Estonia	45.1	111	AGS	na	
	337	851	MGS	na	
Finland		8	SAL	50	
France	544	35	SAL	ni	
Germany	366	1371	SAL	50-200	
Greece	132	1931	SAL	10.2	
Hungary	93.0	86	FGS	na	
Ireland	68.9	342	SAL	50, ni	
Italy(3)	280	436	SAL	ni, 150	
Latvia	63.7	153	AGS	na	
Lithuania	65.2	90	SAL	na	
Luxembourg	2.59	15	SAL	60-110	
Moldova	33.7	64	AGS	na	
Netherlands	41.2	84	SAL	50	
Norway	324	448	SAL	40	
Poland	313	299	SAL	100	
Romania	238	201	SAL	150	
Russia (European part)	3.8	176971	SAL	150-300	
			AGS	na	

Table 2.2 (continued): Summary of deposition measuring techniques and data (De Cort et al., 1998)

Slovak Republic	49.0	411	SAL	30	correction to include global fallout: (Reported level - 0.5) × 1.25 + 2.8 kBq/m ²
Slovenia	20.03.2014	57	SAL	120	
Spain	505	31	SAL	ni	
Sweden	450	135848	AGS	na	1.6 kBq/m ² added to correct for global fallout
Switzerland	41.3	190	SAL	150-200	
			FGS	na	
Turkey (European part)	24	1	SAL	10	
Ukraine	604	11569	SAL	200	
			AGS	na	
United Kingdom	245	395	SAL	50-150	reselection of original data over
		45891	AGS	na	1 kBq/m ²

SAL: soil sample analysis in laboratory
 FGS: field (in-situ) gamma-spectrometry
 MGS: mobile gamma-spectrometry
 AGS: airborne gamma-spectrometry
 ni: no information
 na: not applicable

⁽¹⁾ Some of these data represent aggregated values obtained from more than one measurement; many of the data for Belarus and Ukraine represent aggregated values obtained from several thousands of original measurements

⁽²⁾ Corrections in agreement with the data provider

⁽³⁾ Excluding Sicily

Collected data were used for compiling the maps of total deposition of caesium-137 for European countries (with a few exceptions where insufficient data were available). Figure 2.6 illustrates the deposition levels of caesium after CNPP accident. In several countries outside the former Soviet Union the level 40 kBq/m² (1.08 Curie (Ci)/km²) is exceeded. Areas where deposition exceeds 1480 kBq/m² (40 Ci/km²) are confined to Belarus, Ukraine and Russia. In zones where the deposition level is less than 40 kBq/m² (1.08 Ci/km²), the annual average dose (in 1998) will, with a very high degree of confidence, not exceed 1 mSv (100 millirem (mrem)); this level of dose is adopted by the authorities of Belarus, Russia and Ukraine as a

threshold for taking counter-measures and introducing privileges for the affected population.. In Eastern Europe these levels are found mainly in flat areas while, in Western Europe, they are found largely in mountainous areas. Some spots were formed in precipitation zones, some in regions with increased break of the relief or on mountain slopes blocking or cutting the dispersing radioactive plumes (De Cort et al.,1998).

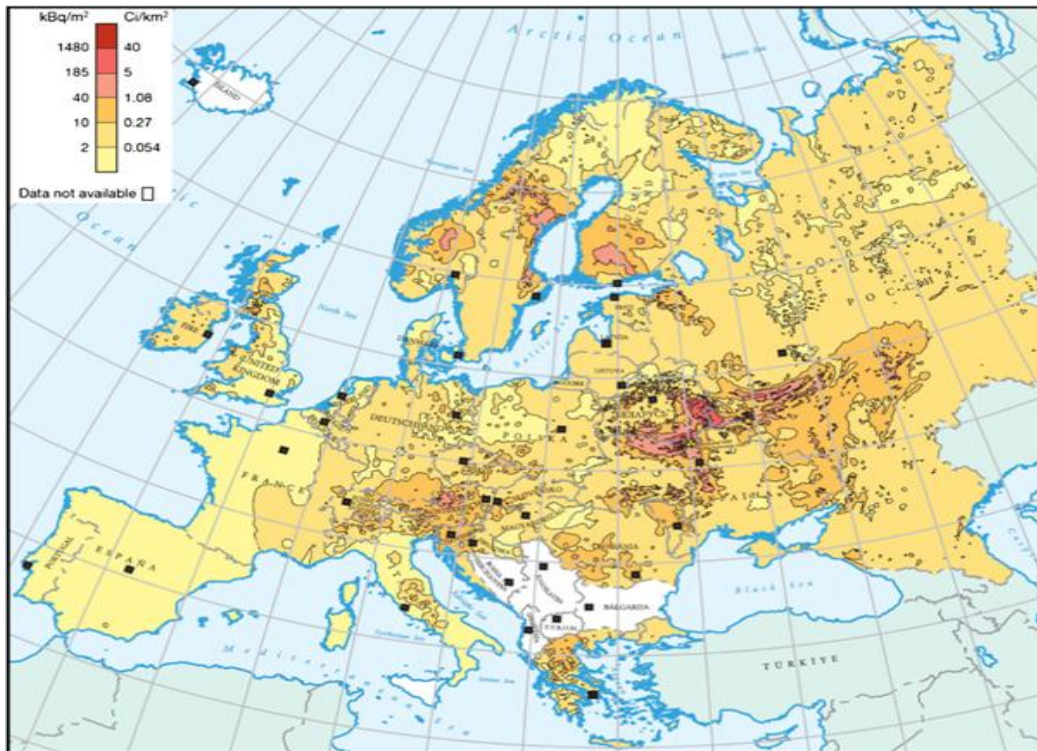


Figure 2.6: Ground deposition of ^{137}Cs in Europe after the CNPP accident (De Cort et al., 1998).

2.1.6 CNPP accident and modeling studies

Since 1960s computer codes were developed and applied for rapid estimates of radioactive material dispersion after nuclear accident fallouts necessary for immediate health assessments (Moroz et al., 2010). A specific field of air quality modeling is related to risk assessment of accidental industrial releases which concerns point emissions (local in space and time) of trace species. In the late 1980s and early 1990s, considerable efforts have been devoted to the development of operational models, especially after the CNPP accident (Quélo et al., 2007). After CNPP accident many research projects have realised models and methods describing separate parts of the nuclear risk assessment problem, e.g. probabilistic safety

assessment, long-range transport and contamination modeling, radioecological sensitivity studies and dose estimation (Baklanov et al., 2007). Some examples of long-range experiments include the Cross Appalachian Tracer Experiment (CAPTEX) in 1983 (Ferber et al., 1986), the Across North America Tracer Experiment (ANATEX) in 1987 (Draxler et al., 1991), and more recently the European Tracer Experiment (ETEX) (van Dop et al., 1998) was progressed to confirm the methods of prediction models. Also studies to estimate the source term after an accident is an important study area. Models such as Flexpart (Stohl et al., 1998), AERMOD (EPA, 2011), CALLPUFF (EPA, 1995) have been extensively used in risk assessment studies to estimate the release and dispersion of radionuclides and the calculation of radiological doses.

In the frame of this thesis, three recent studies are investigated in more details. Brandt et al. (2002) developed an Eulerian Model, DREAM (the Danish Rimpuff and Eulerian Accidental release Model) to model the transport, dispersion and deposition of radioactive material from accidental releases. ^{137}Cs , ^{134}Cs and ^{131}I radionuclides deposition and concentration amounts were estimated from the CNPP accident by using different parameterizations for dry and wet deposition. It is stressed that combination of the relatively simple dry deposition scheme and the wet deposition scheme based on subgrid-scale averaging gave the best performance in reproducing the observed radionuclides deposition and air concentration. Suh et al. (2009) performed a sensitivity analysis on the CNPP accident using different parameters, (like mixing height, diffusion coefficient, etc.) using the Long-range Accident Dose Assessment System (LADAS) and compared the ^{137}Cs air concentrations recorded over Europe during CNPP accident. Evangelidou et al. (2013) performed a coupled LMDzORINCA (The aerosol module INCA (Interactions between Chemistry and Aerosols) is coupled to the general circulation model (GCM), LMDz, developed at the Laboratoire de Meteorologie Dynamique in Paris, and the global vegetation model ORCHIDEE (Organizing Carbon and Hydrology In Dynamic Ecosystems Environment) model. Model was used for simulation of the transport, wet and dry deposition of the radioactive tracer ^{137}Cs after CNPP accident. First they considered, that the altitude of the emissions after the episode assuming that the emissions occurred at the surface and at several heights. And the results of the two versions are

evaluated by using two different vertical resolutions: 19 and 39 vertical layers for the regular grid configuration.

2.2 Biological Effects of Ionizing Radiation

Following the discovery of X-Ray by Roentgen in 1895 the first case of human injury was reported in the literature just a few months later. As early as 1902, the first case of x-ray induced cancer was reported in the literature. In the following years, early human evidence of harmful effects as a result of exposure to radiation in large amounts existed in the 1920s and 1930s, based upon the experience of early radiologists, miners exposed to airborne radioactivity underground, persons working in the radium industry, and other special occupational groups. On the other hand long term effects of ionizing radiation were not understood before World War II (WU, 2006).

Ionizing radiation may be divided into directly and indirectly ionizing for the understanding of biological effects. Most of the particulate types of radiation are directly ionizing i.e. individual particles with adequate kinetic energy can directly disrupt the atomic structure of the absorbing medium through which they pass producing chemical and biological damage to molecules. These are alfa (α) and beta (β) particles. In contrast, electromagnetic radiations, namely, X and γ rays, are indirectly ionizing because they do not produce chemical and biological damage themselves but produce secondary electrons (charged particles) after energy absorption in the material. Figure 2.7 that was adapted from Hall and Giaccia, (2006) shows direct versus indirect action of ionizing radiation. Ionization is the process of removing one or more electrons from atoms by the incident radiation leaving behind electrically charged particles (an electron and a positively charged ion), which may subsequently produce significant biological effects in the irradiated material. The ionized or excited atom or molecule may either fragment producing free radicals or return to the parent state. If the energy transferred by ionizing radiation to the atom is insufficient to eject orbital electrons, the electrons may be raised from lower to higher orbitals and the atom is said to be excited. (IAEA, TCS42, 2010)

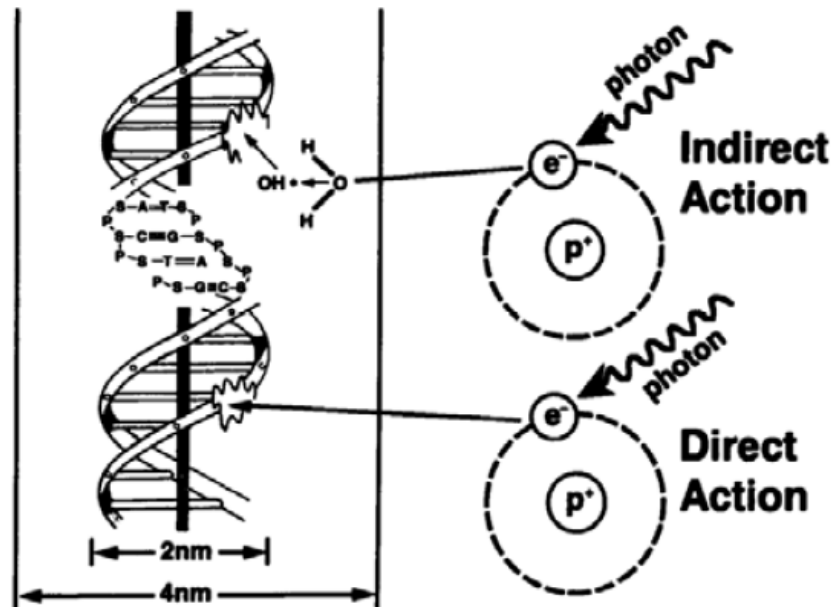


Figure 2.7: Direct vs. indirect actions of ionizing radiation (Hall and Giaccia, 2006).

The atoms of the tissue may be ionized or excited when radiation passes through it. This may cause a change in the structure of the cell and result in damage to the cell. In particular, the genetic material of the cell, the DNA may be changed. Two categories of radiation-induced injury are recognized: deterministic (non-stochastic) and stochastic effects (Magill and Galy, 2005).

Before explaining deterministic (non-stochastic) and stochastic effects we should have a look at the mechanism of cell and radiation interaction. Trapp and Kron (2008) had classified radiation effects in biological matter into three phases:

- 1- The physical phase; includes actual interaction of radiation with matter and the formation of radicals. This can cause indirect radiation damage to cell.
- 2- The chemical phase, when lesions in the DNA may accumulate and enzyme reactions take place. Also some fast and simple repair processes take place
- 3- The biological phase, which encompasses the remainder of the repair process, further cell divisions, mitotic death, apoptosis, and, finally effect on organs and carcinogenesis (Trapp and Kron, 2008).

The structure of the cell may change directly by ionization or indirectly by future changes by transfer of the energy to the medium. Direct effects occur in the DNA in the form of single-strand or double-strand breaks in the molecule. The long term effects include a variety of recombinational changes as well as cross-links,

alterations in sugar and base fractions, base substations, deletions etc. Chromosomal aberrations are a result of DNA variations (ICRP 60, 1990).

Deterministic effects occur when radiation dose kills the cell. Also there is a dose threshold where no effect is observed. Above this threshold the severity of the harm increases with dose. The effect is specific for a particular type of tissue. The actual threshold dose also depends on dose delivery mode, with single exposures being, typically more detrimental than protracted exposure. In general, deterministic effects are of primary concern at high radiation dose levels (Trapp and Kron, 2008). The examples for effect on the CNPP accident of deterministic effects are;

- Erythema (reddening of the skin)
- Epilation (loss of hair)
- Depression of bone marrow cell division (observed in counts of formed elements in peripheral blood)
- NVD (nausea, vomiting, diarrhea), often observed after an exposure to radiation Central nervous system damage
- Damage to unborn child (physical deformities, microcephaly, mental retardation)

One important deterministic effect is death. This results from damage to bone marrow (first), then to the gastrointestinal tract, and then to the nervous system. Also these may be referred to 'Acute Radiation Syndrome' (Stabin, 2008).

The damage of the radiation may not appear for years and to understand the connection of abnormality with the exposure to radiation may be impossible. The predictions on the number of the organisms can be done in case of a large number, but the effect cannot be predicted with certainty for any particular individual. This kind of effect is called stochastic. Stochastic effects of radiation is classified as somatic and genetic (Wootton, 1993). There are main differences between deterministic and stochastic effects. There is not a threshold radiation dose for stochastic effect. And it is possible that the effect is related to radiation exposure and as the dose increase the probability of the damage increases. When talking about stochastic effects there is no doubt that the most serious result is cancer. The relationship between radiation and cancer is well established. Studies on exposure of large populations (the most important one of these studies is the population of

survivors of the Japanese nuclear bomb attacks) and on animals have established this relationship, including leukemia, bone cancer, lung cancer (mainly from radon), thyroid cancer (for example ^{131}I related after CNPP accident) and hereditary effects. The hereditary effects have not been demonstrated in human populations including Japanese bomb survivors, medical populations, and populations affected by CNPP disaster (Stabin, 2008).

2.3 Pathways of Released Radioactive Material to the Environment and to the Human Body

‘An accidental release of radioactive substances from a nuclear plant has a great potential to affect the health of people living in the surroundings of the plant’ (Schnadt and Ivanov, 2012). After the release of radioactive material to the atmosphere, it is transported to the environment and to human body by different pathways. This occurs by air, water (groundwater and surface water), and the food chain. Particles released to the atmosphere, may land in water, on soil, on surfaces. Human activities; eating, drinking, inhalation, or by absorption through the skin result the entrance of radionuclide's to the body. Inhalation of radionuclides suspended in the air (at the moment of release or after resuspension from contaminated surfaces), ingestion of contaminated food (by air, by soil, by ground water), drinking contaminated water (by air, by soil, by ground water) or skin contamination (by air, by water) results the radiation dose of body. Figure 2.8 shows the radioactive materials contamination pathways in the environment and human body.

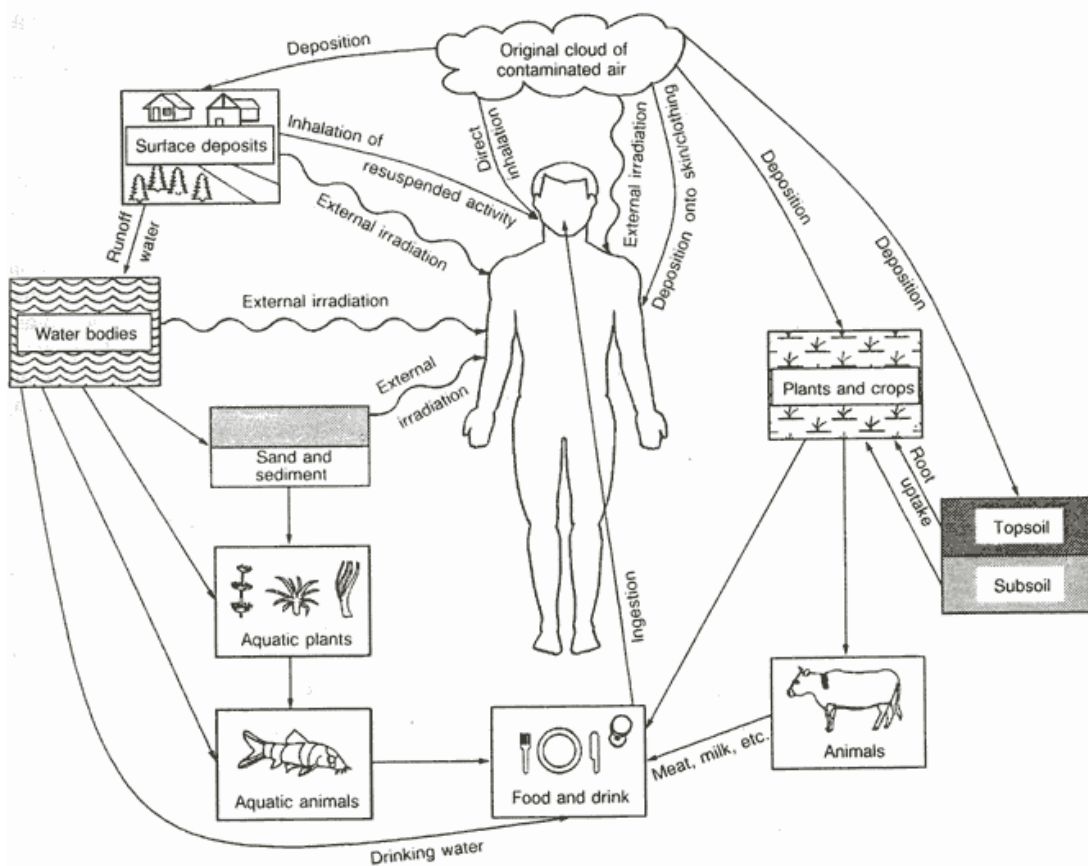


Figure 2.8: The pathways of radionuclides to the body (Url-7).

2.3.1 ^{137}Cs and its effects on the body

Cesium-137 is a man-made radionuclide produced through nuclear fission with a 30.1-year half-life. Since it has a long life time, ^{137}Cs is the main source of the internal and external exposure of the population after power plant accident. On the other hand it is known to migrate through soil and, depending on the mineral composition and presence of organisms such as fungi, exhibits an effective half-life that can be significantly shorter than the physical half-life (Zhdanova et al., 2005; Pröhl et al., 2006; Steinhauser et al., 2013). It has beta radiation. After beta decay either to stable ^{137}Ba or a meta-stable form of barium ($^{137\text{m}}\text{Ba}$) occurs. The meta-stable isotope ($^{137\text{m}}\text{Ba}$) is converted to stable ^{137}Ba . At this moment gamma ray emission with the energy is 0.662 MeV released (Figure 2.9).

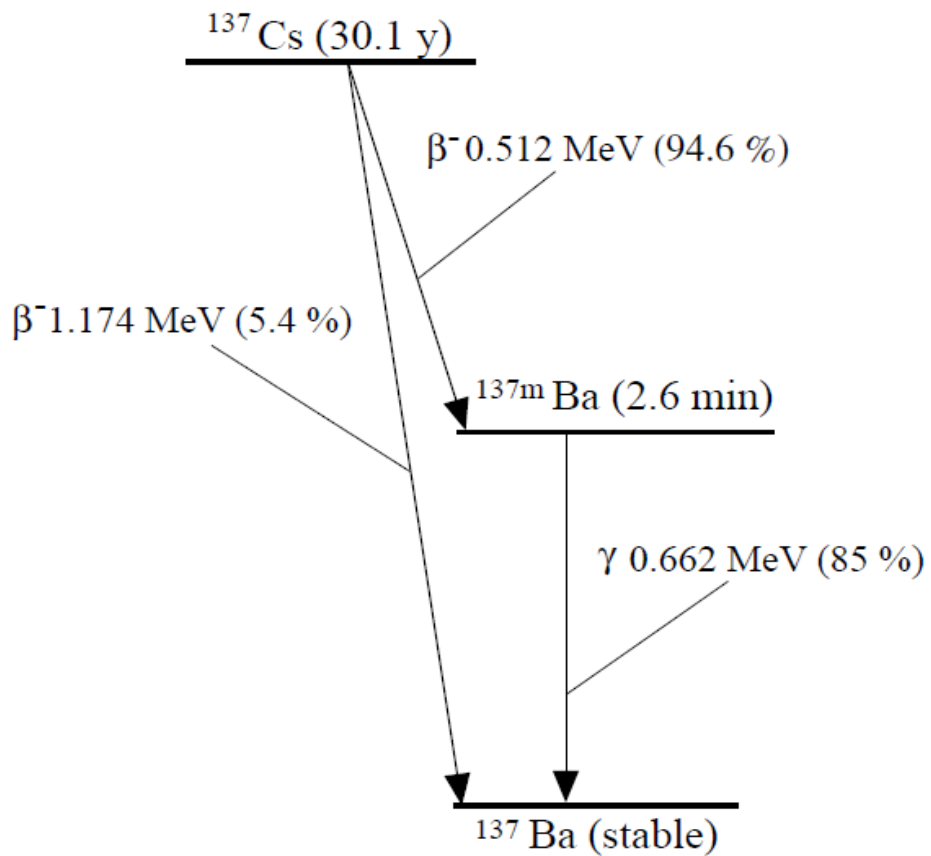


Figure 2.9: ^{137}Cs decay scheme

Caesium compounds can travel long distances in the air before being brought back to the earth by rainfall and gravitational settling (Williams et al., 2004). From studies of ^{137}Cs present in food chains, the biological half-time of this radionuclide found to vary from 15 ± 5 days in infants to 100 ± 50 days in adults (McCraw (1965), NCRP (1977)). In case of inhalation or ingestion ^{137}Cs is distributed to whole body. Reports from Japan and the U.S. indicated concentrations of ^{137}Cs in muscle and bone comparable to, or even greater than, those in the same individual (McCraw, 1965, NCRP 1977, Yamagata et al. 1960).

2.3.2 Radiation doses and health effects after CNPP accident

‘Most of the population of the Northern hemisphere was exposed, to various degrees, to radiation from the CNPP accident’ (OECD/NEA, 2002). CNPP accident affected three major groups of individuals including the workers involved in the actions during the accident or in the mitigation of the aftermath, those individuals who lived close to the vicinity of the accident and were evacuated after the accident, and those

who continued to reside in the contaminated areas further from the CNPP. The estimation of radiation health effects after CNPP is particularly important for these groups (Saenko et al., 2011). Both the workers and the general public resulted or still can result in adverse health effects due to radiation exposure from CNPP accident (IAEA, 2006). Initially an estimated 350000 emergency and recovery operation workers, including army, power plant staff, local police, and fire services, than 600000 registered ‘liquidators’ were involved in containing and cleaning up the accident in 1986–87. The number of the people living in areas of Belarus, Russia, and Ukraine that are contaminated with radionuclides due to the CNPP accident (above 37 kBq/m² or 1Ci/km² of ¹³⁷Cs) is approximately 5 million. Approximately 400000 people lived in the more contaminated areas – classified at the time by Soviet authorities as ‘areas of strict radiation control’ (above 555 kBq/m² or 15 Ci/km² of ¹³⁷Cs), 115000 of these people were evacuated in the spring and summer of 1986 from the area surrounding the CNPP (designated the ‘Exclusion Zone’) to non-contaminated areas. Another 220000 people were relocated in subsequent years (Balonov and Bouville, 2011). Workers and people living close to CNPP site were affected by the gamma radiation just after the accident and following days. The dose rates at 6th May 1986 were the following:

- 12 Gy/h (Gray/h) at distance of 150 m away from the reactor;
- in Pripyat (the closest town in Ukraine to the CNPP) 10 mGy/h in the air, up to 600 mGy/h on roads asphalt, and up to 200 mGy/h in soil.

Three months later (26th July 1986) the dose rate at distance of 150 m away from the ruins of the 4th Unit of CNPP was more than 3 Gy/h. (Kortov et al., 2013). Although some studies are difficult to interpret because of methodological limitations, recent investigations of CNPP clean-up workers (‘liquidators’) have provided evidence of increased risks of leukemia and other hematological malignancies and of cataracts, and suggestions of an increase in the risk of cardiovascular diseases, following low doses and low dose rates of radiation (Cardis and Hatch, 2011).

According to Moller and Mousseau (2006) and Zakharov and Krysanov (1996), the long-term health and environmental consequences of the CNPP catastrophe are not yet fully reported despite 23 years of research (Svendsen et al., 2010). Estimations for the average effective doses (which characterizes the overall health risk due to any combination of radiation) for the general population of ‘contaminated’ areas

accumulated in 1986–2005 were estimated to be between 10 and 30 mSv in various administrative regions of Belarus, Russia and Ukraine. In the areas of strict radiological control, the average dose was around 50 mSv and more (Kinley and Diesner-Kuepfer, 2008). Large areas of Europe were affected to some degree by the CNPP releases.

During the first few weeks after the accident, ^{131}I was the main contributor to the dose, via ingestion of milk. Infant thyroid doses generally ranged from 1 to 20 mGy in Europe, from 0.1 to 5 mGy in Asia, and were about 0.1 mGy in North America. Adult thyroid doses were lower by a factor of about 5. Later on, ^{134}Cs and ^{137}Cs were responsible for most of the dose, through external and internal irradiation. The whole-body doses received during the first year following the accident generally ranged from 0.05 to 0.5 mGy in Europe, from 0.005 to 0.1 mGy in Asia, and of the order of 0.001 mGy in North America. The total whole-body doses expected to be accumulated during the lifetimes of the individuals are estimated to be a factor of 3 greater than the doses received during the first year. (OECD/NEA, 2002)

The CNPP accident in 1986 deposited ^{137}Cs , along with other radioactive debris, over large parts of Europe. This drastically increased the ^{137}Cs concentrations found in the affected areas (Biegalski et al., 2001). Radiocaesium (^{137}Cs and ^{134}Cs) contaminated an area of more than 200000 km² in Europe (above 0.04 MBq of $^{137}\text{Cs}/\text{m}^2$) and Belarus, the Russian Federation and Ukraine were the most affected ones with 71% (IAEA, 2006). And the general public (also for Europe) has been exposed during the past twenty years after the accident both from external sources (^{137}Cs on soil, etc.) and via intake of radionuclide (mainly, ^{137}Cs) with foods, water and air. The study done by Balonov and Bouville (2011), investigates effective doses due to external (based on the numerous measurements of deposition density of ^{137}Cs and other gamma emitters, using a model of radiation transport that takes into account radioactive decay and the migration of the deposited activity to deeper layers of soil) and internal (based on estimation of separately for the inhalation and the ingestion pathways. Consumption of milk and milk products, leafy vegetables, grain products, other fruits and vegetables, and meat was considered for the ingestion pathway irradiation) for the 1986–2005 time period have been estimated for the populations of European countries by means of standard procedures as seen in Figure 2.10.

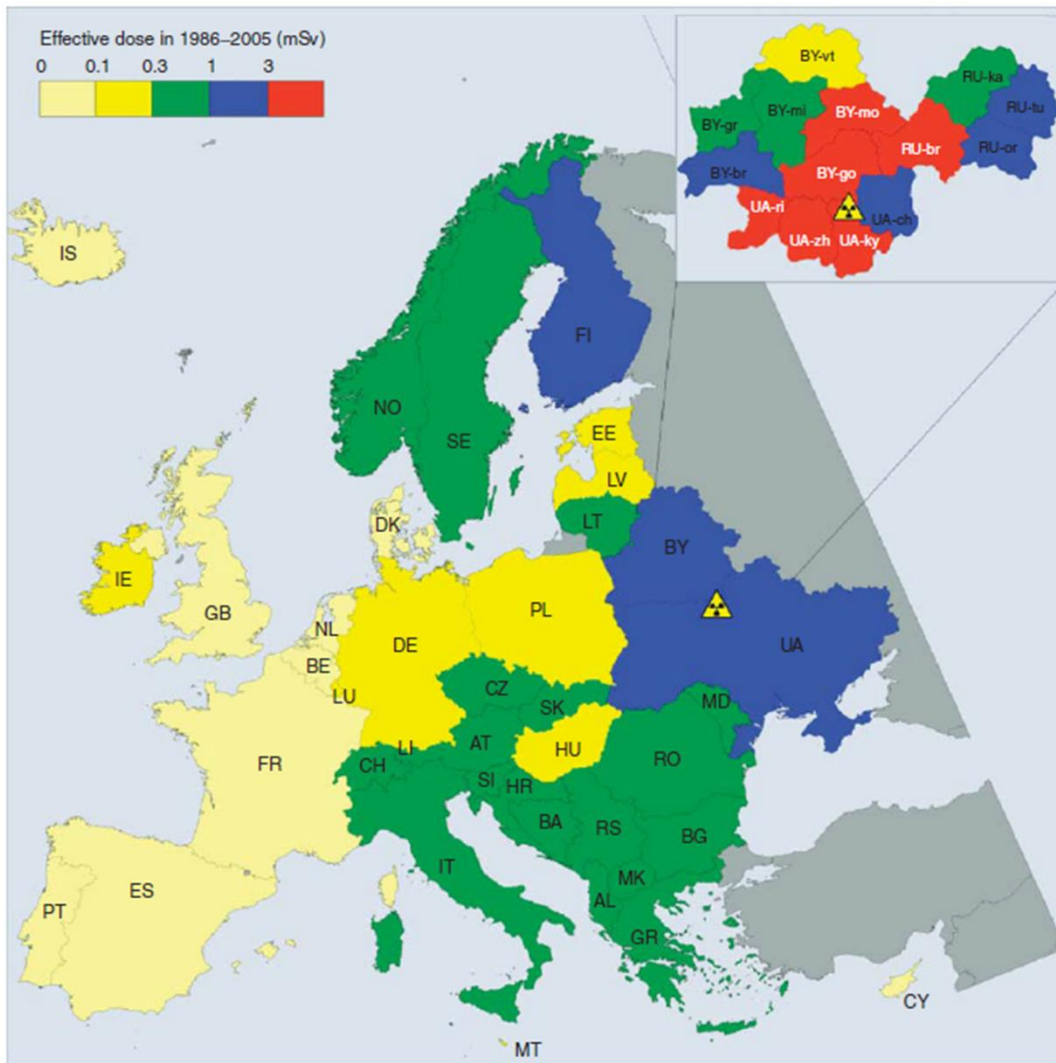


Figure 2.10: Spatial distribution of the effective doses to European populations for the 1986–05 time period. Names of countries are abbreviated according to ISO. For Belarus, Russian Federation, and Ukraine, the spatial distribution of doses is also given by oblast. The oblasts are abbreviated as follows Belarus: Brest, BY-br; Gomel, BY-go; Grodno, BY-gr; Minsk, BY-mi; Mogilev, BY-mo; Vitebsk, BY-vt; Russia: Bryansk, RU-br; Kaluga, RU-ka; Orel, RU-or; Tula, RU-tu; Ukraine: Chernihiv, UA-ch; Kyiv, UA-ky; Rivno, UA-ri; Zhytomir, UA-zh (Balonov M. and Bouville A., 2011).

As seen from Figure 2.10 doses except Belarus, Russian Federation, and Ukraine the doses are not higher than 3 mSv. Because of the very small doses generally received outside Belarus, the Russian Federation and Ukraine, to tell a relationship between cancer and CNPP accident is not possible (Elisabeth et al., 2006). To have an idea about the doses, Table 2.3 (adapted from World Health Organization (Url-1)) gives dose results received after the accident, including doses due to natural background and medical applications.

Table 2.3: Dose results after CNPP accident, natural background and medical applications

Population (years exposed)	Number	Average total in 20 years (mSv) ¹
Liquidators (1986–1987) (high exposed)	240 000	>100
Evacuees (1986)	116 000	>33
Residents SCZs (>555 kBq/m ²) (1986–2005)	270 000	>50
Residents low contam. (37 kBq/m ²) (1986–2005)	5 000 000	10–20
Natural background	2.4 mSv/year (typical range 1–10, max >20)	48
Approximate typical doses from medical x-ray exposures per procedure:		
Whole body CT scan	12 mSv	
Mammogram	0.13 mSv	
Chest x-ray	0.08 mSv	

[1] These doses are additional to those from natural background radiation.

3. METHODOLOGY

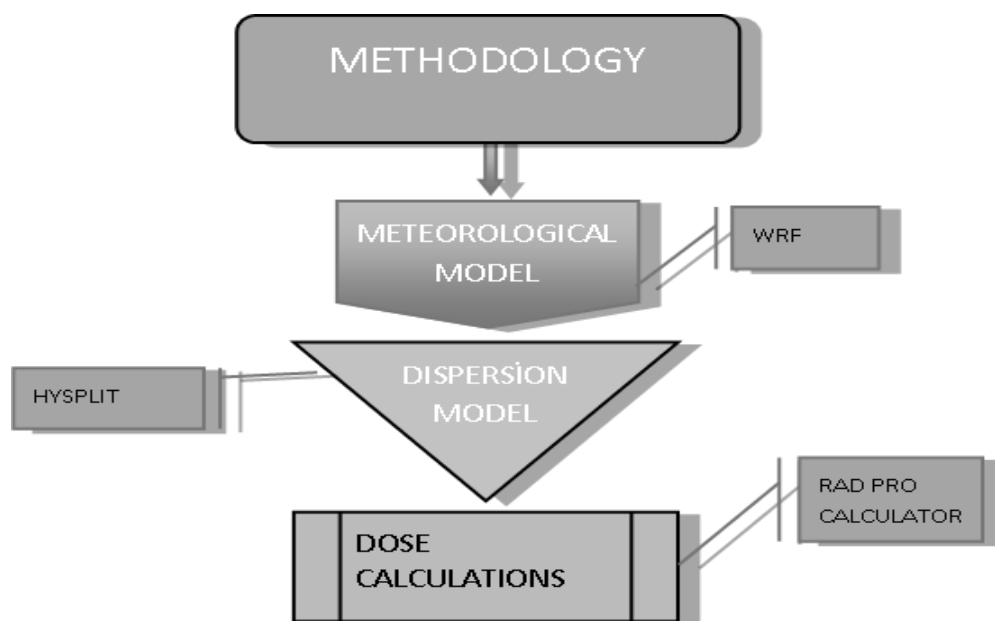


Figure 3.1: Diagram of methodology.

The ^{137}Cs deposition and surface air concentration were estimated for the period of 15 days after the Chernobyl accident, from the 26th of April to the 10th of May, 1986, with a combination of modeling tools that is shown in Figure 3.1. We used the Weather Research Forecast model (WRF version 3.3 <http://www.wrf-model.org>, Skamarmock and Klemp, 2008) to reproduce the meteorological conditions occurred during the CNPP episode. The HYSPLIT (Hybrid Single-Particle Lagrangian Integrated Trajectory) dispersion model was used to simulate the dispersion (deposition and air concentrations) of the radionuclides using the simulated WRF meteorological fields (e.g. wind speed and direction, pressure, temperature, precipitations). The HYSPLIT results were compared with REM dataset (<http://rem.jrc.ec.europa.eu/RemWeb/Download.aspx>) for air concentrations and deposition results, which were used to generate the Atlas of ^{137}Cs on Europe. The radionuclides air concentrations and deposition values were used to estimate the total ^{137}Cs effective doses to which population was exposed. Two methodologies were

used, the first one was performed by according to the coefficients and formulas of UNSCEAR 1988 report UNSCEAR (United Nations Scientific Committee on the Effects of Atomic Radiation) 1988 Report. The second and more recent approach was done according to World Health Organization report (WHO, 2012) published after Fukushima Daiichi nuclear power station accident.

3.1 WRF (Weather Research Forecast model)

The Weather Research and Forecasting (WRF) model is a numerical weather prediction (NWP) and atmospheric simulation model. WRF was developed for the understanding and prediction of mesoscale weather. The WRF model was built upon the MM5 model, which was used primarily as a research tool and whose origins can be traced back to hurricane research done by Rick Anthes in the 1960's (Knievel J., 2005). Since 2006, WRF is used by the United States National Weather Service and has been adopted as the national weather forecast model for many other countries around the world (Schofield J.C.H., 2012). The principle components of WRF model are shown in Figure 3.2. The WRF Software Framework (WSF) provides the infrastructure that accommodates the dynamics solvers, physics packages that interface with the solvers, programs for initialization, WRF-Var (to perform data assimilation), and WRF-Chem (to include the simulation of atmospheric chemistry composition). There are two dynamics solvers in the WRF: the Advanced Research WRF (ARW) solver (originally referred to as the Eulerian mass or "em" solver) developed primarily at NCAR, and the NMM (Nonhydrostatic Mesoscale Model) solver developed at NCEP. WRF is a well-known regional meteorological model, used in several studies also in the area of interest of this study, Eastern Europe and the Mediterranean (i.e., Im et al., 2010; Im et al., 2011). We performed a simulation of the period 20/4/1986 – 21/5/1986 for a domain covering all Europe (160 x 130 grid cells, 53.0 N; 22.0 W central latitude and longitude, Fig. 3.3) with a horizontal resolution of 36 km by 36 km and 31 vertical layers, from surface to 10 hPa. In order to reproduce the specific meteorological conditions occurred during the CNPP episode, we used the National Centers for Environmental Protection (NCEP) Operational Global Analysis data (1° x 1° horizontal and 6 h temporal resolutions) as boundary conditions and to nudge the WRF simulations (temperature, pressure, winds, and specific humidity).

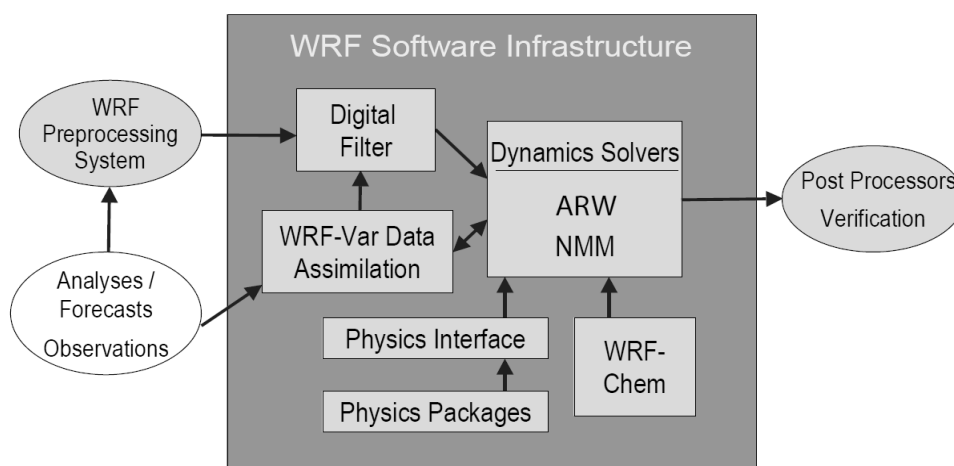


Figure 3.2: WRF system components (Kniewicz J., 2005).

The main WRF physical options chosen for this episode were: the Kessler microphysics scheme (Kessler, 1969); RRTM (rapid radiative transfer model) long-wave radiation scheme (Mlawer et al., 1997); Dudhia short-wave radiation scheme (Dudhia, 1989); NOAA land surface model (Chen and Dudhia, 2001); Yonsei University Planetary Boundary Layer scheme (Hong et al., 2006); and Kain-Fritsch cumulus parameterization scheme (Kain, 2004). Detailed explanations of the options can be found from sections 3.1.1.1 to 3.1.1.6 of the NCAR technical note NCAR/TN-475+STR, written by Skamarmock et al. (2008).

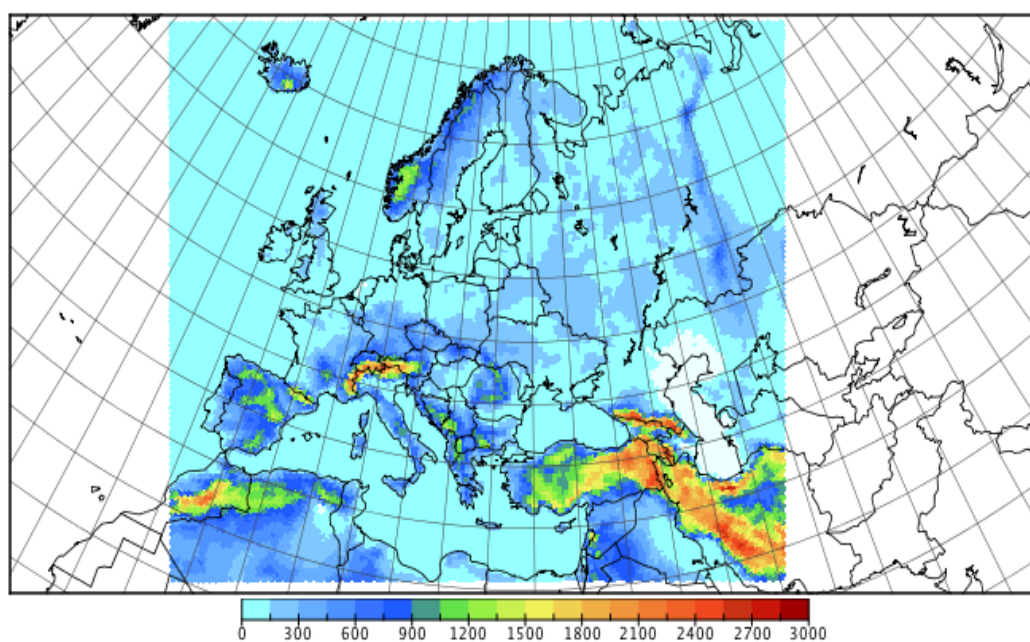


Figure 3.3: Model domain and land/sea mask used of the WRF simulation.

3.2 HYSPLIT

The HYSPLIT (Hybrid Single-Particle Lagrangian Integrated Trajectory, <http://ready.arl.noaa.gov/HYSPLIT.php>, version 4) model from NOAA-ARL's (National Oceanic and Atmospheric Administration Air Resources Laboratory) is a complete system for computing simple air parcel trajectories to complex dispersion and deposition simulations using either puff or particle approaches (Draxler R., et.al., 2009). Some of the applications include tracking and forecasting the release of radioactive material, volcanic ash, wildfire smoke, and pollutants from various stationary and mobile emission sources (Url-11). 'The model calculation method is a hybrid between the Lagrangian approach, which uses a moving frame of reference for the advection and diffusion calculations as the air parcels move from their initial location, and the Eulerian approach, which uses a fixed three-dimensional grid as a frame of reference to compute the pollutant air concentrations' (NOAA, 2013).

We used HYSPLIT to calculate the ^{137}Cs total deposition (wet and dry) and surface air concentrations occurred over Europe and Turkey after the CNPP accident.

The radioactive decay of ^{137}Cs is taken into account in HYSPLIT model to estimate the amount of deposited radioactive materials (Draxler RR and Hess GD, 1997). The decay constant for radioactive processes (β_{rad}) is defined by the half-life $T_{1/2}$,

$$\beta_{\text{rad}} = \ln 2 / T_{1/2} \quad (3.1)$$

And the radioactive mass of a pollutant ($m_{t+\Delta t}$) after a time interval Δt , either in the air or deposited at the soil, becomes,

$$m_{t+\Delta t} = m_t \exp (-\beta_{\text{rad}} \Delta t) \quad (3.2)$$

3.3 HYSPLIT Simulations Setup

The location of Chernobyl nuclear power plant was defined as 51.00 N, 30.00 E. Simulations were processed starting from 26 April 1986 at 00:00 AM and finishing at the end of 10 May 1986. The release point was selected as center of the simulation. Span (deg) latitude and longitude, which sets the total span of the grid in each direction, was set as default: 180 degrees North/South and 360 degrees West/East. The Number of vertical layers was set to two. First layer was set as 0 m for deposition amounts. Second layer was set to 10 m to obtain concentration amount

between surface and 10 m. Sampling interval was set as 6 hours. Definition of pollutant properties was done as preconfigured at HYSPLIT for ^{137}Cs . As a particle, ^{137}Cs , 1.0 μm particle diameter, 1.0 g/cc density and 1.0 shape options were set. The half-life of ^{137}Cs was set as 10960 days. As mentioned in section 3.4.4 resuspension factor was set as 0.0. The release mode was selected as 3D particle. This mixed-mode was selected to take advantage of the more accurate representation of the 3D particle approach near the source and the smoother horizontal distribution provided by one of the hybrid puff approaches at the longer transport distances. (Draxler R., et al. 2009).

An important factor which determines the distribution of pollutants in the atmosphere is the altitude and the time of the injection level. The injection of the radioactive material was described by four different temporal and vertical distributions of the sources. All the performed experiments consider an injection of 85×10^{15} Bq (74×10^{15} Bq for one case) for the entire episode (10 days), as in De Cort et al. (1998). A first experiment was conducted considering continuous emissions at a constant rate of 0.354×10^{12} Bq/hour for 10 consecutive days after the accident and at a constant altitude of 300 m (CONT300). Other three additional cases were considered with more realistic temporal and vertical distributions, according to three different recent studies, Brandt et al. (2002), Suh et al. (2009), and Evangeliou et al. (2013). Sampling dates and emission rates were set according to source terms.

In this study two different dry deposition velocities were tested. HYSPLIT defines a reference dry deposition velocity for ^{137}Cs of 0.1 cm/s. Nevertheless different values for this parameter can be found in previous studies regarding the Chernobyl accident (Brandt et al., 2002 and therein references), ranging from 0.04 cm/s to 0.5 cm/s. For this reason in this study we tested the sensitivity of ^{137}Cs air concentrations and deposition with two different dry deposition velocities, the reference HYSPLIT value of 0.1 cm/s and a larger value of 0.2 cm/s, which was also used in one of the simulations of Brandt et al. (2002). Evangeliou et al. (2013) calculates dry deposition velocities according to Blakanski et al. (1993) and they found values ranging from 0.05 cm/s to 0.2 cm/s. Suh et al. (2009) tested three different dry deposition velocities, 0.1 cm/s, 0.15 cm/s, and 0.05 cm/s.

Wet deposition processes impose difficulties in meteorological computer models. The difficulty stems from the simplified assumptions incorporated into wet deposition models coupled with a general lack of reliable precipitation observations in the meteorological input data (Moroz et al., 2010). For wet deposition, options pre-defined at HYSPLIT users guide for ^{137}Cs were chosen. In-cloud removal is defined as a ratio of the pollutant in air (g/liter of air in the cloud layer) to that in rain (g/liter) measured at the ground and was set as $3.2\text{E}+05$ (l/l). Below-cloud removal is defined through a removal time constant and was set as $5.0\text{E}-05$ (1/s) (Draxler R., et.al. 2009).

Seven different simulations were performed using HYSPLIT model. All simulations were processed by the HYSPLIT concentration mode. From now on the experiments will be named as BR1 (sources based on Brandt et al., 2002), EV1 (sources based on Evangeliou et al., 2013) and SU1 (sources based on Suh et al., 2009), with dry deposition velocity of 0.1 cm/s. BR2, EV2, SU2 (sources based on Brandt et al., 2002, Evangeliou et al., 2013, Suh et al., 2009), and CONT300 (constant emission rate at 300 m) with dry deposition velocity of 0.2 cm/s (Table 3.1). For all simulations deposition and concentration values for our domain were obtained by 12 days and 0.2×0.2 degrees simulations.

Table 3.1: Summary of the simulations performed with HYSPLIT.

Simulation	Emission Description	Dry Deposition Velocity
BR1	Brandt et al. (2002), Table 3.1	0.1 cm/s
BR2	Brandt et al. (2002), Table 3.1	0.2 cm/s
EV1	Suh et al. (2009), Table 3.2	0.1 cm/s
EV2	Suh et al. (2009), Table 3.2	0.2 cm/s
SU1	Evangeliou et al. (2013), Table 3.3	0.1 cm/s
SU2	Evangeliou et al. (2013), Table 3.3	0.2 cm/s
CONT300	Constant 0.354×10^{12} Bq/hour at 300 m	0.2 cm/s

BR1 and BR2 simulations were done using source term described in Table 3.2, according to Hass et al. (1990), Devell et al. (1995), Waight et al., (1995) and De Cort et al. (1998) (Brandt et al., 2002). The table shows the approximate height of release and release amounts of ^{137}Cs as Bq/per day for 10 days following the CNPP accident.

Table 3.2: Source term after CNPP accident according to Brand et al. (2002).

Approximate Height [m]	25-26 April	27 April	28 April	29 April	30 April
225	-	-	2.9×10^{15}	2.0×10^{15}	1.7×10^{15}
425	-	6.7×10^{14}	2.9×10^{15}	2.0×10^{15}	1.7×10^{15}
715	-	3.4×10^{15}	-	-	-
1090	1.0×10^{16}	2.7×10^{15}	-	-	-
1575	8.1×10^{15}				
Approximate Height [m]	May 1	May 2	May 3	May 4	May 5
225	1.7×10^{15}	3.4×10^{15}	4.3×10^{15}	6.1×10^{15}	7.0×10^{15}
425	1.7×10^{15}	3.4×10^{15}	4.3×10^{15}	6.1×10^{15}	7.0×10^{15}

The simulations SU1 and SU2 were performed using the source term as presented by Suh et al. (2009). The source term data for the release between 26 April and 6 May 1986 is shown in Table 3.3 and is based on a study of Klug and et al. (Suh et al., 2009).

Table 3.3: Source term after CNPP accident according to Suh et al. (2009)

Effective initial plume height [m]	26 April ^a	27 April	28 April	29 April	30 April	
600	2.2×10^{16}	7.7×10^{15}	-	-	-	
300	-	-	5.5×10^{15}	4.1×10^{15}	3.0×10^{15}	
Approximate Height [m]	May 1	May 2	May 3	May 4	May 5	May 6
300	3.0×10^{15}	5.5×10^{15}	6.3×10^{15}	8.1×10^{15}	8.9×10^{15}	1.1×10^{14}

^a For initial explosion, 20 % of the first day released activity was assumed to be released in the first 6 h at an effective initial height of 1500 m.

Table 3.4 shows the source term for EV1 and EV2 simulations as described in Evangelidou et al. (2013).

Table 3.4: Source term after CNPP accident according to Evangelidou et al. (2013).

Mid-Point in 19 Layers [m]	26 April	27 April	28 April	29 April	30 April
140	-	-	1.450×10^{15}	1.000×10^{15}	0.85×10^{15}
360	-	0.335×10^{15}	2.900×10^{15}	2.000×10^{15}	1.7×10^{15}
690	-	3.735×10^{15}	1.450×10^{15}	1.000×10^{15}	0.85×10^{15}
1200	1.405×10^{15}	2.700×10^{15}	-	-	-
1900	5.050×10^{15}	-	-	-	-
2900	1.000×10^{15}	-	-	-	-

Mid-Point in 19 Layers [m]	May 1	May 2	May 3	May 4	May 5
140	0.850×10^{15}	1.700×10^{15}	2.150×10^{15}	3.050×10^{15}	3.050×10^{15}
360	1.700×10^{15}	3.400×10^{15}	4.300×10^{15}	6.100×10^{15}	6.100×10^{15}
690	0.850×10^{15}	1.700×10^{15}	2.150×10^{15}	3.050×10^{15}	3.050×10^{15}

3.4 Radiation Dose Calculations

The main exposure pathways to radioactive material are: a) external effective dose from cloud gamma (Dc); b) internal effective dose from inhalation (Da) during radioactive cloud passage; c) external effective dose from radionuclides deposited on soil and other surfaces (Dg); d) internal effective dose from the consumption of contaminated food and water (IAEA, 2006). In this study we considered only the first three processes, as the estimation of the internal effective dose from ingestion (d) would require a separate study which includes measurements of water, animal, and crop products contamination. Effective dose calculations were estimated by using two different methodologies. The first one was performed according to the UNSCEAR 1988 report (United Nations Scientific Committee on the Effects of Atomic Radiation). The second and more recent approach was done according to World Health Organization report (WHO, 2012) published after Fukushima Daiichi nuclear power station accident. In both approaches, the effective dose due to ground deposition was calculated for one year, which reflects as nearly as possible the prevailing conditions, not only in terms of measured ^{137}Cs values, but also in terms of shielding and occupancy factors and protective measures (ANNEX D, UNSCEAR, 1988). The total effective dose was calculated separately for adults, child (age < 10 years), and infants (age < 1 year) for the first year after the accident.

Since inhalation of resuspended radionuclides is only significant for those radionuclides, which do not present an external radiation hazard (McColl and Prosser, 2012), the effective dose due to resuspension was neglected.

3.4.1 Effective dose calculation from UNSCEAR and Radiological Toolbox

3.4.1.1 Radiological Tool Box

The Radiological Toolbox, developed for the U.S. Nuclear Regulatory Commission (NRC) provides access to physical, chemical, anatomical, physiological and mathematical data (and models) relevant to the protection of workers and the public from exposures to ionizing radiation (K. F. Eckerman, A. L. Sjoreen). In our study Radiological Toolbox is used to obtain dose coefficients for external dose calculations due to ground deposition and cloud gamma and dose calculation due to inhalation. For external dose calculation Radiological Toolbox uses dose coefficients taken from the Federal Guidance Report no. 12 External Exposure to Radionuclides in Air, Water, and Soil which was prepared by Keith F. Eckerman and Jeffrey C. Ryman for U.S. Environmental Protection Agency's Office of Radiation and Indoor Air. Public inhalation dose coefficients were taken from International Commission on Radiological Protection report ICRP Publication 72: Age-dependent Doses to the Members of the Public from Intake of Radionuclides.

3.4.1.2 Dose from ground deposition

For external effective dose calculation (D_g and D_c) Radiological Toolbox uses effective dose coefficients according to Eckerman and Ryman (1993).

$$D_g = C_g \times S_g \times M_o + C_g \times S_g \times M_i \times B_s \quad (3.3)$$

where C_g is the deposition value ($Bq\ m^{-2}$) simulated by HYSPLIT, S_g is the external effective dose coefficient from ground ($9.44 \times 10^{-11}\ Sv\ Bq^{-1}\ year^{-1}\ m^{-2}$ for ^{137}Cs and $1.83 \times 10^{-08}\ Sv\ Bq^{-1}\ year^{-1}\ m^{-2}$ for ^{137m}Ba), M_o is the outdoor occupancy factor, and M_i is the indoor occupancy factor. B_s is the building shielding factor.

3.4.1.3 Cloud gamma doses

Whereas γ radiation from airborne radionuclides is the main exposure pathway of dose from external exposure, some radionuclide's give rise to β radiation, which can lead to exposure to the skin. Cloud gamma doses were calculated by the formula;

$$D_c = C_a \times S_a \times M_o + C_a \times S_a \times M_i \times B_a \quad (3.4)$$

Where C_a is the air concentration value ($Bq\ m^{-3}$) simulated by HYSPLIT, S_a is the external cloud gamma coefficient ($8.02 \times 10^{-12}\ Sv\ Bq^{-1}\ day^{-1}\ m^{-3}$). In formulas 3.3 and 3.4, the values for M_o , M_i , and B_s are 0.2, 0.8 and 0.2 (ANNEX D, UNSCEAR, 1988), respectively.

3.4.1.4 Inhalation doses

Public inhalation effective dose (D_a) was calculated using the coefficients from the report No. 72 of the International Commission on Radiological Protection report (ICRP, 1995);

$$D_a = C_a \times I_a \times M_o \times R + C_a \times I_a \times M_i \times B_r \times R \quad (3.5)$$

where C_a is the air concentration value ($Bq\ m^{-3}$) simulated by HYSPLIT, I_a is the public inhalation effective dose coefficient ($3.9 \times 10^{-8}\ Sv\ Bq^{-1}$ for adults, $4.8 \times 10^{-8}\ Sv\ Bq^{-1}$ for child, and $10^{-7}\ Sv\ Bq^{-1}$ for infants), R is the breathing rate ($m^3\ h^{-1}$), and B_r is the indoor air reduction factor (0.3) (ANNEX D, UNSCEAR, 1998). Breathing rates were $19.2\ m^3\ day^{-1}$ for an adult, $14.4\ m^3\ day^{-1}$ for 10 years old child and $4.8\ m^3\ day^{-1}$ for 1 year old infants (Robinson, 1996). Since the cloud gamma and inhalation effective doses depend on the concentrations of ^{137}Cs in the air, D_a and D_c were simulated by HYSPLIT for the 15 days of the episode.

3.4.2 Effective dose calculation from WHO

The second approach for calculation of the effective doses for the first year after CNPP accident was performed according to the World Health Organization report (2012) and therein references.

3.4.2.1 Dose from ground deposition

For external effective dose calculation from ground deposition we used the formula adapted from Annex 7 of WHO report (2012);

$$Dg=RF \times Cg \times de^{dep} \quad (3.6)$$

where Cg is the total activity density of radionuclide on the ground (i.e. deposited ^{137}Cs in Bq/m^2 simulated by HYSPLIT), de^{dep} is the effective external effective dose coefficient per unit deposit of radionuclide for age group, $1.2 \times 10^{-8} \text{ Sv Bq}^{-1} \text{ year}^{-1} \text{ m}^{-2}$ for adults and child, and $1.6 \times 10^{-8} \text{ Sv Bq}^{-1} \text{ year}^{-1} \text{ m}^{-2}$ for infants (Jacob et al., 1990). RF is the reduction factor of 0.3624 as indicated in Annex 3, Table A3.8 of WHO report (2012),

3.4.2.2 Cloud gamma doses

For external effective dose from radioactive cloud, the method described at the study of Bedwell et al., 2010 was used. Effective dose rate from radioactive cloud is calculated by the formula;

$$Dc=RF \times Ca \times k \times I \times E \times A \quad (3.7)$$

where RF is the same reduction factor used before, Ca is the activity concentration in air (Bq/m^3) simulated by HYSPLIT, k is a conversion factor ($2 \times 10^{-6} \text{ Gy y}^{-1} \text{ MeV}^{-1} \text{ m}^{-3} \text{ s}^{-1}$) (Bedwell et al., 2010), I is the photon intensity (ICRP 38, 1983), E is the photon energy (MeV) (ICRP 38, 1983), A is the effective dose per unit air kerma (ICRP 74, 1996).

3.4.2.3 Inhalation doses

The effective dose of population age group from inhalation of radioactive materials was calculated according to:

$$Da=Ca \times Ia \times R \quad (3.8)$$

where Ca is the activity concentration in air (Bq/m^3) simulated by HYSPLIT, R is the breathing rate for age group ($22.18 \text{ m}^3 \text{ day}^{-1}$ for adults, $15.28 \text{ m}^3 \text{ day}^{-1}$ for child, and $5.2 \text{ m}^3 \text{ day}^{-1}$ for infants, ICRP 66, 1994), Ia is the effective inhalation effective dose coefficient for each age group and radionuclide in Sv Bq^{-1} ($4.6 \times 10^{-9} \text{ Sv Bq}^{-1}$ for adults, $3.7 \times 10^{-9} \text{ Sv Bq}^{-1}$ for child, and $5.4 \times 10^{-9} \text{ Sv Bq}^{-1}$ for infants). (ICRP database : (v2.0.1)) Since the cloud gamma and inhalation effective doses depends on the concentrations of ^{137}Cs in the air, Dc and Da are calculated for every day using daily average ^{137}Cs air concentrations simulated with HYSPLIT, and the total effective

doses from radioactive cloud and inhalation are the sum of D_c and D_a for every day of the simulation.

3.5 REM Database

The Radioactivity Environmental Monitoring (REM) data bank (Url-5) was set-up in 1988 to collect environmental radioactivity produced in the aftermath of the Chernobyl accident. To have a historical record of the Chernobyl accident and preparing a monitoring report after CNPP accident were the main goals of building the data bank. Data from 27 European Commission Member States and other European countries are included in the database. In this study we made comparison of simulated air concentration and deposition values (Figure 3.4) of ^{137}Cs after CNPP accident with the measurements collected in the REM database (2013). A detailed description of the REM database (2013) and measuring techniques is provided in APPENDIX B of the Atlas of Caesium deposition on Europe after the Chernobyl accident (De Cort et al., 1998). Air concentrations of ^{137}Cs are available at 90 stations, while deposition was measured at almost 2500 locations.

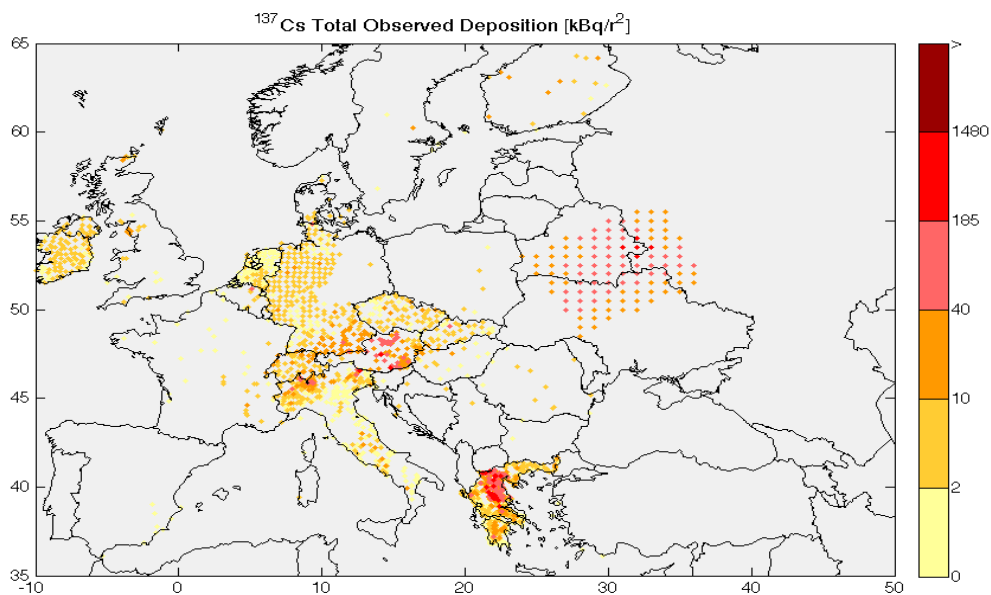


Figure 3.4: Measured (REM) total deposition of ^{137}Cs over Europe.

The density of measuring locations is very variable (see also Table 2.2), with high number of measurements only for few countries (Ireland, the Netherlands, West Germany, Switzerland, Austria, Italy, Czech Republic, Slovakia, and Greece). All other countries have only few scattered measurement sites to represent vast territories.

4. RESULTS AND DISCUSSION

4.1 Meteorology

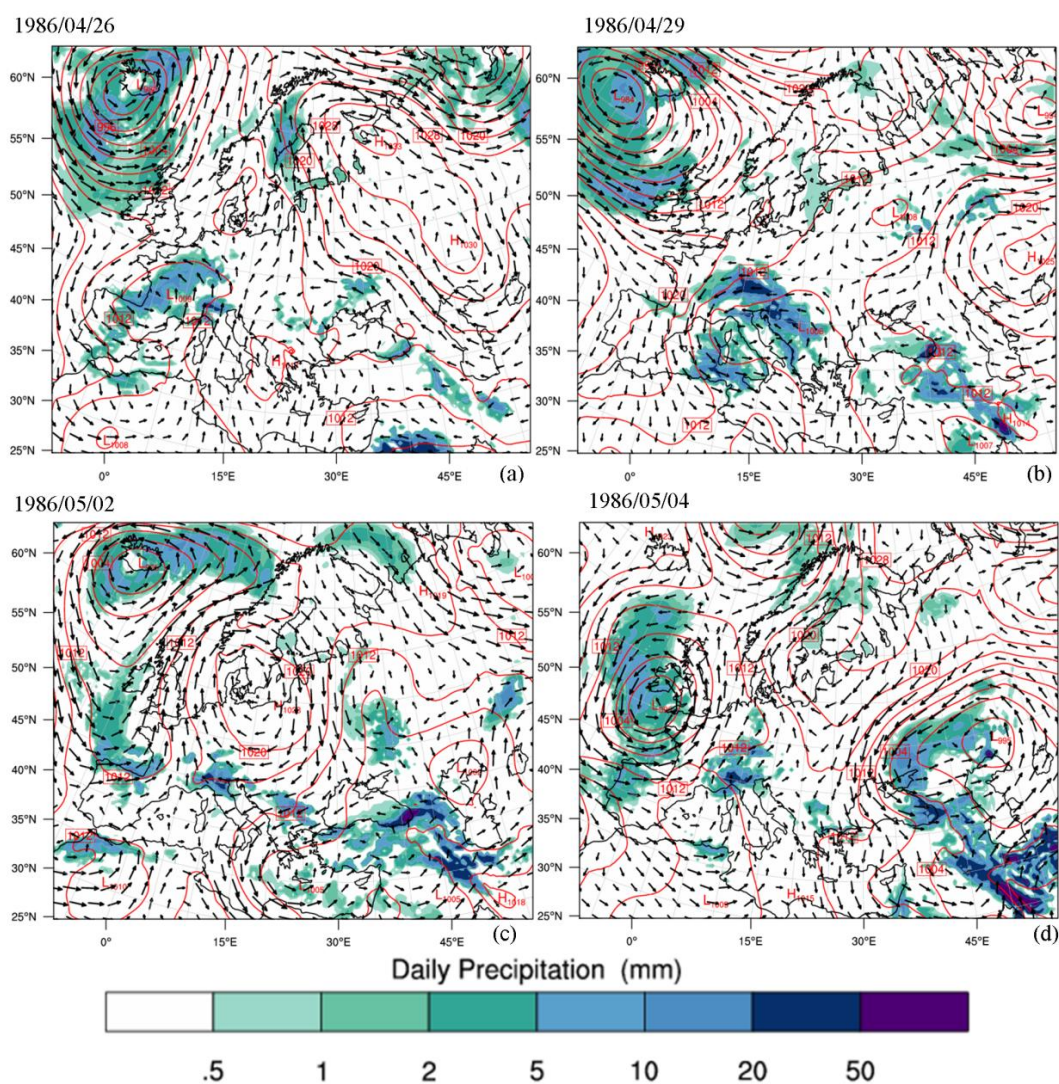


Figure 4.1: Daily mean wind speed, sea level pressure and precipitations for the days: a) 26/04/1986. b) 29/04/1986. c) 02/05/1986. d) 04/05/1986.

The meteorology is a key component in order to simulate correctly the transport, arrival time and deposition of the radioactive material at the different areas in Europe, which were affected by the Chernobyl accident. Figures 4.1, A.1, and A.2 show the meteorology as simulated by WRF model for the CNPP accident episode.

When the explosion occurred, surface winds at the Chernobyl site were very weak and variable in direction (UNSCEAR, 1998). During the first two days after the accident (26-27/4/1986) a high pressure system over Russia generated strong south-easterly winds, which transported the radioactive cloud to North-West from the reactor, reaching the Scandinavia Peninsula (Figure 4.1 a). The high pressure system over Russia moved south during 28-29/4/1986 and eastward in the following days. This changed the wind direction first towards east, from Chernobyl over Russia (Figure 4.1 b) and after toward south. The high pressure system over Europe and low pressure system over Siberia forced the wind direction over Turkey and Balkan countries (Figure 4.1 c, 02/05/1986), a condition that persists until the 06/05/1986 (Figure 4.1 d). Figure 4.2 gives the daily 850 hPa level pressure and wind patterns as described in the Atlas (de Cort et al., 1998). The pressure and wind patterns are well represented also in our simulation, which give us enough confidence in reproducing the transport of the radioactive cloud.

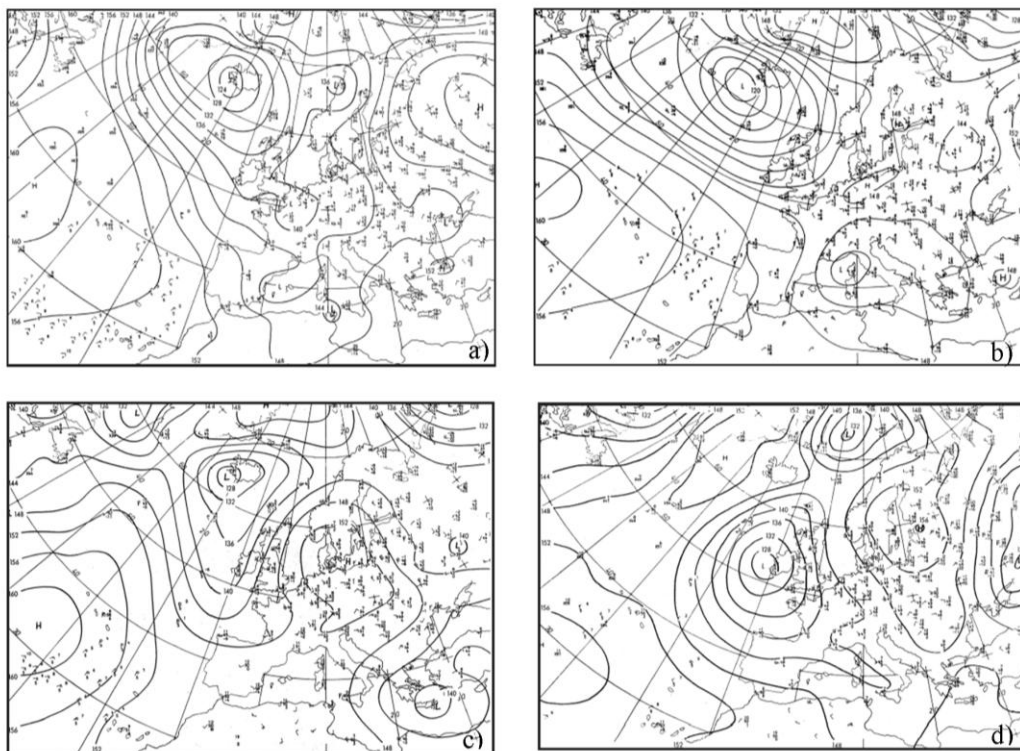


Figure 4.2: Daily 850 hPa level pressure for the days: a) 26/04/1986. b) 29/04/1986. c) 02/05/1986. d) 04/05/1986 (de Cort et al., 1998).

An important parameter which largely determines the deposition of ^{137}Cs is the precipitation, as the major part of total deposition consists of wet deposition (Brandt et al., 2002). Our simulation generally shows similar precipitation patterns as in the Atlas (daily meteorology maps 61-64, de Cort et al., 1998). During the first 3 days after the accident (26-29/04/1986) both the Atlas and our simulation show precipitations (5-20 mm/day) occurring south of the Chernobyl Nuclear Power Plant and moving towards east. At dates 29-30/04/1986 precipitations were observed in the Scandinavian Peninsula (south western Finland and central Sweden), which is only partially reproduced in our model simulation over the Baltic Sea. On 01/05/1986 the main precipitation patterns is located North East of the CNPP (mainly in Russia), which is also well represented in the WRF simulation. Precipitation affected south Eastern Europe, mainly Turkey and Bulgaria (not included in the Atlas), between the 2nd and 4th of May 1986. These precipitation patterns are important because the radioactive clouds were carried to these regions during these days, as we will show in the next section. Kindap et al. (2008) conducted a similar study obtaining similar results by using the MM5T model, which was developed by Chen et al. (2008) based on the fifth-generation Penn State/NCAR Mesoscale model (MM5; Grell et al. 1995). Also in their simulation the radioactive material was transported from Chernobyl to North Europe at 26-27 April, and then affected Central Europe 5 days after the CNPP accident and on 3rd of May reached to the Balkan countries, including Turkey.

4.2 Air concentrations and deposition of ^{137}Cs over Europe

4.2.1 Air concentrations of ^{137}Cs over Europe

The simulated radioactive cloud is simulated by HYSPLIT coherently with the wind patterns and precipitations shown in the previous section. In Figure 4.3 we present the daily mean ^{137}Cs air concentrations at surface for simulation BR1 and the entire simulated episode (Figures A3, A4, A5, A6, A7, A8 in Appendix A show the results for all the other simulations). In the same figure we plot ^{137}Cs measurement from the REM dataset. The largest ^{137}Cs air concentrations were observed and simulated mainly in three regions during the episode, the Scandinavian Peninsula and toward East (Belarus, Ukraine and Russia) in the first days, Central Europe and the Balkan Peninsula after the 1st of May.

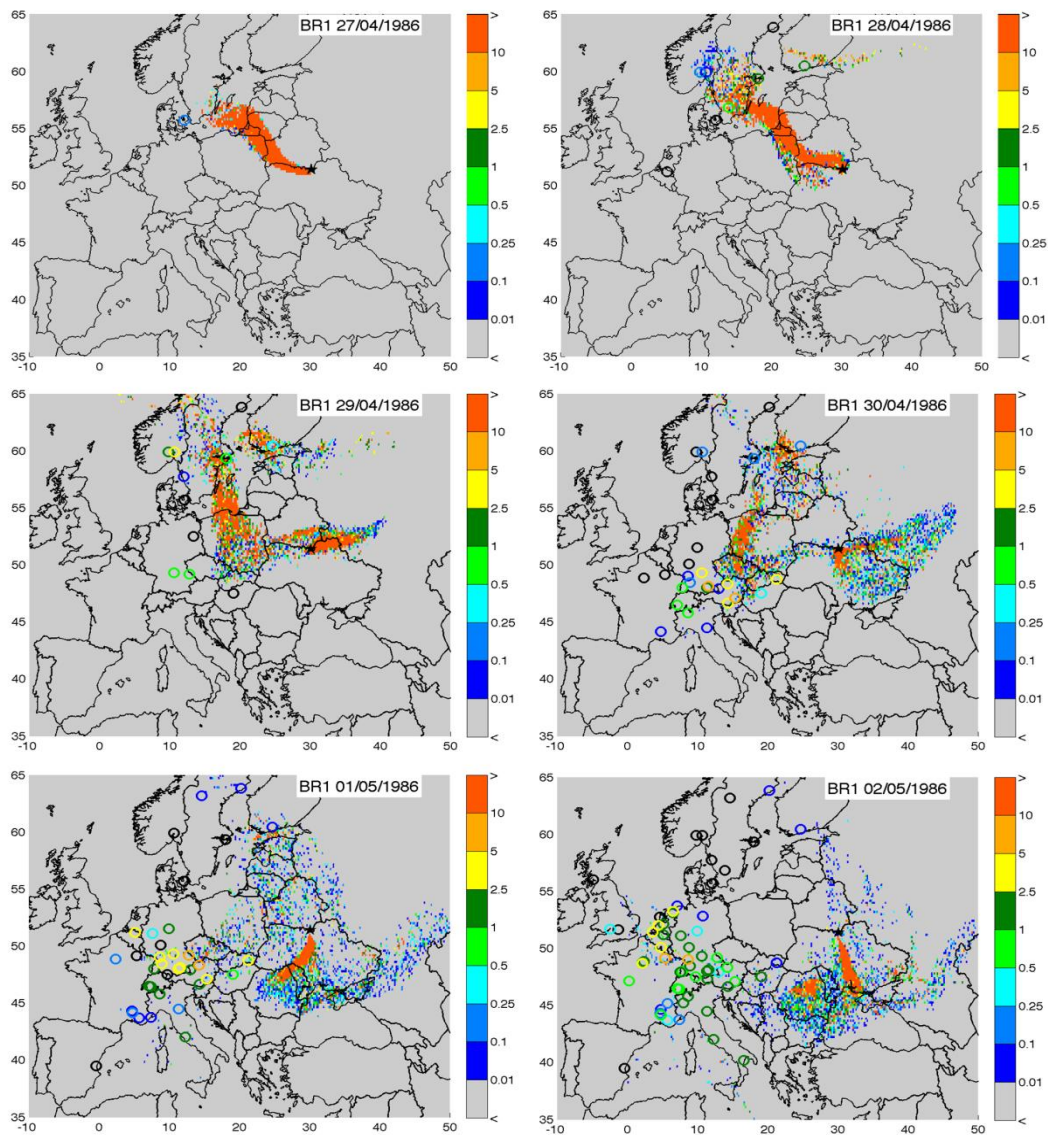


Figure 4.3: Caesium-137 air concentrations [Bq/m^3] simulated by HYSPLIT at surface for the BR1 simulation, 27/04/1986–08/05/1986. REM measurements are plotted as colored open circles (black circles correspond to measurements below $0.01 \text{ Bq}/\text{m}^3$).

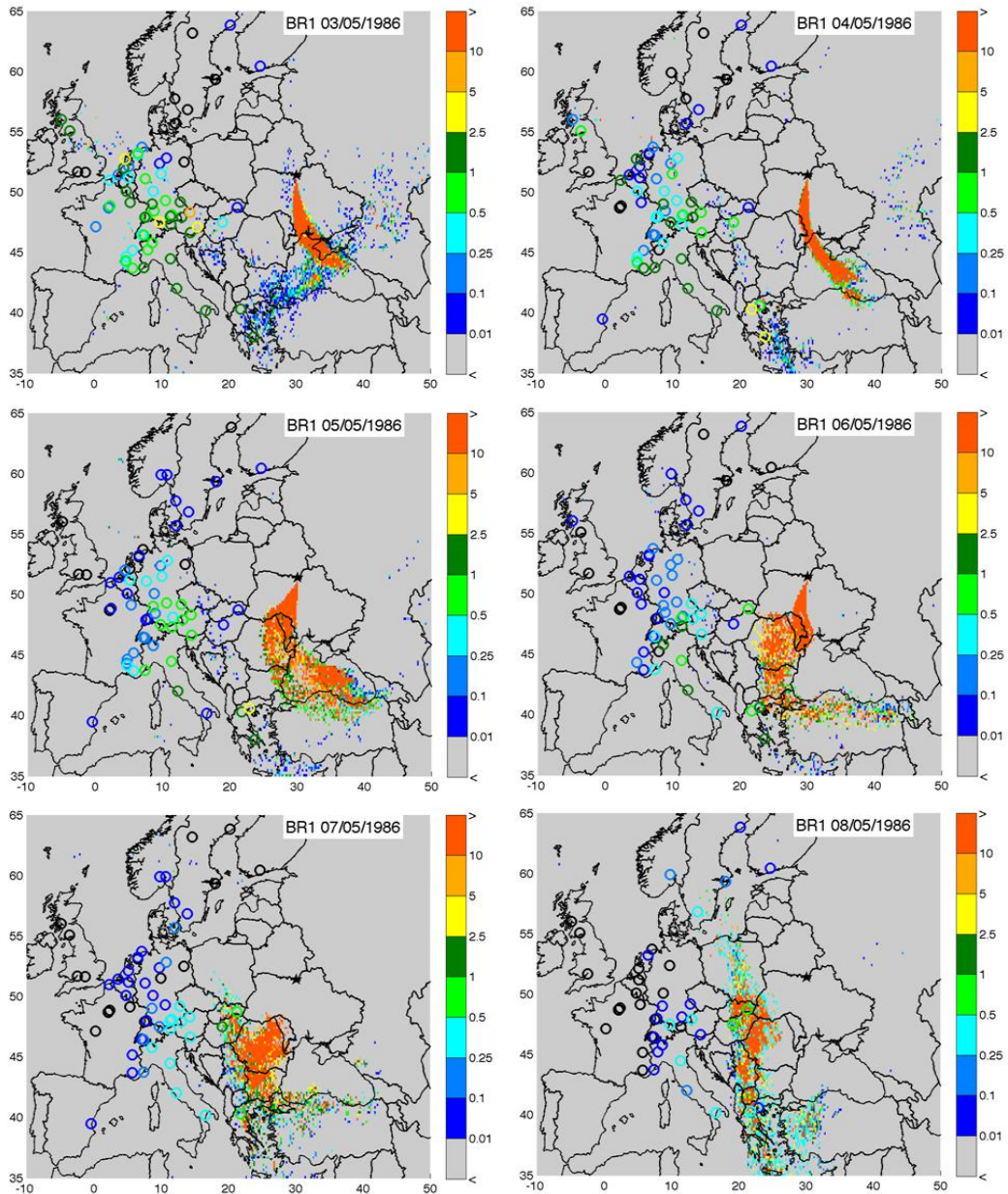


Figure 4.3 (continued): Caesium-137 air concentrations [Bq/m^3] simulated by HYSPLIT at surface for the BR1 simulation, 27/04/1986–08/05/1986. REM measurements are plotted as colored open circles (black circles correspond to measurements below $0.01 \text{ Bq}/\text{m}^3$).

The first observed ¹³⁷Cs air concentrations after the CNPP accident were reported by Sweden on the 27th of April (Devell et al., 1986). Also in our simulations the strong south-easterly winds (described in section 4.1) transported ¹³⁷Cs to Finland and Sweden in the first days after the CNPP accident (Figure 4.3). On the 28th - 29th of May the wind direction changes, the ¹³⁷Cs plume moves from Scandinavia Peninsula towards Central European countries, mainly Poland, while a second plume is moving

towards East from Chernobyl affecting Belarus, Ukraine and Russia. On the 1st of May the winds bring the ¹³⁷Cs plume to the south of the CNPP, reaching the Balkan Peninsula and Turkey on the 2nd of May. The plume first arrived to the European part of Turkey and moved in the following days above the Aegean Sea, affecting both Turkey and Greece. Until the 5th of May high ¹³⁷Cs concentrations persist over the Black Sea and all Northern Turkey. The contaminated air affects Turkey until the 8th of May moving again towards the Aegean region. The largest ¹³⁷Cs concentrations in the last 2 days of the episode are simulated over the Balkan Peninsula, in particular Romania and Bulgaria. All the HYSPLIT simulations, performed using three different source terms (Table 3.1, Table 3.2., Table 3.3.), reproduced similar transport patterns (Appendix A). The main differences between the simulations were found for the CONT300 simulation, which considers a rather simple and unrealistic source term description (constant emission rate at 300 m altitude). The HYSPLIT simulations cannot always reproduce the observed values at the same locations of the observations, but in general similar values can be observed in the vicinity of the measuring sites. This might be due to several factors, such as the uncertainty in the amount of emitted radionuclides, the source term temporal and vertical distribution, and biases in the meteorological simulation, which determines transport and deposition of the radionuclides. On the other hand, the distribution of the observed ¹³⁷Cs air concentrations is generally well represented by the model simulations both temporally and spatially, but in general the transport in the model shows smaller values in Western Europe.

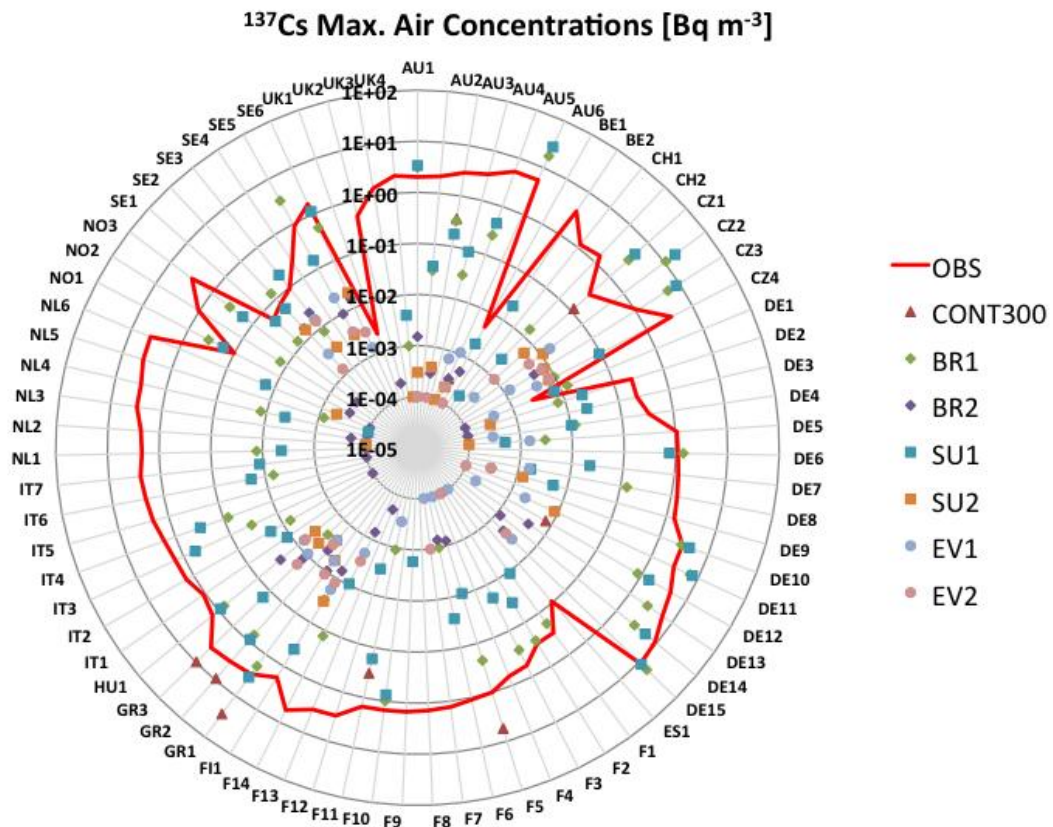


Figure 4.4: Observed and simulated Caesium-137 maximum air concentrations at REM database measuring stations.

Figure 4.4 shows the maximum ^{137}Cs air concentrations observed at several locations included in the REM dataset (Table B.1, in the Appendix B) and simulated by all HYSPLIT simulations. In general BR1 and SU1 better represented the observed maximum concentrations. These two simulations can reproduce the peak concentrations at several locations in those regions where the radioactive cloud was mainly transported, such as the Scandinavian Peninsula (Sweden, Finland and Norway), Central Europe (Austria and Germany), and South Europe (Greece).

A more general comparison of the observed and simulated range of ^{137}Cs air concentrations over all Europe is shown in Figure 4.5. The box plots represent the 25th, 50th and 75th percentiles; the whiskers represent the 1st and 99th percentiles. We excluded from the comparison the simulated air concentrations lower than 10^{-5} Bq/m³, which is the minimum air concentration detected by the measurements (Evangelidou et al., 2013). Generally for all simulations the range of air concentrations is larger than the observed in REM database. The BR1 simulation (Figure 4.3) is the closest to the REM observations, with a median and 75th percentile

close to 0.1 Bq/m^3 and 1 Bq/m^3 , respectively, while smaller values are simulated for the 25th percentile. The effect of the different source terms is generally resulting in larger values; EV1 shows maximum air concentrations up to 10 Bq/m^3 , SU1 up to $20\text{-}30 \text{ Bq/m}^3$, and BR1 up to 100 Bq/m^3 . The effect of different dry deposition velocity is to reduce the median and 25th percentile with the larger value (0.2 cm/s), the results of BR2 and SU2 simulations show that increasing dry deposition velocity affected Central European countries (Austria, Belgium, Germany), West European countries (France and Italy) and Norway by reducing mean air concentrations at these countries, while only small differences are seen between the EV1 and EV2 simulations. The transport of the radioactive cloud in our simulations is also in good agreement with previous studies (Brandt et. 2002, Kindap et al. 2008, Suh et al. 2009, Evangeliou et al., 2013) that show similar mean air concentrations and transport over Turkey.

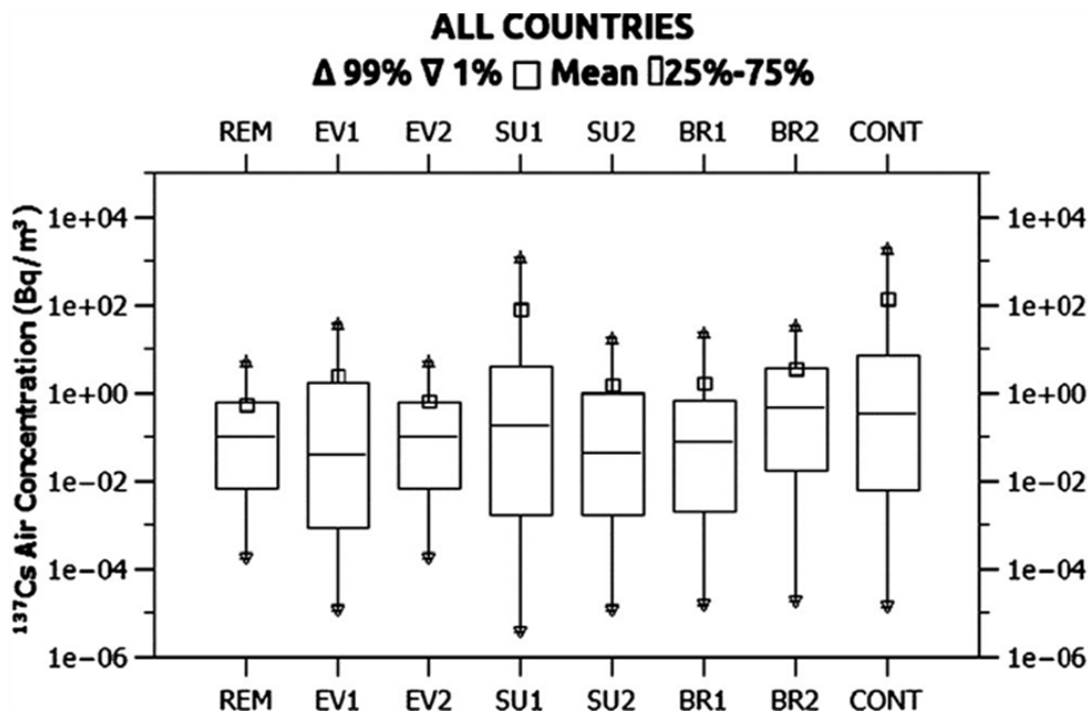


Figure 4.5: Box and Whisker plots of the surface activity concentrations (Bq/m^3) of ^{137}Cs .

4.2.2 Deposition of ^{137}Cs over Europe

The results in terms of total ^{137}Cs deposition for the entire episode (Bq/m^2) from six of the seven simulations are presented in Figure 4.6 (CONT300 simulation not shown).

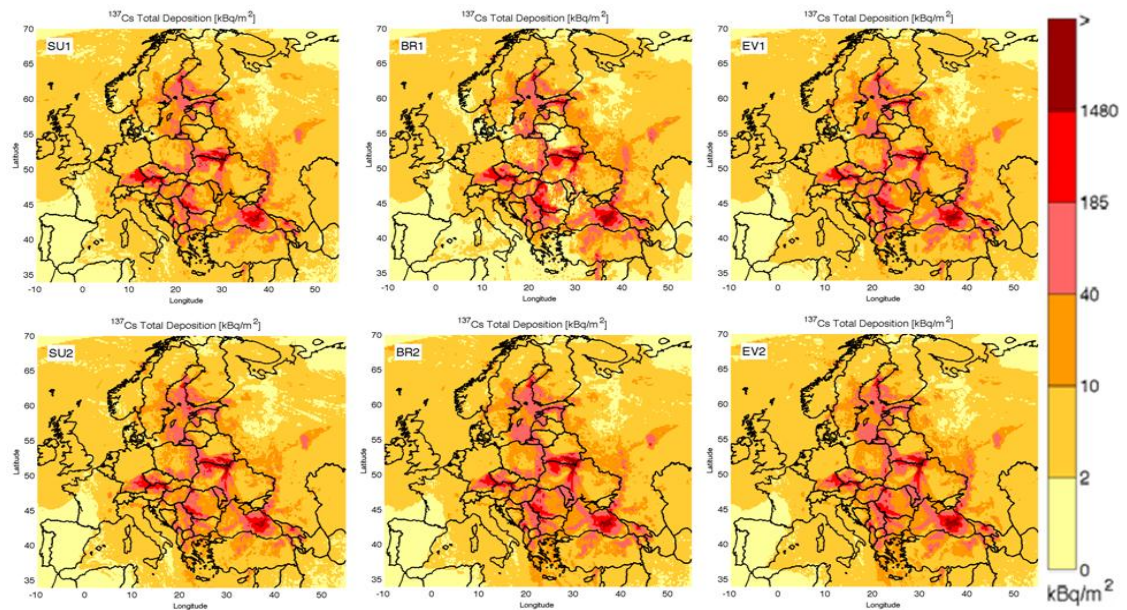


Figure 4.6: Total deposition of ^{137}Cs over Europe after Chernobyl accident for six simulations.

All the simulations show similar deposition patterns of ^{137}Cs , with values larger than 40 kBq/m^2 mainly at the surroundings of the Chernobyl power plant (Ukraine and Belarus), and other 3 regions, the Scandinavian Peninsula and Baltic countries, Central Europe, and the Balkan Peninsula and Turkey. Figure 3.4 shows the total deposition measurements from the REM dataset, which were used to derive the map of ^{137}Cs deposition in the Atlas (Figure 2.6).

Table 4.1 shows the cumulative deposition results provided by De Cort et al. (1998, Table III.1) and our simulations. The total ^{137}Cs deposition over the entire continent (44.3 PBq , excluding Russia) is generally well represented by the simulations, with differences ranging from about -24% to 1% . Almost 90% of the total ^{137}Cs is deposited in 8 countries, Belarus, Ukraine, Finland, Sweden, Norway, Austria, Romania and Germany (de Cort et al., 1998). The same countries in our simulations represent from 77% to 82% of total deposition, except for CNT300, where almost all deposition occurs near the CNPP, in Ukraine. In the countries closest to the CNPP the total ^{137}Cs deposition differs from the Atlas by $6\text{-}48\%$ (Ukraine) and $53\text{-}70\%$ (Belarus).

The cumulative deposition amounts for Scandinavian Peninsula and Baltic countries Sweden, Finland, Norway, are smaller compared to the Atlas, on the other hand results for Estonia and Latvia are larger, while the closest results were obtained for Lithuania. This might be due to the WRF meteorological simulation, with

precipitations mainly located over the Baltic Sea instead of the Scandinavian countries, as observed in de Cort et al. (1998) in the first days after the CNPP accident (Figure 4.1). In Central Europe the simulated deposition values agree fairly well with the Atlas for Austria, which is one of the main affected countries, the differences are in the range of $\pm 30\%$. In other countries like Poland, Czech Republic, Slovakia, Romania, and Germany the simulated deposition values are a factor from 2 to 4 larger than in the Atlas. In Western Europe and Balkan Peninsula, cumulative deposition is underestimated by model simulations, while Greece and European part of Turkey are closer to the values reported in the Atlas. Changing dry deposition velocity did not affect significantly the total deposition amounts for each country. On the other hand simulations with low deposition velocity (EV1, SU1, and BR1) have lower deposition values around Chernobyl whereas they have higher deposition values at longer distances from Chernobyl. Figure 4.7 shows the distribution of cumulative deposition values for REM observations and simulations for all countries. All simulations generally show lower depositions with lower medians, 25th and 75th percentiles, but the largest deposition values (99th percentile) are in the order of 100 kBq/m^2 , as the REM dataset. The mean values of each simulation are also closer to the REM mean value ($\sim 10 \text{ kBq/m}^2$). The dry deposition velocity of 0.2 cm/s (EV2, BR2, and SU2) determines a 10% larger total ^{137}Cs deposition over the entire continent when compared to a 0.1 cm/s dry deposition velocity (EV1, BR1, and SU1).

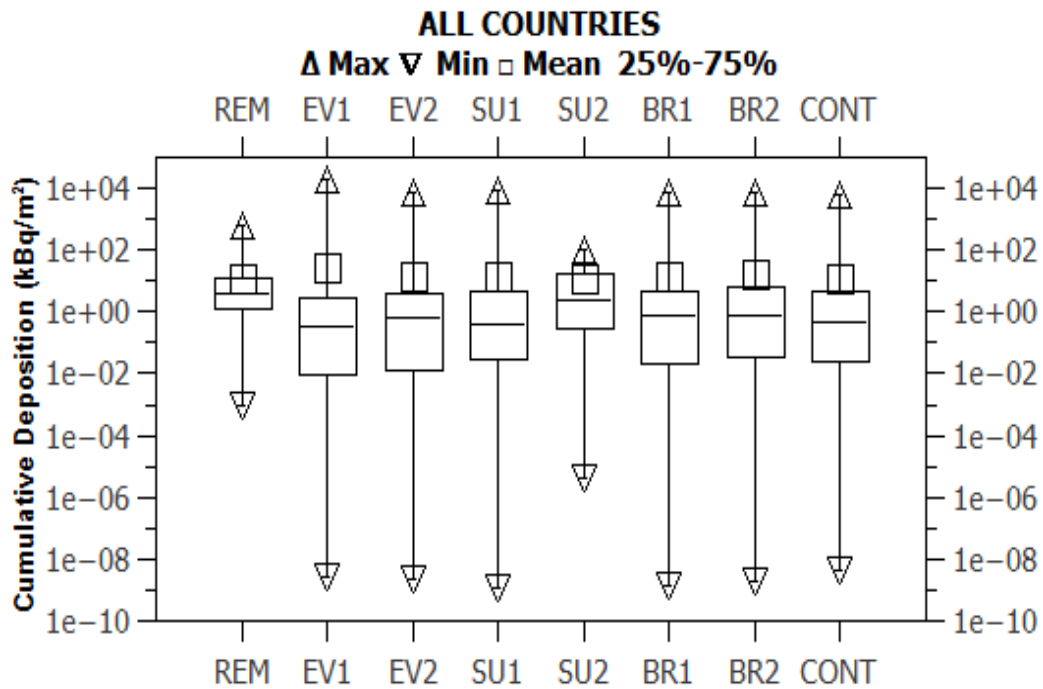


Figure 4.7: Box and Whisker plots of the cumulative deposition (kBq/m²) of ¹³⁷Cs.

Over Ukraine we found total deposition 17-25% larger with 0.2 cm/s dry deposition velocity, and 7-10% larger over Belarus. But the effect of dry deposition velocity can be different using different source terms, for example over Norway the effect of dry deposition is larger than 25% for BR2 and SU2, compared to BR1 and SU1, while less deposition is simulated in EV2 compared to EV1 (-11%). Similar feature is observed for Austria, with no effect of dry deposition velocity for the simulations SU1-SU2 and EV1-EV2, but a lower deposition of almost 30% in BR2 compared to BR1. Over Germany the total deposition is lower with higher dry deposition velocity, from 7% to 20%. The discrepancies between our model simulations and the Atlas can be due to several reasons: the exact emission values for Chernobyl are still not known (50% uncertainty was estimated for the emissions, de Cort et al., 1998), the heterogeneity of measurements used to generate the Atlas of ¹³⁷Cs deposition (Figure 3.4); and the smoothing methodology applied to the observations can be easily affected by the distribution of observational data points; the meteorological simulation can be also a source of possible differences in some specific regions, even if the general transport and precipitation patterns are well represented by the model (Section 3.1). Similar results were found by previous studies, Brandt et al. (2002), Suh et al. (2009), and Evangelidou et al. (2013), which used different methodologies.

Table 4.1 : Cumulative ¹³⁷Cs deposition results for Europe after CNPP accident (De Cort et al., 2008).

Country	(Cumulative Deposition Results (kBq/m ²))							
	Atlas (REM)	Simulations						
	SU1	BR1	EV1	cont 300 m	EV2	BR2	SU2	
Austria	1,60E+00	2,05E+00	1,80E+00	1,12E+00	6,48E-01	1,14E+00	1,29E+00	2,00E+00
Belarus	1,50E+01	5,30E+00	6,57E+00	4,42E+00	5,81E+00	4,72E+00	7,07E+00	5,86E+00
Belgium	1,00E-02	2,47E-03	1,76E-03	1,64E-03	4,22E-04	1,62E-03	2,17E-03	4,24E-03
Croatia	2,10E-01	1,38E-01	1,97E-01	1,56E-01	1,64E-01	1,36E-01	1,96E-01	1,30E-01
Czech Republic	3,40E-01	1,52E+00	1,74E+00	1,59E+00	3,64E-01	1,41E+00	1,48E+00	1,38E+00
Denmark	1,60E-02	1,61E-03	5,29E-04	6,71E-04	1,45E-05	4,55E-04	2,07E-03	6,40E-04
Estonia	5,10E-02	6,61E-01	8,25E-01	8,61E-01	2,49E-01	7,03E-01	7,46E-01	6,50E-01
Finland	3,10E+00	8,90E-01	8,54E-01	8,86E-01	4,03E-01	9,28E-01	8,96E-01	8,75E-01
France	3,50E-01	1,62E-01	8,03E-02	1,11E-01	4,80E-02	6,81E-02	7,36E-02	1,60E-01
Germany	1,20E+00	3,07E+00	2,80E+00	2,83E+00	4,87E-01	2,47E+00	2,60E+00	2,45E+00
Greece	6,90E-01	4,95E-01	3,02E-01	7,03E-01	4,77E-01	8,35E-01	7,97E-01	5,30E-01
Hungary	1,50E-01	7,90E-01	9,23E-01	9,29E-01	6,35E-01	9,85E-01	9,73E-01	7,43E-01
Ireland	2,10E-01	2,06E-03	3,84E-03	3,39E-03	6,53E-07	2,27E-03	3,22E-03	9,38E-04
Italy	5,70E-01	1,59E-01	1,08E-01	9,33E-02	4,68E-02	7,77E-02	7,68E-02	1,34E-01
Latvia	5,50E-02	1,29E-01	1,33E-01	1,38E-01	5,70E-02	2,17E-01	2,35E-01	1,36E-01
Lithuania	2,40E-01	1,38E-01	1,74E-01	2,01E-01	9,35E-02	3,74E-01	3,75E-01	2,60E-01
Luxembourg	3,00E-03	2,63E-03	1,11E-03	3,69E-03	5,27E-04	1,54E-03	5,91E-04	3,36E-03
Moldova	3,40E-01	1,97E-01	1,41E-01	2,76E-01	4,72E-01	5,35E-01	5,32E-01	3,46E-01
Netherlands	1,00E-02	2,70E-03	5,90E-04	3,15E-03	1,50E-04	9,28E-04	1,67E-03	2,40E-03
Norway	2,00E+00	8,88E-02	1,05E-01	1,09E-01	3,34E-02	9,70E-02	1,31E-01	1,18E-01
Poland	4,00E-01	1,73E+00	2,17E+00	1,98E+00	1,11E+00	2,17E+00	2,35E+00	2,00E+00
Romania	1,50E+00	3,61E+00	5,66E+00	4,90E+00	5,96E+00	5,19E+00	5,47E+00	3,74E+00
Slovakia	1,80E-01	5,63E-01	5,53E-01	4,56E-01	2,98E-01	4,96E-01	5,16E-01	5,35E-01

Table 4.1 (continued): deposition results for Europe after CNPP accident (De Cort et al., 2008).

Slovenia	3,30E-01	7,35E-02	7,99E-02	5,87E-02	4,96E-02	5,00E-02	5,01E-02	5,90E-02
Spain	3,10E-02	2,91E-03	6,91E-05	2,03E-03	5,39E-04	1,79E-03	1,10E-03	6,47E-04
Sweden	2,90E+00	6,99E-01	8,39E-01	7,22E-01	4,10E-01	9,54E-01	1,00E+00	8,61E-01
Switzerland	2,70E-01	1,23E-02	1,00E-02	8,92E-03	5,83E-03	6,63E-03	9,25E-03	1,14E-02
Ukraine	1,20E+01	1,34E+01	1,42E+01	1,12E+01	2,64E+01	1,38E+01	1,78E+01	1,58E+01
United Kingdom	5,30E-01	6,44E-03	1,31E-02	1,35E-02	9,89E-04	8,04E-03	1,09E-02	5,25E-03
TOTAL	4,43E+01	3,59E+01	4,03E+01	3,38E+01	4,42E+01	3,74E+01	4,46E+01	3,88E+01
Turkey (European side)	1,00E-01	6,05E-02	9,85E-02	8,16E-02	1,11E-01	1,08E-01	1,03E-01	7,34E-02
Turkey (All)	Not available	2,16E+00	3,56E+00	3,28E+00	2,78E+00	3,19E+00	3,00E+00	2,01E+00

4.2.3 Radiological doses over Europe

A brief description of the radiological doses due to ^{137}Cs after the CNPP accident is presented at the continental scale. Radiological doses for adults, child and infants were calculated according to two approaches described in Section 3.4. Over Europe the simulated (Figure 4.8) doses for adults and simulation BR1 (Figure A.9 and A10 for other simulations) are lower than 5 mSv/year, except in the vicinity of the CNPP, where adult doses goes up to 50 mSv/year and 33 mSv/year, for the UNSCEAR and WHO approaches, respectively.

The components that can determine the differences between two approaches are occupancy factors, external, internal and cloud gamma dose coefficients, as well as breathing rates. Nevertheless the largest difference between the two approaches is due to the external dose coefficients, since the effect of ^{137}Cs deposition contributes between 60% and 100% to the total dose. External dose coefficient used at WHO approach is $1.2 \times 10^{-8} \text{ Sv Bq}^{-1} \text{ year}^{-1} \text{ m}^{-2}$ for adults whereas this is $1.84 \times 10^{-8} \text{ Sv Bq}^{-1} \text{ year}^{-1} \text{ m}^{-2}$. The ratio between these coefficients is 65%. This is nearly the same ratio between the dose results from the two approaches.

For both approaches external exposure from ground deposition is by far the dominant pathway contributing to effective dose, as reported also by WHO (2012). Another reason making external dose dominant is the longer duration of exposure from deposited material. The inhalation and cloud gamma doses are calculated only for the travel time of contaminated air (from few days to some weeks), while the external dose is normally estimated at least for one year after the accident.

With UNSCEAR approach and BR1 simulation, the first year doses were estimated separately for adults, up to 49.726 mSv, children, up to 49.647 mSv, and infants, up to 49.586 mSv. With WHO approach and BR1 simulation, maximum dose results were 33.041 mSv for adults, 32.809 mSv for children, and 43.502 for infants. Differences doses between different age groups are due to breathing rates and occupancy factors. On the other hand the WHO approach considers a higher external dose coefficient for infants, with total doses 30% larger than adult doses.

Table 4.2 presents the calculated maximum adult dose results for all simulations with two approaches. As indicated above, higher dry deposition velocity increased

deposition of ^{137}Cs closer to CNPP, and consequently higher dose values (BR2, EV2, SU2, and CONT300). The maximum adult dose in CONT300 simulation is two times higher than the maximum dose of the other simulations. This is a result of deposition of most of the ^{137}Cs in vicinity of CNPP, but this scenario is the less realistic of the all set of simulations.

Table 4.2: Calculated maximum adult doses.

Approach	Maximum adult dose values (mSv/year)						
	BR1	BR2	EV1	EV2	SU1	SU2	CONT300
UNSCEAR	49.726	61.972	40.741	42.703	47.174	48.904	125.13
WHO	33.041	41.228	27.129	28.463	31.396	32.579	83.144

As presented at Figure 4.7 calculated doses also represent the spread of the plume. Higher radiation doses in the Baltic and Scandinavian region are found, as the winds direction was toward northeast for the first two days after the CNPP accident. High doses were found also over Central and Eastern Europe countries, which were reached by a second plume. After 1st of May wind direction mainly changed toward south, affecting the doses in the Balkan Peninsula, Black Sea and Turkey. But generally it is possible to say that the accident caused whole continent to receive doses. In some regions of Ukraine, Belarus doses were around 1 mSv/year and higher than 5 mSv/year. The other main countries in the three regions described above show doses between 0.1 mSv/year and 1 mSv/year. The radiological doses for Turkey will be discussed in Section 4.3.

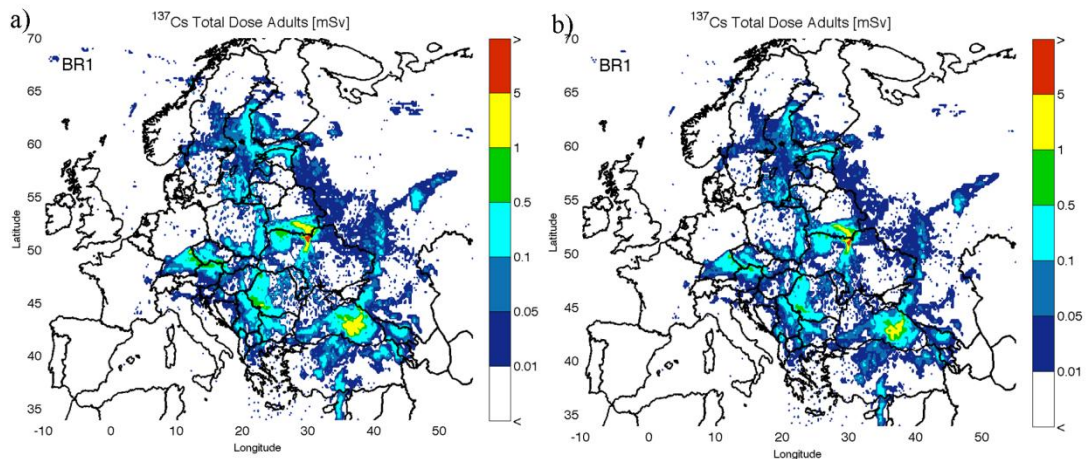


Figure 4.8: Effective dose values for Europe for two approaches. a) UNSCEAR Approach, b) WHO Approach.

4.3 Air concentrations and deposition of ^{137}Cs over Turkey

4.3.1 Air concentrations and deposition of ^{137}Cs over Turkey

In this section we focus on air concentrations and deposition of ^{137}Cs over Turkey, a country which was interested by the radioactive cloud for large part of its territory (Figure 4.3, from 03/05/1986 to 08/05/1986), but only a small fraction of Turkey (the European part) was included in the Atlas of Caesium deposition, with values ranging between 2 and 10 kBq/m². The total deposition estimated in the Atlas for the European part of Turkey is 0.1 PBq, while the simulated total deposition is ranging between 0.06 and 0.11 PBq. The estimate in the Atlas is based on a single measurement available in the Turkish territory. Over Greece, where almost 2000 observations were available, the simulated ^{137}Cs total deposition values were ranging between 0.3 PBq and 0.83 PBq, fairly similar to the Atlas, 0.69 PBq (Table 4.1). This gives some confidence on the simulation of the radioactive cloud transport to the South of the CNPP. On the 30th of April with the change of wind direction toward south the radioactive cloud emitted from Chernobyl moved towards the Balkan peninsula and reaching the European part of Turkey on the 2nd of May (Figure 4.3, BR1 simulation) and staying on Western Turkey until the 4th of May, with air concentrations generally below 1 Bq/m³. On the 4th of May the main radioactive cloud is crossing the Black Sea and reaching the Eastern part of Turkey and ^{137}Cs air concentrations are transported from North Eastern to North Western Turkey for the following 2 days, with concentrations larger than 10 Bq/m³. On the 7th of May concentrations larger than 10 Bq/m³ are found again in the European part of Turkey and in the South West on the 8th of May. Figure 4.9 shows the simulated average daily air concentrations of ^{137}Cs over Turkey. The averages are calculated over each grid cell for the days with ^{137}Cs concentrations larger than zero.

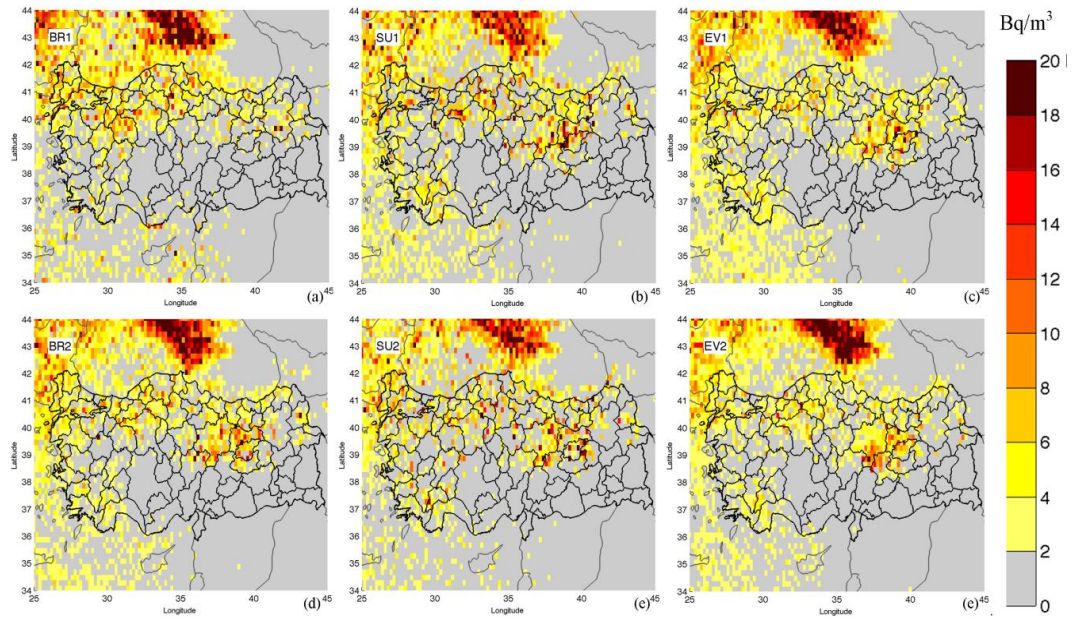


Figure 4.9: Mean ^{137}Cs air concentration values for Turkey.

All the simulations show the main impact of CNPP accident in North Turkey, from East to West, and also in South West Turkey. Some differences are found when analyzing single provinces, but in general the main affected regions are the European part of Turkey, the Black Sea costs, but also some provinces in Central and East Anatolia, with values which are generally below 4 Bq/m^3 , but can reach 20 Bq/m^3 in some grid cells. Using dry deposition velocity of 0.2 cm/s (BR2, SU2, and EV2) is not changing significantly the air concentration distribution. The ^{137}Cs air concentrations and deposition amounts averaged over 6 experiments and for each Turkish province are provided in the Appendices B at Tables B2, B3, B4, B5, B6, and B7 and for BR1 simulation at Table 4.3.

Figure 4.10 shows the deposition values for 6 different simulations. The total ^{137}Cs deposition over Turkey during the entire episode is ranging between 2 PBq and 3.5 PBq (2.8 PBq average of 6 experiments, excluding CONT300), which would rank Turkey as the fourth country in Europe in terms of cumulative ^{137}Cs deposition (fifth if we compare the mean of model simulations with the values in the Atlas, Table 4.3).

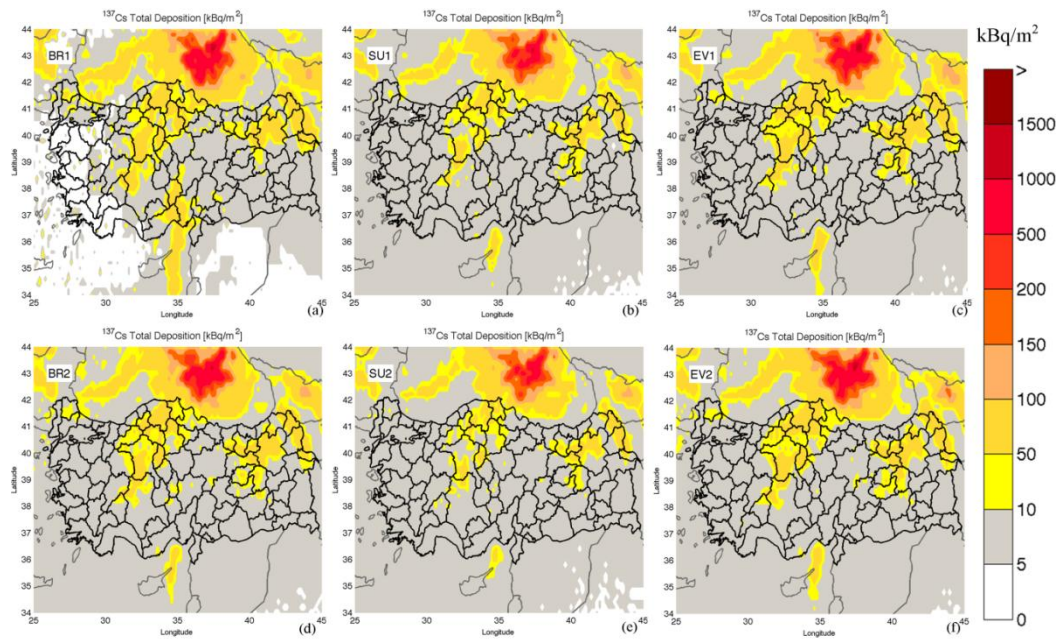


Figure 4.10: Total ^{137}Cs deposition amounts of Turkey with 6 different simulations.

We should note that the deposition of ^{137}Cs is high in all simulations over the Black Sea, with values up to 1000 kBq/m^2 . Similar patterns and values were found by Brandt et al. (2002) based on subgrid-scale averaging for wet deposition and a simple method for dry deposition. Their study showed that the effect of wet deposition is larger than dry deposition for the simulations based on precipitation rates which is partially simulated at our study. High deposition values over the Black Sea could be important through the effects on the food chain and people, but this aspect is not addressed in this study. Compared to the distribution of ^{137}Cs air concentrations, the deposition occurs in all simulations mainly over two regions with values between 10 kBq/m^2 and 100 kBq/m^2 , in East Turkey (mainly the provinces of Ardahan, Kars, Iğdir, Erzurum, Bayburt), and a region which is going from central coasts of Black Sea (i.e. Sinop, Kastamonu, and Samsun) towards south west until Ankara and Konya. In BR1 simulation deposition values larger than 10 kBq/m^2 are also simulated in a small region of South Turkey (Adana, Nigde, and Mersin). The simulations with 0.2 cm/s dry deposition velocity do not show significant differences compared to the corresponding simulations with 0.1 cm/s dry deposition velocity.

Table 4.3: BR1 Simulation results for Turkish Provinces.

City	Mean Deposition (Bq/m ²)	Total Deposition (Bq)	Mean Air Concentration (Bq/m ³)
NIGDE	2,298E+04	1,682E+14	3,178E-02
IGDIR	2,000E+04	7,049E+13	5,198E-02
KARS	1,773E+04	1,701E+14	1,504E-01
ARDAHAN	1,602E+04	8,508E+13	5,217E-02
KASTAMONU	1,488E+04	1,943E+14	6,389E-01
BAYBURT	1,299E+04	4,824E+13	4,665E-01
KIRIKKALE	1,270E+04	6,001E+13	3,694E-01
ERZURUM	1,138E+04	2,830E+14	3,958E-01
ANKARA	1,137E+04	2,874E+14	5,087E-01
ÇORUM	1,136E+04	1,449E+14	9,907E-01
ADANA	1,133E+04	1,591E+14	6,643E-02
İÇEL	1,021E+04	1,639E+14	6,350E-02
KARABK	1,003E+04	4,060E+13	5,530E-01
SAMSUN	9,476E+03	9,299E+13	1,230E+00
ARTVIN	9,183E+03	6,763E+13	2,515E-01
ÇANKIRI	9,092E+03	6,625E+13	9,003E-01
SINOP	8,959E+03	5,103E+13	5,949E-01
AMASYA	8,913E+03	4,979E+13	9,068E-01
KONYA	6,365E+03	2,564E+14	7,448E-02
KIRKLARELI	5,628E+03	3,647E+13	7,133E-01
OSMANIYE	5,493E+03	1,759E+13	6,851E-03
KIRSEHIR	5,387E+03	3,535E+13	1,453E-01
GIRESUN	5,313E+03	3,716E+13	6,402E-01
BOLU	5,224E+03	4,405E+13	7,472E-01
ISPARTA	5,200E+03	4,683E+13	1,814E-01
GÜMÜSHANE	5,023E+03	3,391E+13	6,538E-01
ISTANBUL	4,925E+03	2,567E+13	1,040E+00
AGRI	4,623E+03	5,185E+13	1,077E-01
ERZINCAN	4,366E+03	5,146E+13	2,630E-01
BINGÖL	4,120E+03	3,469E+13	5,310E-02
TEKIRDAG	3,862E+03	2,445E+13	1,006E+00
ESKISEHIR	3,815E+03	5,266E+13	1,037E+00
YOZGAT	3,713E+03	5,115E+13	1,910E-01
HATAY	3,433E+03	1,910E+13	7,496E-02
RIZE	3,172E+03	1,203E+13	5,809E-01
TOKAT	3,135E+03	3,224E+13	5,725E-01
KAYSERI	2,670E+03	4,528E+13	3,259E-02
AFYON	2,652E+03	3,794E+13	3,322E-01
BARTIN	2,563E+03	5,829E+12	7,772E-01
ORDU	2,491E+03	1,491E+13	1,029E+00
YALOVA	2,467E+03	1,869E+12	8,693E-01
KARAMAN	2,437E+03	2,131E+13	3,654E-02
TRABZON	2,300E+03	1,055E+13	9,976E-01
GAZIANTEP	1,965E+03	1,299E+13	1,814E-02

Table 4.3 (continued): BR1 Simulation results for Turkish Provinces.

ADIYAMAN	1,904E+03	1,431E+13	6,892E-03
USAK	1,862E+03	1,007E+13	4,258E-01
NEVSEHIR	1,833E+03	1,001E+13	1,102E-01
EDIRNE	1,823E+03	1,127E+13	1,286E+00
BILECIK	1,761E+03	7,361E+12	1,090E+00
K.MARAS	1,674E+03	2,435E+13	1,280E-02
DÜZCE	1,660E+03	4,439E+12	8,351E-01
TUNCELI	1,550E+03	1,180E+13	1,933E-01
ZONGULDAK	1,539E+03	5,074E+12	6,822E-01
KÜTAHYA	1,515E+03	1,765E+13	6,401E-01
SAKARYA	1,478E+03	7,180E+12	7,197E-01
DENIZLI	1,447E+03	1,697E+13	2,232E-01
SIVAS	1,429E+03	3,985E+13	2,999E-01
BURSA	1,324E+03	1,447E+13	7,114E-01
AKSARAY	1,150E+03	9,300E+12	1,263E-02
MUS	7,716E+02	6,548E+12	6,097E-02
KILIS	7,438E+02	1,057E+12	6,481E-03
DIYARBAKIR	6,927E+02	1,063E+13	3,834E-03
SANLIURFA	6,560E+02	1,266E+13	9,751E-03
BITLIS	6,145E+02	5,105E+12	1,111E-06
ELAZIG	5,803E+02	5,404E+12	4,386E-02
MANISA	4,922E+02	6,544E+12	2,015E-01
MUGLA	4,828E+02	6,143E+12	2,113E-01
MALATYA	4,436E+02	5,335E+12	1,883E-02
MARDIN	3,845E+02	3,380E+12	6,355E-04
KOCAELI	3,690E+02	1,257E+12	7,687E-01
ANTALYA	3,288E+02	6,768E+12	1,077E-01
VAN	2,366E+02	4,934E+12	3,748E-05
SIIRT	2,322E+02	1,382E+12	9,581E-08
BATMAN	2,263E+02	1,015E+12	6,870E-12
BALIKESIR	2,126E+02	3,096E+12	3,832E-01
SIRNAK	1,690E+02	1,189E+12	3,684E-03
IZMIR	6,968E+01	8,466E+11	2,896E-01
ÇANAKKALE	6,815E+01	6,731E+11	7,327E-01
HAKKARI	2,598E+01	1,835E+11	8,889E-05
AYDIN	2,563E+01	2,059E+11	9,307E-02
BURDUR	3,839E-01	2,714E+09	1,059E-01

4.3.2 Radiological doses of ¹³⁷Cs over Turkey

The effective radiation doses affecting adults, child (<10 years age), and infants (<1 year age) in Turkey were calculated using the formulas described in Section 2.3. Mean effective dose values for 6 simulations (CONT300 excluded) for Turkey are shown in Figure 4.11. Effective doses are calculated with two approaches using the simulated ¹³⁷Cs air concentrations and deposition, the differences between doses of

adults, child and infants are due to breathing rate and occupancy factor (Section 2.3). The mean effective doses over Turkey for adults vary between 1.40×10^{-4} mSv/year and 1.15×10^{-1} mSv/year for the first approach (UNSCEAR), and between 9.36×10^{-5} mSv/year and 7.56×10^{-2} mSv/year for the second approach (WHO). The WHO approach results in smaller effective doses over Turkey, between 66% and 77% of the UNSCEAR results. The distribution of effective doses reflects more the ^{137}Cs deposition than the air concentrations. External radiation from ground deposition has a contribution on total dose between 25%-100%, while inhalation has a contribution between 0.1% and 74%. Compared with ground deposition and inhalation, cloud gamma has a smaller effect on total dose with a value smaller than 1%. Almost all Turkey was interested by the CNPP radioactive cloud, according to our simulations only few provinces in the South East were not affected, for all North and East of Turkey the effective doses are ranging between 0.01 mSv/year and 0.1 mSv/year, with few provinces above 0.1 mSv/year. The largest values were found in the Northern part of Turkey (Ardahan, Bayburt, Kastamonu), and in Central and East Anatolia (Kars, Kirikkale, Iğdir, Erzurum). The effect of dry deposition velocity on effective doses is not large, but can be visible in some provinces due to higher ^{137}Cs air concentrations simulated with 0.1 cm s^{-1} dry deposition velocity, for example in South Western Turkey. Table 4.4 and Table 4.5 list the effective doses affecting adults averaged over 6 simulations (CONT300 excluded) for each Turkish province, together with minimum and maximum effective dose in the provinces and standard deviation (Effective radiological dose results of 7 simulations with both approaches are provided at Appendices B at Tables B8, B9, B10, B11, B12, B13, B14, B15, B16, B17, B18, B19, B20, and B21). De Cort et al. (1998) estimated that an effective dose of 0.01-0.02 mSv corresponds to a ^{137}Cs deposition of 10 kBq/m^2 and 0.1-0.2 mSv to 100 kBq/m^2 . These values are similar with our effective dose calculations, which include also the effect of air concentrations, but do not include the effect due to ingestion of contaminated food and water. Over Turkey we found deposition generally below 10 kBq/m^2 and only in two regions between 10 and 100 kBq/m^2 , with corresponding doses below 0.1 mSv/year. The effective doses estimated for Turkey are lower compared to the 4.2 mSv considered as the per capita dose in Europe from other sources of radiation exposure, such as cosmic radiation, medicine diagnosis and therapy, terrestrial radiation (De Cort et al., 1998). Annual natural

background doses of humans worldwide is on average 2.4 mSv, with a typical range of 1–10 mSv, while the average accumulated effective doses from Chernobyl fallout was approximately 50 mSv and more for residents of ‘strict-control zones’ and 10-20 mSv for residents of other contaminated area in Ukraine and Belarus. For other countries in Europe, excluding Turkey, the estimated per capita effective dose was 0.3 mSv, over the 1986–2005 time period (Balonov and Bouville, 2013). Maximum doses calculated in our simulations did not exceed 1 mSv, which is the annual effective dose limit according to the International Commission on Radiological Protection (ICRP, 1991).

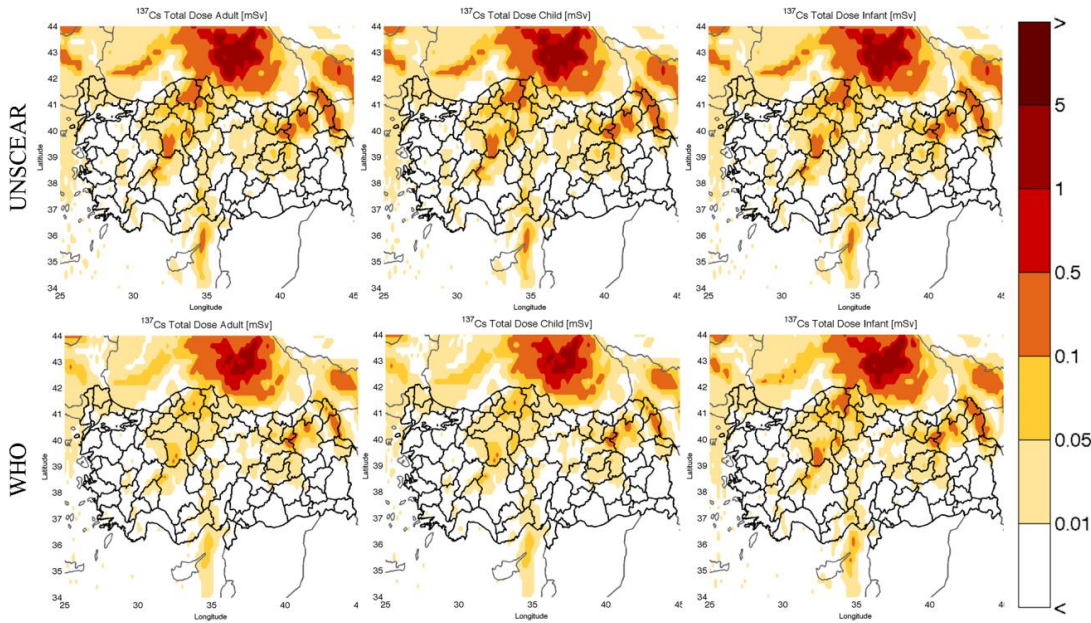


Figure 4.11: Mean ^{137}Cs effective dose values for 6 simulations (CONT300 excluded) for adults (left), child (b10 years age, center), and infants (b1 year age, right), and with UNSCEAR (top) and WHO (bottom) methodologies.

Table 4.4: Mean, minimum, maximum, and standard deviation (6 simulations) of ^{137}Cs adult dose values (mSv/year) for each province in Turkey (UNSCEAR approach).

PROVINCE	Mean	Min	Max	Std.dev	PROVINCE	Mean	Min	Max	Std.dev
ARDAHAN	1,149E-01	7,829E-02	1,483E-01	2,454E-02	MALATYA	1,202E-02	2,950E-03	2,009E-02	5,074E-03
BAYBURT	1,113E-01	8,632E-02	1,337E-01	2,046E-02	USAK	1,172E-02	8,931E-03	1,387E-02	1,892E-03
KASTAMONU	9,516E-02	6,767E-02	1,281E-01	1,983E-02	ZONGULDAK	1,141E-02	6,844E-03	1,551E-02	3,448E-03
KARS	8,971E-02	6,396E-02	1,175E-01	1,797E-02	DIYARBAKIR	1,013E-02	4,591E-03	1,359E-02	3,417E-03
KIRIKKALE	8,808E-02	6,217E-02	1,156E-01	1,765E-02	DENIZLI	1,008E-02	6,598E-03	1,363E-02	2,106E-03
SINOP	8,131E-02	5,970E-02	1,181E-01	2,027E-02	TOKAT	9,809E-03	4,098E-03	2,111E-02	5,442E-03
IGDIR	7,094E-02	4,179E-02	1,325E-01	2,976E-02	KAYSERI	9,644E-03	6,459E-03	1,770E-02	4,027E-03
ERZURUM	6,956E-02	5,022E-02	8,143E-02	1,268E-02	BURDUR	9,427E-03	9,083E-05	1,584E-02	5,276E-03
KARABÜK	6,703E-02	4,554E-02	8,262E-02	1,279E-02	CANAKKALE	8,685E-03	8,877E-04	1,490E-02	4,684E-03
ANKARA	6,652E-02	4,271E-02	8,595E-02	1,605E-02	TRABZON	8,611E-03	4,634E-03	1,583E-02	3,483E-03
CANKIRI	6,055E-02	4,159E-02	7,905E-02	1,198E-02	SAKARYA	8,576E-03	5,514E-03	1,157E-02	2,241E-03
CORUM	6,044E-02	3,904E-02	7,587E-02	1,292E-02	ORDU	8,530E-03	3,436E-03	1,711E-02	4,429E-03
ARTVIN	5,661E-02	3,765E-02	6,751E-02	1,012E-02	AYDIN	8,247E-03	2,385E-04	1,312E-02	4,461E-03
ERZINCAN	4,806E-02	2,908E-02	6,462E-02	1,408E-02	HATAY	8,176E-03	3,872E-03	2,279E-02	6,574E-03
BOLU	4,565E-02	3,059E-02	5,897E-02	1,164E-02	MUGLA	7,576E-03	3,799E-03	1,197E-02	2,891E-03
SAMSUN	4,415E-02	2,367E-02	6,350E-02	1,260E-02	BILECIK	7,332E-03	4,594E-03	1,231E-02	2,816E-03
BINGOL	4,249E-02	2,732E-02	5,248E-02	8,554E-03	OSMANIYE	7,268E-03	9,505E-04	3,639E-02	1,303E-02
GUMUSHANE	4,205E-02	2,846E-02	5,349E-02	9,925E-03	IZMIR	6,783E-03	6,340E-04	1,180E-02	3,526E-03
AMASYA	3,533E-02	2,365E-02	5,958E-02	1,170E-02	KUTAHYA	6,760E-03	4,049E-03	1,042E-02	2,069E-03
NIGDE	3,255E-02	6,750E-03	1,522E-01	5,355E-02	ANTALYA	6,510E-03	2,659E-03	1,061E-02	2,661E-03
TUNCELI	3,009E-02	1,038E-02	4,150E-02	1,144E-02	ADIYAMAN	6,141E-03	2,709E-03	1,262E-02	3,189E-03
KIRKLARELI	2,968E-02	2,136E-02	3,770E-02	5,792E-03	YALOVA	5,874E-03	3,603E-04	1,686E-02	5,474E-03
GIRESUN	2,963E-02	1,933E-02	3,558E-02	6,582E-03	KARAMAN	5,682E-03	1,504E-03	1,617E-02	5,024E-03
ELAZIG	2,622E-02	3,870E-03	4,014E-02	1,179E-02	BATMAN	5,041E-03	1,205E-03	1,164E-02	4,052E-03

Table 4.4 (continued): Mean, minimum, maximum, and standard deviation (6 simulations) of ^{137}Cs adult dose values (mSv/year) for each province in Turkey (UNSCEAR approach).

KONYA	2,397E-02	1,513E-02	4,221E-02	8,837E-03	BALIKESIR	4,943E-03	1,636E-03	7,624E-03	2,100E-03
ISPARTA	2,365E-02	1,555E-02	3,456E-02	6,241E-03	BURSA	4,715E-03	1,251E-03	9,193E-03	2,433E-03
ESKISEHIR	2,318E-02	1,443E-02	2,787E-02	5,135E-03	KOCAELI	4,593E-03	2,902E-03	7,312E-03	1,807E-03
KIRSEHIR	2,174E-02	1,044E-02	3,577E-02	8,755E-03	K.MARAS	4,269E-03	1,612E-03	1,110E-02	3,163E-03
RIZE	2,098E-02	1,650E-02	2,611E-02	3,146E-03	AKSARAY	4,248E-03	2,570E-03	7,623E-03	1,648E-03
ISTANBUL	2,050E-02	1,292E-02	3,325E-02	6,232E-03	MANISA	4,161E-03	2,445E-03	5,895E-03	1,269E-03
ICEL	2,049E-02	7,779E-03	6,770E-02	2,118E-02	MUS	3,994E-03	1,981E-03	5,167E-03	1,145E-03
TEKIRDAG	1,955E-02	1,229E-02	2,618E-02	4,425E-03	GAZIANTEP	3,476E-03	1,355E-03	1,303E-02	4,276E-03
AGRI	1,780E-02	9,055E-03	3,069E-02	6,706E-03	SANLIURFA	2,636E-03	2,046E-03	4,351E-03	7,865E-04
NEVSEHIR	1,701E-02	8,873E-03	2,430E-02	5,577E-03	KILIS	2,048E-03	5,305E-04	4,931E-03	1,450E-03
DUZCE	1,679E-02	1,068E-02	2,656E-02	5,924E-03	BITLIS	1,932E-03	5,496E-04	4,071E-03	1,116E-03
YOZGAT	1,592E-02	8,812E-03	2,471E-02	4,823E-03	MARDIN	1,828E-03	6,962E-04	2,547E-03	6,281E-04
BARTIN	1,575E-02	9,957E-03	1,852E-02	2,860E-03	VAN	1,665E-03	1,391E-03	2,146E-03	2,903E-04
ADANA	1,452E-02	1,579E-03	7,510E-02	2,710E-02	SIIRT	8,020E-04	2,765E-04	1,538E-03	4,175E-04
SIVAS	1,426E-02	9,647E-03	1,913E-02	3,766E-03	SIRNAK	7,588E-04	5,085E-04	1,122E-03	2,149E-04
EDIRNE	1,414E-02	8,420E-03	2,049E-02	4,008E-03	HAKKARI	1,423E-04	3,185E-05	2,621E-04	7,272E-05
AFYON	1,350E-02	6,757E-03	1,777E-02	4,457E-03					

Table 4.5: Mean, minimum, maximum, and standard deviation (6 simulations) of ^{137}Cs adult dose values (mSv/year) for each province in Turkey (WHO Approach).

PROVINCE	Mean	Min	Max	Std.dev	City	PROVINCE	Min	Max	Std.dev
ARDAHAN	7,564E-02	5,155E-02	9,758E-02	1,61E-02	MALATYA	8,447E-03	1,958E-03	1,423E-02	3,631E-03
BAYBURT	7,350E-02	5,721E-02	8,810E-02	1,34E-02	ZONGULDAK	7,928E-03	4,656E-03	1,053E-02	2,305E-03
KASTAMONU	6,295E-02	4,473E-02	8,471E-02	1,31E-02	USAK	7,896E-03	5,934E-03	9,269E-03	1,294E-03
KARS	5,920E-02	4,224E-02	7,734E-02	1,18E-02	DENIZLI	7,177E-03	4,970E-03	9,760E-03	1,416E-03
KIRIKKALE	5,819E-02	4,123E-02	7,617E-02	1,15E-02	BURDUR	7,068E-03	2,298E-04	1,161E-02	3,760E-03
SINOP	5,378E-02	3,988E-02	7,782E-02	1,33E-02	TOKAT	6,812E-03	2,963E-03	1,452E-02	3,717E-03
IGDIR	4,673E-02	2,756E-02	8,705E-02	1,95E-02	DIYARBAKIR	6,703E-03	3,019E-03	8,995E-03	2,264E-03
ERZURUM	4,590E-02	3,312E-02	5,367E-02	8,37E-03	CANAKKALE	6,673E-03	1,433E-03	1,091E-02	3,168E-03
KARABUK	4,456E-02	3,032E-02	5,474E-02	8,47E-03	KAYSERI	6,613E-03	4,499E-03	1,166E-02	2,596E-03
ANKARA	4,416E-02	2,844E-02	5,689E-02	1,06E-02	SAKARYA	6,209E-03	3,948E-03	8,138E-03	1,562E-03
CANKIRI	4,054E-02	2,772E-02	5,292E-02	8,01E-03	TRABZON	6,188E-03	3,287E-03	1,155E-02	2,565E-03
CORUM	4,029E-02	2,595E-02	5,096E-02	8,73E-03	AYDIN	6,164E-03	2,710E-04	9,458E-03	3,180E-03
ARTVIN	3,757E-02	2,497E-02	4,470E-02	6,71E-03	ORDU	6,141E-03	2,565E-03	1,243E-02	3,207E-03
ERZINCAN	3,236E-02	1,940E-02	4,350E-02	9,55E-03	MUGLA	5,659E-03	2,774E-03	8,757E-03	2,063E-03
BOLU	3,067E-02	2,041E-02	3,966E-02	7,84E-03	HATAY	5,410E-03	2,584E-03	1,505E-02	4,336E-03
SAMSUN	2,955E-02	1,589E-02	4,312E-02	8,56E-03	BILECIK	5,361E-03	3,265E-03	9,349E-03	2,165E-03
BINGOL	2,806E-02	1,800E-02	3,472E-02	5,67E-03	IZMIR	5,106E-03	7,524E-04	8,582E-03	2,445E-03
GUMUSHANE	2,804E-02	1,907E-02	3,551E-02	6,51E-03	ANTALYA	4,811E-03	1,894E-03	7,697E-03	1,900E-03
AMASYA	2,364E-02	1,568E-02	4,017E-02	7,97E-03	OSMANIYE	4,781E-03	6,278E-04	2,390E-02	8,554E-03
NIGDE	2,139E-02	4,443E-03	9,998E-02	3,52E-02	KUTAHYA	4,729E-03	2,764E-03	7,581E-03	1,561E-03
KIRKLARELI	2,076E-02	1,513E-02	2,558E-02	3,85E-03	YALOVA	4,479E-03	2,377E-04	1,208E-02	3,886E-03
TUNCELI	2,070E-02	7,039E-03	2,853E-02	7,91E-03	ADIYAMAN	4,081E-03	1,782E-03	8,291E-03	2,093E-03
GIRESUN	1,996E-02	1,291E-02	2,410E-02	4,48E-03	BALIKESIR	3,803E-03	1,519E-03	5,592E-03	1,465E-03
ELAZIG	1,755E-02	2,592E-03	2,686E-02	7,90E-03	KARAMAN	3,794E-03	1,041E-03	1,066E-02	3,289E-03
ISPARTA	1,592E-02	1,062E-02	2,290E-02	4,04E-03	BURSA	3,520E-03	9,651E-04	6,861E-03	1,789E-03

Table 4.5 (continued): Mean, minimum, maximum, and standard deviation (6 simulations) of ^{137}Cs adult dose values (mSv/year) for each province in Turkey (WHO Approach).

KONYA	1,581E-02	1,001E-02	2,780E-02	5,81E-03	KOCAELI	3,508E-03	2,249E-03	5,253E-03	1,177E-03
ESKISEHIR	1,568E-02	9,715E-03	1,857E-02	3,50E-03	BATMAN	3,310E-03	7,916E-04	7,643E-03	2,661E-03
KIRSEHIR	1,437E-02	6,941E-03	2,365E-02	5,77E-03	MANISA	3,052E-03	1,888E-03	4,241E-03	8,843E-04
RIZE	1,429E-02	1,131E-02	1,764E-02	2,12E-03	K.MARAS	2,864E-03	1,098E-03	7,300E-03	2,062E-03
ISTANBUL	1,400E-02	8,840E-03	2,303E-02	4,39E-03	AKSARAY	2,811E-03	1,702E-03	5,019E-03	1,078E-03
TEKIRDAG	1,370E-02	8,466E-03	1,835E-02	3,15E-03	MUS	2,644E-03	1,301E-03	3,450E-03	7,630E-04
ICEL	1,361E-02	5,251E-03	4,452E-02	1,39E-02	GAZIANTEP	2,297E-03	9,042E-04	8,576E-03	2,810E-03
AGRI	1,178E-02	6,010E-03	2,027E-02	4,42E-03	SANLIURFA	1,739E-03	1,351E-03	2,868E-03	5,179E-04
DUZCE	1,160E-02	7,085E-03	1,847E-02	4,06E-03	KILIS	1,355E-03	3,575E-04	3,245E-03	9,501E-04
NEVSEHIR	1,147E-02	6,168E-03	1,640E-02	3,72E-03	BITLIS	1,268E-03	3,608E-04	2,673E-03	7,328E-04
YOZGAT	1,071E-02	6,017E-03	1,644E-02	3,17E-03	MARDIN	1,206E-03	4,634E-04	1,673E-03	4,113E-04
BARTIN	1,070E-02	6,721E-03	1,235E-02	1,99E-03	VAN	1,095E-03	9,137E-04	1,417E-03	1,929E-04
EDIRNE	1,044E-02	6,406E-03	1,485E-02	2,73E-03	SIIRT	5,267E-04	1,815E-04	1,010E-03	2,741E-04
SIVAS	1,020E-02	6,681E-03	1,373E-02	2,74E-03	SIRNAK	4,993E-04	3,347E-04	7,407E-04	1,420E-04
ADANA	9,559E-03	1,042E-03	4,938E-02	1,78E-02	HAKKARI	9,361E-05	2,091E-05	1,731E-04	4,802E-05
AFYON	9,221E-03	4,680E-03	1,205E-02	2,99E-03					

5. CONCLUSIONS

The transport and deposition of ^{137}Cs over Europe occurred after the CNPP accident has been simulated using the WRF-HYSPLIT modeling system. The model results are compared to the Atlas of Caesium deposition on Europe after the Chernobyl accident (de Cort et al., 1998), which is the main reference study resulted from a joint effort to collect radiological data after the Chernobyl accident in several countries in Europe. The dispersion of the radioactive cloud over Europe has been compared as well with more recent studies (Brandt et al., 2002, Suh et al., 2009, Evangelidou et al., 2013), which used different modeling techniques. Totally seven WRF/HYSPLIT simulations were performed to assess the uncertainty associated to the vertical distribution of the emitted radionuclides and the dry deposition process. Four different vertical and temporal emission rate profiles have been tested, as well as two different dry deposition velocities, 0.1 cm/s and 0.2 cm/s, which are in the range of the literature values. An additional focus was given on ^{137}Cs deposition and air concentrations over Turkey, which closes a historic gap in the Atlas. The Anatolian peninsula was one of the main affected countries, but not included in the results of the Atlas, except for the small European part of Turkey. Radiological doses from simulated air concentrations and deposition has been estimated for Europe and Turkey according to two separate methodologies based on the UNSCEAR (1988) and WHO (2012) reports, respectively.

The main results are summarized in the following points:

- The transport of the radioactive cloud was simulated fairly well by the WRF-HYSPLIT modeling system. The meteorological simulation and the transport patterns agree with de Cort et al. (1998) and more recent studies discussed in this study. The distribution of air concentrations of ^{137}Cs agrees well with the measurements collected in the REM dataset (Figures 4.3, 4.5, and 4.7). Three main regions were involved by the radioactive cloud, the Scandinavian Peninsula, in the first days after the CNPP accident, East and Central Europe,

and after 5 days from the explosion the Balkan Peninsula and Turkey. All the simulations could not capture the ^{137}Cs concentrations at the same location of the measurements in Western Europe, but in some cases similar levels were predicted in close regions;

- The total deposition of ^{137}Cs during the entire episode is fairly well simulated compared to de Cort et al. (1998), which estimated 44.3 PBq deposited over Europe (Excluding Russia) based on the REM measurement dataset. The simulated total deposition is ranging between 33.8 PBq and 44.6 PBq for the seven WRF/HYSPLIT simulations. In the Atlas, 90% of the total deposition is distributed within 9 countries (Belarus, Ukraine, Finland, Sweden, Norway, Austria, Romania and Germany, Table 4.1). The same countries are generally found in all the simulations, except for Norway, Sweden (for all experiments with dry deposition velocity of 0.1 cm/s), Finland (only in CONT300 and BR2), and Germany in CONT300. In the simulations other countries are more affected by ^{137}Cs deposition (Poland, Czech Republic, and Hungary). Deposition is generally underestimated in Western Europe.
- The temporal and vertical distribution on the emission rates produce rather similar deposition and air concentration patterns, except for the unrealistic CONT300 experiment (constant emission rate at 300 m), which results in most of the deposition in Ukraine (26.4 PBq). Within the other experiments the variability associated to different source distribution is in the range of -8% -10% for total deposition over entire Europe and -30% and 20% in the countries with largest ^{137}Cs deposition. We must note that an uncertainty of 50% was estimated for the total amount of emitted radioactive material from CNPP (de Cort et al., 1998).
- The effect of dry deposition velocity was in the range of -10% for total deposition over Europe when using a value of 0.1 cm/s. The effect of dry deposition is also different when considering different emission distribution. As expected countries closer to the CNPP show smaller deposition values with 0.1 cm/s velocity (e.g. from -20% to -15% in Ukraine, from -10% to -6% in Belarus, and larger deposition values far from CNPP (e.g. from 8% to 25% in Germany).

- Turkey was not included in the Atlas of Caesium deposition over Europe, and, according to the simulations, is one of the countries with largest ^{137}Cs deposition in Europe. The radioactive cloud interested Turkey from the 2nd of May until the 8th of May, with mean air concentrations up to 25 Bq/m³ in the province of Edirne, and larger than 10 Bq/m³ in many provinces of Black Sea and Marmara regions. The total deposition over Turkey estimated in the set of simulations is ranging between 2 PBq (5% of total deposition in Europe) and 3.5 PBq (10% of total deposition in Europe), which would rank Turkey at the 5th place if compared to the country totals in the Atlas (de Cort et al., 1998). In all simulations mainly the ^{137}Cs deposition, with values between 10 kBq/m² and 100 kBq/m², occurs over two regions, in East Turkey, and a region which is going from central Anatolian coastline of Black Sea towards south west until the provinces of Ankara and Konya.
- Radiological effective doses have been estimated for Europe according to the simulated ^{137}Cs air concentrations and deposition for the first year. Calculations were done by using two different approaches, based on UNSCEAR and WHO reports. The results of the two approaches show very similar dose distribution patterns, while doses calculated according to the WHO report are in general lower from 23% to 34%. Almost all Europe was affected by radiological doses after the accident, with values below 0.01 mSv/year for the more distant regions from the CNPP, to values above 5 mSv/year in the vicinity of the CNPP.
- Almost all the Anatolian peninsula was interested by the CNPP radioactive cloud. According to our simulations only few provinces in the South East were not affected, adult effective doses reach values up to 0.15 mSv/year in North Eastern Turkey. The results of simulations EV1, EV2, SU1 shows that the province of Ardahan has the highest dose values reaching up to 0,148 mSv/year, whereas BR2 and SU2 give the highest value of effective radiation doses for the province of Bayburt. The dose values averaged over each province are highest around the Black Sea region, North and Central Anatolia. The lowest mean dose value was found for Hakkari. The deposited ^{137}Cs determines the largest part of the total radiological dose, almost 100% in some cases, while the cloud gamma (^{137}Cs air concentrations) generally

plays a minor role. The simulated dose values over the Anotolian peninsula due to the CNPP accident are very small compared to the 4.2 mSv/year, considered as the per capita effective dose in Europe from other sources of radiation exposure, and the ICRP (1995) annual mean effective dose limit of 1 mSv/year.

- In this study the estimated effective doses do not consider the ingestion of contaminated food and water. With a half life of 30 years ^{137}Cs can accumulate to soil and plant roots affecting agricultural products. In the long term the consumption of contaminated agricultural products will result in higher effects compared to the other exposure pathways. All the simulations indicated that one of the most affected region by total ^{137}Cs deposition was the Black Sea (Figure 4.10), with possible implications for the marine ecosystem and fisheries product.
- Nuclear power plant accidents are still a serious threat to world population and environment, as the Fukushima Nuclear Power Plant accident reminded us, recently. With increasing number of new nuclear power plants and the existing and obsolete power plants, like the Metsamor Nuclear Power Plant (Armenia), which is located in area with high seismic risk, a fast methodology to estimate accurately the dispersion and deposition of radioactive material is of high importance and it should be done in the future. In this study we have shown the capabilities of a methodology and associated uncertainties, which can be used for a quick emergency response.

REFERENCES

- Baklanov A., Jens Havskov Sørensen J.H., Mahura A.** (2008). Methodology for Probabilistic Atmospheric Studies using Long-Term Dispersion Modelling, *Environmental Modeling & Assessment*, 13 (4), 541-552, doi: 10.1007/s10666-007-9124-4
- Balonov M., Bouville A.** (2013). Radiation Exposures Due to the Chernobyl Accident, *Encyclopedia of Environmental Health*, pp.709-720, <http://dx.doi.org/10.1016/B978-0-444-52272-6.00086-6>
- Bedwell P, Wellings J. , Haywood M.S. and Hort M.C.** (2010). Cloud gamma modelling in the UK Met Office's NAME III model. *Proceedings of the 13th Conference on Harmonisation within Atmospheric Dispersion Modelling for Regulatory Purposes (HARMO13)*, Paris, France.
- Bennett B., Bouville A., Hall P., Savkin M. and Storm H.** (2000). Chernobyl Accident: Exposures and Effects, *International congress, IRPA 10 Hiroshima*, May 2000.
- Biegalski S. R., Hosticka B., Mason L. R.** (2001). Cesium-137 concentrations, trends, and sources observed in Kuwait City, Kuwait. *Journal of Radioanalytical and Nuclear Chemistry*, 248(3), 643–649.
- Brandt J., Christensen J. H., and Frohn L. M.** (2002). Modelling transport and deposition of caesium and iodine from the Chernobyl accident using the DREAM model, *Atmospheric Chemistry and Physics*, 2, 397–417.
- Cardis E., and Hatch M.** (2011).The Chernobyl accident — an epidemiological perspective, *Clinical Oncology*, 23, 251–260. <http://dx.doi.org/10.1016/j.clon.2011.01.510>
- Cetiner M.A. and Ozmen A.** (1995). Transfer of 137cs in tea and other foods to man after the Chernobyl accident in Turkey, *Radiation Physics and Chemistry*,46,(1), 77-82
- Chen, S. H., Dudhia, J., Kain, J. S., Kindap, T., & Tan, E.** (2008). Development of the online MM5 tracer model and its applications to air pollution episodes in Istanbul, Turkey and Sahara dust transport. *Journal of Geophysical Research*, 113, D11203. doi:10.1029/2007JD009244.
- De Cort, M., Dubois, G., Fridman, Sh. D., Germenchuk, M. G., Izrael, Yu. A., Janssens, A., Jones, A. R., Kelly, G. N., Kvasnikova, E. V., Matveenko, I. I., Nazarov, I. M., Pokumeiko, Yu. M., Sitak, V. A., Stukin, E. D., Tabachny, L. Ya., Tsaturov, Yu. S., and Avdyushin, S. I.** (1998). Atlas of caesium deposition on Europe after the Chernobyl accident, *Office for Official Publications of the European*

Communities EUR 16733, ISBN 92-828-3140-X, Catalogue number CG-NA-16-733-29-C., Luxembourg

- Draxler RR, Dietz R, Lagomarsino RJ, Start G.** (1991). Across North America tracer experiment (ANATEX): Sampling and analysis. *Atmospheric Environment*, 25A: 2815–2836.
- Draxler R., Stunder B., Rolph G., Stein A., Taylor A.** (2009). *Hysplit 4 user's guide (Version 4.9)*, NOAA, Silver Spring, MD.
- Draxler R.R., Hess G.D.**, (1997). *Description of the HYSPLIT_4 modeling system*. NOAA Tech. Memo. ERL ARL-224, pp 24, Silver Spring, MD.
- Devell L., Tovedal H., Bergström U., Appelgren A., Chyssler J. Andersson L.** (1986). Initial observations of fallout from the reactor accident at Chernobyl., *Nature*, 321, 192-193
- Eckerman K.F. and Sjoreen A.L.** (2006). *Radiological Toolbox User's Manual*, Oak Ridge National Laboratory U.S. Department of Energy
- Elisabeth C. , Krewski D., Boniol M., Drozdovitch V., , Darby S.C. , Gilbert E. S., Akiba S., Benichou J., Ferlay J., Gandini S., Hill C., Howe G. , Kesminiene A., Moser M., Sanchez M. , Storm H., Voisin L. and Boyle P.** (2006). Estimates of the cancer burden in Europe from radioactive fallout from the Chernobyl accident, *Int. J. Cancer*, 119, 1224–1235, Wiley-Liss, Inc.
- Environmental Protection Agency (EPA).** (1995). User's Guide for the Industrial Source Complex (ISC3) Dispersion Models. *I - III*. EPA-454/B-95-003a-c.
- Environmental Protection Agency (EPA).** (2011). Addendum to User's Guide of the AMS/EPA Regulatory Model AERMOD (version 11103), March 2011
- Evangelidou N., Balkanski Y., Cozic A. and Møller P.** (2013). *Simulations of the transport and deposition of 137 Cs after Chernobyl*, *Atmospheric Chemistry and Physics*, 13, 7681–7736 doi:10.5194/acpd-13-7681-2013
- Ferber GJ, Heffter JL, Lagomarsino RJ, Thomas FL, Dietz RN, Benkovitz CM.** (1986). *Cross-Appalachian tracer experiment (CAPTEX '83) final report, Technical Report*, ERL ARL-142, NOAA.
- Grell, G. A., Dudhia, J., & Stauffer, D. R.** (1995). *A description of the fifth-generation Penn State/NCAR mesoscale model (MM5)*. NCAR/TN-398 + STR. Boulder: National Center for Atmospheric Research.
- IAEA-RDS-1/32.** (2012). *Energy, Electricity and Nuclear Power Estimates for the Period up to 2050*, ISBN 978–92–0–133510–4 ISSN 1011–2642, Vienna
- IAEA-RDS-2/33.** (2013). *Nuclear Power Reactors In The World IAEA*, ISBN 978–92–0–144110–ISSN 1011–2642, Vienna
- IAEA TRS 42.** (2010). *Radiation Biology: A Handbook for Teachers and Students, Training Course Series 42*, ISSN 1018-5518, Vienna

- IAEA SRS 53.** (2008). *Derivation of the Source Term and Analysis of the Radiological Consequences of Research Reactor Accidents, Safety Report Series No:53* ISBN 978-92-0-109707-1, Vienna.
- IAEA RARS 1239.** (2006). *Environmental consequences of the Chernobyl accident and their remediation: twenty years of experience / report of the Chernobyl Forum Expert Group, Radiological assessment reports series No: 1239*, (ISSN 1020-6566) ISBN 92-0-114705-8, Vienna
- IAEA SRS 19.** (2001). *Generic models for use in assessing the impact of discharges of radioactive substances to the environment, Safety Report Series No:19*, Vienna.
- ICRP 38.** (1983) *Radionuclide Transformations - Energy and Intensity of Emissions. ICRP Publication 38.* Ann. ICRP 11-13
- ICRP 60.** (1991). *1990 Recommendations of the International Commission on Radiological Protection, ICRP publication 60.* Ann ICRP 21: 1-201.
- ICRP 66.** (1994). *Human Respiratory Tract Model for Radiological Protection. ICRP Publication 66,* Ann. ICRP 24 (1-3).
- ICRP Database of dose coefficients: workers and members of the public** (version 2.0.1) (2009).
- ICRP 72.** (1995). Age-dependent Doses to the Members of the Public from Intake of Radionuclides - Part 5 Compilation of Ingestion and Inhalation Coefficients. *ICRP Publication 72.* Ann. ICRP 26 (1).
- ICRP 74.** (1996). Conversion Coefficients for use in Radiological Protection against External Radiation. *ICRP Publication 74.* Ann. ICRP 26 (3-4).
- Im U., Markakis K., Unal A., Kindap T., Poupkou A., Incecik S., Yenigun O., Melas D., Theodosi C., Mihalopoulos N.** (2010). Study of a winter PM episode in Istanbul using the high resolution WRF/CMAQ modeling system, *Atmospheric Environment*, 44 (26), 3085-3094, doi:10.1016/j.atmosenv.2010.05.036
- Im, U., Markakis, K., Poupkou, A., Melas, D., Unal, A., Gerasopoulos, E., Daskalakis, N., Kindap, T., Kanakidou, M.** (2011). The impact of temperature changes on summer time ozone and its precursors in the Eastern Mediterranean, *Atmospheric Chemistry and Physics*, 11, 3847-3864, doi:10.5194/acp-11-3847-2011.
- Izrael Yu A., De Cort M., Jones A.R., Kelly G.N., Matveenko I.I., Pokumeiko Yu M., Tabatchnyi L.Ya, Tsaturov Yu.** (1996). The Atlas of Caesium-137 Contamination of Europe after the Chernobyl Accident, *Proceedings of the first international conference Minsk, Belarus*, 1-10, EUR 16544 EN.
- Kindap, T., Turuncoglu, U.U., Chen, S.H., Unal A. and Karaca, M.** (2009). Potential Threats from a Likely Nuclear Power Plant Accident: a Climatological Trajectory Analysis and Tracer Study. *Water Air Soil Pollution*, 198, 393-405. doi:10.1007/s11270-008-9853-2
- Kinley III D. and Diesner-Kuepfer A.** (2008). IAEA Division of Public Information: , Chernobyl's Legacy: Health, Environmental and

Socio-Economic Impacts and Recommendations to the Governments of Belarus, the Russian Federation and Ukraine, April 2006
IAEA/PIA.87 Rev.2 / 06-09181 The International Nuclear and Radiological Event Scale International Atomic Energy Agency, Vienna

- Knivel J.** (2005). The WRF Model, *ATEC Forecasters Conference*, Boulder, 5.
- Kortov V. and Ustyantsev Yu.** (2013). Chernobyl accident: Causes, consequences and problems of radiation measurements, *Radiation Measurements*, 55, 12-16, doi:10.1016/j.radmeas.2012.05.015.
- Lelieveld J., D. Kunkel D., Lawrence M. G.** (2012). Global risk of radioactive fallout after major nuclear reactor accidents, *Atmospheric Chemistry and Physics*, 12, 4245–4258, doi:10.5194/acp-12-4245-2012
- Magill J. and Galy J.** (2005). Radioactivity Radionuclide's Radiation, *Springer-Verlag Berlin Heidelberg and European Communities*, ISBN 3-540-21116-0, Karlsruhe
- McCraw, T.F.** (1965). The half time of Cesium in man, page 281 in Fallout Program Quarterly Summary Report, *HASL-164 (Health and Safety Laboratory, U.S. Atomic Energy Commission)* New York
- McCull, N. P. and Prosser, S. L.** (2012). *NRPB - W19 Emergency Data Handbook*, ISBN: 0-85951-490-0
- Mould RF.** (2000). *Chernobyl Record. The Definitive History of the Chernobyl Catastrophe*. Institute of Physics Publishing, Bristol.
- Moroz BE, Beck HL, Bouville A, Simon SL.** (2010). Predictions of dispersion and deposition of fallout from nuclear testing using the noaa-hysplit meteorological model, *Health Physics*, 99(2) doi:10.1097/HP.0b013e3181b43697
- NCRP 52.** (1977). National Council on Radiation Protection and Measurements, ¹³⁷Cs From The Environment to Man: Metabolism and Dose, *NCRP Report NO.52, National Council on Radiation Protection and Measurements*. Washington.
- NOAA** (2013). *A Complete Modeling System for Simulating Dispersion of Harmful Atmospheric Material*, National Oceanic and Atmospheric Administration, Air Resources Laboratory
- OECD/NEA.** (2002). *CHERNOBYL Assessment of Radiological and Health Impacts 2002 Update of Chernobyl: Ten Years On*. France
- Povinec P. P., Katsumi Hirose Michio Aoyama.** (2013). Fukushima Accident, *Radioactivity Impact on the Environment*, Pages 55–102, <http://dx.doi.org/10.1016/B978-0-12-408132-1.00003-6>
- Pröhl G., Ehlken S., Fiedler I., Kirchner G., Klemt E., Zibold G.** (2006). Ecological half-lives of 90Sr and 137Cs in terrestrial and aquatic ecosystems, *Journal of Environmental Radioactivity*, 91(1–2), 41–72., doi:10.1016/j.jenvrad.2006.08.004.

- Quelo, D.; Krysta, M.; Bocquet, M.; Isnard, O.; Minier, Y.; Sportisse, B.** (2007). Validation of the Polyphemus platform on the ETEX, Chernobyl and Algeciras cases. *Atmospheric Environment*, 41, 5300–5315. Cambray, R. S.; Cawse, P. A.; Garland, J. A.; Gibson, J. A. B.; Johnson, P.; Lewis, G. N. J.; Newton, D; Salmon, L; Wade, B. O.
- Robinson C.A.** (1996). *Generalised habit data for radiological assessments*, NRPB-M636 Chilton.
- Saenko V. Ivanov V. , Tsyb A., Bogdanova T., Tronko M. , Demidchik Yu., Yamashita S.** (2011). Overview The Chernobyl Accident and its Consequences, *Clinical Oncology*, 23, 234-243 doi:10.1016/j.clon.2011.01.502.
- Sadeghi N. and Sadrnia M.** (2011). Cancer risk assessment for Tehran research reactor and radioisotope laboratory with CAP88-PC code (Gaussian plume model), *Nuclear Engineering and Design*. 241, 1795–1798.
- Schnadt H., and Ivanov I.** (2012). Environmental Consequences and Management of a Severe Accident Nuclear Safety in Light Water Reactors, *Nuclear Safety in Light Water Reactor*, pp. 589-621, –124DOI: 10.1016/B978-0-12-388446-6.00007-1
- Schöppner M., Plastino W., Povinec P.P. , Wotawa G., Bella F., Budano A., Vincenzi M., Ruggieri F.** (2012). Estimation of the time-dependent radioactive source-term from the Fukushima nuclear power plant accident using atmospheric transport modeling, *Journal of Environmental Radioactivity* 114, 10-14, doi: 10.1016/j.jenvrad.2011.11.008.
- Schofield J.C.H.** (2012). *Mappping Nuclear Fallout Using the Weather Research & Forecasting (WRF) Model*, Air Force Institute of Technology Wright-Patterson Air Force Base, Ohio.
- Skamarock W.C., Klemp J. B., Dudhia J., Gill D.O., Barker D.M., Duda G.M., Huang X.Y., Wang W., Powers J.G.** (2008). *A Description of the Advanced Research WRF* (Version 3), National Center for Atmospheric Research, Boulder, Colorado, USA.
- Skamarock W.C. and Klemp J.B.** (2008). A time-split non-hydrostatic atmospheric model. *Journal of Computational Physics*, 227, 3465–3485.
- Stabin M.G.** (2008). Radiation protection and Dosimetry, *Springer Science+Business Media, LLC*, New York.
- Steinhauser G., Merz S., Hainz D., Sterba J. H.** (2013). Artificial radioactivity in environmental media (air, rainwater, soil, vegetation) in Austria after the Fukushima nuclear accident, *Environmental Science and Pollution Research*, 20(4), 2527-2534. doi: 10.1007/s11356-012-1140-5
- Steinhauser, G., Brandl, A., and Johnson, T. E.** (2014). Comparison of the Chernobyl and Fukushima nuclear accidents: A review of the environmental impacts, *Science of The Total Environment*, 470–471, 800–817, doi : 10.1016/j.scitotenv.2013.10.029S

- Stohl, A., Hittenberger M., Wotawa G.** (1998). Validation of the Lagrangian particle dispersion model FLEXPART against large scale tracer experiments. *Atmospheric Environment*, 32, 4245-4264.
- Suh K.S., Han M.H., Jung S.H. and Lee C.W.** (2009). Numerical simulation for a long-range dispersion of a pollutant using Chernobyl data, *Mathematical and Computer Modelling*, 4, 337–343.
- Svendsen E.R., Kolpakov I.E., Stepanova Y.I., Vdovenko V.Y., Naboka M.V., Mousseau T. A., Mohr L.C., Hoel D.G. and Karmaus W.J.J.** (2010). ¹³⁷Cesium Exposure and Spirometry Measures in Ukrainian Children Affected by the Chernobyl Nuclear Incident, *Environmental Health Perspectives*, 118, 720-725.
- Thakur P., Ballard S. and Nelson R.** (2013). An overview of Fukushima radionuclides measured in the northern hemisphere, *Science of the Total Environment*, 458–460, 577–613.
- Trapp J.V. and Krojn T.** (2008). An introduction to Radiation Protection in Medicine, *Taylor&Francis Group*, ISBN:978-1-58488-964-9, New York
- UNSCEAR.** (2000). *Exposures and effects of the Chernobyl accident* (Annex J).
- WHO (World Health Organization).** (2012). Preliminary dose estimation from the nuclear accident after the 2011 Great East Japan earthquake and tsunami, ISBN 978 92 4 150366, (http://whqlibdoc.who.int/publications/2012/9789241503662_eng.pdf)
- WU.** (2006). Principles of Radiation Protection, *Environmental Health and Safety, UW Environmental Health and Safety*, University Of Washington, Seattle
- UNSCEAR.** (1998). *United Nations Scientific Committee on the Effects of Atomic Radiation 1988 Report to the General Assembly*, with Annexes
- Url-1**<<http://www.euronuclear.org/info/encyclopedia/n/nuclear-power-plant-world-wide.html>>, date retrieved 27.02.2012
- Url-2**<<http://www.unscear.org/unscear/en/chernobyl.html>>, date retrieved 11.03.2014
- Url-3**<<http://www.unscear.org/unscear/en/chernobyl.html>>, date retrieved 29.06.2013
- Url-4**<<http://rem.jrc.ec.europa.eu/RemWeb/pastprojects/Atlas.aspx>>, date retrieved 19.03.2013
- Url-5**<<http://rem.jrc.ec.europa.eu/RemWeb/Download.aspx>>, date retrieved 19.03.2013
- Url-6** <<http://www.iaea.org>> date retrieved 15.04.2013
- Url-7**<<http://www.world-nuclear.org/info/Safety-and-Security/Safety-of-Plants/Chernobyl-Accident>>, date retrieved 11.03.2014
- Url-8**<<http://www.dalje.com>>, date retrieved 10.02.2014
- Url-9**<<http://www.oecd-nea.org/rp/chernobyl/c01.html>>, date retrieved 11.03.2014

- Url-10**<http://www.who.int/ionizing_radiation/chernobyl/background/en/, date retrieved 31.03.2014
- Url-11**<http://www.arl.noaa.gov/documents/Summaries/Dispersion_HYSPLIT.pdf> date retrieved 30.06.2012
- Wootton, R.** (2003). Radiation Protection of patients, *Cambridge University Press*, London
- van Dop H, Addis R, Fraser G, Girardi F, Graziani G, Inoue Y, Kelly N, Klug W, Kulmala A, Nodop K, Pretel J.** (1998). ETEX: A European tracer experiment; observations, dispersion modelling and emergency response, *Atmospheric Environment*, 32,4089–4094.
- Williams M., Wohlers D.W., Citra M., Diamond, G.L and SwartsS.G.** (2004). Toxicological profile for cesium, *U.S. Department of Health and Human Services Public Health Service Agency for Toxic Substances and Disease Registry*.
- Yamagata N. and Yamagata T.** (1960). The concentration of caesium-137 in human tissues and organs. *Bull.Inst.Public Health*, 9(2), 72. Tokyo
- Zhdanova N.N., Zakharchenko V.A., Haselwandter K.** (2005). Radionuclides and fungal communities. In: Dighton J, White JF, Oudemans P (eds). *The fungal community*, 3rd edn. CRC Press, Boca Raton, pp 759-768

APPENDICES

APPENDIX A: Maps

APPENDIX B: Tables

APPENDIX A: Maps

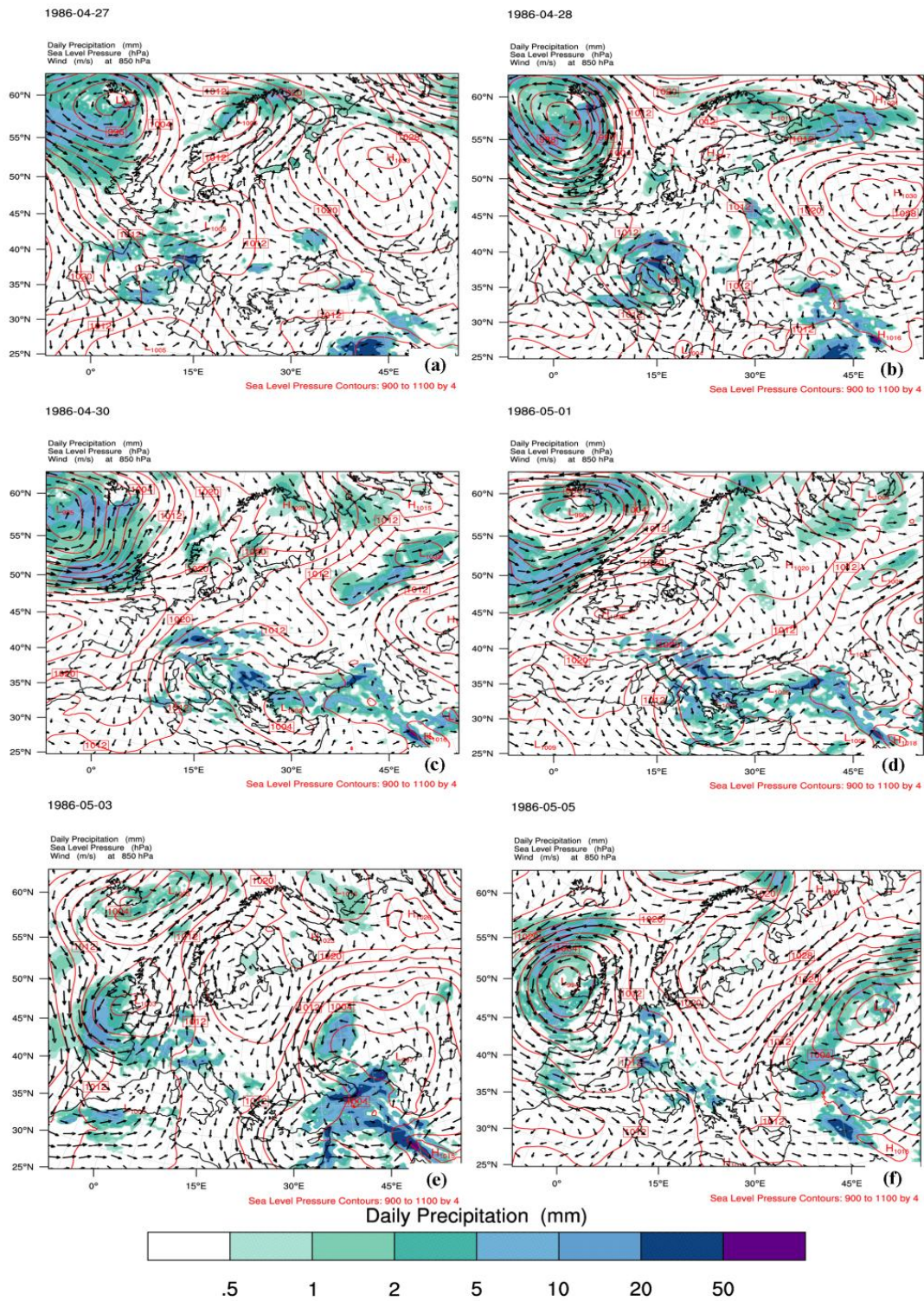


Figure A.1: Daily mean wind speed, sea level pressure and precipitation amounts for a) 27 April 1986. b) 28 April 1986. c) 30 April 1986. d) 01 May 1986. e) 03 May 1986. f) 05 May 1986.

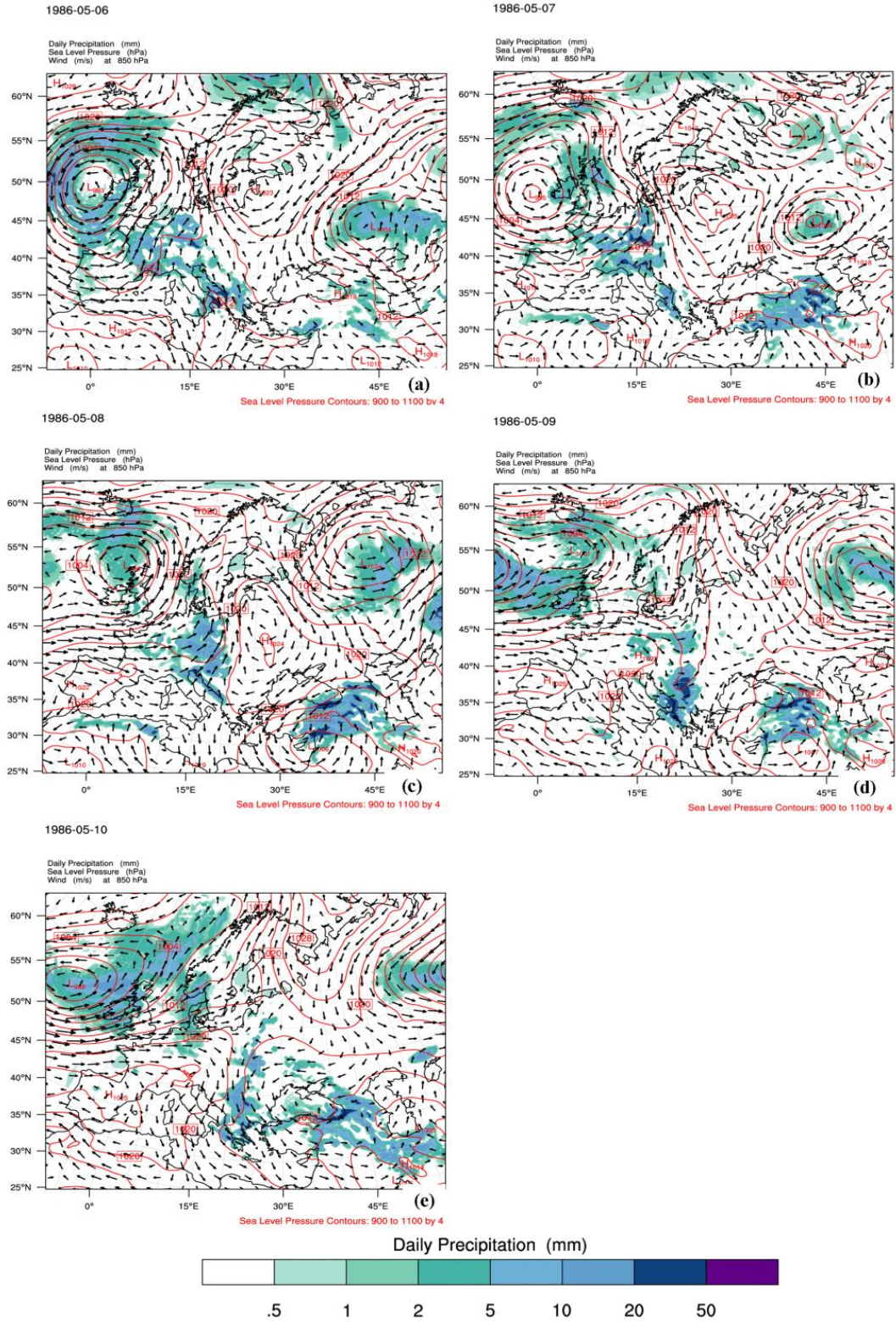


Figure A.2: Daily mean wind speed, Sea level pressure and precipitation amounts for: a) 06/05/1986. b) 07/05/1986. c) 08/05/1986. d) 09/05/1986. e) 10/05/1986.

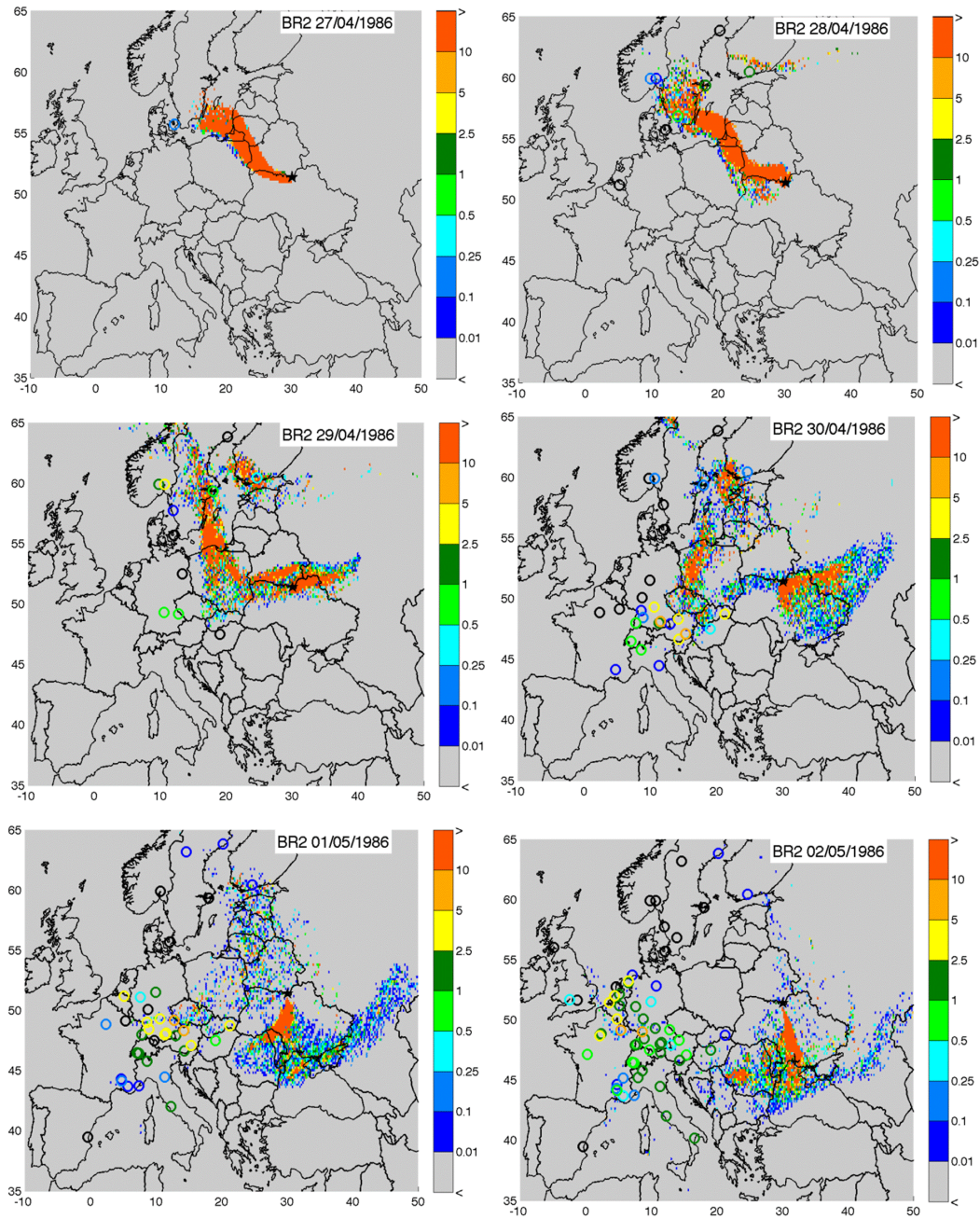


Figure A.3: Caesium-137 air concentrations [Bq/m^3] simulated by HYSPLIT at surface for the BR2 simulation, 27/04/1986–08/05/1986. REM measurements are plotted as colored open circles (black circles correspond to measurements below $0.01 \text{ Bq}/\text{m}^3$).

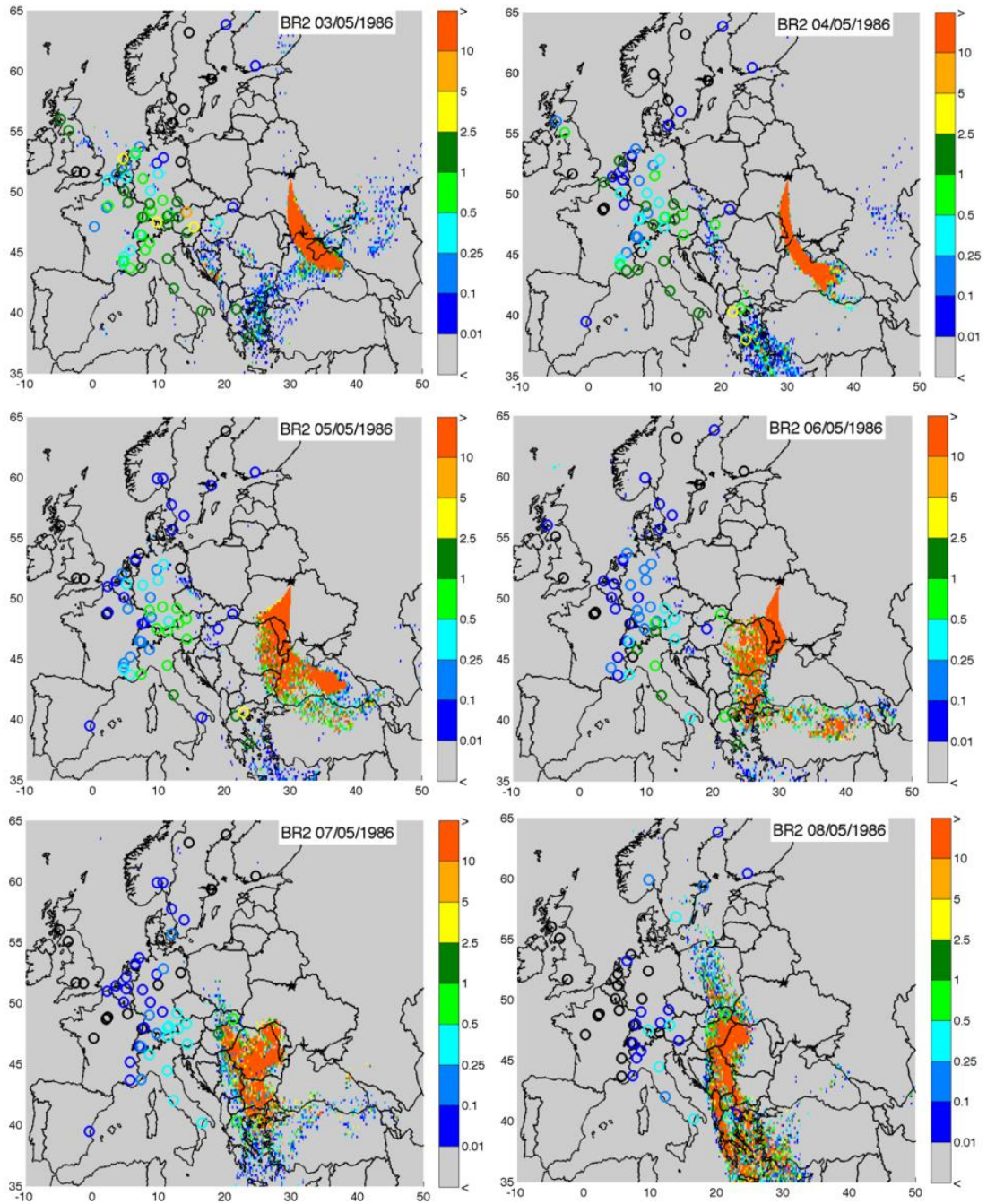


Figure A.3 (continued): Caesium-137 air concentrations [Bq/m^3] simulated by HYSPLIT at surface for the BR2 simulation, 27/04/1986–08/05/1986. REM measurements are plotted as colored open circles (black circles correspond to measurements below 0.01 Bq/m^3).

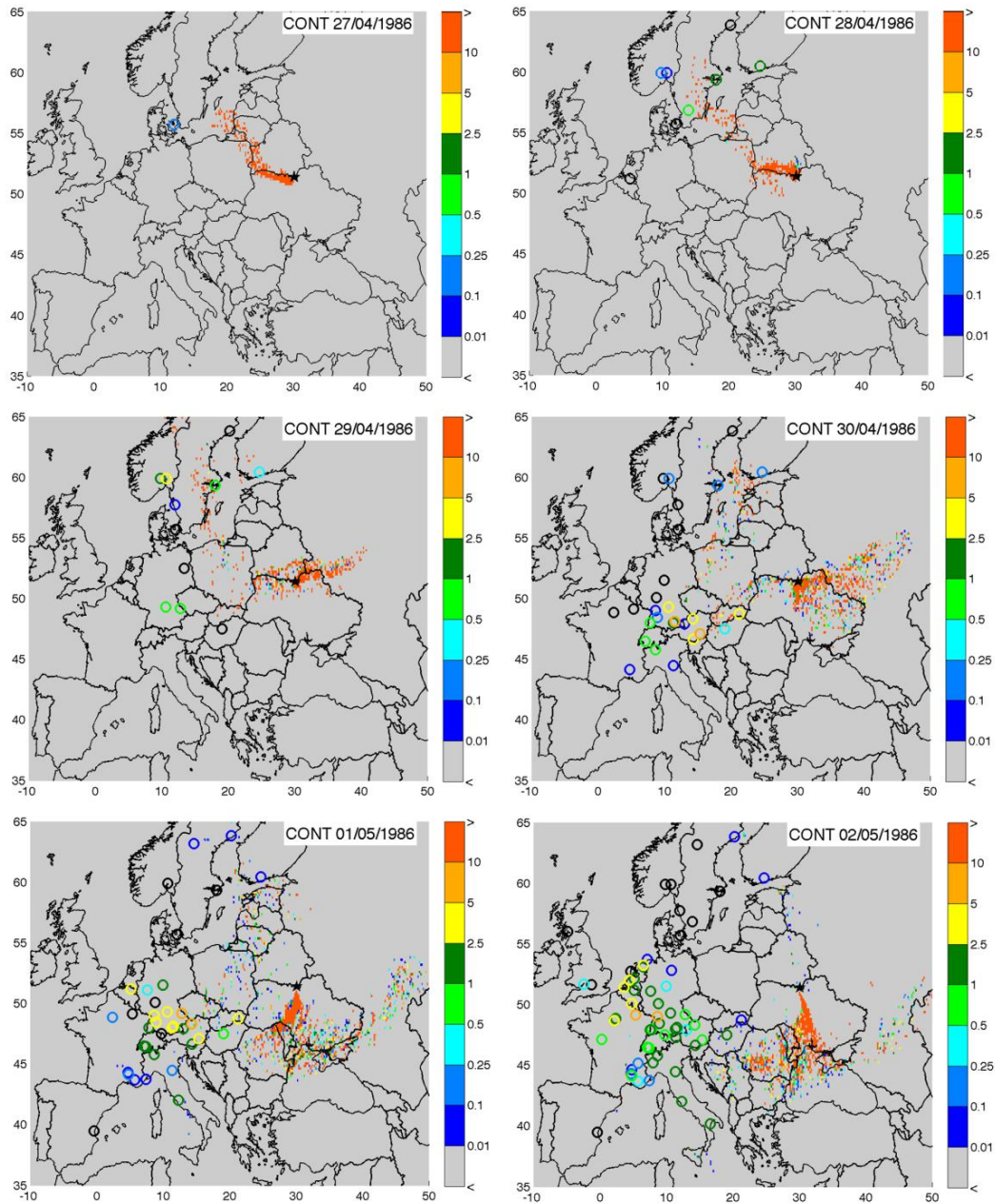


Figure A.4: Caesium-137 air concentrations [Bq/m^3] simulated by HYSPLIT at surface for the CONT simulation, 27/04/1986–08/05/1986. REM measurements are plotted as colored open circles (black circles correspond to measurements below 0.01 Bq/m^3).

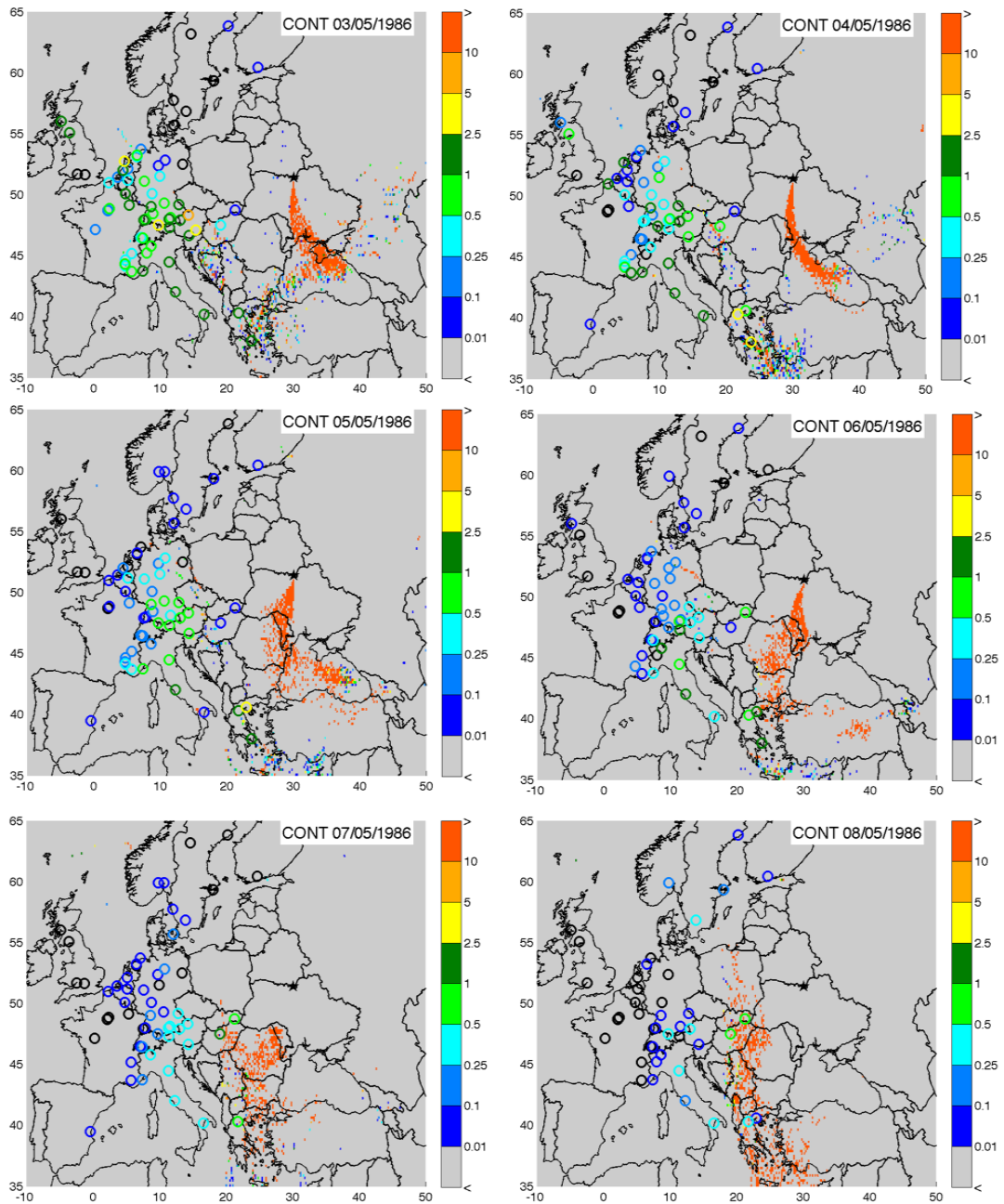


Figure A.4 (continued): Caesium-137 air concentrations [Bq/m^3] simulated by HYSPLIT at surface for the CONT simulation, 27/04/1986–08/05/1986. REM measurements are plotted as colored open circles (black circles correspond to measurements below 0.01 Bq/m^3).

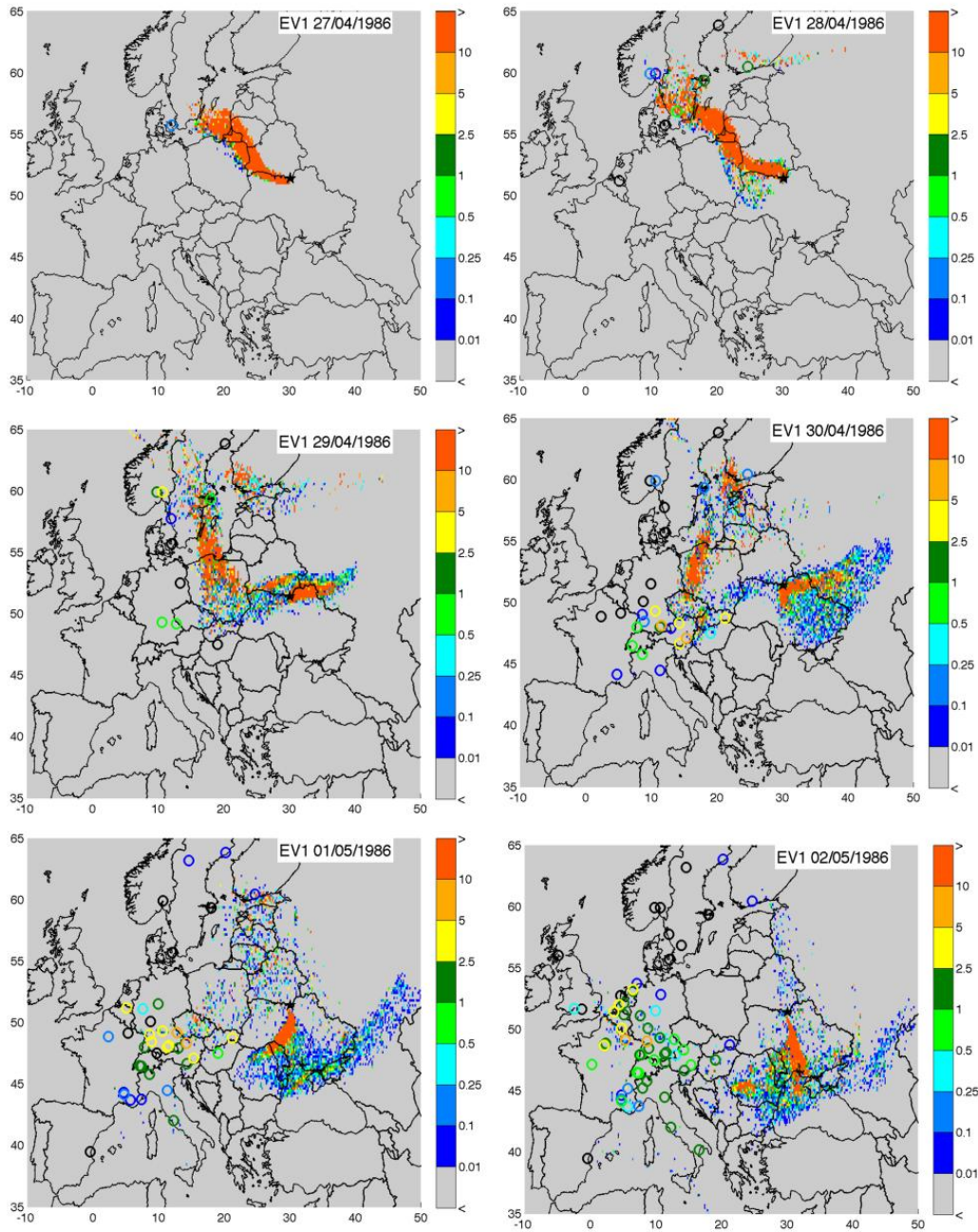


Figure A.5: Caesium-137 air concentrations [Bq/m^3] simulated by HYSPLIT at surface for the EV1 simulation, 27/04/1986–08/05/1986. REM measurements are plotted as colored open circles (black circles correspond to measurements below 0.01 Bq/m^3).

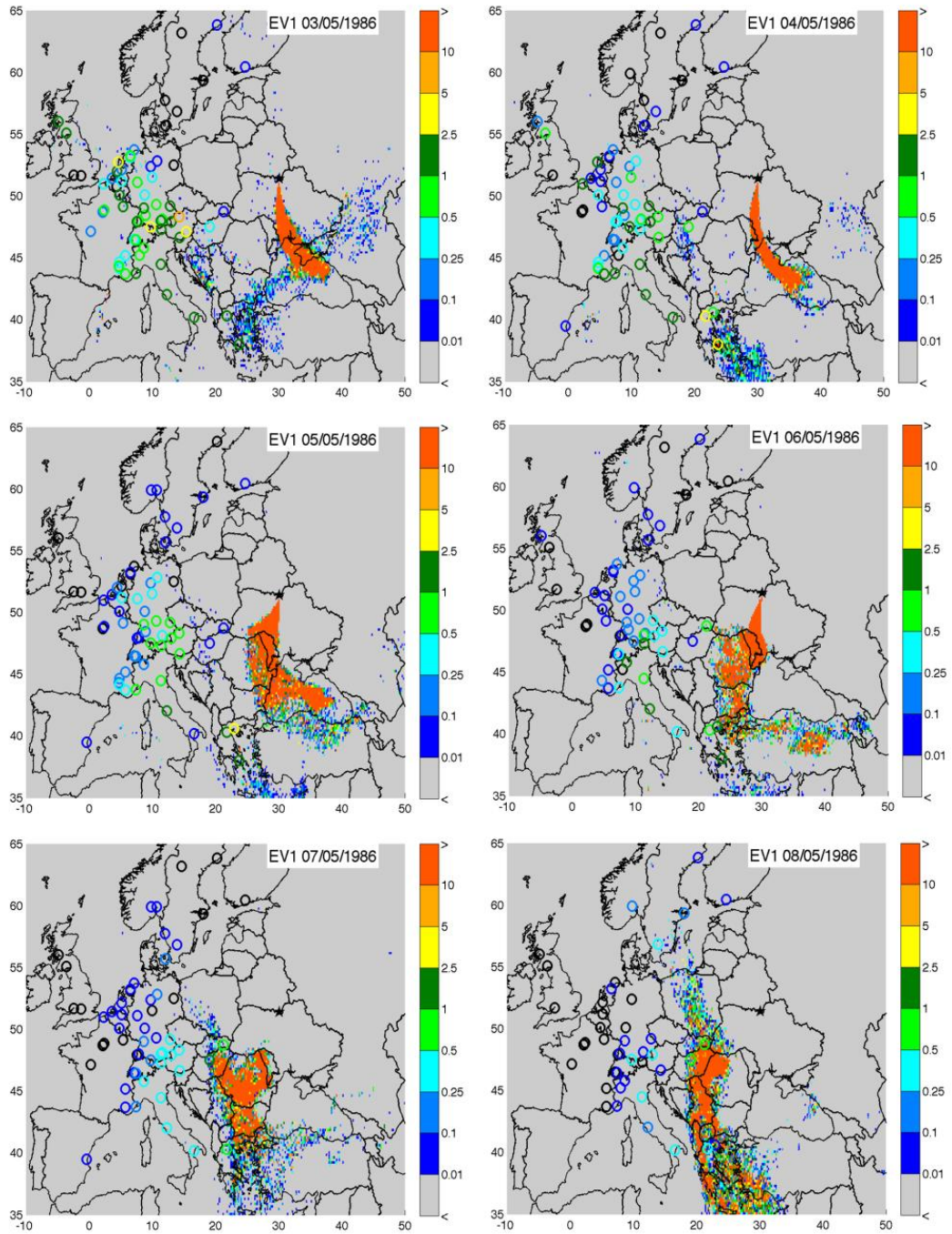


Figure A.5 (continued): Caesium-137 air concentrations [Bq/m^3] simulated by HYSPLIT at surface for the EV1 simulation, 27/04/1986–08/05/1986. REM measurements are plotted as colored open circles (black circles correspond to measurements below $0.01 \text{ Bq}/\text{m}^3$).

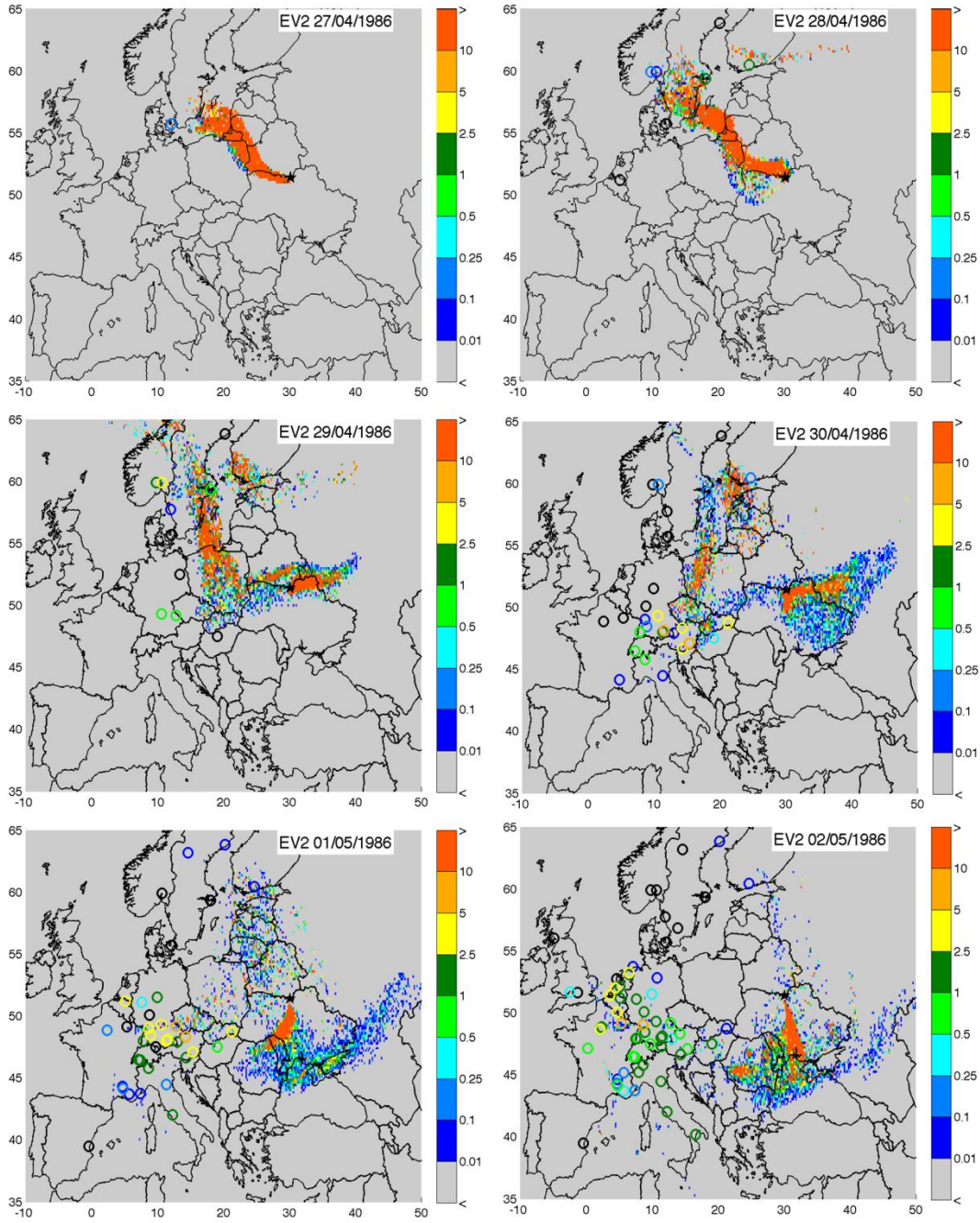


Figure A.6: Caesium-137 air concentrations [Bq/m^3] simulated by HYSPLIT at surface for the EV2 simulation, 27/04/1986–08/05/1986. REM measurements are plotted as colored open circles (black circles correspond to measurements below $0.01 \text{ Bq}/\text{m}^3$).

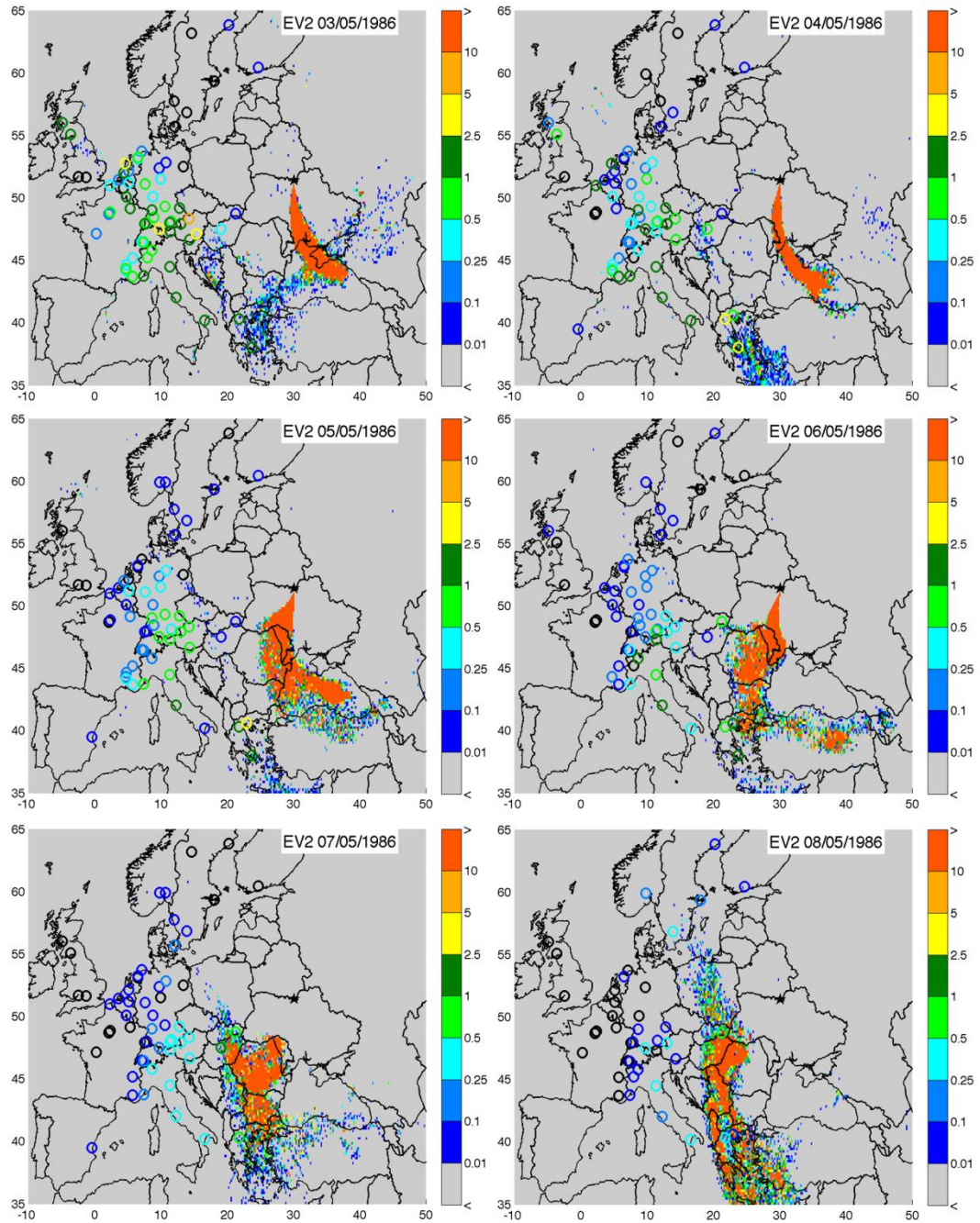


Figure A.6 (continued): Caesium-137 air concentrations [Bq/m^3] simulated by HYSPLIT at surface for the EV2 simulation, 27/04/1986–08/05/1986. REM measurements are plotted as colored open circles (black circles correspond to measurements below $0.01 \text{ Bq}/\text{m}^3$).

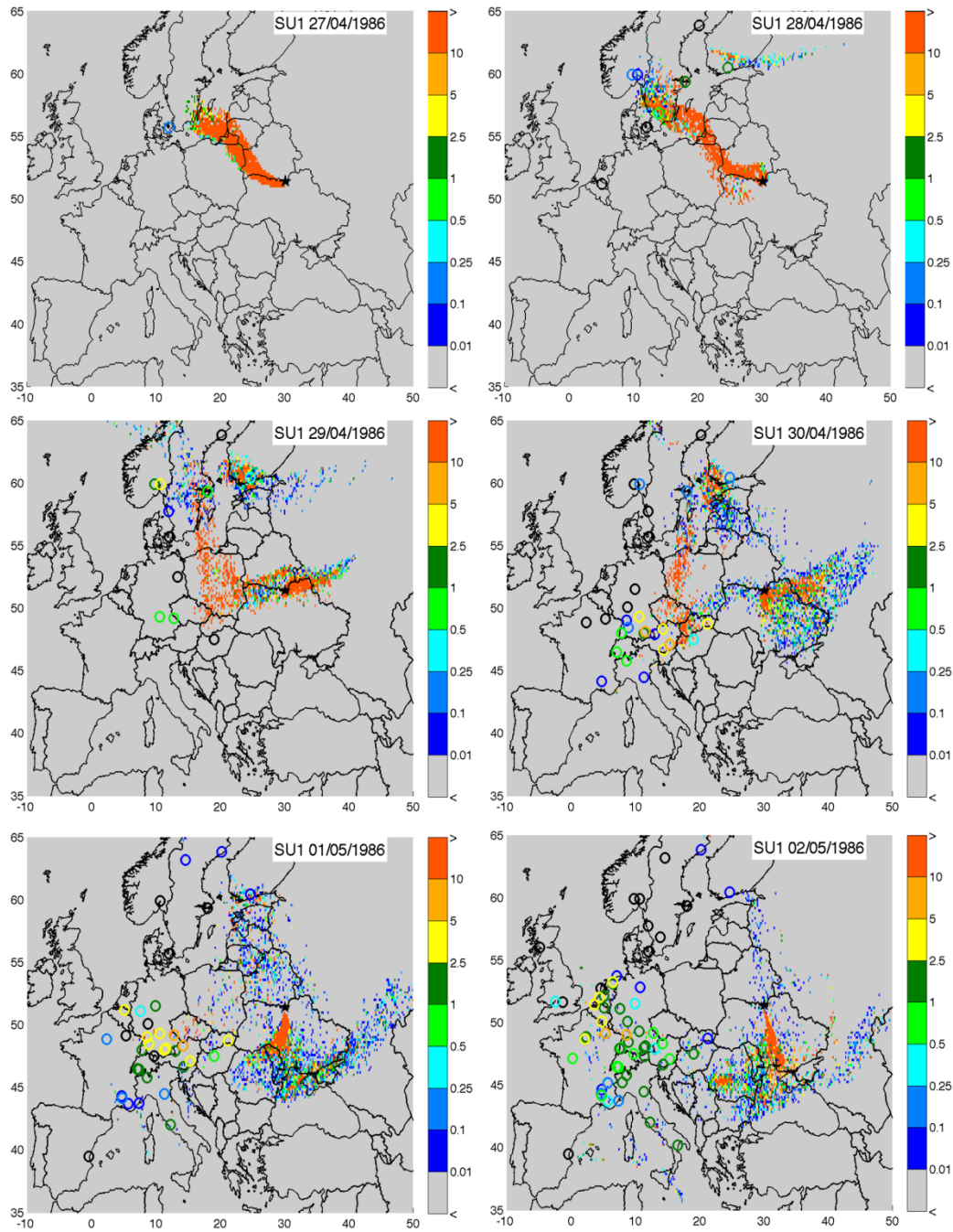


Figure A.7: Caesium-137 air concentrations [Bq/m^3] simulated by HYSPLIT at surface for the SU1 simulation, 27/04/1986–08/05/1986. REM measurements are plotted as colored open circles (black circles correspond to measurements below $0.01 \text{ Bq}/\text{m}^3$).

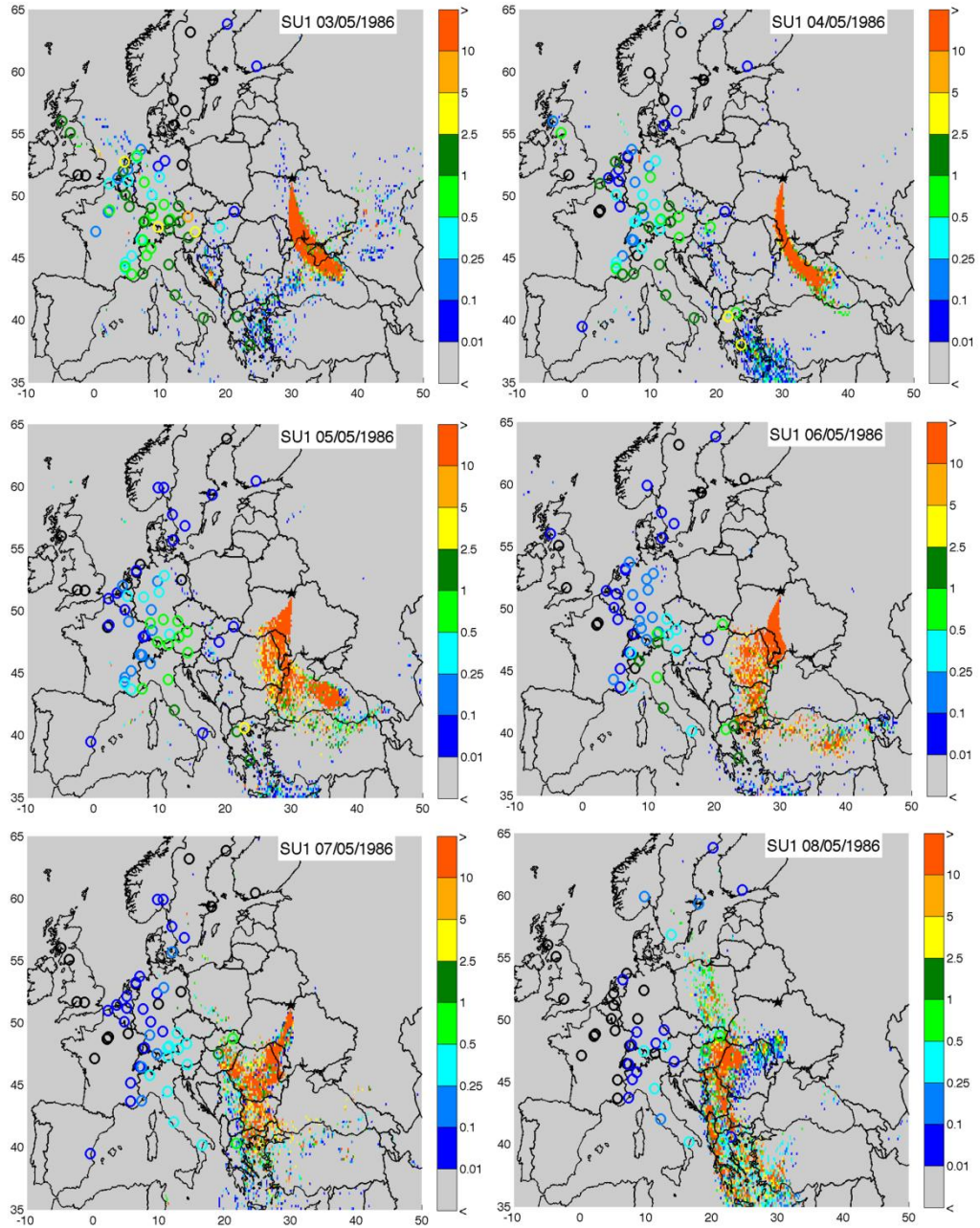


Figure A.7 (continued): Caesium-137 air concentrations [Bq/m^3] simulated by HYSPLIT at surface for the SU1 simulation, 27/04/1986–08/05/1986. REM measurements are plotted as colored open circles (black circles correspond to measurements below $0.01 \text{ Bq}/\text{m}^3$).

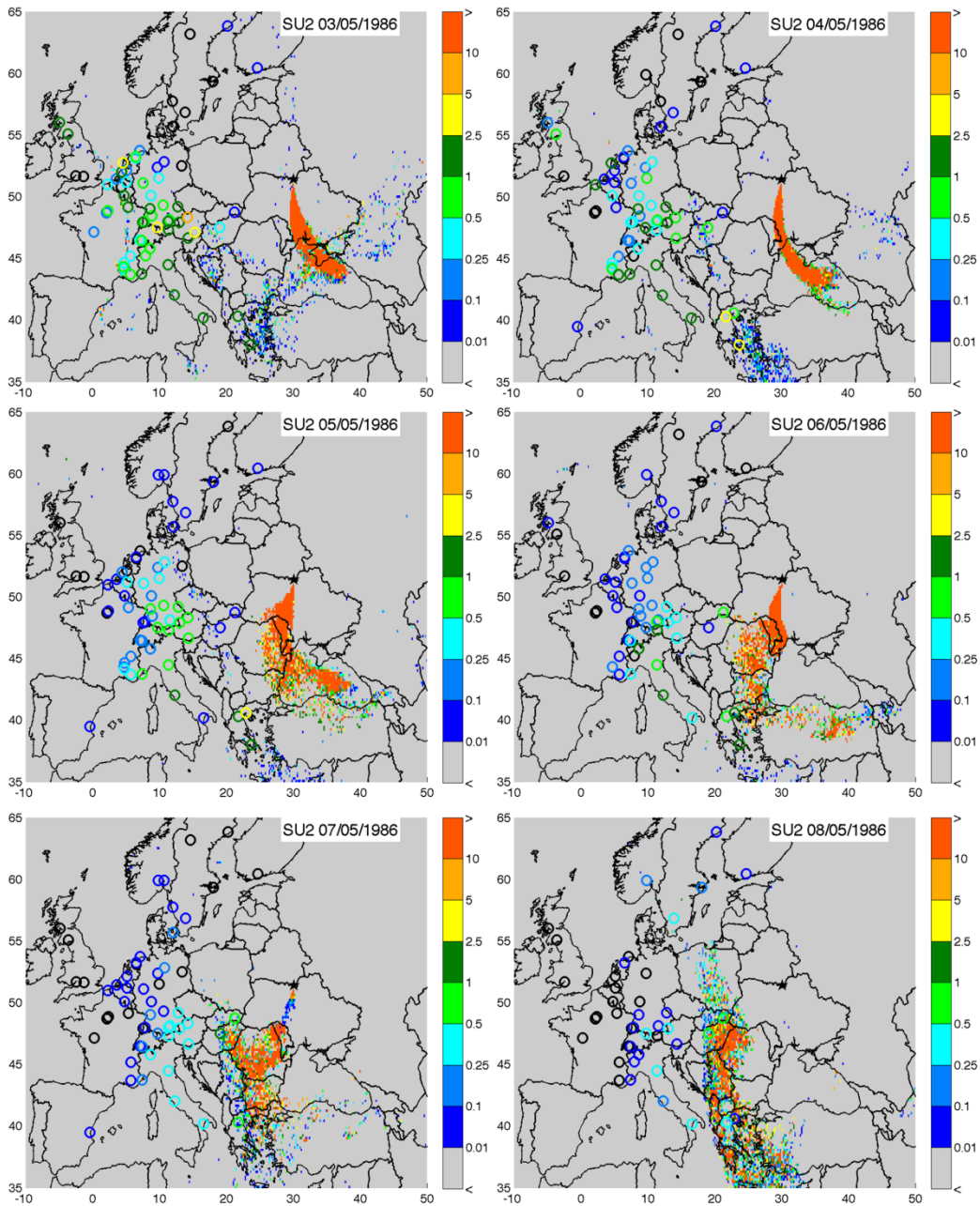


Figure A.8: Caesium-137 air concentrations [Bq/m^3] simulated by HYSPLIT at surface for the SU2 simulation, 27/04/1986–08/05/1986. REM measurements are plotted as colored open circles (black circles correspond to measurements below $0.01 \text{ Bq}/\text{m}^3$).

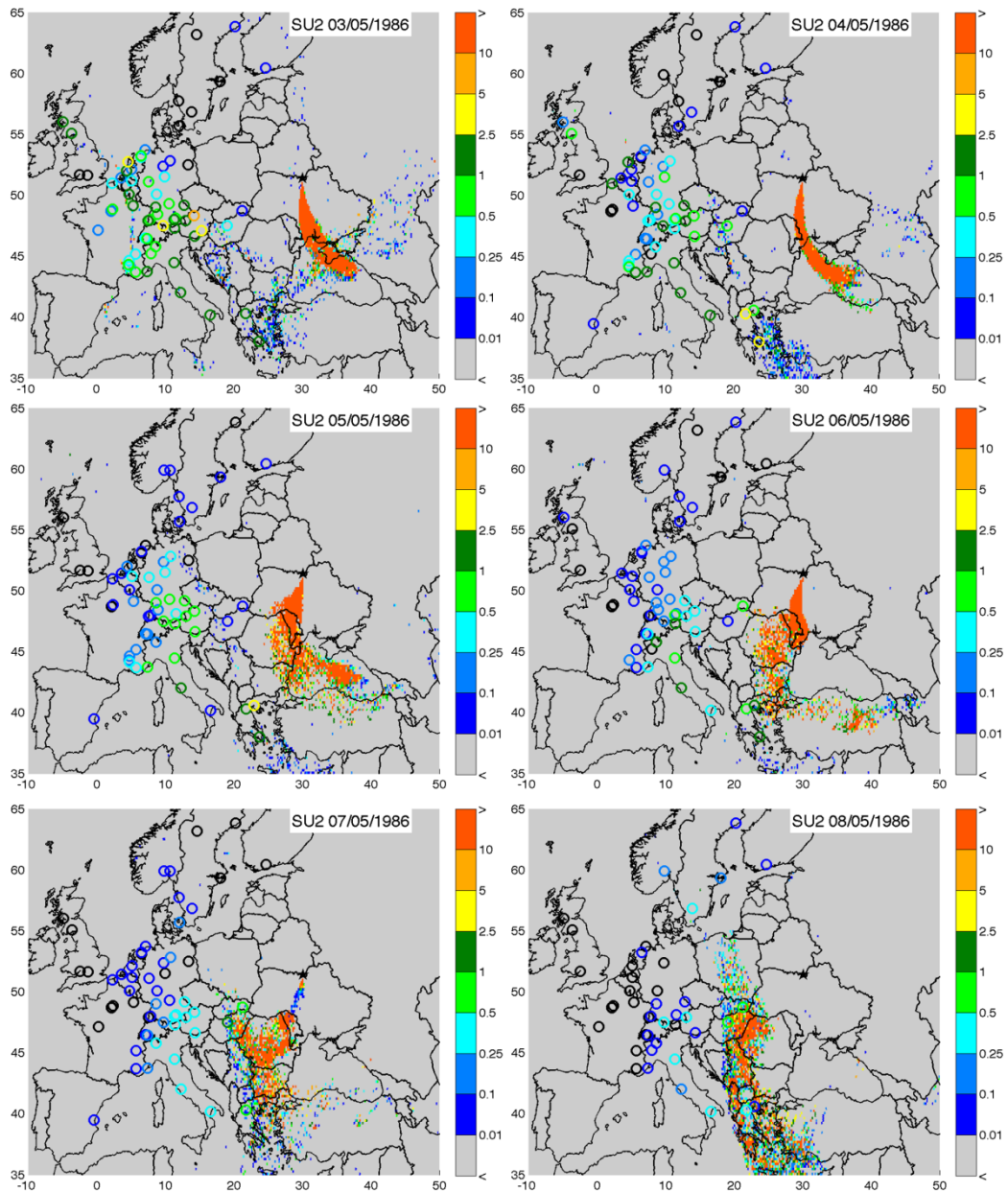


Figure A.8 (continued): Caesium-137 air concentrations [Bq/m^3] simulated by HYSPLIT at surface for the SU2 simulation, 27/04/1986–08/05/1986. REM measurements are plotted as colored open circles (black circles correspond to measurements below $0.01 \text{ Bq}/\text{m}^3$).

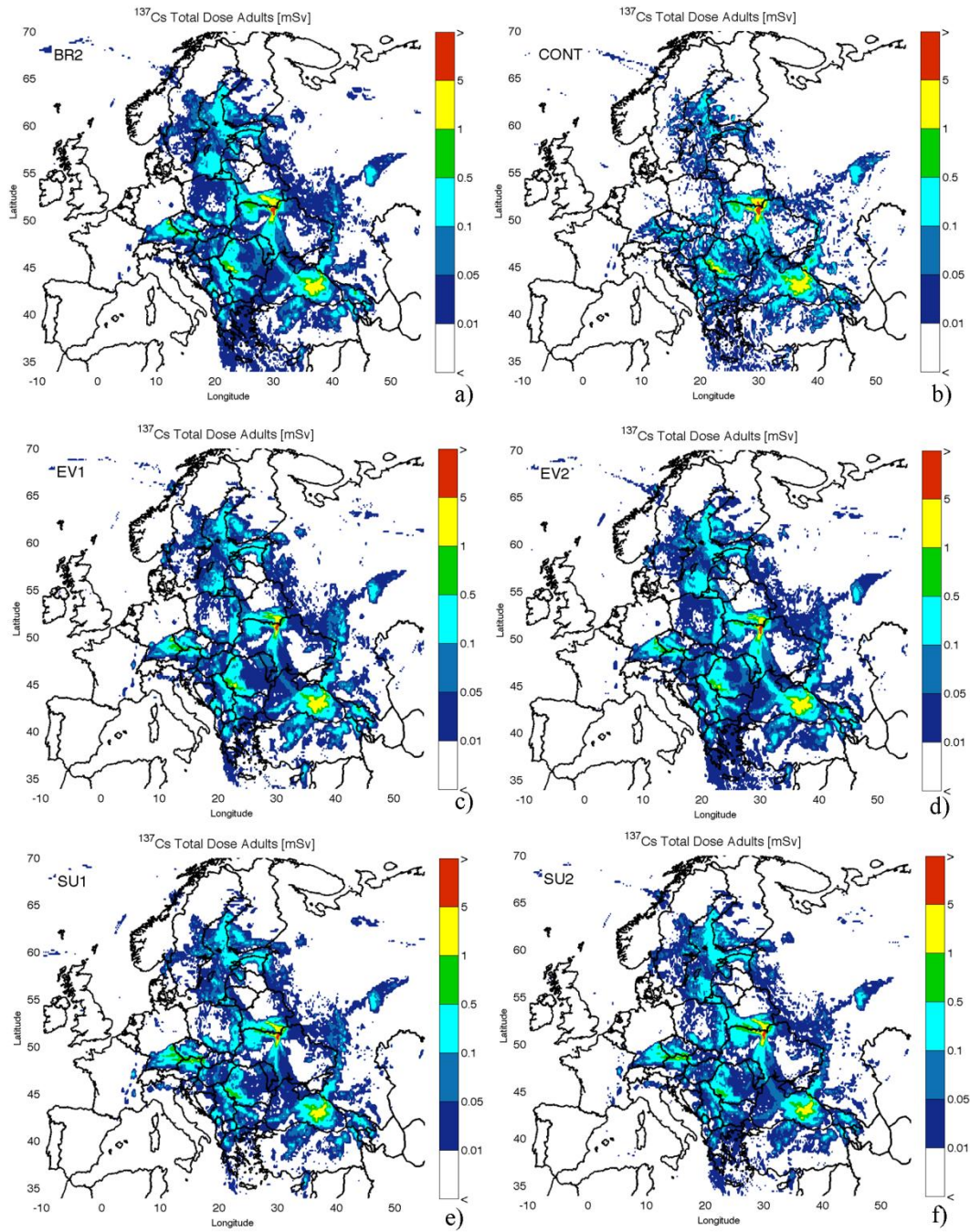


Figure A.9: Adult dose results (mSv) of the simulations for Europe calculated by UNSCEAR Approach: a) BR2 b) CONT c) EV1 d) EV2. e) SU1. f) SU2.

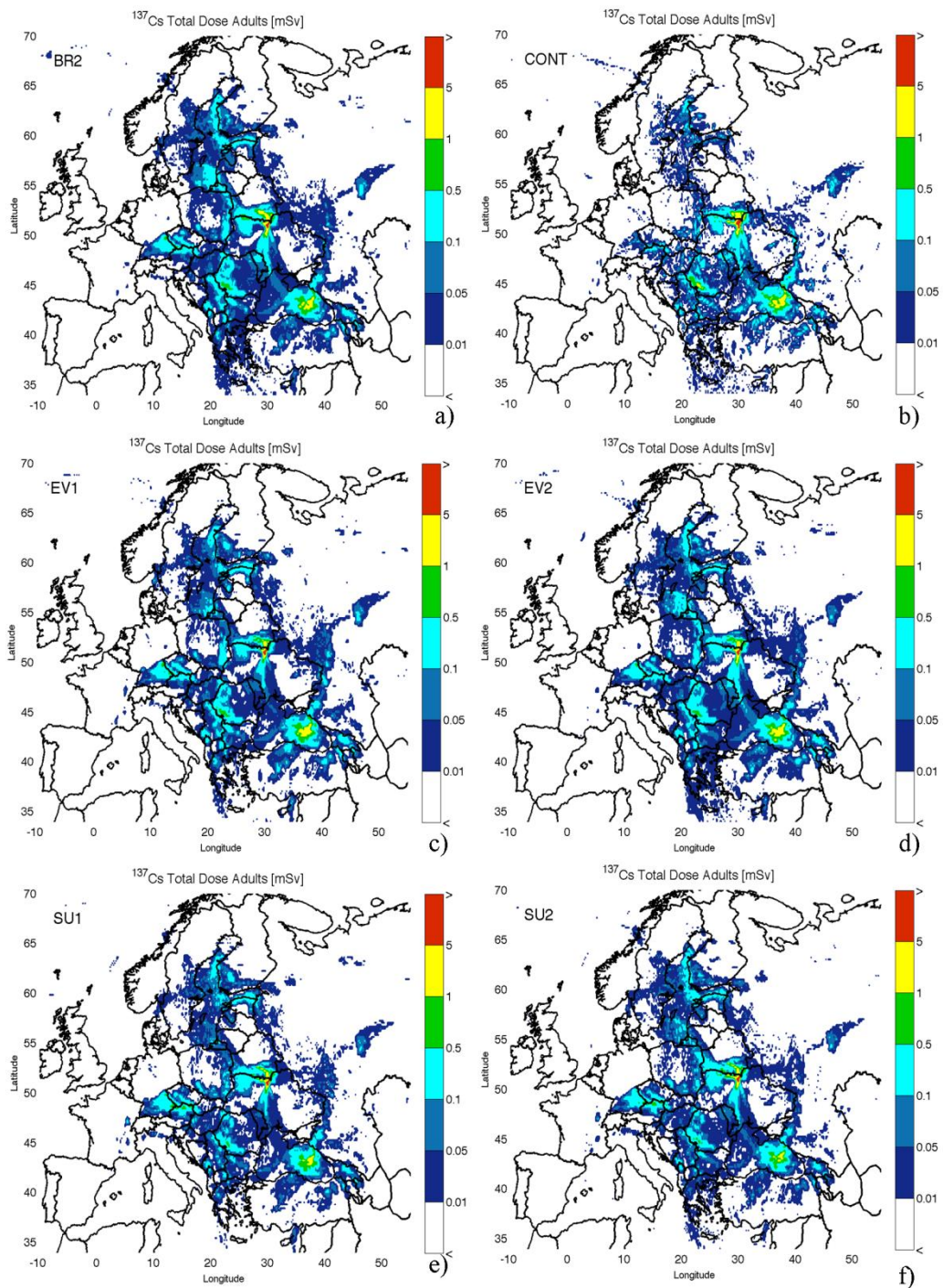


Figure A.10: Adult dose results (mSv) of the simulations for Europe calculated by WHO Approach: a) BR2 b) CONT c) EV1 d) EV2. e) SU1. f) SU2.

APPENDIX B: Tables

Table B.1: List of REM database stations which were used for comparisons with simulated ^{137}Cs air concentrations.

CT	CITY	LON	LAT	CT	CITY	LON	LAT
AU1	SALZBURG	13.05	47.90	F9	PARIS	2.36	48.85
AU2	INNSBRUCK	11.41	47.28	F10	FESSENHEIM	7.56	47.91
AU3	KLAGENFURT	14.33	46.63	F11	MONACO	7.42	43.73
AU4	BREGENZ	9.78	47.51	F12	CHOOZ	4.81	50.10
AU5	GRAZ	15.36	47.08	F13	ORSAY	2.18	48.68
AU6	LINZ	14.30	48.31	F14	VERDUN	5.38	49.15
BE1	BRUXELLES(Ixelles)	4.33	50.78	FI1	NURMIJAERVI	24.70	60.45
BE2	MOL	5.12	51.18	GR1	THESSALONIKI	22.95	40.59
CH1	FRIBOURG	7.12	46.49	GR2	KOZANIS	21.79	40.31
CH2	SPIEZ	7.42	46.42	GR3	ATTIKIS	23.78	38.00
CZ1	CESKE	14.43	48.97	HU1	BUDAPEST	19.10	47.50
CZ2	JASLOVSKE	17.45	48.50	IT1	CASACCIA	12.30	42.03
CZ3	BRATISLAVA	17.17	48.17	IT2	BRASIMONE	11.33	44.48
CZ4	KOSICE	21.25	48.73	IT3	SALUGGIA	8.02	45.21
DE1	BERLIN-WEST	13.42	52.50	IT4	ISPRA	8.63	45.80
DE2	HANNOVER	9.73	52.38	IT5	TRISAIA	16.63	40.17
DE3	NORDERNEY	7.15	53.71	IT6	BOLOGNA	11.33	44.48
DE4	WALDHOF	10.75	52.81	IT7	CAPANNA	12.30	42.03
DE5	MEINERZHAGEN	7.65	51.11	NL1	EELDE	6.56	53.13
DE6	FREIBURG	7.87	48.00	NL2	BILTHOVEN	5.18	52.11
DE7	AACHEN	6.10	50.76	NL3	VLISSINGEN	3.58	51.45
DE8	GOETTINGEN	9.95	51.53	NL4	GRONINGEN	6.53	53.25
DE9	OFFENBACH	8.77	50.10	NL5	DELFT	4.38	52.00
DE10	ROTTENBURG	8.94	48.46	NL6	PETTEN	4.64	52.76
DE11	ANSBACH	10.59	49.30	NO1	BERGEN	10.66	59.90
DE12	STARNBERG	11.34	48.00	NO2	OSLO	9.80	59.90
DE13	KARLSRUHE	8.67	49.00	NO3	KJELLER	10.66	59.90
DE14	NEUHERBERG	11.58	48.13	SE1	UMEAA	20.25	63.83
DE15	BROTJACKLRIEGEL	12.78	49.20	SE2	OESTERSUND	14.67	63.17
ES1	TARRAGONA	-0.40	39.48	SE3	GOETEBORG	12.00	57.75
F1	CRUAS	4.80	44.63	SE4	RISOE	12.07	55.70
F2	GRENOBLE	5.72	45.18	SE5	LJUNGBYHED	13.92	56.82
F3	TRICASTIN	4.73	44.33	SE6	STOCKHOLM	18.08	59.33
F4	CHINON	0.25	47.15	UK1	HARWELL	-1.3	51.62
F5	MARCOULE	4.80	44.13	UK2	BERKELEY	-2.45	51.69
F6	CADARACHE	5.75	43.71	UK3	GLASGOW	-4.83	56.00
F7	GRAVELINES	2.31	51.00	UK4	CHAPELCROSS	-3.61	55.06

Table B.2: BR2 Simulation results for Turkish Provinces.

City	Mean Deposition (Bq/m ²)	Total Deposition (Bq)	Mean Air Concentration (Bq/m ³)
BAYBURT	1,938E+04	7,197E+13	1,484E-01
ARDAHAN	1,861E+04	9,885E+13	1,878E-01
KASTAMONU	1,456E+04	1,901E+14	3,225E-01
KIRIKKALE	1,352E+04	6,388E+13	3,121E-01
KARS	1,338E+04	1,283E+14	3,141E-01
ERZURUM	1,192E+04	2,965E+14	1,653E-01
SINOP	1,071E+04	6,100E+13	3,100E-01
KARABUK	1,061E+04	4,297E+13	6,572E-01
CANKIRI	1,017E+04	7,413E+13	5,673E-01
CORUM	1,005E+04	1,281E+14	5,380E-01
ANKARA	9,854E+03	2,490E+14	3,896E-01
IGDIR	9,840E+03	3,469E+13	1,658E-01
ARTVIN	8,857E+03	6,523E+13	4,208E-01
ERZINCAN	8,845E+03	1,042E+14	1,030E+00
BOLU	7,982E+03	6,731E+13	7,287E-01
GUMUSHANE	7,375E+03	4,979E+13	3,640E-01
BINGOL	6,796E+03	5,722E+13	1,474E-01
TUNCELI	6,165E+03	4,694E+13	1,106E+00
SAMSUN	5,705E+03	5,598E+13	3,317E-01
GIRESUN	5,227E+03	3,655E+13	4,078E-01
KIRKLARELI	5,019E+03	3,252E+13	1,451E+00
AMASYA	4,780E+03	2,670E+13	3,003E-01
ELAZIG	4,426E+03	4,122E+13	3,749E-01
ESKISEHIR	3,837E+03	5,296E+13	2,892E-01
ISPARTA	3,716E+03	3,347E+13	3,544E-01
NEVSEHIR	3,634E+03	1,985E+13	3,859E-01
KONYA	3,478E+03	1,401E+14	4,434E-02
RIZE	3,442E+03	1,305E+13	4,842E-01
TEKIRDAG	3,157E+03	1,999E+13	8,377E-01
ISTANBUL	2,844E+03	1,482E+13	2,719E-01
AGRI	2,777E+03	3,114E+13	1,107E-01
SIVAS	2,734E+03	7,621E+13	9,163E-01
BARTIN	2,667E+03	6,064E+12	3,867E-01
EDIRNE	2,642E+03	1,632E+13	8,928E-01
KIRSEHIR	2,624E+03	1,722E+13	5,221E-02
DUZCE	2,598E+03	6,949E+12	3,183E-01
AFYON	2,580E+03	3,691E+13	3,110E-01
YOZGAT	2,499E+03	3,444E+13	2,789E-01
ZONGULDAK	2,243E+03	7,395E+12	4,267E-01
BURDUR	2,098E+03	1,483E+13	8,709E-01
USAK	2,077E+03	1,123E+13	1,518E-01
DIYARBAKIR	2,046E+03	3,139E+13	6,349E-02
CANAKKALE	1,929E+03	1,905E+13	9,311E-01
AYDIN	1,915E+03	1,538E+13	7,287E-01
MALATYA	1,897E+03	2,282E+13	3,485E-01

Table B.2 (continued): BR2 Simulation results for Turkish Provinces

ICEL	1,804E+03	2,894E+13	1,486E-01
NIGDE	1,763E+03	1,290E+13	1,883E-02
MUGLA	1,737E+03	2,210E+13	7,746E-01
IZMIR	1,717E+03	2,086E+13	7,187E-01
KAYSERI	1,714E+03	2,907E+13	4,565E-01
DENIZLI	1,479E+03	1,735E+13	4,047E-01
TOKAT	1,439E+03	1,479E+13	2,955E-01
ANTALYA	1,349E+03	2,776E+13	5,329E-01
ORDU	1,304E+03	7,804E+12	5,100E-01
SAKARYA	1,265E+03	6,147E+12	5,487E-01
TRABZON	1,133E+03	5,198E+12	2,509E-01
BALIKESIR	1,106E+03	1,610E+13	5,052E-01
YALOVA	9,842E+02	7,456E+11	8,375E-01
KOCAELI	9,723E+02	3,313E+12	4,686E-01
KUTAHYA	9,604E+02	1,119E+13	1,285E-01
HATAY	9,248E+02	5,144E+12	1,376E-02
BURSA	8,764E+02	9,579E+12	3,317E-01
MANISA	8,431E+02	1,121E+13	3,518E-01
BATMAN	7,637E+02	3,425E+12	1,794E-04
BILECIK	7,086E+02	2,962E+12	1,185E-01
AKSARAY	5,676E+02	4,591E+12	2,138E-02
MUS	5,593E+02	4,746E+12	1,389E-02
ADIYAMAN	5,269E+02	3,962E+12	1,424E-02
KARAMAN	4,622E+02	4,041E+12	8,876E-02
K.MARAS	3,756E+02	5,464E+12	3,265E-02
KILIS	3,595E+02	5,111E+11	4,906E-04
ADANA	3,084E+02	4,330E+12	9,137E-03
OSMANIYE	3,084E+02	9,873E+11	1,637E-02
SANLIURFA	3,083E+02	5,952E+12	6,454E-03
VAN	2,100E+02	4,379E+12	2,795E-04
GAZIANTEP	2,033E+02	1,344E+12	1,287E-02
BITLIS	1,612E+02	1,339E+12	6,111E-30
SIRNAK	1,302E+02	9,160E+11	3,062E-05
MARDIN	1,046E+02	9,198E+11	5,449E-03
SIIRT	8,953E+01	5,330E+11	1,210E-06
HAKKARI	2,642E+01	1,866E+11	5,222E-22

Table B.3: CONT Simulation results for Turkish Provinces.

City	Mean Deposition (Bq/m ²)	Total Deposition (Bq)	Mean Air Concentration (Bq/m ³)
KARABUK	2,197E+04	8,897E+13	1,547E-01
KASTAMONU	2,165E+04	2,826E+14	3,922E-01
SINOP	1,973E+04	1,124E+14	3,397E-01
ARDAHAN	1,836E+04	9,749E+13	2,052E-01
KARS	1,378E+04	1,321E+14	2,184E-01
ERZURUM	1,224E+04	3,046E+14	1,126E-01
KIRIKKALE	1,109E+04	5,240E+13	5,960E-01
CANKIRI	1,015E+04	7,397E+13	3,768E-01
BOLU	1,009E+04	8,511E+13	1,214E-01
BAYBURT	9,934E+03	3,689E+13	1,938E-01
ARTVIN	9,607E+03	7,075E+13	3,254E-01
GUMUSHANE	8,295E+03	5,600E+13	5,113E-01
ANKARA	7,894E+03	1,995E+14	2,136E-01
ERZINCAN	7,605E+03	8,962E+13	8,458E-01
TUNCELI	7,002E+03	5,331E+13	1,404E+00
BINGOL	6,921E+03	5,827E+13	4,954E-02
ELAZIG	6,880E+03	6,407E+13	3,583E-01
CORUM	6,758E+03	8,614E+13	2,004E-01
ISTANBUL	5,693E+03	2,967E+13	7,094E-01
NEVSEHIR	4,531E+03	2,475E+13	4,531E-03
DUZCE	4,335E+03	1,159E+13	4,317E-01
KIRKLARELI	4,125E+03	2,673E+13	8,959E-01
SAMSUN	4,026E+03	3,951E+13	1,933E-01
BARTIN	3,962E+03	9,008E+12	0,000E+00
TEKIRDAG	3,908E+03	2,475E+13	6,046E-01
ZONGULDAK	3,547E+03	1,169E+13	4,402E-01
AMASYA	3,234E+03	1,806E+13	5,005E-01
ESKISEHIR	3,049E+03	4,209E+13	2,827E-02
USAK	2,919E+03	1,579E+13	1,211E-01
AYDIN	2,756E+03	2,214E+13	1,202E+00
MALATYA	2,590E+03	3,115E+13	7,350E-01
RIZE	2,562E+03	9,715E+12	1,322E-01
IGDIR	2,496E+03	8,799E+12	1,667E-14
EDIRNE	2,390E+03	1,476E+13	6,833E-01
ISPARTA	2,136E+03	1,924E+13	2,477E-01
SAKARYA	1,989E+03	9,665E+12	2,973E-01
KONYA	1,935E+03	7,794E+13	2,300E-02
SIVAS	1,820E+03	5,075E+13	6,021E-01
ORDU	1,734E+03	1,038E+13	1,451E-01
MUGLA	1,728E+03	2,198E+13	5,629E-01
DENIZLI	1,685E+03	1,977E+13	2,162E-01
GIRESUN	1,553E+03	1,086E+13	3,509E-01
BURDUR	1,551E+03	1,097E+13	7,411E-01
KIRSEHIR	1,527E+03	1,002E+13	3,148E-05
CANAKKALE	1,513E+03	1,494E+13	5,334E-01

Table B.3 (continued): CONT Simulation results for Turkish Provinces.

KUTAHYA	1,398E+03	1,629E+13	7,132E-02
YOZGAT	1,320E+03	1,819E+13	2,712E-02
NIGDE	1,314E+03	9,623E+12	2,459E-02
AFYON	1,293E+03	1,850E+13	2,624E-01
IZMIR	1,238E+03	1,505E+13	5,586E-01
KAYSERI	1,188E+03	2,015E+13	2,871E-01
KOCAELI	1,179E+03	4,018E+12	2,708E-01
MANISA	9,689E+02	1,288E+13	2,627E-01
BILECIK	8,631E+02	3,608E+12	1,930E-01
AGRI	8,023E+02	8,997E+12	9,524E-15
ICEL	7,135E+02	1,145E+13	1,663E-01
YALOVA	6,670E+02	5,053E+11	3,722E-04
BALIKESIR	6,646E+02	9,679E+12	3,228E-01
ANTALYA	6,587E+02	1,356E+13	1,783E-01
K.MARAS	5,698E+02	8,289E+12	7,839E-02
TOKAT	5,690E+02	5,851E+12	3,084E-01
BURSA	4,524E+02	4,944E+12	1,957E-01
HATAY	4,503E+02	2,505E+12	4,064E-03
DIYARBAKIR	4,149E+02	6,366E+12	1,535E-01
ADIYAMAN	3,002E+02	2,257E+12	1,453E-08
TRABZON	2,725E+02	1,250E+12	8,940E-02
MUS	2,621E+02	2,224E+12	1,806E-08
AKSARAY	1,711E+02	1,384E+12	6,459E-03
VAN	1,615E+02	3,367E+12	8,951E-20
MARDIN	1,049E+02	9,227E+11	0,000E+00
ADANA	7,995E+01	1,122E+12	3,083E-03
SIIRT	7,870E+01	4,685E+11	0,000E+00
SIRNAK	7,767E+01	5,465E+11	1,491E-08
KARAMAN	6,287E+01	5,497E+11	3,515E-03
BATMAN	5,993E+01	2,688E+11	0,000E+00
KILIS	3,278E+01	4,659E+10	3,333E-03
HAKKARI	3,196E+01	2,257E+11	0,000E+00
BITLIS	2,168E+01	1,801E+11	1,587E-30
GAZIANTEP	1,683E+01	1,113E+11	1,257E-03
SANLIURFA	1,288E+01	2,486E+11	9,524E-04
OSMANIYE	1,008E+01	3,226E+10	1,879E-03

Table B.4: EV1 Simulation results for Turkish Provinces.

City	Mean Deposition (Bq/m ²)	Total Deposition (Bq)	Mean Air Concentration (Bq/m ³)
ARDAHAN	2,098E+04	1,114E+14	2,222E-01
BAYBURT	1,977E+04	7,343E+13	4,012E-01
KASTAMONU	1,929E+04	2,519E+14	5,208E-01
SINOP	1,780E+04	1,014E+14	2,545E-01
KIRIKKALE	1,744E+04	8,240E+13	2,130E-01
KARS	1,592E+04	1,528E+14	3,218E-01
ANKARA	1,294E+04	3,270E+14	3,975E-01
KARABÜK	1,244E+04	5,035E+13	4,234E-01
ERZURUM	1,228E+04	3,054E+14	1,796E-01
ÇANKIRI	1,185E+04	8,638E+13	8,779E-01
İGDIR	1,053E+04	3,712E+13	1,876E-01
ÇORUM	1,044E+04	1,330E+14	6,138E-01
ARTVIN	1,016E+04	7,485E+13	3,220E-01
ERZINCAN	9,153E+03	1,079E+14	8,866E-01
BOLU	8,788E+03	7,411E+13	7,461E-01
SAMSUN	8,188E+03	8,035E+13	3,961E-01
GÜMÜSHANE	8,046E+03	5,432E+13	3,338E-01
BİNGÖL	7,903E+03	6,654E+13	2,241E-01
TUNCELI	5,532E+03	4,213E+13	1,100E+00
AMASYA	5,518E+03	3,082E+13	4,203E-01
ELAZIG	5,476E+03	5,099E+13	4,830E-01
GİRESUN	5,250E+03	3,671E+13	6,198E-01
KİRSEHIR	4,531E+03	2,973E+13	4,999E-02
ESKİSEHIR	4,187E+03	5,779E+13	2,353E-01
KIRKLARELI	4,112E+03	2,665E+13	1,373E+00
ISPARTA	3,867E+03	3,483E+13	3,873E-01
KONYA	3,593E+03	1,447E+14	6,078E-02
NEVSEHIR	3,536E+03	1,931E+13	2,884E-01
DÜZCE	3,317E+03	8,871E+12	4,745E-01
RİZE	3,089E+03	1,171E+13	5,135E-01
İSTANBUL	3,006E+03	1,567E+13	4,138E-01
TEKİRDAĞ	2,848E+03	1,803E+13	7,446E-01
AGRI	2,838E+03	3,182E+13	7,043E-02
YOZGAT	2,326E+03	3,205E+13	1,943E-01
BARTIN	2,300E+03	5,231E+12	1,906E-01
SİVAS	2,126E+03	5,926E+13	9,432E-01
AFYON	2,085E+03	2,982E+13	3,933E-01
USAK	2,084E+03	1,127E+13	1,184E-01
MALATYA	2,080E+03	2,502E+13	6,653E-01
İÇEL	1,970E+03	3,161E+13	1,710E-01
DIYARBAKIR	1,963E+03	3,012E+13	3,654E-02
ZONGULDAK	1,943E+03	6,406E+12	3,206E-01
BATMAN	1,757E+03	7,881E+12	2,326E-04
EDİRNE	1,678E+03	1,037E+13	1,036E+00
SAKARYA	1,416E+03	6,878E+12	4,974E-01

Table B.4 (continued): EV1 Simulation results for Turkish Provinces.

DENIZLI	1,357E+03	1,591E+13	5,278E-01
KAYSERI	1,280E+03	2,170E+13	3,312E-01
NIGDE	1,252E+03	9,169E+12	1,258E-02
BURDUR	1,242E+03	8,780E+12	9,964E-01
TOKAT	1,212E+03	1,247E+13	2,493E-01
AYDIN	1,140E+03	9,160E+12	1,030E+00
ÇANAKKALE	1,100E+03	1,086E+13	1,089E+00
KARAMAN	1,045E+03	9,134E+12	5,482E-02
TRABZON	9,848E+02	4,519E+12	5,549E-01
MUGLA	9,627E+02	1,225E+13	8,303E-01
IZMIR	9,352E+02	1,136E+13	8,178E-01
BILECIK	8,986E+02	3,756E+12	4,060E-01
KÜTAHYA	8,911E+02	1,039E+13	2,073E-01
ADIYAMAN	8,651E+02	6,504E+12	4,066E-02
HATAY	8,645E+02	4,809E+12	1,982E-02
ANTALYA	7,954E+02	1,637E+13	5,992E-01
MUS	7,790E+02	6,610E+12	1,254E-02
BALIKESIR	6,794E+02	9,895E+12	6,218E-01
K.MARAS	6,456E+02	9,392E+12	7,817E-02
ORDU	6,324E+02	3,785E+12	2,548E-01
MANISA	5,571E+02	7,407E+12	3,150E-01
BURSA	5,289E+02	5,781E+12	4,853E-01
AKSARAY	5,176E+02	4,187E+12	5,627E-02
ADANA	4,407E+02	6,187E+12	1,607E-02
KOCAELI	4,306E+02	1,467E+12	2,426E-01
SANLIURFA	3,716E+02	7,174E+12	8,230E-03
BITLIS	3,446E+02	2,863E+12	8,415E-14
VAN	3,234E+02	6,742E+12	7,104E-03
YALOVA	2,697E+02	2,043E+11	2,512E-01
GAZIANTEP	2,423E+02	1,601E+12	2,139E-02
OSMANIYE	2,401E+02	7,685E+11	1,367E-02
MARDIN	2,357E+02	2,073E+12	7,124E-03
SIIRT	1,730E+02	1,030E+12	2,212E-04
KILIS	1,431E+02	2,034E+11	1,657E-02
SIRNAK	1,059E+02	7,453E+11	6,151E-04
HAKKARI	1,336E+01	9,433E+10	4,333E-25

Table B.5: EV2 Simulation results for Turkish Provinces.

City	Mean Deposition (Bq/m ²)	Total Deposition (Bq)	Mean Air Concentration (Bq/m ³)
ARDAHAN	2,236E+04	1,187E+14	2,166E-01
BAYBURT	2,016E+04	7,485E+13	2,865E-01
KASTAMONU	1,576E+04	2,058E+14	4,320E-01
KIRIKKALE	1,549E+04	7,319E+13	3,305E-01
SINOP	1,464E+04	8,338E+13	4,900E-01
KARS	1,329E+04	1,275E+14	2,556E-01
ANKARA	1,212E+04	3,064E+14	5,239E-01
KARABÜK	1,198E+04	4,851E+13	5,392E-01
ERZURUM	1,170E+04	2,910E+14	1,756E-01
IGDIR	1,064E+04	3,751E+13	1,525E-01
ARTVIN	9,726E+03	7,163E+13	5,351E-01
ERZINCAN	9,672E+03	1,140E+14	9,302E-01
ÇORUM	9,606E+03	1,224E+14	4,713E-01
ÇANKIRI	9,532E+03	6,945E+13	6,879E-01
BOLU	8,830E+03	7,446E+13	8,137E-01
GÜMÜŞHANE	7,883E+03	5,323E+13	3,969E-01
BİNGÖL	7,518E+03	6,329E+13	1,917E-01
SAMSUN	6,734E+03	6,608E+13	3,379E-01
ELAZIG	6,021E+03	5,607E+13	4,327E-01
TUNCELI	6,020E+03	4,583E+13	1,097E+00
KIRKLARELI	4,878E+03	3,161E+13	1,227E+00
GIRESUN	4,623E+03	3,233E+13	4,373E-01
ESKISEHIR	4,113E+03	5,678E+13	3,667E-01
AMASYA	3,957E+03	2,210E+13	2,721E-01
DÜZCE	3,929E+03	1,051E+13	8,934E-01
RIZE	3,904E+03	1,480E+13	4,257E-01
ISPARTA	3,593E+03	3,235E+13	3,781E-01
KONYA	3,489E+03	1,405E+14	4,904E-02
KIRSEHIR	3,300E+03	2,166E+13	1,175E-01
TEKIRDAG	3,232E+03	2,047E+13	9,184E-01
ISTANBUL	3,040E+03	1,584E+13	4,972E-01
EDIRNE	2,986E+03	1,845E+13	1,204E+00
MALATYA	2,952E+03	3,551E+13	8,936E-01
SIVAS	2,798E+03	7,799E+13	1,009E+00
BARTIN	2,786E+03	6,334E+12	1,214E-01
AGRI	2,554E+03	2,865E+13	7,619E-02
YOZGAT	2,539E+03	3,498E+13	2,893E-01
AFYON	2,534E+03	3,625E+13	3,743E-01
NEVSEHIR	2,412E+03	1,318E+13	2,115E-01
ZONGULDAK	2,313E+03	7,626E+12	3,041E-01
BURDUR	2,298E+03	1,625E+13	1,043E+00
ÇANAKKALE	2,161E+03	2,135E+13	9,753E-01
DENIZLI	1,995E+03	2,340E+13	6,981E-01
AYDIN	1,893E+03	1,520E+13	7,869E-01
İÇEL	1,817E+03	2,916E+13	1,905E-01

Table B.5 (continued): EV2 Simulation results for Turkish Provinces.

DIYARBAKIR	1,781E+03	2,733E+13	4,996E-02
SAKARYA	1,704E+03	8,280E+12	4,675E-01
USAK	1,685E+03	9,112E+12	1,358E-01
ANTALYA	1,544E+03	3,178E+13	6,323E-01
MUGLA	1,480E+03	1,883E+13	6,544E-01
TOKAT	1,442E+03	1,483E+13	4,073E-01
BILECIK	1,440E+03	6,021E+12	5,013E-01
BATMAN	1,377E+03	6,177E+12	1,711E-07
ORDU	1,335E+03	7,990E+12	4,507E-01
IZMIR	1,330E+03	1,616E+13	5,267E-01
TRABZON	1,318E+03	6,046E+12	3,677E-01
KÜTAHYA	1,224E+03	1,426E+13	2,969E-01
KOCAELI	1,069E+03	3,641E+12	3,903E-01
BALIKESIR	1,023E+03	1,489E+13	5,855E-01
NIGDE	1,019E+03	7,462E+12	6,859E-03
KAYSERI	9,551E+02	1,620E+13	2,226E-01
YALOVA	9,313E+02	7,055E+11	6,882E-01
ADIYAMAN	8,695E+02	6,537E+12	1,077E-01
MANISA	8,612E+02	1,145E+13	3,197E-01
HATAY	5,813E+02	3,234E+12	3,637E-02
BURSA	5,768E+02	6,305E+12	2,770E-01
K.MARAS	4,955E+02	7,208E+12	9,925E-02
MUS	4,901E+02	4,158E+12	2,396E-02
AKSARAY	3,869E+02	3,130E+12	1,277E-02
ADANA	3,257E+02	4,572E+12	1,158E-02
SANLIURFA	3,130E+02	6,042E+12	4,276E-03
VAN	2,986E+02	6,226E+12	4,262E-04
MARDIN	2,909E+02	2,557E+12	1,145E-02
KARAMAN	2,798E+02	2,446E+12	5,786E-02
BITLIS	2,413E+02	2,005E+12	1,905E-06
OSMANIYE	2,116E+02	6,775E+11	1,973E-03
GAZIANTEP	2,081E+02	1,376E+12	4,523E-03
KILIS	1,852E+02	2,632E+11	9,009E-03
SIRNAK	1,278E+02	8,994E+11	1,305E-04
SIIRT	1,034E+02	6,152E+11	6,557E-04
HAKKARI	3,949E+01	2,788E+11	8,556E-04

Table B.6: SU1 Simulation results for Turkish Provinces.

City	Mean Deposition (Bq/m ²)	Total Deposition (Bq)	Mean Air Concentration (Bq/m ³)
ARDAHAN	1,421E+04	7,546E+13	2,179E-01
BAYBURT	1,309E+04	4,860E+13	2,618E-01
SINOP	1,156E+04	6,584E+13	2,673E-01
KASTAMONU	1,128E+04	1,473E+14	2,870E-01
KARS	1,116E+04	1,071E+14	2,924E-01
KIRIKKALE	9,353E+03	4,420E+13	3,590E-01
KARABUK	8,558E+03	3,465E+13	3,169E-01
ERZURUM	8,058E+03	2,004E+14	1,513E-01
CANKIRI	7,584E+03	5,526E+13	6,678E-01
ARTVIN	7,498E+03	5,523E+13	3,316E-01
ANKARA	7,320E+03	1,850E+14	3,458E-01
CORUM	7,135E+03	9,094E+13	2,606E-01
BINGOL	6,673E+03	5,619E+13	7,017E-02
IGDIR	6,299E+03	2,220E+13	1,065E-01
SAMSUN	6,080E+03	5,967E+13	3,031E-01
ERZINCAN	6,048E+03	7,128E+13	6,387E-01
BOLU	5,612E+03	4,733E+13	2,866E-01
AMASYA	5,073E+03	2,834E+13	2,499E-01
TUNCELI	4,598E+03	3,501E+13	8,655E-01
GUMUSHANE	4,267E+03	2,881E+13	3,282E-01
ELAZIG	3,894E+03	3,626E+13	8,859E-02
GIRESUN	3,284E+03	2,296E+13	3,300E-01
KIRKLARELI	3,140E+03	2,035E+13	9,518E-01
RIZE	2,709E+03	1,027E+13	2,296E-01
ESKISEHIR	2,676E+03	3,694E+13	2,332E-01
ISTANBUL	2,578E+03	1,344E+13	2,558E-01
ISPARTA	2,550E+03	2,296E+13	3,627E-01
KONYA	2,481E+03	9,991E+13	5,132E-02
BARTIN	2,298E+03	5,224E+12	1,972E-01
AGRI	1,858E+03	2,083E+13	6,204E-02
TEKIRDAG	1,825E+03	1,156E+13	3,409E-01
DIYARBAKIR	1,720E+03	2,638E+13	7,503E-02
MALATYA	1,627E+03	1,957E+13	5,568E-01
DUZCE	1,607E+03	4,299E+12	6,088E-02
KIRSEHIR	1,569E+03	1,029E+13	7,662E-02
ICEL	1,524E+03	2,445E+13	9,258E-02
USAK	1,473E+03	7,967E+12	1,427E-01
NIGDE	1,440E+03	1,055E+13	2,209E-02
SIVAS	1,422E+03	3,963E+13	5,553E-01
NEVSEHIR	1,313E+03	7,172E+12	2,951E-01
YOZGAT	1,312E+03	1,808E+13	1,998E-01
EDIRNE	1,203E+03	7,433E+12	7,567E-01
ZONGULDAK	1,072E+03	3,535E+12	3,857E-01
AFYON	1,001E+03	1,432E+13	2,100E-01
KAYSERI	9,718E+02	1,648E+13	2,542E-01

Table B.6 (continued): SU1 Simulation results for Turkish Provinces.

ADIYAMAN	9,655E+02	7,259E+12	8,263E-02
DENIZLI	9,467E+02	1,110E+13	5,494E-01
BURDUR	8,696E+02	6,148E+12	7,483E-01
HATAY	8,469E+02	4,711E+12	5,462E-02
SAKARYA	8,279E+02	4,022E+12	4,786E-01
CANAKKALE	7,815E+02	7,719E+12	7,127E-01
AYDIN	7,800E+02	6,265E+12	5,778E-01
ANTALYA	7,130E+02	1,467E+13	5,060E-01
MUS	7,091E+02	6,017E+12	2,431E-05
TRABZON	6,805E+02	3,123E+12	2,112E-01
KARAMAN	6,709E+02	5,866E+12	4,402E-02
BILECIK	6,588E+02	2,754E+12	3,875E-01
MUGLA	6,457E+02	8,215E+12	4,981E-01
IZMIR	6,401E+02	7,778E+12	5,502E-01
KUTAHYA	6,030E+02	7,027E+12	9,150E-02
TOKAT	5,976E+02	6,146E+12	2,344E-01
ORDU	4,947E+02	2,961E+12	2,666E-01
ADANA	4,946E+02	6,943E+12	3,144E-02
AKSARAY	4,935E+02	3,992E+12	5,631E-03
BALIKESIR	4,380E+02	6,380E+12	3,145E-01
KOCAELI	4,306E+02	1,467E+12	4,003E-01
K.MARAS	4,067E+02	5,917E+12	6,235E-02
SANLIURFA	3,680E+02	7,105E+12	1,208E-02
MANISA	3,472E+02	4,616E+12	2,437E-01
KILIS	3,397E+02	4,829E+11	1,050E-02
BITLIS	3,053E+02	2,537E+12	0,000E+00
BATMAN	2,592E+02	1,162E+12	2,084E-04
MARDIN	2,583E+02	2,271E+12	5,828E-04
GAZIANTEP	2,373E+02	1,569E+12	7,682E-03
VAN	2,254E+02	4,699E+12	7,108E-06
OSMANIYE	1,819E+02	5,824E+11	8,755E-03
BURSA	1,777E+02	1,942E+12	1,240E-01
SIIRT	8,654E+01	5,152E+11	8,202E-07
SIRNAK	7,670E+01	5,398E+11	7,406E-04
YALOVA	5,431E+01	4,114E+10	9,889E-04
HAKKARI	4,809E+00	3,395E+10	0,000E+00

Table B.7: SU2 Simulation results for Turkish Provinces.

City	Mean Deposition (Bq/m ²)	Total Deposition (Bq)	Mean Air Concentration (Bq/m ³)
BAYBURT	1,525E+04	5,664E+13	5,975E-01
ARDAHAN	1,181E+04	6,270E+13	1,348E-01
KIRIKKALE	1,111E+04	5,250E+13	3,233E-01
KASTAMONU	1,019E+04	1,331E+14	2,599E-01
SINOP	9,800E+03	5,582E+13	1,289E-01
KARS	9,637E+03	9,244E+13	2,112E-01
ERZURUM	7,569E+03	1,883E+14	1,353E-01
IGDIR	6,874E+03	2,423E+13	1,297E-01
KARABUK	6,841E+03	2,770E+13	3,661E-01
ANKARA	6,417E+03	1,622E+14	3,450E-01
ÇANKIRI	6,248E+03	4,552E+13	3,532E-01
ÇORUM	5,869E+03	7,480E+13	2,736E-01
ARTVIN	5,665E+03	4,172E+13	2,161E-01
BINGÖL	5,397E+03	4,544E+13	1,572E-01
GUMUSHANE	5,292E+03	3,573E+13	1,597E-01
ERZINCAN	5,069E+03	5,973E+13	4,553E-01
BOLU	4,592E+03	3,873E+13	2,806E-01
AMASYA	3,559E+03	1,988E+13	1,288E-01
SAMSUN	3,545E+03	3,479E+13	3,037E-01
KIRKLARELI	3,519E+03	2,280E+13	8,772E-01
ELAZIG	3,201E+03	2,981E+13	3,142E-01
TUNCELI	2,955E+03	2,250E+13	5,090E-01
GIRESUN	2,900E+03	2,028E+13	1,918E-01
NEVSEHIR	2,536E+03	1,385E+13	2,951E-01
RIZE	2,454E+03	9,305E+12	4,140E-01
TEKIRDAG	2,380E+03	1,507E+13	6,441E-01
ISPARTA	2,316E+03	2,086E+13	3,501E-01
KONYA	2,279E+03	9,179E+13	6,088E-02
KIRSEHIR	2,238E+03	1,468E+13	4,248E-02
ESKISEHIR	2,160E+03	2,982E+13	2,057E-01
SIVAS	2,024E+03	5,642E+13	5,921E-01
EDIRNE	1,935E+03	1,196E+13	8,235E-01
ISTANBUL	1,922E+03	1,002E+13	3,092E-01
YOZGAT	1,911E+03	2,633E+13	1,942E-01
DUZCE	1,834E+03	4,904E+12	3,774E-01
MALATYA	1,624E+03	1,953E+13	4,040E-01
BURDUR	1,623E+03	1,148E+13	7,389E-01
BARTIN	1,489E+03	3,385E+12	1,592E-01
DENIZLI	1,432E+03	1,679E+13	4,564E-01
CANAKKALE	1,376E+03	1,359E+13	5,791E-01
AYDIN	1,367E+03	1,098E+13	6,538E-01
AGRI	1,362E+03	1,527E+13	5,641E-02
USAK	1,343E+03	7,263E+12	6,113E-02
ORDU	1,219E+03	7,295E+12	2,834E-01
AFYON	1,208E+03	1,728E+13	2,360E-01

Table B.7 (continued): SU2 Simulation results for Turkish Provinces.

MUGLA	1,167E+03	1,485E+13	5,432E-01
ICEL	1,163E+03	1,866E+13	1,239E-01
IZMIR	1,148E+03	1,395E+13	4,719E-01
TRABZON	1,135E+03	5,210E+12	3,822E-01
ZONGULDAK	1,021E+03	3,364E+12	1,406E-01
NIGDE	1,017E+03	7,447E+12	2,028E-02
KAYSERI	1,014E+03	1,720E+13	1,590E-01
DIYARBAKIR	9,523E+02	1,461E+13	3,311E-02
BILECIK	9,198E+02	3,845E+12	3,260E-01
TOKAT	8,863E+02	9,114E+12	1,657E-01
ANTALYA	8,563E+02	1,762E+13	3,785E-01
SAKARYA	8,070E+02	3,920E+12	2,824E-01
KUTAHYA	7,943E+02	9,257E+12	1,419E-01
BALIKESIR	7,604E+02	1,108E+13	4,705E-01
HATAY	7,362E+02	4,095E+12	1,708E-02
AKSARAY	7,224E+02	5,844E+12	7,121E-03
KOCAELI	6,603E+02	2,250E+12	2,743E-01
BURSA	5,906E+02	6,455E+12	2,617E-01
MANISA	5,189E+02	6,898E+12	2,263E-01
ADIYAMAN	4,087E+02	3,072E+12	2,875E-03
MARDIN	3,797E+02	3,338E+12	4,263E-03
SANLIURFA	3,666E+02	7,077E+12	2,338E-03
YALOVA	3,256E+02	2,467E+11	5,683E-01
MUS	2,990E+02	2,537E+12	1,444E-04
GAZIANTEP	2,853E+02	1,886E+12	1,164E-02
K.MARAS	2,403E+02	3,495E+12	3,390E-02
ADANA	2,379E+02	3,340E+12	4,875E-03
KARAMAN	2,229E+02	1,949E+12	4,600E-02
VAN	2,137E+02	4,456E+12	2,210E-06
BATMAN	1,818E+02	8,155E+11	4,760E-04
OSMANIYE	1,432E+02	4,584E+11	3,284E-03
BITLIS	8,297E+01	6,893E+11	3,581E-12
KILIS	7,937E+01	1,128E+11	7,958E-03
SIRNAK	7,721E+01	5,433E+11	3,555E-04
SIIRT	4,174E+01	2,485E+11	1,580E-06
HAKKARI	1,875E+01	1,324E+11	0,000E+00

Table B.8: Calculated doses for Turkish Provinces by using BR1 simulation results (UNSCEAR Approach).

Province	Doses (mSv)		
	Adult	Child	Infant
NIGDE	1,52E-01	1,52E-01	1,52E-01
IGDIR	1,33E-01	1,32E-01	1,32E-01
KARS	1,18E-01	1,18E-01	1,17E-01
ARDAHAN	1,06E-01	1,06E-01	1,06E-01
KASTAMONU	9,90E-02	9,88E-02	9,87E-02
BAYBURT	8,63E-02	8,62E-02	8,61E-02
KIRIKKALE	8,43E-02	8,43E-02	8,42E-02
ÇORUM	7,59E-02	7,56E-02	7,55E-02
ANKARA	7,56E-02	7,55E-02	7,54E-02
ERZURUM	7,56E-02	7,55E-02	7,54E-02
ADANA	7,51E-02	7,51E-02	7,51E-02
İÇEL	6,77E-02	6,77E-02	6,77E-02
KARABÜK	6,68E-02	6,66E-02	6,65E-02
SAMSUN	6,35E-02	6,32E-02	6,30E-02
ARTVIN	6,10E-02	6,09E-02	6,09E-02
ÇANKIRI	6,08E-02	6,06E-02	6,04E-02
SINOP	5,97E-02	5,96E-02	5,95E-02
AMASYA	5,96E-02	5,94E-02	5,92E-02
KONYA	4,22E-02	4,22E-02	4,22E-02
KIRKLARELI	3,77E-02	3,75E-02	3,74E-02
OSMANIYE	3,64E-02	3,64E-02	3,64E-02
KIRSEHIR	3,58E-02	3,57E-02	3,57E-02
GIRESUN	3,56E-02	3,54E-02	3,53E-02
BOLU	3,51E-02	3,49E-02	3,47E-02
ISPARTA	3,46E-02	3,45E-02	3,45E-02
GÜMÜSHANE	3,37E-02	3,35E-02	3,34E-02
ISTANBUL	3,32E-02	3,30E-02	3,28E-02
AGRI	3,07E-02	3,07E-02	3,06E-02
ERZINCAN	2,91E-02	2,90E-02	2,90E-02
BINGÖL	2,73E-02	2,73E-02	2,73E-02
TEKIRDAG	2,62E-02	2,59E-02	2,58E-02
ESKISEHIR	2,59E-02	2,56E-02	2,55E-02
YOZGAT	2,47E-02	2,47E-02	2,46E-02
HATAY	2,28E-02	2,28E-02	2,28E-02
RIZE	2,14E-02	2,12E-02	2,11E-02
TOKAT	2,11E-02	2,10E-02	2,09E-02
AFYON	1,78E-02	1,77E-02	1,76E-02
KAYSERI	1,77E-02	1,77E-02	1,77E-02
BARTIN	1,74E-02	1,73E-02	1,71E-02
ORDU	1,71E-02	1,69E-02	1,67E-02
YALOVA	1,69E-02	1,67E-02	1,65E-02
KARAMAN	1,62E-02	1,62E-02	1,62E-02
TRABZON	1,58E-02	1,56E-02	1,54E-02
GAZIANTEP	1,30E-02	1,30E-02	1,30E-02
EDIRNE	1,28E-02	1,25E-02	1,23E-02

Table B.8 (continued): Calculated doses for Turkish Provinces by using BR1 simulation results (UNSCEAR Approach).

ADYAMAN	1,26E-02	1,26E-02	1,26E-02
USAK	1,26E-02	1,25E-02	1,24E-02
BILECIK	1,23E-02	1,21E-02	1,19E-02
NEVSEHIR	1,22E-02	1,22E-02	1,22E-02
DÜZCE	1,15E-02	1,13E-02	1,11E-02
DENIZLI	1,12E-02	1,11E-02	1,11E-02
K.MARAS	1,11E-02	1,11E-02	1,11E-02
ZONGULDAK	1,06E-02	1,04E-02	1,03E-02
KÜTAHYA	1,04E-02	1,03E-02	1,02E-02
TUNCELI	1,04E-02	1,03E-02	1,03E-02
SAKARYA	1,02E-02	1,01E-02	9,92E-03
SIVAS	9,65E-03	9,58E-03	9,52E-03
BURSA	9,19E-03	9,03E-03	8,90E-03
AKSARAY	7,62E-03	7,62E-03	7,62E-03
MUS	5,15E-03	5,13E-03	5,12E-03
KILIS	4,93E-03	4,93E-03	4,93E-03
DIYARBAKIR	4,59E-03	4,59E-03	4,59E-03
SANLIURFA	4,35E-03	4,35E-03	4,35E-03
BITLIS	4,07E-03	4,07E-03	4,07E-03
ELAZIG	3,87E-03	3,86E-03	3,85E-03
MUGLA	3,80E-03	3,74E-03	3,70E-03
MANISA	3,38E-03	3,33E-03	3,30E-03
MALATYA	2,95E-03	2,95E-03	2,94E-03
KOCAELI	2,90E-03	2,72E-03	2,59E-03
ANTALYA	2,66E-03	2,63E-03	2,61E-03
MARDIN	2,55E-03	2,55E-03	2,55E-03
BALIKESIR	1,64E-03	1,55E-03	1,48E-03
VAN	1,57E-03	1,57E-03	1,57E-03
SIIRT	1,54E-03	1,54E-03	1,54E-03
BATMAN	1,50E-03	1,50E-03	1,50E-03
SIRNAK	1,12E-03	1,12E-03	1,12E-03
ÇANAKKALE	8,88E-04	7,18E-04	5,86E-04
İZMİR	6,34E-04	5,67E-04	5,15E-04
AYDIN	2,38E-04	2,16E-04	1,98E-04
HAKKARI	1,72E-04	1,72E-04	1,72E-04
BURDUR	9,08E-05	5,69E-05	3,04E-05

Table B.9: Calculated doses for Turkish Provinces by using BR1 simulation results (WHO Approach).

Province	Doses (mSv)		
	Adult	Child	Infant
NIGDE	1,00E-01	1,00E-01	1,33E-01
IGDIR	8,71E-02	8,70E-02	1,16E-01
KARS	7,73E-02	7,72E-02	1,03E-01
ARDAHAN	6,98E-02	6,97E-02	9,29E-02
KASTAMONU	6,57E-02	6,53E-02	8,66E-02
BAYBURT	5,72E-02	5,69E-02	7,55E-02
KIRIKKALE	5,58E-02	5,55E-02	7,38E-02
ÇORUM	5,10E-02	5,03E-02	6,63E-02
ANKARA	5,02E-02	4,99E-02	6,62E-02
ERZURUM	5,01E-02	4,98E-02	6,61E-02
ADANA	4,94E-02	4,93E-02	6,57E-02
İÇEL	4,45E-02	4,45E-02	5,93E-02
KARABÜK	4,45E-02	4,41E-02	5,84E-02
SAMSUN	4,31E-02	4,23E-02	5,55E-02
ÇANKIRI	4,09E-02	4,03E-02	5,31E-02
ARTVIN	4,03E-02	4,02E-02	5,34E-02
AMASYA	4,02E-02	3,96E-02	5,21E-02
SINOP	3,99E-02	3,95E-02	5,22E-02
KONYA	2,78E-02	2,77E-02	3,69E-02
KIRKLARELI	2,56E-02	2,51E-02	3,29E-02
GIRESUN	2,41E-02	2,37E-02	3,11E-02
OSMANIYE	2,39E-02	2,39E-02	3,19E-02
BOLU	2,39E-02	2,34E-02	3,06E-02
KIRSEHIR	2,37E-02	2,36E-02	3,13E-02
ISTANBUL	2,30E-02	2,23E-02	2,90E-02
ISPARTA	2,29E-02	2,28E-02	3,02E-02
GÜMÜSHANE	2,29E-02	2,24E-02	2,94E-02
AGRI	2,03E-02	2,02E-02	2,69E-02
ERZINCAN	1,94E-02	1,92E-02	2,54E-02
TEKIRDAG	1,84E-02	1,77E-02	2,28E-02
ESKISEHIR	1,82E-02	1,75E-02	2,26E-02
BINGÖL	1,80E-02	1,80E-02	2,39E-02
YOZGAT	1,64E-02	1,63E-02	2,16E-02
HATAY	1,50E-02	1,50E-02	1,99E-02
RIZE	1,47E-02	1,43E-02	1,87E-02
TOKAT	1,45E-02	1,41E-02	1,84E-02
ORDU	1,24E-02	1,17E-02	1,49E-02
BARTIN	1,24E-02	1,18E-02	1,52E-02
YALOVA	1,21E-02	1,15E-02	1,47E-02
AFYON	1,20E-02	1,18E-02	1,55E-02
KAYSERI	1,17E-02	1,16E-02	1,55E-02
TRABZON	1,16E-02	1,09E-02	1,38E-02
KARAMAN	1,07E-02	1,06E-02	1,41E-02
EDIRNE	9,93E-03	9,05E-03	1,11E-02
BILECIK	9,35E-03	8,61E-03	1,07E-02

Table B.9 (continued): Calculated doses for Turkish Provinces by using BR1 simulation results (WHO Approach).

USAK	8,76E-03	8,47E-03	1,10E-02
GAZIANTEP	8,58E-03	8,56E-03	1,14E-02
DÜZCE	8,51E-03	7,94E-03	9,99E-03
ADYAMAN	8,29E-03	8,29E-03	1,10E-02
NEVSEHIR	8,14E-03	8,07E-03	1,07E-02
ZONGULDAK	7,75E-03	7,29E-03	9,23E-03
DENIZLI	7,62E-03	7,45E-03	9,75E-03
KÜTAHYA	7,58E-03	7,14E-03	9,07E-03
SAKARYA	7,54E-03	7,05E-03	8,89E-03
K.MARAS	7,30E-03	7,29E-03	9,71E-03
TUNCELI	7,04E-03	6,91E-03	9,07E-03
BURSA	6,86E-03	6,38E-03	7,99E-03
SIVAS	6,68E-03	6,48E-03	8,42E-03
AKSARAY	5,02E-03	5,01E-03	6,67E-03
MUS	3,45E-03	3,41E-03	4,50E-03
KILIS	3,24E-03	3,24E-03	4,32E-03
DIYARBAKIR	3,02E-03	3,02E-03	4,02E-03
SANLIURFA	2,87E-03	2,86E-03	3,81E-03
KOCAELI	2,80E-03	2,27E-03	2,48E-03
MUGLA	2,77E-03	2,61E-03	3,31E-03
BITLIS	2,67E-03	2,67E-03	3,56E-03
ELAZIG	2,59E-03	2,56E-03	3,38E-03
MANISA	2,45E-03	2,32E-03	2,94E-03
MALATYA	1,96E-03	1,95E-03	2,58E-03
ANTALYA	1,89E-03	1,81E-03	2,32E-03
MARDIN	1,67E-03	1,67E-03	2,23E-03
BALIKESIR	1,52E-03	1,26E-03	1,40E-03
ÇANAKKALE	1,43E-03	9,33E-04	7,19E-04
VAN	1,03E-03	1,03E-03	1,37E-03
SIIRT	1,01E-03	1,01E-03	1,35E-03
BATMAN	9,84E-04	9,84E-04	1,31E-03
IZMIR	7,52E-04	5,55E-04	5,32E-04
SIRNAK	7,41E-04	7,38E-04	9,82E-04
AYDIN	2,71E-04	2,04E-04	2,01E-04
BURDUR	2,30E-04	1,30E-04	6,80E-05
HAKKARI	1,13E-04	1,13E-04	1,51E-04

Table B.10: Calculated doses for Turkish Provinces by using BR2 simulation results (UNSCEAR Approach).

Province	Doses (mSv)		
	Adult	Child	Infant
BAYBURT	1,28E-01	1,28E-01	1,28E-01
ARDAHAN	1,23E-01	1,23E-01	1,23E-01
KASTAMONU	9,66E-02	9,66E-02	9,65E-02
KIRIKKALE	8,97E-02	8,97E-02	8,96E-02
KARS	8,88E-02	8,87E-02	8,87E-02
ERZURUM	7,91E-02	7,90E-02	7,90E-02
SINOP	7,11E-02	7,10E-02	7,10E-02
KARABÜK	7,07E-02	7,05E-02	7,04E-02
ÇANKIRI	6,77E-02	6,76E-02	6,75E-02
ÇORUM	6,69E-02	6,68E-02	6,67E-02
ANKARA	6,55E-02	6,54E-02	6,53E-02
IGDIR	6,53E-02	6,52E-02	6,52E-02
ERZINCAN	5,92E-02	5,90E-02	5,88E-02
ARTVIN	5,89E-02	5,88E-02	5,87E-02
BOLU	5,33E-02	5,31E-02	5,30E-02
GÜMÜSHANE	4,91E-02	4,90E-02	4,89E-02
BINGÖL	4,51E-02	4,51E-02	4,50E-02
TUNCELI	4,15E-02	4,12E-02	4,10E-02
SAMSUN	3,80E-02	3,79E-02	3,79E-02
GİRESUN	3,49E-02	3,48E-02	3,47E-02
KIRKLARELI	3,41E-02	3,38E-02	3,35E-02
AMASYA	3,18E-02	3,18E-02	3,17E-02
ELAZIG	2,95E-02	2,95E-02	2,94E-02
ESKİSEHIR	2,56E-02	2,55E-02	2,55E-02
ISPARTA	2,48E-02	2,47E-02	2,47E-02
NEVSEHIR	2,43E-02	2,42E-02	2,41E-02
RIZE	2,31E-02	2,30E-02	2,29E-02
KONYA	2,31E-02	2,31E-02	2,30E-02
TEKIRDAG	2,14E-02	2,12E-02	2,11E-02
ISTANBUL	1,90E-02	1,89E-02	1,89E-02
SIVAS	1,87E-02	1,84E-02	1,83E-02
AGRI	1,85E-02	1,84E-02	1,84E-02
EDİRNE	1,80E-02	1,78E-02	1,77E-02
BARTIN	1,79E-02	1,78E-02	1,77E-02
KİRSEHIR	1,74E-02	1,74E-02	1,74E-02
DÜZCE	1,74E-02	1,73E-02	1,73E-02
AFYON	1,73E-02	1,72E-02	1,71E-02
YOZGAT	1,67E-02	1,67E-02	1,66E-02
ZONGULDAK	1,51E-02	1,50E-02	1,49E-02
BURDUR	1,44E-02	1,42E-02	1,41E-02
USAK	1,39E-02	1,38E-02	1,38E-02
DIYARBAKIR	1,36E-02	1,36E-02	1,36E-02
ÇANAĞKALE	1,33E-02	1,31E-02	1,29E-02
AYDIN	1,31E-02	1,29E-02	1,28E-02
MALATYA	1,28E-02	1,27E-02	1,26E-02

Table B.10 (continued): Calculated doses for Turkish Provinces by using BR2 simulation results (UNSCEAR Approach).

İÇEL	1,20E-02	1,20E-02	1,20E-02
MUGLA	1,20E-02	1,18E-02	1,16E-02
IZMIR	1,18E-02	1,16E-02	1,15E-02
NIGDE	1,17E-02	1,17E-02	1,17E-02
KAYSERI	1,16E-02	1,15E-02	1,14E-02
DENIZLI	1,00E-02	9,94E-03	9,87E-03
TOKAT	9,70E-03	9,64E-03	9,58E-03
ANTALYA	9,25E-03	9,13E-03	9,03E-03
ORDU	8,94E-03	8,82E-03	8,73E-03
SAKARYA	8,71E-03	8,58E-03	8,48E-03
TRABZON	7,65E-03	7,59E-03	7,55E-03
BALIKESIR	7,62E-03	7,51E-03	7,42E-03
YALOVA	7,02E-03	6,82E-03	6,67E-03
KOCAELI	6,72E-03	6,61E-03	6,53E-03
KÜTAHYA	6,44E-03	6,41E-03	6,39E-03
HATAY	6,13E-03	6,13E-03	6,13E-03
BURSA	6,00E-03	5,93E-03	5,87E-03
MANISA	5,79E-03	5,71E-03	5,65E-03
BATMAN	5,06E-03	5,06E-03	5,06E-03
BILECIK	4,76E-03	4,74E-03	4,72E-03
AKSARAY	3,77E-03	3,77E-03	3,76E-03
MUS	3,71E-03	3,71E-03	3,71E-03
ADIYAMAN	3,50E-03	3,50E-03	3,49E-03
KARAMAN	3,11E-03	3,09E-03	3,08E-03
K.MARAS	2,51E-03	2,50E-03	2,49E-03
KILIS	2,38E-03	2,38E-03	2,38E-03
OSMANIYE	2,05E-03	2,05E-03	2,05E-03
ADANA	2,05E-03	2,05E-03	2,04E-03
SANLIURFA	2,05E-03	2,04E-03	2,04E-03
VAN	1,39E-03	1,39E-03	1,39E-03
GAZIANTEP	1,35E-03	1,35E-03	1,35E-03
BITLIS	1,07E-03	1,07E-03	1,07E-03
SIRNAK	8,62E-04	8,62E-04	8,62E-04
MARDIN	6,96E-04	6,95E-04	6,94E-04
SIIRT	5,93E-04	5,93E-04	5,93E-04
HAKKARI	1,75E-04	1,75E-04	1,75E-04

Table B.11: Calculated doses for Turkish Provinces by using BR2 simulation results (WHO Approach).

Province	Doses (mSv)		
	Adult	Child	Infant
BAYBURT	8,45E-02	8,44E-02	1,12E-01
ARDAHAN	8,12E-02	8,11E-02	1,08E-01
KASTAMONU	6,38E-02	6,36E-02	8,46E-02
KIRIKKALE	5,93E-02	5,91E-02	7,85E-02
KARS	5,87E-02	5,85E-02	7,77E-02
ERZURUM	5,21E-02	5,20E-02	6,92E-02
KARABK	4,72E-02	4,67E-02	6,18E-02
SINOP	4,70E-02	4,68E-02	6,22E-02
ÇANKIRI	4,51E-02	4,47E-02	5,92E-02
ÇORUM	4,45E-02	4,42E-02	5,85E-02
ANKARA	4,35E-02	4,32E-02	5,73E-02
IGDIR	4,31E-02	4,29E-02	5,71E-02
ERZINCAN	4,01E-02	3,94E-02	5,17E-02
ARTVIN	3,92E-02	3,89E-02	5,15E-02
BOLU	3,58E-02	3,53E-02	4,66E-02
GUMUSHANE	3,26E-02	3,24E-02	4,29E-02
BINGÖL	2,98E-02	2,97E-02	3,95E-02
TUNCELI	2,85E-02	2,78E-02	3,62E-02
SAMSUN	2,53E-02	2,51E-02	3,32E-02
KIRKLARELI	2,41E-02	2,31E-02	2,97E-02
GIRESUN	2,34E-02	2,31E-02	3,05E-02
AMASYA	2,13E-02	2,10E-02	2,78E-02
ELAZIG	1,98E-02	1,96E-02	2,58E-02
ESKISEHIR	1,71E-02	1,69E-02	2,24E-02
ISPARTA	1,67E-02	1,65E-02	2,17E-02
NEVSEHIR	1,64E-02	1,61E-02	2,12E-02
RIZE	1,57E-02	1,54E-02	2,02E-02
KONYA	1,52E-02	1,52E-02	2,02E-02
TEKIRDAG	1,50E-02	1,45E-02	1,87E-02
SIVAS	1,33E-02	1,27E-02	1,63E-02
EDIRNE	1,29E-02	1,23E-02	1,57E-02
ISTANBUL	1,28E-02	1,26E-02	1,66E-02
AGRI	1,22E-02	1,22E-02	1,62E-02
BARTIN	1,22E-02	1,19E-02	1,56E-02
DZCE	1,18E-02	1,16E-02	1,52E-02
AFYON	1,17E-02	1,15E-02	1,51E-02
KIRSEHIR	1,15E-02	1,15E-02	1,52E-02
YOZGAT	1,13E-02	1,11E-02	1,46E-02
BURDUR	1,05E-02	9,88E-03	1,25E-02
ZONGULDAK	1,04E-02	1,01E-02	1,32E-02
ÇANAkkALE	9,83E-03	9,20E-03	1,16E-02
AYDIN	9,46E-03	8,96E-03	1,14E-02
USAK	9,27E-03	9,17E-03	1,21E-02
DIYARBAKIR	8,99E-03	8,95E-03	1,19E-02
MALATYA	8,79E-03	8,55E-03	1,12E-02

Table B.11 (continued): Calculated doses for Turkish Provinces by using BR2 simulation results (WHO Approach).

MUGLA	8,76E-03	8,23E-03	1,04E-02
IZMIR	8,58E-03	8,09E-03	1,03E-02
KAYSERI	8,16E-03	7,85E-03	1,01E-02
IÇEL	8,07E-03	7,97E-03	1,05E-02
NIGDE	7,69E-03	7,68E-03	1,02E-02
DENIZLI	7,06E-03	6,78E-03	8,75E-03
TOKAT	6,71E-03	6,51E-03	8,47E-03
ANTALYA	6,69E-03	6,33E-03	8,06E-03
ORDU	6,46E-03	6,11E-03	7,79E-03
SAKARYA	6,35E-03	5,98E-03	7,58E-03
BALIKESIR	5,59E-03	5,25E-03	6,63E-03
YALOVA	5,58E-03	5,01E-03	6,08E-03
TRABZON	5,32E-03	5,14E-03	6,68E-03
KOCAELI	4,96E-03	4,64E-03	5,85E-03
KÜTAHYA	4,38E-03	4,29E-03	5,63E-03
BURSA	4,33E-03	4,10E-03	5,23E-03
MANISA	4,21E-03	3,97E-03	5,04E-03
HATAY	4,04E-03	4,03E-03	5,37E-03
BATMAN	3,32E-03	3,32E-03	4,43E-03
BILECIK	3,27E-03	3,18E-03	4,16E-03
AKSARAY	2,50E-03	2,49E-03	3,30E-03
MUS	2,45E-03	2,44E-03	3,25E-03
ADIYAMAN	2,31E-03	2,30E-03	3,06E-03
KARAMAN	2,15E-03	2,09E-03	2,72E-03
K.MARAS	1,68E-03	1,66E-03	2,19E-03
KILIS	1,56E-03	1,56E-03	2,09E-03
OSMANIYE	1,37E-03	1,36E-03	1,80E-03
ADANA	1,36E-03	1,35E-03	1,79E-03
SANLIURFA	1,35E-03	1,35E-03	1,79E-03
VAN	9,14E-04	9,14E-04	1,22E-03
GAZIANTEP	9,04E-04	8,95E-04	1,18E-03
BITLIS	7,01E-04	7,01E-04	9,35E-04
SIRNAK	5,66E-04	5,66E-04	7,55E-04
MARDIN	4,63E-04	4,60E-04	6,09E-04
SIIRT	3,89E-04	3,89E-04	5,19E-04
HAKKARI	1,15E-04	1,15E-04	1,53E-04

Table B.12: Calculated doses for Turkish Provinces by using EV1 simulation results (UNSCEAR Approach).

Province	Doses (mSv)		
	Adult	Child	Infant
ARDAHAN	1,39E-01	1,39E-01	1,39E-01
BAYBURT	1,31E-01	1,31E-01	1,31E-01
KASTAMONU	1,28E-01	1,28E-01	1,28E-01
SINOP	1,18E-01	1,18E-01	1,18E-01
KIRIKKALE	1,16E-01	1,16E-01	1,16E-01
KARS	1,06E-01	1,06E-01	1,06E-01
ANKARA	8,59E-02	8,59E-02	8,58E-02
KARABÜK	8,26E-02	8,25E-02	8,24E-02
ERZURUM	8,14E-02	8,14E-02	8,14E-02
ÇANKIRI	7,90E-02	7,88E-02	7,87E-02
IGDIR	6,99E-02	6,98E-02	6,98E-02
ÇORUM	6,95E-02	6,94E-02	6,93E-02
ARTVIN	6,75E-02	6,74E-02	6,74E-02
ERZINCAN	6,12E-02	6,10E-02	6,08E-02
BOLU	5,87E-02	5,85E-02	5,83E-02
SAMSUN	5,45E-02	5,44E-02	5,43E-02
GÜMÜSHANE	5,35E-02	5,34E-02	5,34E-02
BINGÖL	5,25E-02	5,24E-02	5,24E-02
TUNCELI	3,73E-02	3,70E-02	3,68E-02
AMASYA	3,68E-02	3,67E-02	3,66E-02
ELAZIG	3,66E-02	3,64E-02	3,64E-02
GIRESUN	3,51E-02	3,50E-02	3,49E-02
KIRSEHIR	3,00E-02	3,00E-02	3,00E-02
KIRKLARELI	2,81E-02	2,77E-02	2,75E-02
ESKISEHIR	2,79E-02	2,78E-02	2,78E-02
ISPARTA	2,58E-02	2,58E-02	2,57E-02
KONYA	2,38E-02	2,38E-02	2,38E-02
NEVSEHIR	2,36E-02	2,35E-02	2,35E-02
DÜZCE	2,23E-02	2,21E-02	2,21E-02
RIZE	2,08E-02	2,06E-02	2,06E-02
ISTANBUL	2,02E-02	2,01E-02	2,00E-02
TEKIRDAG	1,93E-02	1,91E-02	1,90E-02
AGRI	1,88E-02	1,88E-02	1,88E-02
YOZGAT	1,55E-02	1,55E-02	1,54E-02
BARTIN	1,54E-02	1,53E-02	1,53E-02
SIVAS	1,46E-02	1,44E-02	1,43E-02
MALATYA	1,42E-02	1,40E-02	1,39E-02
AFYON	1,40E-02	1,40E-02	1,39E-02
USAK	1,39E-02	1,38E-02	1,38E-02
İÇEL	1,32E-02	1,31E-02	1,31E-02
ZONGULDAK	1,31E-02	1,30E-02	1,29E-02
DIYARBAKIR	1,30E-02	1,30E-02	1,30E-02
EDİRNE	1,17E-02	1,15E-02	1,13E-02
BATMAN	1,16E-02	1,16E-02	1,16E-02
SAKARYA	9,67E-03	9,56E-03	9,47E-03

Table B.12 (continued): Calculated doses for Turkish Provinces by using EV1 simulation results (UNSCEAR Approach).

DENIZLI	9,30E-03	9,18E-03	9,08E-03
BURDUR	8,82E-03	8,59E-03	8,41E-03
KAYSERI	8,67E-03	8,60E-03	8,54E-03
NIGDE	8,30E-03	8,30E-03	8,30E-03
TOKAT	8,18E-03	8,12E-03	8,08E-03
AYDIN	8,17E-03	7,93E-03	7,74E-03
ÇANAKKALE	7,93E-03	7,68E-03	7,48E-03
KARAMAN	6,95E-03	6,94E-03	6,93E-03
MUGLA	6,87E-03	6,68E-03	6,53E-03
TRABZON	6,85E-03	6,73E-03	6,63E-03
IZMIR	6,68E-03	6,49E-03	6,34E-03
BILECIK	6,19E-03	6,10E-03	6,03E-03
KÜTAHYA	6,03E-03	5,98E-03	5,94E-03
ADIYAMAN	5,75E-03	5,75E-03	5,74E-03
HATAY	5,74E-03	5,73E-03	5,73E-03
ANTALYA	5,63E-03	5,49E-03	5,38E-03
MUS	5,17E-03	5,16E-03	5,16E-03
BALIKESIR	4,87E-03	4,73E-03	4,61E-03
ORDU	4,34E-03	4,28E-03	4,24E-03
K.MARAS	4,32E-03	4,31E-03	4,29E-03
MANISA	3,88E-03	3,81E-03	3,75E-03
BURSA	3,79E-03	3,68E-03	3,59E-03
AKSARAY	3,46E-03	3,45E-03	3,44E-03
KOCAELI	3,00E-03	2,94E-03	2,90E-03
ADANA	2,93E-03	2,93E-03	2,92E-03
SANLIURFA	2,47E-03	2,46E-03	2,46E-03
BITLIS	2,28E-03	2,28E-03	2,28E-03
VAN	2,15E-03	2,14E-03	2,14E-03
YALOVA	1,94E-03	1,88E-03	1,83E-03
GAZIANTEP	1,62E-03	1,61E-03	1,61E-03
OSMANIYE	1,60E-03	1,60E-03	1,59E-03
MARDIN	1,57E-03	1,56E-03	1,56E-03
SIIRT	1,15E-03	1,15E-03	1,15E-03
KILIS	9,58E-04	9,54E-04	9,51E-04
SIRNAK	7,02E-04	7,02E-04	7,02E-04
HAKKARI	8,85E-05	8,85E-05	8,85E-05

Table B.13: Calculated doses for Turkish Provinces by using EV1 simulation results (WHO Approach).

Province	Doses (mSv)		
	Adult	Child	Infant
ARDAHAN	9,16E-02	9,14E-02	1,22E-01
BAYBURT	8,66E-02	8,63E-02	1,15E-01
KASTAMONU	8,47E-02	8,44E-02	1,12E-01
SINOP	7,78E-02	7,76E-02	1,03E-01
KIRIKKALE	7,62E-02	7,60E-02	1,01E-01
KARS	6,98E-02	6,95E-02	9,25E-02
ANKARA	5,69E-02	5,66E-02	7,52E-02
KARABK	5,47E-02	5,44E-02	7,23E-02
ERZURUM	5,37E-02	5,35E-02	7,13E-02
ANKIRI	5,29E-02	5,23E-02	6,91E-02
ORUM	4,63E-02	4,59E-02	6,08E-02
IGDIR	4,61E-02	4,60E-02	6,11E-02
ARTVIN	4,47E-02	4,45E-02	5,91E-02
ERZINCAN	4,12E-02	4,06E-02	5,35E-02
BOLU	3,94E-02	3,89E-02	5,13E-02
SAMSUN	3,62E-02	3,60E-02	4,77E-02
GÜMÜSHANE	3,55E-02	3,53E-02	4,68E-02
BINGÖL	3,47E-02	3,46E-02	4,59E-02
TUNCELI	2,58E-02	2,50E-02	3,26E-02
AMASYA	2,47E-02	2,44E-02	3,22E-02
ELAZIG	2,46E-02	2,42E-02	3,20E-02
GIRESUN	2,38E-02	2,34E-02	3,07E-02
KIRKLARELI	2,00E-02	1,91E-02	2,45E-02
KIRSEHIR	1,98E-02	1,97E-02	2,63E-02
ESKISEHIR	1,86E-02	1,84E-02	2,44E-02
ISPARTA	1,74E-02	1,72E-02	2,26E-02
NEVSEHIR	1,58E-02	1,56E-02	2,06E-02
KONYA	1,57E-02	1,57E-02	2,09E-02
DÜZCE	1,52E-02	1,48E-02	1,94E-02
RIZE	1,42E-02	1,39E-02	1,81E-02
ISTANBUL	1,37E-02	1,34E-02	1,76E-02
TEKIRDAG	1,35E-02	1,30E-02	1,68E-02
AGRI	1,24E-02	1,24E-02	1,65E-02
SIVAS	1,07E-02	1,01E-02	1,27E-02
YOZGAT	1,04E-02	1,03E-02	1,36E-02
BARTIN	1,03E-02	1,02E-02	1,34E-02
MALATYA	1,01E-02	9,62E-03	1,24E-02
AFYON	9,68E-03	9,41E-03	1,23E-02
USAK	9,25E-03	9,17E-03	1,21E-02
ZONGULDAK	8,95E-03	8,73E-03	1,14E-02
EDIRNE	8,91E-03	8,20E-03	1,02E-02
İÇEL	8,83E-03	8,72E-03	1,15E-02
DIYARBAKIR	8,59E-03	8,57E-03	1,14E-02
BATMAN	7,64E-03	7,64E-03	1,02E-02
BURDUR	6,95E-03	6,27E-03	7,64E-03

Table B.13 (continued): Calculated doses for Turkish Provinces by using EV1 simulation results (WHO Approach).

SAKARYA	6,93E-03	6,59E-03	8,43E-03
DENIZLI	6,72E-03	6,36E-03	8,10E-03
AYDIN	6,56E-03	5,85E-03	7,07E-03
ÇANAKKALE	6,47E-03	5,73E-03	6,86E-03
KAYSERI	6,08E-03	5,85E-03	7,57E-03
TOKAT	5,66E-03	5,49E-03	7,14E-03
MUGLA	5,48E-03	4,91E-03	5,95E-03
NIGDE	5,47E-03	5,46E-03	7,27E-03
IZMIR	5,34E-03	4,78E-03	5,78E-03
TRABZON	5,14E-03	4,77E-03	5,96E-03
KARAMAN	4,63E-03	4,59E-03	6,08E-03
BILECIK	4,54E-03	4,26E-03	5,39E-03
ANTALYA	4,39E-03	3,98E-03	4,88E-03
KÜTAHYA	4,20E-03	4,06E-03	5,26E-03
BALIKESIR	3,92E-03	3,50E-03	4,21E-03
ADIYAMAN	3,83E-03	3,80E-03	5,03E-03
HATAY	3,79E-03	3,78E-03	5,02E-03
MUS	3,41E-03	3,40E-03	4,52E-03
ORDU	3,15E-03	2,97E-03	3,78E-03
BURSA	3,05E-03	2,72E-03	3,28E-03
K.MARAS	2,93E-03	2,88E-03	3,78E-03
MANISA	2,91E-03	2,70E-03	3,37E-03
AKSARAY	2,34E-03	2,30E-03	3,03E-03
KOCAELI	2,25E-03	2,08E-03	2,60E-03
ADANA	1,94E-03	1,93E-03	2,56E-03
SANLIURFA	1,63E-03	1,62E-03	2,16E-03
YALOVA	1,56E-03	1,39E-03	1,67E-03
BITLIS	1,50E-03	1,50E-03	2,00E-03
VAN	1,42E-03	1,41E-03	1,88E-03
GAZIANTEP	1,09E-03	1,07E-03	1,41E-03
OSMANIYE	1,07E-03	1,06E-03	1,40E-03
MARDIN	1,04E-03	1,03E-03	1,37E-03
SIIRT	7,53E-04	7,53E-04	1,00E-03
KILIS	6,48E-04	6,37E-04	8,37E-04
SIRNAK	4,62E-04	4,61E-04	6,14E-04
HAKKARI	5,81E-05	5,81E-05	7,75E-05

Table B.14: Calculated doses for Turkish Provinces by using EV2 simulation results (UNSCEAR Approach).

Province	Doses (mSv)		
	Adult	Child	Infant
ARDAHAN	1,48E-01	1,48E-01	1,48E-01
BAYBURT	1,34E-01	1,34E-01	1,34E-01
KASTAMONU	1,05E-01	1,05E-01	1,05E-01
KIRIKKALE	1,03E-01	1,03E-01	1,03E-01
SINOP	9,72E-02	9,71E-02	9,70E-02
KARS	8,82E-02	8,81E-02	8,81E-02
ANKARA	8,06E-02	8,05E-02	8,04E-02
KARABÜK	7,97E-02	7,96E-02	7,95E-02
ERZURUM	7,76E-02	7,76E-02	7,75E-02
IGDIR	7,06E-02	7,05E-02	7,05E-02
ARTVIN	6,47E-02	6,46E-02	6,45E-02
ERZINCAN	6,46E-02	6,44E-02	6,42E-02
ÇORUM	6,39E-02	6,38E-02	6,37E-02
ÇANKIRI	6,36E-02	6,34E-02	6,33E-02
BOLU	5,90E-02	5,88E-02	5,86E-02
GÜMÜSHANE	5,25E-02	5,24E-02	5,23E-02
BINGÖL	4,99E-02	4,99E-02	4,98E-02
SAMSUN	4,48E-02	4,47E-02	4,47E-02
TUNCELI	4,05E-02	4,03E-02	4,01E-02
ELAZIG	4,01E-02	4,00E-02	4,00E-02
KIRKLARELI	3,30E-02	3,28E-02	3,25E-02
GIRESUN	3,09E-02	3,08E-02	3,07E-02
ESKISEHIR	2,75E-02	2,74E-02	2,73E-02
DÜZCE	2,66E-02	2,64E-02	2,62E-02
AMASYA	2,64E-02	2,63E-02	2,63E-02
RIZE	2,61E-02	2,60E-02	2,59E-02
ISPARTA	2,40E-02	2,39E-02	2,39E-02
KONYA	2,31E-02	2,31E-02	2,31E-02
TEKIRDAG	2,20E-02	2,17E-02	2,16E-02
KIRSEHIR	2,19E-02	2,19E-02	2,19E-02
EDIRNE	2,05E-02	2,02E-02	2,00E-02
ISTANBUL	2,04E-02	2,03E-02	2,02E-02
MALATYA	2,01E-02	1,99E-02	1,97E-02
SIVAS	1,91E-02	1,89E-02	1,87E-02
BARTIN	1,85E-02	1,85E-02	1,85E-02
AFYON	1,70E-02	1,69E-02	1,69E-02
YOZGAT	1,70E-02	1,69E-02	1,69E-02
AGRI	1,70E-02	1,69E-02	1,69E-02
NEVSEHIR	1,61E-02	1,61E-02	1,60E-02
BURDUR	1,58E-02	1,56E-02	1,54E-02
ZONGULDAK	1,55E-02	1,54E-02	1,54E-02
ÇANAKKALE	1,49E-02	1,47E-02	1,45E-02
DENIZLI	1,36E-02	1,35E-02	1,33E-02
AYDIN	1,30E-02	1,28E-02	1,27E-02
İÇEL	1,22E-02	1,21E-02	1,21E-02

Table B.14 (continued): Calculated doses for Turkish Provinces by using EV2 simulation results (UNSCEAR Approach).

DIYARBAKIR	1,18E-02	1,18E-02	1,18E-02
SAKARYA	1,16E-02	1,15E-02	1,14E-02
USAK	1,12E-02	1,12E-02	1,12E-02
ANTALYA	1,06E-02	1,05E-02	1,03E-02
MUGLA	1,02E-02	1,00E-02	9,92E-03
BILECIK	9,84E-03	9,72E-03	9,63E-03
TOKAT	9,80E-03	9,70E-03	9,63E-03
IZMIR	9,12E-03	9,00E-03	8,91E-03
BATMAN	9,12E-03	9,12E-03	9,12E-03
ORDU	9,11E-03	9,01E-03	8,92E-03
TRABZON	8,95E-03	8,86E-03	8,80E-03
KÜTAHYA	8,28E-03	8,22E-03	8,16E-03
KOCAELI	7,31E-03	7,22E-03	7,15E-03
BALIKESIR	7,12E-03	6,99E-03	6,88E-03
NIGDE	6,76E-03	6,75E-03	6,75E-03
YALOVA	6,58E-03	6,42E-03	6,30E-03
KAYSERI	6,46E-03	6,41E-03	6,37E-03
MANISA	5,90E-03	5,82E-03	5,76E-03
ADYAMAN	5,82E-03	5,80E-03	5,78E-03
BURSA	3,99E-03	3,92E-03	3,87E-03
HATAY	3,87E-03	3,86E-03	3,86E-03
K.MARAS	3,34E-03	3,32E-03	3,30E-03
MUS	3,26E-03	3,25E-03	3,25E-03
AKSARAY	2,57E-03	2,57E-03	2,57E-03
ADANA	2,16E-03	2,16E-03	2,16E-03
SANLIURFA	2,08E-03	2,07E-03	2,07E-03
VAN	1,98E-03	1,98E-03	1,98E-03
MARDIN	1,93E-03	1,93E-03	1,93E-03
KARAMAN	1,89E-03	1,87E-03	1,86E-03
BITLIS	1,60E-03	1,60E-03	1,60E-03
OSMANIYE	1,40E-03	1,40E-03	1,40E-03
GAZIANTEP	1,38E-03	1,38E-03	1,38E-03
KILIS	1,23E-03	1,23E-03	1,23E-03
SIRNAK	8,47E-04	8,47E-04	8,47E-04
SIIRT	6,85E-04	6,85E-04	6,85E-04
HAKKARI	2,62E-04	2,62E-04	2,62E-04

Table B.15: Calculated doses for Turkish Provinces by using EV2 simulation results (WHO Approach).

Province	Doses (mSv)		
	Adult	Child	Infant
ARDAHAN	9,76E-02	9,74E-02	1,30E-01
BAYBURT	8,81E-02	8,79E-02	1,17E-01
KASTAMONU	6,92E-02	6,89E-02	9,16E-02
KIRIKKALE	6,79E-02	6,76E-02	9,00E-02
SINOP	6,44E-02	6,41E-02	8,51E-02
KARS	5,82E-02	5,80E-02	7,72E-02
ANKARA	5,35E-02	5,32E-02	7,05E-02
KARABK	5,29E-02	5,26E-02	6,97E-02
ERZURUM	5,11E-02	5,10E-02	6,79E-02
IGDIR	4,65E-02	4,64E-02	6,18E-02
ERZINCAN	4,35E-02	4,29E-02	5,65E-02
ARTVIN	4,31E-02	4,28E-02	5,66E-02
ÇANKIRI	4,25E-02	4,21E-02	5,56E-02
ÇORUM	4,25E-02	4,22E-02	5,59E-02
BOLU	3,97E-02	3,91E-02	5,16E-02
GÜMÜSHANE	3,49E-02	3,46E-02	4,59E-02
BINGÖL	3,30E-02	3,29E-02	4,37E-02
SAMSUN	2,98E-02	2,96E-02	3,92E-02
TUNCELI	2,79E-02	2,71E-02	3,54E-02
ELAZIG	2,69E-02	2,66E-02	3,51E-02
KIRKLARELI	2,31E-02	2,23E-02	2,88E-02
GIRESUN	2,08E-02	2,05E-02	2,70E-02
DÜZCE	1,85E-02	1,79E-02	2,32E-02
ESKISEHIR	1,85E-02	1,82E-02	2,40E-02
RIZE	1,76E-02	1,73E-02	2,28E-02
AMASYA	1,76E-02	1,74E-02	2,31E-02
ISPARTA	1,62E-02	1,60E-02	2,10E-02
TEKIRDAG	1,55E-02	1,49E-02	1,91E-02
KONYA	1,52E-02	1,52E-02	2,03E-02
EDIRNE	1,49E-02	1,40E-02	1,78E-02
KIRSEHIR	1,45E-02	1,45E-02	1,92E-02
MALATYA	1,42E-02	1,36E-02	1,75E-02
ISTANBUL	1,40E-02	1,37E-02	1,78E-02
SIVAS	1,37E-02	1,30E-02	1,67E-02
BARTIN	1,23E-02	1,22E-02	1,62E-02
BURDUR	1,16E-02	1,09E-02	1,38E-02
AFYON	1,16E-02	1,13E-02	1,49E-02
YOZGAT	1,15E-02	1,13E-02	1,49E-02
AGRI	1,12E-02	1,12E-02	1,48E-02
ÇANAKKALE	1,09E-02	1,02E-02	1,30E-02
NEVSEHIR	1,08E-02	1,07E-02	1,41E-02
ZONGULDAK	1,05E-02	1,03E-02	1,35E-02
DENIZLI	9,76E-03	9,28E-03	1,19E-02
AYDIN	9,45E-03	8,91E-03	1,13E-02
İÇEL	8,20E-03	8,07E-03	1,06E-02

Table B.15 (continued): Calculated doses for Turkish Provinces by using EV2 simulation results (WHO Approach).

SAKARYA	8,14E-03	7,82E-03	1,01E-02
DIYARBAKIR	7,82E-03	7,79E-03	1,04E-02
ANTALYA	7,70E-03	7,27E-03	9,23E-03
USAK	7,54E-03	7,44E-03	9,83E-03
MUGLA	7,45E-03	7,00E-03	8,87E-03
BILECIK	7,04E-03	6,70E-03	8,57E-03
TOKAT	6,90E-03	6,63E-03	8,54E-03
IZMIR	6,60E-03	6,24E-03	7,94E-03
ORDU	6,50E-03	6,20E-03	7,94E-03
TRABZON	6,30E-03	6,05E-03	7,80E-03
BATMAN	5,99E-03	5,99E-03	7,99E-03
KÜTAHYA	5,78E-03	5,58E-03	7,23E-03
BALIKESIR	5,36E-03	4,96E-03	6,19E-03
KOCAELI	5,25E-03	4,99E-03	6,37E-03
YALOVA	5,12E-03	4,65E-03	5,70E-03
KAYSERI	4,50E-03	4,35E-03	5,64E-03
NIGDE	4,44E-03	4,44E-03	5,91E-03
MANISA	4,24E-03	4,02E-03	5,14E-03
ADIYAMAN	3,95E-03	3,88E-03	5,09E-03
BURSA	2,94E-03	2,75E-03	3,47E-03
HATAY	2,58E-03	2,56E-03	3,39E-03
K.MARAS	2,31E-03	2,24E-03	2,92E-03
MUS	2,17E-03	2,15E-03	2,85E-03
AKSARAY	1,70E-03	1,69E-03	2,25E-03
ADANA	1,43E-03	1,43E-03	1,89E-03
SANLIURFA	1,37E-03	1,36E-03	1,82E-03
KARAMAN	1,31E-03	1,27E-03	1,65E-03
VAN	1,30E-03	1,30E-03	1,73E-03
MARDIN	1,28E-03	1,27E-03	1,69E-03
BITLIS	1,05E-03	1,05E-03	1,40E-03
OSMANIYE	9,23E-04	9,22E-04	1,23E-03
GAZIANTEP	9,12E-04	9,09E-04	1,21E-03
KILIS	8,19E-04	8,13E-04	1,08E-03
SIRNAK	5,56E-04	5,56E-04	7,41E-04
SIIRT	4,50E-04	4,50E-04	6,00E-04
HAKKARI	1,73E-04	1,72E-04	2,29E-04

Table B.16: Calculated doses for Turkish Provinces by using SU1 simulation results (UNSCEAR Approach).

Province	Doses (mSv)		
	Adult	Child	Infant
ARDAHAN	9,43E-02	9,42E-02	9,42E-02
BAYBURT	8,68E-02	8,68E-02	8,67E-02
SINOP	7,67E-02	7,67E-02	7,66E-02
KASTAMONU	7,49E-02	7,48E-02	7,48E-02
KARS	7,41E-02	7,41E-02	7,40E-02
KIRIKKALE	6,22E-02	6,21E-02	6,20E-02
KARABÜK	5,69E-02	5,68E-02	5,67E-02
ERZURUM	5,35E-02	5,34E-02	5,34E-02
ÇANKIRI	5,06E-02	5,05E-02	5,04E-02
ARTVIN	4,99E-02	4,98E-02	4,97E-02
ANKARA	4,87E-02	4,86E-02	4,85E-02
ÇORUM	4,74E-02	4,74E-02	4,73E-02
BINGÖL	4,42E-02	4,42E-02	4,42E-02
IGDIR	4,18E-02	4,18E-02	4,17E-02
SAMSUN	4,05E-02	4,04E-02	4,03E-02
ERZINCAN	4,04E-02	4,03E-02	4,02E-02
BOLU	3,73E-02	3,73E-02	3,72E-02
AMASYA	3,38E-02	3,37E-02	3,36E-02
TUNCELI	3,10E-02	3,08E-02	3,06E-02
GÜMÜSHANE	2,85E-02	2,84E-02	2,83E-02
ELAZIG	2,58E-02	2,58E-02	2,58E-02
GIRESUN	2,19E-02	2,19E-02	2,18E-02
KIRKLARELI	2,14E-02	2,11E-02	2,10E-02
RIZE	1,81E-02	1,80E-02	1,80E-02
ESKISEHIR	1,79E-02	1,78E-02	1,78E-02
ISTANBUL	1,72E-02	1,72E-02	1,71E-02
ISPARTA	1,71E-02	1,70E-02	1,70E-02
KONYA	1,65E-02	1,65E-02	1,64E-02
BARTIN	1,53E-02	1,53E-02	1,53E-02
AGRI	1,28E-02	1,28E-02	1,28E-02
TEKIRDAG	1,23E-02	1,22E-02	1,22E-02
DIYARBAKIR	1,14E-02	1,14E-02	1,14E-02
MALATYA	1,11E-02	1,10E-02	1,09E-02
DÜZCE	1,07E-02	1,07E-02	1,07E-02
KIRSEHIR	1,04E-02	1,04E-02	1,04E-02
İÇEL	1,02E-02	1,01E-02	1,01E-02
USAK	9,84E-03	9,81E-03	9,78E-03
SIVAS	9,75E-03	9,62E-03	9,52E-03
NIGDE	9,55E-03	9,55E-03	9,55E-03
NEVSEHIR	8,87E-03	8,80E-03	8,75E-03
YOZGAT	8,81E-03	8,77E-03	8,73E-03
EDIRNE	8,42E-03	8,25E-03	8,11E-03
ZONGULDAK	7,33E-03	7,24E-03	7,17E-03
AFYON	6,76E-03	6,71E-03	6,67E-03
DENIZLI	6,60E-03	6,47E-03	6,37E-03

Table B.16 (continued): Calculated doses for Turkish Provinces by using SU1 simulation results (UNSCEAR Approach).

KAYSERI	6,59E-03	6,53E-03	6,48E-03
ADIYAMAN	6,44E-03	6,43E-03	6,41E-03
BURDUR	6,21E-03	6,03E-03	5,90E-03
SAKARYA	5,77E-03	5,66E-03	5,57E-03
HATAY	5,64E-03	5,63E-03	5,62E-03
ÇANAKKALE	5,60E-03	5,44E-03	5,31E-03
AYDIN	5,51E-03	5,38E-03	5,27E-03
ANTALYA	5,02E-03	4,91E-03	4,82E-03
MUS	4,70E-03	4,70E-03	4,70E-03
TRABZON	4,63E-03	4,58E-03	4,55E-03
BILECIK	4,59E-03	4,50E-03	4,43E-03
MUGLA	4,57E-03	4,46E-03	4,37E-03
IZMIR	4,57E-03	4,44E-03	4,34E-03
KARAMAN	4,47E-03	4,46E-03	4,45E-03
TOKAT	4,10E-03	4,04E-03	4,00E-03
KÜTAHYA	4,05E-03	4,03E-03	4,01E-03
ORDU	3,44E-03	3,37E-03	3,33E-03
ADANA	3,29E-03	3,29E-03	3,28E-03
AKSARAY	3,27E-03	3,27E-03	3,27E-03
KOCAELI	3,09E-03	3,00E-03	2,93E-03
BALIKESIR	3,09E-03	3,02E-03	2,96E-03
K.MARAS	2,73E-03	2,72E-03	2,71E-03
SANLIURFA	2,45E-03	2,44E-03	2,44E-03
MANISA	2,44E-03	2,39E-03	2,34E-03
KILIS	2,26E-03	2,25E-03	2,25E-03
BITLIS	2,02E-03	2,02E-03	2,02E-03
BATMAN	1,72E-03	1,72E-03	1,72E-03
MARDIN	1,71E-03	1,71E-03	1,71E-03
GAZIANTEP	1,58E-03	1,58E-03	1,57E-03
VAN	1,49E-03	1,49E-03	1,49E-03
BURSA	1,25E-03	1,22E-03	1,20E-03
OSMANIYE	1,21E-03	1,21E-03	1,21E-03
SIIRT	5,73E-04	5,73E-04	5,73E-04
SIRNAK	5,09E-04	5,08E-04	5,08E-04
YALOVA	3,60E-04	3,60E-04	3,60E-04
HAKKARI	3,19E-05	3,19E-05	3,19E-05

Table B.17: Calculated doses for Turkish Provinces by using SU1 simulation results (WHO Approach).

Province	Doses (mSv)		
	Adult	Child	Infant
ARDAHAN	6,21E-02	6,20E-02	8,25E-02
BAYBURT	5,73E-02	5,71E-02	7,60E-02
SINOP	5,07E-02	5,05E-02	6,71E-02
KASTAMONU	4,95E-02	4,93E-02	6,55E-02
KARS	4,90E-02	4,88E-02	6,49E-02
KIRIKKALE	4,12E-02	4,10E-02	5,44E-02
KARABK	3,77E-02	3,75E-02	4,98E-02
ERZURUM	3,53E-02	3,52E-02	4,68E-02
ANKIRI	3,40E-02	3,36E-02	4,43E-02
ARTVIN	3,31E-02	3,29E-02	4,36E-02
ANKARA	3,24E-02	3,21E-02	4,26E-02
ÇORUM	3,14E-02	3,13E-02	4,15E-02
BINGÖL	2,91E-02	2,91E-02	3,87E-02
IGDIR	2,76E-02	2,75E-02	3,66E-02
ERZINCAN	2,73E-02	2,69E-02	3,54E-02
SAMSUN	2,69E-02	2,67E-02	3,54E-02
BOLU	2,49E-02	2,47E-02	3,27E-02
AMASYA	2,24E-02	2,23E-02	2,95E-02
TUNCELI	2,13E-02	2,07E-02	2,70E-02
GÜMÜSHANE	1,91E-02	1,88E-02	2,49E-02
ELAZIG	1,71E-02	1,70E-02	2,26E-02
KIRKLARELI	1,51E-02	1,45E-02	1,86E-02
GIRESUN	1,48E-02	1,46E-02	1,92E-02
RIZE	1,21E-02	1,20E-02	1,58E-02
ESKISEHIR	1,20E-02	1,18E-02	1,56E-02
ISPARTA	1,17E-02	1,14E-02	1,49E-02
ISTANBUL	1,16E-02	1,14E-02	1,51E-02
KONYA	1,09E-02	1,08E-02	1,44E-02
BARTIN	1,03E-02	1,02E-02	1,34E-02
AGRI	8,48E-03	8,43E-03	1,12E-02
TEKIRDAG	8,47E-03	8,23E-03	1,07E-02
MALATYA	7,94E-03	7,56E-03	9,68E-03
DIYARBAKIR	7,59E-03	7,54E-03	1,00E-02
DÜZCE	7,08E-03	7,04E-03	9,35E-03
SIVAS	7,04E-03	6,67E-03	8,49E-03
KIRSEHIR	6,94E-03	6,89E-03	9,13E-03
İÇEL	6,77E-03	6,71E-03	8,88E-03
USAK	6,63E-03	6,53E-03	8,60E-03
EDIRNE	6,41E-03	5,89E-03	7,31E-03
NIGDE	6,30E-03	6,28E-03	8,36E-03
NEVSEHIR	6,17E-03	5,97E-03	7,74E-03
YOZGAT	6,02E-03	5,88E-03	7,70E-03
ZONGULDAK	5,26E-03	5,00E-03	6,39E-03
DENIZLI	4,97E-03	4,59E-03	5,73E-03
BURDUR	4,94E-03	4,43E-03	5,37E-03

Table B.17 (continued): Calculated doses for Turkish Provinces by using SU1 simulation results (WHO Approach).

AFYON	4,68E-03	4,54E-03	5,90E-03
KAYSERI	4,62E-03	4,45E-03	5,75E-03
ÇANAKKALE	4,50E-03	4,02E-03	4,85E-03
SAKARYA	4,34E-03	4,02E-03	5,01E-03
ADİYAMAN	4,33E-03	4,27E-03	5,63E-03
AYDIN	4,29E-03	3,89E-03	4,78E-03
ANTALYA	3,89E-03	3,54E-03	4,36E-03
HATAY	3,77E-03	3,73E-03	4,94E-03
İZMİR	3,64E-03	3,26E-03	3,96E-03
MUGLA	3,58E-03	3,24E-03	3,96E-03
BİLECİK	3,47E-03	3,20E-03	3,99E-03
TRABZON	3,29E-03	3,14E-03	4,04E-03
MUS	3,08E-03	3,08E-03	4,11E-03
KARAMAN	2,99E-03	2,96E-03	3,91E-03
TOKAT	2,96E-03	2,80E-03	3,57E-03
KÜTAHYA	2,76E-03	2,70E-03	3,54E-03
ORDU	2,57E-03	2,38E-03	2,99E-03
KOCAELİ	2,49E-03	2,22E-03	2,67E-03
BALIKESİR	2,39E-03	2,18E-03	2,68E-03
ADANA	2,20E-03	2,18E-03	2,88E-03
AKSARAY	2,15E-03	2,15E-03	2,86E-03
MANISA	1,89E-03	1,72E-03	2,12E-03
K.MARAS	1,87E-03	1,82E-03	2,39E-03
SANLIURFA	1,62E-03	1,61E-03	2,14E-03
KILIS	1,49E-03	1,49E-03	1,97E-03
BITLİS	1,33E-03	1,33E-03	1,77E-03
BATMAN	1,13E-03	1,13E-03	1,50E-03
MARDIN	1,12E-03	1,12E-03	1,50E-03
GAZİANTEP	1,04E-03	1,04E-03	1,38E-03
VAN	9,80E-04	9,80E-04	1,31E-03
BURSA	9,65E-04	8,80E-04	1,09E-03
OSMANIYE	8,05E-04	7,99E-04	1,06E-03
SIİRT	3,76E-04	3,76E-04	5,02E-04
SIRNAK	3,35E-04	3,34E-04	4,45E-04
YALOVA	2,38E-04	2,37E-04	3,15E-04
HAKKARI	2,09E-05	2,09E-05	2,79E-05

Table B.18: Calculated doses for Turkish Provinces by using SU2 simulation results (UNSCEAR Approach).

Province	Doses (mSv)		
	Adult	Child	Infant
BAYBURT	1,01E-01	1,01E-01	1,01E-01
ARDAHAN	7,83E-02	7,83E-02	7,82E-02
KIRIKKALE	7,38E-02	7,37E-02	7,37E-02
KASTAMONU	6,77E-02	6,76E-02	6,76E-02
SINOP	6,50E-02	6,50E-02	6,49E-02
KARS	6,40E-02	6,39E-02	6,39E-02
ERZURUM	5,02E-02	5,02E-02	5,02E-02
IGDIR	4,56E-02	4,56E-02	4,56E-02
KARABÜK	4,55E-02	4,55E-02	4,54E-02
ANKARA	4,27E-02	4,26E-02	4,26E-02
ÇANKIRI	4,16E-02	4,15E-02	4,14E-02
ÇORUM	3,90E-02	3,90E-02	3,89E-02
ARTVIN	3,77E-02	3,76E-02	3,76E-02
BINGÖL	3,58E-02	3,58E-02	3,58E-02
GÜMÜSHANE	3,51E-02	3,51E-02	3,51E-02
ERZINCAN	3,38E-02	3,37E-02	3,37E-02
BOLU	3,06E-02	3,05E-02	3,05E-02
KIRKLARELI	2,38E-02	2,36E-02	2,35E-02
SAMSUN	2,37E-02	2,36E-02	2,35E-02
AMASYA	2,37E-02	2,36E-02	2,36E-02
ELAZIG	2,14E-02	2,13E-02	2,13E-02
TUNCELI	1,99E-02	1,98E-02	1,97E-02
GIRESUN	1,93E-02	1,93E-02	1,92E-02
NEVSEHIR	1,70E-02	1,69E-02	1,69E-02
RIZE	1,65E-02	1,64E-02	1,63E-02
TEKIRDAG	1,62E-02	1,60E-02	1,59E-02
ISPARTA	1,56E-02	1,55E-02	1,54E-02
KONYA	1,51E-02	1,51E-02	1,51E-02
KIRSEHIR	1,48E-02	1,48E-02	1,48E-02
ESKISEHIR	1,44E-02	1,44E-02	1,43E-02
SIVAS	1,38E-02	1,36E-02	1,35E-02
EDIRNE	1,33E-02	1,31E-02	1,30E-02
ISTANBUL	1,29E-02	1,28E-02	1,28E-02
YOZGAT	1,28E-02	1,27E-02	1,27E-02
DÜZCE	1,24E-02	1,23E-02	1,22E-02
BURDUR	1,12E-02	1,10E-02	1,09E-02
MALATYA	1,10E-02	1,09E-02	1,08E-02
BARTIN	9,96E-03	9,92E-03	9,89E-03
DENIZLI	9,76E-03	9,65E-03	9,57E-03
ÇANAKKALE	9,46E-03	9,33E-03	9,22E-03
AYDIN	9,44E-03	9,29E-03	9,17E-03
AGRI	9,05E-03	9,04E-03	9,03E-03
USAK	8,93E-03	8,92E-03	8,91E-03
ORDU	8,24E-03	8,18E-03	8,12E-03
AFYON	8,14E-03	8,09E-03	8,04E-03

Table B.18 (continued): Calculated doses for Turkish Provinces by using SU2 simulation results (UNSCEAR Approach).

MUGLA	8,05E-03	7,93E-03	7,83E-03
IZMIR	7,89E-03	7,78E-03	7,69E-03
IÇEL	7,78E-03	7,75E-03	7,73E-03
TRABZON	7,75E-03	7,66E-03	7,59E-03
ZONGULDAK	6,84E-03	6,81E-03	6,79E-03
KAYSERI	6,81E-03	6,78E-03	6,75E-03
NIGDE	6,75E-03	6,75E-03	6,74E-03
DIYARBAKIR	6,33E-03	6,32E-03	6,31E-03
BILECIK	6,29E-03	6,21E-03	6,15E-03
TOKAT	5,97E-03	5,93E-03	5,90E-03
ANTALYA	5,90E-03	5,81E-03	5,74E-03
SAKARYA	5,51E-03	5,45E-03	5,40E-03
KÜTAHYA	5,35E-03	5,31E-03	5,29E-03
BALIKESIR	5,32E-03	5,21E-03	5,12E-03
HATAY	4,89E-03	4,88E-03	4,88E-03
AKSARAY	4,79E-03	4,79E-03	4,79E-03
KOCAELI	4,54E-03	4,47E-03	4,42E-03
BURSA	4,07E-03	4,01E-03	3,96E-03
MANISA	3,57E-03	3,52E-03	3,48E-03
ADIYAMAN	2,71E-03	2,71E-03	2,71E-03
MARDIN	2,52E-03	2,52E-03	2,52E-03
YALOVA	2,50E-03	2,36E-03	2,26E-03
SANLIURFA	2,43E-03	2,43E-03	2,43E-03
MUS	1,98E-03	1,98E-03	1,98E-03
GAZIANTEP	1,90E-03	1,89E-03	1,89E-03
K.MARAS	1,61E-03	1,60E-03	1,60E-03
ADANA	1,58E-03	1,58E-03	1,58E-03
KARAMAN	1,50E-03	1,49E-03	1,49E-03
VAN	1,42E-03	1,42E-03	1,42E-03
BATMAN	1,20E-03	1,20E-03	1,20E-03
OSMANIYE	9,50E-04	9,50E-04	9,49E-04
BITLIS	5,50E-04	5,50E-04	5,50E-04
KILIS	5,31E-04	5,29E-04	5,27E-04
SIRNAK	5,12E-04	5,12E-04	5,12E-04
SIIRT	2,77E-04	2,77E-04	2,77E-04
HAKKARI	1,24E-04	1,24E-04	1,24E-04

Table B.19: Calculated doses for Turkish Provinces by using SU2 simulation results (WHO Approach).

Province	Doses (mSv)		
	Adult	Child	Infant
BAYBURT	6,73E-02	6,69E-02	8,87E-02
ARDAHAN	5,16E-02	5,15E-02	6,85E-02
KIRIKKALE	4,88E-02	4,86E-02	6,46E-02
KASTAMONU	4,47E-02	4,45E-02	5,92E-02
SINOP	4,28E-02	4,27E-02	5,69E-02
KARS	4,22E-02	4,21E-02	5,60E-02
ERZURUM	3,31E-02	3,30E-02	4,39E-02
KARABÜK	3,03E-02	3,01E-02	3,98E-02
IGDIR	3,01E-02	3,00E-02	3,99E-02
ANKARA	2,84E-02	2,82E-02	3,74E-02
ÇANKIRI	2,77E-02	2,75E-02	3,64E-02
ÇORUM	2,59E-02	2,58E-02	3,42E-02
ARTVIN	2,50E-02	2,48E-02	3,29E-02
BINGÖL	2,37E-02	2,36E-02	3,14E-02
GÜMÜSHANE	2,33E-02	2,32E-02	3,08E-02
ERZINCAN	2,27E-02	2,24E-02	2,96E-02
BOLU	2,04E-02	2,02E-02	2,68E-02
KIRKLARELI	1,67E-02	1,61E-02	2,08E-02
SAMSUN	1,59E-02	1,57E-02	2,07E-02
AMASYA	1,57E-02	1,56E-02	2,07E-02
ELAZIG	1,44E-02	1,42E-02	1,87E-02
TUNCELI	1,36E-02	1,33E-02	1,74E-02
GIRESUN	1,29E-02	1,28E-02	1,69E-02
NEVSEHIR	1,15E-02	1,13E-02	1,48E-02
TEKIRDAG	1,14E-02	1,09E-02	1,41E-02
RIZE	1,13E-02	1,10E-02	1,44E-02
ISPARTA	1,06E-02	1,04E-02	1,36E-02
KONYA	1,00E-02	9,96E-03	1,32E-02
KIRSEHIR	9,80E-03	9,77E-03	1,30E-02
SIVAS	9,72E-03	9,32E-03	1,20E-02
ESKISEHIR	9,71E-03	9,57E-03	1,26E-02
EDIRNE	9,69E-03	9,13E-03	1,16E-02
ISTANBUL	8,84E-03	8,63E-03	1,13E-02
YOZGAT	8,61E-03	8,48E-03	1,12E-02
DZCE	8,56E-03	8,30E-03	1,08E-02
BURDUR	8,21E-03	7,70E-03	9,74E-03
MALATYA	7,69E-03	7,41E-03	9,59E-03
AYDIN	6,96E-03	6,51E-03	8,21E-03
DENIZLI	6,93E-03	6,62E-03	8,50E-03
ÇANAKKALE	6,88E-03	6,49E-03	8,24E-03
BARTIN	6,72E-03	6,61E-03	8,70E-03
AGRI	6,01E-03	5,97E-03	7,92E-03
USAK	5,93E-03	5,89E-03	7,81E-03
MUGLA	5,92E-03	5,55E-03	7,01E-03
ORDU	5,74E-03	5,55E-03	7,19E-03

Table B.19 (continued): Calculated doses for Turkish Provinces by using SU2 simulation results (WHO Approach).

IZMIR	5,73E-03	5,40E-03	6,87E-03
AFYON	5,62E-03	5,46E-03	7,11E-03
TRABZON	5,53E-03	5,27E-03	6,75E-03
IÇEL	5,25E-03	5,17E-03	6,80E-03
KAYSERI	4,66E-03	4,55E-03	5,95E-03
ZONGULDAK	4,66E-03	4,56E-03	5,98E-03
BILECIK	4,51E-03	4,28E-03	5,48E-03
NIGDE	4,46E-03	4,44E-03	5,91E-03
ANTALYA	4,31E-03	4,05E-03	5,13E-03
DIYARBAKIR	4,19E-03	4,17E-03	5,54E-03
TOKAT	4,11E-03	4,00E-03	5,21E-03
BALIKESIR	4,04E-03	3,72E-03	4,62E-03
SAKARYA	3,95E-03	3,76E-03	4,80E-03
KÜTAHYA	3,67E-03	3,58E-03	4,67E-03
KOCAELI	3,30E-03	3,11E-03	3,95E-03
HATAY	3,23E-03	3,22E-03	4,28E-03
AKSARAY	3,15E-03	3,15E-03	4,19E-03
BURSA	2,97E-03	2,80E-03	3,54E-03
MANISA	2,61E-03	2,45E-03	3,11E-03
YALOVA	2,30E-03	1,91E-03	2,14E-03
ADIYAMAN	1,78E-03	1,78E-03	2,37E-03
MARDIN	1,66E-03	1,65E-03	2,20E-03
SANLIURFA	1,60E-03	1,60E-03	2,13E-03
MUS	1,30E-03	1,30E-03	1,73E-03
GAZIANTEP	1,26E-03	1,25E-03	1,66E-03
K.MARAS	1,10E-03	1,07E-03	1,41E-03
ADANA	1,04E-03	1,04E-03	1,38E-03
KARAMAN	1,04E-03	1,01E-03	1,31E-03
VAN	9,29E-04	9,29E-04	1,24E-03
BATMAN	7,92E-04	7,91E-04	1,05E-03
OSMANIYE	6,28E-04	6,26E-04	8,32E-04
BITLIS	3,61E-04	3,61E-04	4,81E-04
KILIS	3,58E-04	3,52E-04	4,64E-04
SIRNAK	3,36E-04	3,36E-04	4,48E-04
SIIRT	1,82E-04	1,82E-04	2,42E-04
HAKKARI	8,15E-05	8,15E-05	1,09E-04

Table B.20: Calculated doses for Turkish Provinces by using CONT simulation results (UNSCEAR Approach).

Province	Doses (mSv)		
	Adult	Child	Infant
KARABÜK	1,46E-01	1,46E-01	1,46E-01
KASTAMONU	1,44E-01	1,44E-01	1,43E-01
SINOP	1,31E-01	1,31E-01	1,31E-01
ARDAHAN	1,22E-01	1,22E-01	1,22E-01
KARS	9,50E-02	9,50E-02	9,49E-02
ERZURUM	8,12E-02	8,11E-02	8,11E-02
KIRIKKALE	7,38E-02	7,37E-02	7,36E-02
ÇANKIRI	6,75E-02	6,74E-02	6,73E-02
BOLU	6,69E-02	6,69E-02	6,69E-02
BAYBURT	6,59E-02	6,59E-02	6,58E-02
ARTVIN	6,38E-02	6,38E-02	6,37E-02
GÜMÜSHANE	5,52E-02	5,51E-02	5,50E-02
ANKARA	5,24E-02	5,24E-02	5,23E-02
ERZINCAN	5,09E-02	5,07E-02	5,05E-02
TUNCELI	4,72E-02	4,69E-02	4,66E-02
BINGÖL	4,59E-02	4,59E-02	4,59E-02
ELAZIG	4,58E-02	4,57E-02	4,56E-02
ÇORUM	4,49E-02	4,48E-02	4,48E-02
İSTANBUL	3,81E-02	3,80E-02	3,78E-02
NEVSEHIR	3,00E-02	3,00E-02	3,00E-02
DÜZCE	2,90E-02	2,89E-02	2,88E-02
KIRKLARELI	2,79E-02	2,76E-02	2,75E-02
SAMSUN	2,68E-02	2,67E-02	2,67E-02
TEKIRDAG	2,62E-02	2,61E-02	2,60E-02
BARTIN	2,62E-02	2,62E-02	2,62E-02
ZONGULDAK	2,38E-02	2,37E-02	2,36E-02
AMASYA	2,17E-02	2,16E-02	2,15E-02
ESKİSEHIR	2,08E-02	2,08E-02	2,07E-02
USAK	1,94E-02	1,94E-02	1,94E-02
AYDIN	1,90E-02	1,87E-02	1,85E-02
MALATYA	1,76E-02	1,74E-02	1,73E-02
RIZE	1,71E-02	1,70E-02	1,70E-02
IGDIR	1,65E-02	1,65E-02	1,65E-02
EDİRNE	1,62E-02	1,61E-02	1,60E-02
ISPARTA	1,43E-02	1,42E-02	1,42E-02
SAKARYA	1,34E-02	1,33E-02	1,32E-02
YALOVA	1,33E-02	1,33E-02	1,33E-02
BURDUR	1,29E-02	1,27E-02	1,25E-02
KONYA	1,28E-02	1,28E-02	1,28E-02
SIVAS	1,24E-02	1,23E-02	1,22E-02
MUGLA	1,22E-02	1,20E-02	1,19E-02
ORDU	1,16E-02	1,15E-02	1,15E-02
DENİZLİ	1,13E-02	1,12E-02	1,12E-02
ÇANAKKALE	1,07E-02	1,06E-02	1,05E-02
GİRESUN	1,05E-02	1,04E-02	1,04E-02

Table B.20 (continued): Calculated doses for Turkish Provinces by using CONT simulation results (UNSCEAR Approach).

KIRSEHIR	1,01E-02	1,01E-02	1,01E-02
KOCAELI	9,74E-03	9,67E-03	9,61E-03
KÜTAHYA	9,30E-03	9,28E-03	9,27E-03
IZMIR	8,82E-03	8,69E-03	8,58E-03
YOZGAT	8,76E-03	8,75E-03	8,75E-03
AFYON	8,72E-03	8,66E-03	8,61E-03
NIGDE	8,72E-03	8,72E-03	8,71E-03
KAYSERI	8,04E-03	7,98E-03	7,92E-03
MANISA	7,45E-03	7,38E-03	7,33E-03
AGRI	6,47E-03	6,47E-03	6,47E-03
BILECIK	5,83E-03	5,79E-03	5,75E-03
BALIKESIR	5,01E-03	4,93E-03	4,87E-03
IÇEL	4,95E-03	4,91E-03	4,88E-03
ANTALYA	4,56E-03	4,52E-03	4,48E-03
HATAY	4,31E-03	4,31E-03	4,31E-03
K.MARAS	4,06E-03	4,04E-03	4,03E-03
TOKAT	3,95E-03	3,88E-03	3,83E-03
BURSA	3,68E-03	3,63E-03	3,58E-03
DIYARBAKIR	3,48E-03	3,44E-03	3,40E-03
MUS	2,08E-03	2,08E-03	2,08E-03
ADIYAMAN	1,99E-03	1,99E-03	1,99E-03
TRABZON	1,86E-03	1,84E-03	1,82E-03
AKSARAY	1,14E-03	1,14E-03	1,13E-03
VAN	1,11E-03	1,11E-03	1,11E-03
MARDIN	1,09E-03	1,09E-03	1,09E-03
ADANA	5,31E-04	5,31E-04	5,30E-04
SIIRT	5,21E-04	5,21E-04	5,21E-04
SIRNAK	5,14E-04	5,14E-04	5,14E-04
KARAMAN	4,63E-04	4,62E-04	4,61E-04
BATMAN	3,97E-04	3,97E-04	3,97E-04
KILIS	2,19E-04	2,18E-04	2,18E-04
HAKKARI	2,12E-04	2,12E-04	2,12E-04
SANLIURFA	1,83E-04	1,82E-04	1,82E-04
BITLIS	1,68E-04	1,68E-04	1,68E-04
GAZIANTEP	1,28E-04	1,28E-04	1,28E-04
OSMANIYE	7,92E-05	7,87E-05	7,83E-05

Table B.21: Calculated doses for Turkish Provinces by using CONT simulation results (WHO Approach).

Province	Doses (mSv)		
	Adult	Child	Infant
KARABÜK	9,58E-02	9,57E-02	1,27E-01
KASTAMONU	9,48E-02	9,45E-02	1,26E-01
SINOP	8,63E-02	8,61E-02	1,15E-01
ARDAHAN	8,02E-02	8,00E-02	1,07E-01
KARS	6,27E-02	6,25E-02	8,32E-02
ERZURUM	5,34E-02	5,33E-02	7,10E-02
KIRIKKALE	4,91E-02	4,87E-02	6,46E-02
ÇANKIRI	4,47E-02	4,45E-02	5,90E-02
BOLU	4,41E-02	4,40E-02	5,86E-02
BAYBURT	4,35E-02	4,34E-02	5,77E-02
ARTVIN	4,23E-02	4,21E-02	5,58E-02
GÜMÜSHANE	3,69E-02	3,65E-02	4,83E-02
ANKARA	3,47E-02	3,45E-02	4,59E-02
ERZINCAN	3,44E-02	3,38E-02	4,45E-02
TUNCELI	3,26E-02	3,17E-02	4,12E-02
ELAZIG	3,05E-02	3,02E-02	4,01E-02
BINGÖL	3,02E-02	3,01E-02	4,02E-02
ÇORUM	2,97E-02	2,96E-02	3,93E-02
İSTANBUL	2,59E-02	2,54E-02	3,33E-02
NEVSEHIR	1,97E-02	1,97E-02	2,63E-02
DÜZCE	1,95E-02	1,92E-02	2,53E-02
KIRKLARELI	1,93E-02	1,87E-02	2,43E-02
TEKIRDAG	1,79E-02	1,75E-02	2,29E-02
SAMSUN	1,78E-02	1,77E-02	2,34E-02
BARTIN	1,72E-02	1,72E-02	2,30E-02
ZONGULDAK	1,61E-02	1,58E-02	2,08E-02
AMASYA	1,48E-02	1,45E-02	1,90E-02
AYDIN	1,39E-02	1,30E-02	1,65E-02
ESKISEHIR	1,37E-02	1,36E-02	1,82E-02
USAK	1,29E-02	1,28E-02	1,70E-02
MALATYA	1,24E-02	1,19E-02	1,53E-02
EDİRNE	1,15E-02	1,10E-02	1,42E-02
RIZE	1,13E-02	1,13E-02	1,49E-02
IGDIR	1,09E-02	1,09E-02	1,45E-02
ISPARTA	9,67E-03	9,50E-03	1,25E-02
BURDUR	9,47E-03	8,87E-03	1,12E-02
SAKARYA	9,11E-03	8,91E-03	1,17E-02
SIVAS	8,85E-03	8,44E-03	1,08E-02
YALOVA	8,70E-03	8,70E-03	1,16E-02
MUGLA	8,66E-03	8,26E-03	1,06E-02
KONYA	8,45E-03	8,44E-03	1,12E-02
ORDU	7,76E-03	7,67E-03	1,01E-02
ÇANAKKALE	7,69E-03	7,31E-03	9,35E-03
DENİZLİ	7,67E-03	7,52E-03	9,87E-03

Table B.21 (continued): Calculated doses for Turkish Provinces by using CONT simulation results (WHO Approach).

GIRESUN	7,30E-03	7,06E-03	9,16E-03
KOCAELI	6,78E-03	6,56E-03	8,50E-03
KIRSEHIR	6,64E-03	6,64E-03	8,86E-03
IZMIR	6,46E-03	6,07E-03	7,68E-03
KÜTAHYA	6,19E-03	6,14E-03	8,14E-03
AFYON	6,03E-03	5,85E-03	7,61E-03
YOZGAT	5,78E-03	5,76E-03	7,67E-03
NIGDE	5,75E-03	5,74E-03	7,63E-03
KAYSERI	5,61E-03	5,42E-03	7,02E-03
MANISA	5,24E-03	5,03E-03	6,50E-03
AGRI	4,25E-03	4,25E-03	5,66E-03
BILECIK	4,05E-03	3,92E-03	5,09E-03
BALIKESIR	3,70E-03	3,46E-03	4,36E-03
İÇEL	3,45E-03	3,33E-03	4,32E-03
ANTALYA	3,20E-03	3,08E-03	3,98E-03
TOKAT	2,95E-03	2,74E-03	3,44E-03
HATAY	2,84E-03	2,83E-03	3,77E-03
K.MARAS	2,76E-03	2,71E-03	3,55E-03
BURSA	2,68E-03	2,53E-03	3,20E-03
DIYARBAKIR	2,50E-03	2,38E-03	3,03E-03
MUS	1,37E-03	1,37E-03	1,82E-03
TRABZON	1,32E-03	1,26E-03	1,62E-03
ADIYAMAN	1,31E-03	1,31E-03	1,74E-03
AKSARAY	7,54E-04	7,50E-04	9,95E-04
VAN	7,29E-04	7,29E-04	9,72E-04
MARDIN	7,17E-04	7,17E-04	9,56E-04
ADANA	3,52E-04	3,50E-04	4,65E-04
SIIRT	3,42E-04	3,42E-04	4,56E-04
SIRNAK	3,38E-04	3,38E-04	4,50E-04
KARAMAN	3,08E-04	3,06E-04	4,05E-04
BATMAN	2,61E-04	2,61E-04	3,48E-04
KILIS	1,48E-04	1,45E-04	1,92E-04
HAKKARI	1,39E-04	1,39E-04	1,85E-04
SANLIURFA	1,22E-04	1,21E-04	1,60E-04
BITLIS	1,10E-04	1,10E-04	1,47E-04
GAZIANTEP	8,59E-05	8,49E-05	1,12E-04
OSMANIYE	5,45E-05	5,30E-05	6,91E-05

CURRICULUM VITAE



Name Surname: Volkan ŞİMŞEK

Place and Date of Birth: Yozgat 18/06/1978

Address: Çekmece Nuclear Research and Training Center Yarımurgaz Mah.
Nükleer Araştırma Merkezi Yolu, 34303, Küçükçekmece İSTANBUL

E-Mail: volkan.simsek@taek.gov.tr

B.Sc.: Eskişehir Osmangazi University, Physics

M.Sc.: Muğla University, Physics

Professional Experience and Rewards:

2003-2006, Research Assistant, Physics Dept., Muğla University.

2006-..., Çekmece Nuclear Research and Training Center

List of Publications and Patents:

- **Simsek V.**, G.Karahan Dose Assessment For People Living In Most Crowded City Of Turkey, *International Conference of Young Scientists and Specialists dedicated to the 20'th Anniversary of NNC and the 55th Anniversary of NCC and the 55th Anniversary of INP NC RK*, June 6 – 8, 2012. Almaty, Kazakhstan.
- **Şimşek V**, Oktik Ş., Cankoçak K., Güneş Isınımının 200-1100 nm Arasında Spektral Analizi Yoluyla Mugla Atmosferinde NO₂, SO₂ Ve Ozon Gazlarının Miktarlarının Belirlenmesi, *2005 Dünya Fizik Yılı-Türk Fizik Derneği 23. Uluslararası Fizik Kongresi*, 13-16 Eylül 2005, Muğla, Türkiye.
- **Şimşek V**, Oktik Ş., Cankoçak K, Güneş Isınımının 200-1100 nm Arasında Spektral Analizi Yoluyla Mugla Atmosferinde NO₂, SO₂ Ve Ozon Gazlarının Miktarlarının Belirlenmesi *I.Ulusal Güneş ve Hidrojen Enerjisi Kongresi*, pp 242-247, 21-23 Haziran 2006, Muğla, Türkiye

PUBLICATIONS/PRESENTATIONS ON THE THESIS

- **Simsek V.**, Pozzoli L., Unal A., Kindap T., Karaca M., 2014. Simulation of ^{137}Cs transport and deposition after the Chernobyl Nuclear Power Plant accident and radiological doses over the Anatolian Peninsula, *Science of the Total Environment*, pp. 74–88, Elsevier B.V., <http://dx.doi.org/10.1016/j.scitotenv.2014.08.038>
- **Simsek V.**, Kindap T., Unal A., Pozzoli L., Karaca M., 2012. Calculation of Radiation Doses Due to Release of ^{137}Cs and ^{131}I using Atmospheric Dispersion and Dose Calculation Models ,*Nuclear Science and its Application*, pp378, September 25-28 Samarkand , Uzbekistan.
- **Simsek V.**, Kindap T., Unal A., Pozzoli L., Karaca M., 2012. Estimation Of ^{137}Cs Using Atmospheric Dispersion Models After A Nuclear Reactor Accident, *EGU General Assembly 2012*, April 22-27 Vienna, Austria.